Identification and Characterization of Cold-Tolerance Associated Genes in Wheat

Muhammad Zayed

A Thesis

In the Department

of

Biology

Presented in Partial Fulfilment of the Requirements

For the Degree of

Doctor of Philosophy (Biology) at

Concordia University

Montreal, Quebec, Canada

October 2018

CONCORDIA UNIVERSITY
School of Graduate Studies

This is to certify that the thesis prepared

By: **Muhammad Zayed**

Entitled: **Identification and Characterization of Cold-Tolerance Associated Genes in Wheat**

and submitted in partial fulfilment of the requirements for the degree of

Doctor of Philosophy (Biology)

complies with the regulations of the University and meets the accepted standards with respect to originality and quality.

Signed by the final Examining Committee:

---------- Chair

Dr. Karen Li

---------- External Examiner

Dr. Mirwais Qaderi

---------- External to Program

Dr. Andreas Bergdahl

---------- Examiner

Dr. Jinsuk Lee

---------- Examiner

Dr. Patrick Gulick

---------- Thesis Supervisor

Dr. Selvadurai Dayanandan

Approved by ----------

Dr. Robert Weladji, Graduate Program Director

Date of defense: Thursday, November 8, 2018 ----------

André Roy, Dean

Faculty of Arts and Science

ABSTRACT

Identification and characterization of cold-tolerance associated genes in wheat

Muhammad Zayed, Ph.D.

Concordia University, 2018

The low temperature remains as one of the major limiting factors of crop productivity in the temperate region, and identification of cold tolerance related genes is crucial for developing cold tolerant crop plants to increase agricultural productivity. The objective of my thesis is to identify cold tolerance related candidate genes in wheat, one of the major crops in the temperate region. In Chapter 2, I have reviewed the literature pertaining to the mechanisms of cold tolerance in plants with specific emphasis on Wheat. In Chapter 3, forty candidate genes with increased expression under cold exposure based on published microarray data were selected and further characterized. These genes belonging to four categories namely defense-related regulators; transcriptional and epigenetic regulators; post-transcriptional and post-translational regulators; and genes of unknown functions revealed many differentially expressed genes including Remorin – upregulated in response to cold; a novel gene in wheat homologous to RD29B of Arabidopsis- upregulated in response to cold and ABA; and another novel gene regulated by both ABA and MetJA.

In chapter 4, the results of genome-wide identification and characterization of the wheat remorin family and its association with cold tolerance are presented. A search of the wheat database revealed the existence of twenty different remorin genes that we classified into six groups sharing a common structure and phylogenetic origin. Promoter analysis of TaREM genes revealed the presence of putative cis-elements related to diverse functions like development, hormonal regulation, biotic and abiotic stress responsiveness. Expression levels of TaREM genes were measured in plants grown under in field and laboratory conditions and in response to hormone treatment. Our analyses revealed twelve members of the remorin family that are regulated during

cold acclimation of wheat in four different tissues (root, crown, stem and leaves), with the highest expression in roots. Differential gene expression was found between wheat cultivars with contrasting degree of cold tolerance suggesting the implication of TaREM genes in cold response and tolerance. Additionally, eight genes were induced in response to ABA and MetJA treatment. This genome-wide analysis of TaREM genes provides valuable resources for functional analysis aimed at understanding their role in stress adaptation.

The chapter 5 is focused on gaining insights into the evolutionary history and in-silico functional characterization of a novel cold-responsive gene in wheat. This gene in wheat has distant homology to known abiotic stress-related genes in other plants including CAP160 in *Spinacia oleracea*, RD29B in Arabidopsis and CDeT11-24 in *Craterostigma plantagineum*. The results show that these genes are homologous and may have evolved from a common ancestor. The Bayesian phylogenetic analyses of the protein sequences of this gene from various plant species revealed three distinctive clades. Further analyses revealed that this gene has predominantly evolved through neutral processes with some regions experiencing signatures of negative selections and some regions showing signatures of episodic positive selections. These genes contained common K-like segments and function predictions revealed that these protein-coding genes may share at least two functions related to abiotic stress conditions. One function is similar to the cryoprotective function of LEA protein, and the second function as a signalling molecule by binding specifically to phosphatidic acid.

ACKNOWLEDGMENTS

Above all, I would like to thank ALLAH “God” Almighty for giving me the patience, strength and knowledge to complete this work reasonably. Without his mercy and blessings, this work will never be accomplished. During my Ph.D. journey, ALLAH blesses me with many individuals who supported and helped me to complete this work, and herby I will only try to express my gratitude to them.

First, I would like to express my sincere appreciation to my supervisor, Prof. Selvadurai Dayanandan. Also, I would like to express my great thanks to Prof. Fathey Sarhan and Prof. Jean Danyluk from UQAM university. I am thankful to Dr. Sarhan for welcoming me into his laboratory and his support during my study. I am particularly indebted to Prof. Jean Danyluk, from UQAM university, for his guidance, inspirational ideas, training and support. My most profound appreciation to my committee members Prof. Patrick Gulick and Prof. Jinsuk Lee, I owe a very important debt to Prof. Patrick Gulick for his insightful comments and suggestions into my thesis. Special thanks to Dr. Guillaume Larocque from the Quebec Centre For Biodiversity Science (QCBS) for his help with plotting the graphs and statistical analysis using R-programming language.

My profound thanks to all members from Prof. Selvadurai Dayanandan laboratory, with special thanks to Shiva Prakash and Sachin Naik for their valuable discussions and Kyle Grant for proofreading many parts of my thesis. I would like to thank all staff members from Concordia University for their generous help. I truly thank Dr. Mohamed Badawi and Dr. Zahra Agharbaoui from Prof. Fathey Sarhan laboratory for their contributions to my thesis research work. Furthermore, I would like to thank all staff members of UQAM.

Special thanks from the bottom of my heart to the Egyptian Bureau of Cultural and Educational Affairs in Montreal, the Mission Sector in Egypt, the Egyptian Ministry of Higher Education, and Prof. Selvadurai Dayanandan for sponsoring my study for six years during my Ph.D. program at Concordia University.

In Egypt, I would like to sincerely thank all teachers of the Botany Department, Faculty of Science, Menoufia University, those who taught me during my undergraduate and Master studies with special gratitude to the spirit of Prof. Mohamed Ali Afifi Hefnawy, his memory will be eternal, Prof. Mohamed Medhat Gharieb, Prof. Mohamed Tawfik, Prof. Mohamed Zayed, Prof. Zaki Turki, Prof. Mamdouh Elamry, Prof. Mohamed E. El-lithy, Prof. Omaima Eissa, Prof. Magdy

Mattar and Prof. Fathey El-Shayeb. My sincerest thanks for Prof. Abd-Elfattah Selim, Faculty of Agriculture, Menoufia University.

Forever, I would like to express my deepest gratitude to my father Atef, my mother Fawzia, my sisters Kholoud and Jana, my brother Amr, my aunt Amal, my uncles Hussein, Raafat, Salah and their families, my parents-in-law Mohamed and Samia, my brothers-in-law Abd-Elfattah and Ahmed and my sister-in-law Basma, all my relatives and to the spirits of my grandfathers Mohamed Zayed and Hashem Nour Eldin and to my granduncle Mohamed Elnoamany and uncle Sameh, whose memories are everlasting.

Special thanks to my wife Sara, for her continuous support and her cups of Turkish coffee, my daughter Mariam and my son Atef, those who make my life delightful. My heartily thanks to my family of lovely friends. This includes, Dr. Esam Orabi and his family, Taryn Boudreau, Jean-Marc Nielly, Dr. Hala Khalil, Darya Mitrofanova and all my friends.

Dedication

To my grandmother

Samah Elnoamany

Who gifted her time to take care of me since my birth and granted me with her endless love.
Your voice is in my ears, your love is in my heart, and your soul lights my way.

CONTRIBUTIONS OF AUTHORS

Chapter Three: Identification of Cold-Tolerance Associated Genes in Wheat

Author names:

Muhammad Zayed[1,3], Mohamed A. Badawi[2], Zahra Agharbaoui[2], Jean Danyluk[2] and Fathey Sarhan[2]

Affiliations :

[1]Department of Biology, Concordia University, 7141 Sherbrooke St. W. Montreal, Quebec H4B 1R6, Canada; [2]Département des Sciences Biologiques, Université du Québec à Montréal, Montréal, Quebec H3C 3P8, Canada. [3]Botany Department, Faculty of Science, Menoufia University, Shebin El Kom, Egypt.

Authors' contributions:

M.Z., F.S. and J.D. designed the overall study. M.Z., M.A.B and Z.A. selected the candidate genes. M.A.B and M.Z. performed the qPCR experiments. M.A.B and J.D performed the biological experiments under controlled conditions and provided samples of the biological experiments under field condition. M.Z. and Z.A performed the biological experiments for ABA and MetJA. M.Z. analyse the qPCR data and wrote the article.

Chapter Four: Genome-Wide Identification and Characterization of the Wheat Remorin (TaREM) Family and its Association with Cold Tolerance

Author names:

Mohamed A. Badawi[1, 4], Zahra Agharbaoui[1], Muhammad Zayed[5, 6], Qiang Li[2, 3], Brook Byrns[2], Jitao Zou[3], D. Brian Fowler[2], Jean Danyluk[1] and Fathey Sarhan[1]

Affiliations:

[1]Département des Sciences Biologiques, Université du Québec à Montréal, Montréal, Quebec H3C 3P8, Canada; [2]Department of Plant Sciences, University of Saskatchewan, Saskatoon, Saskatchewan S7N 5A8, Canada; [3]National Research Council Canada, Saskatoon, Saskatchewan S7N 0W9, Canada; [4]Agricultural Genetic Engineering Research Institute (AGERI), Agricultural Research Centre, Giza, Egypt 12619; [5]Department of Biology, Concordia University, 7141 Sherbrooke St. W. Montreal, Quebec H4B 1R6, Canada. [6]Botany Department, Faculty of Science, Menoufia University, Shebin El Kom, Egypt.

Authors' contributions:

M.A.B, J.D and F.S designed the overall study. M.A.B and J.D performed the biological experiments under controlled conditions. M.Z. and Z.A performed the biological experiments for ABA and MetJA. D.B.F, J.Z and Q.L performed the biological experiments under field condition and provided the RNA-Seq data. M.Z performed the selection of remorin gene from the RNA-Seq data. M.Z performed the Genevestigator analysis and Bayesian phylogenetic analysis. M.A.B and M.Z. performed the qPCR experiments. M.A.B performed the bioinformatics analyses. M.A.B, Z.A and F.S wrote the article.

Chapter Five: Evolutionary and In-Silico Functional Analysis of A Novel Cold Responsive Gene in Wheat

Author names:

Muhammad Zayed[1,2] and Selvadurai Dayanandan[1]

Affiliations:

[1]Department of Biology, Concordia University, 7141 Sherbrooke St. W. Montreal, Quebec H4B 1R6, Canada. [2]Botany Department, Faculty of Science, Menoufia University, Shebin El Kom, Egypt.

Authors' contributions:

M.Z.: Designing the overall study, performing the analyses and writing the draft manuscript. S.D.: Manuscript revision, results validation and supervision.

TABLE OF CONTENTS

List of Figures

CHAPTER 2

CHAPTER 3

CHAPTER 5

List of Tables

List of Appendices

1. List of Appendix Datasets

Dataset S3.1: List of predicted gene sequences with the start and stop codons.

Dataset S3.2: List of primers used in qPCR.

Dataset S4.1: List of wheat remorin CDS sequences.

Dataset S4.2: List of remorin protein sequences.

Dataset S4.3: List of remorin sequences used in the phylogenetic analyses though Maximum Likelihood Phylogenetic and Bayesian methods.

Dataset S4.4: List of wheat remorin-C domain sequences.

Dataset S4.5: List of the twenty wheat remorin-C domain sequences.

Dataset S4.6: List of remorin promoter sequences.

Dataset S4.7: List of wheat remorin nucleotide sequences that were used for gene structure analysis.

Dataset S5.1: List of the retrieved genomic DNA sequences, Coding Sequences and Predicted Proteins of different plant CAP160 genes.

Dataset S5.2: Sequence data of promoters of various plant CAP160 homologous genes.

Dataset S5.3: Comparison between positive co-expression networks of RD29B (Ath1.1, AT5G52300), CAP160 (Ath1.2, AT4G25580.1) in Arabidopsis and the co-expression network of their homologous gene in rice (Os, LOC_OS10g36180) with limiting the number of the analysed co-expressed genes to 25. The degree of positive co-expression between each pair of genes is calculated using Pearson's correlation coefficient. This is followed by a Table that annotates the co-expressed genes and then by a heatmap that explores the conditions where the mutually correlated genes from each network are differentially expressed with a cut-off fold-change value of 3 and a p-value equals to or less than 0.05. The analysis was performed using Genevestigator software (Zimmermann et al. 2014).

A. Positive co-expression analysis of RD29B (Ath1.1, AT5G52300.1). Genes with mutual correlation of at least 0.8 were connected.
B. Descriptions of positively correlated genes.
C. Conditions where gene (Ath1.1) and mutually correlated genes exhibit similar profiles of differential expression.

D. Positive co-expression analysis of CAP160 (Ath1.2, AT4G25580.1). Genes with mutual correlation of at least 0.8 were connected.
E. Descriptions of positively correlated genes.
F. Conditions where gene (Ath1.2) and mutually correlated genes exhibit similar profiles of differential expression.
G. Positive co-expression analysis of Loc-Os10g36180.1 from rice. Genes with mutual correlation of at least 0.8 were connected.
H. Descriptions of positively correlated genes.
I. Conditions where gene (Os) and mutually correlated genes exhibit similar profiles of differential expression.

Dataset S5.4: The Predicted MEME-Multiple EM for Motif Elicitation (Bailey et al. 2009).

Dataset S5.5A: Multiple sequence alignment of the retrieved plant CAP160 proteins as performed by Decipher, an R-based alignment software (Wright 2015).

Dataset S5.5B: Multiple sequence alignment of the retrieved plant CAP160 proteins from clade I with *Amborella trichopoda* CAP160 protein, and as performed by Decipher, an R-based alignment software (Wright 2015).

Dataset S5.5C: Multiple sequence alignment of the retrieved plant CAP160 proteins from clade II, and as performed by Decipher, an R-based alignment software (Wright 2015).

Dataset S5.5D: Multiple sequence alignment of the retrieved plant CAP160 proteins from clade III, and as performed by Decipher, an R-based alignment software (Wright 2015).

2. List of Appendix Figures

Figure S4.1: Phylogenetic tree of all wheat REM genes from genome A, B and D. The amino acids corresponding to the conserved C-motif of the 20 REMs genes were aligned by MUSCLE in MEGA6. A Maximum Likelihood tree (ML) was derived from this alignment using LG + Gamma model and bootstrap value with 500 replicates.

Figure S4.2: A Gene expression analysis of twenty TaREM genes from published RNA-Seq data. Relative gene expression is presented as a colored heat-map where yellow color indicates up-regulated genes, blue color indicates down-regulated genes and black color represents unchanged relative gene expression. Pearson's based hierarchical clustering algorithm is used to cluster REM genes and different perturbations based on the pattern of gene expression. The color reflected the

log ratio with yellow indicating up-regulation and blue down-regulation. The analysis was performed using Genevestigator software (Zimmermann et al. 2014).

Figure S4.3: A gene expression analysis of twenty *TaREM* genes from published RNA-Seq data from different anatomical parts and developmental stages. Relative gene expression is presented as a colored heat-map where burgundy-white color-coding in a log scale represents the minimum level and burgundy color represents the maximum level of expression. **(A)** Expression of *TaREM* genes across different wheat tissues. **(B)** Expression of *TaREM* genes across different wheat developmental stages. Pearson's based hierarchical clustering algorithm is used to group genes and different tissues or developmental stages based on the pattern of gene expression. The color reflected the log ratio with burgundy indicating up-regulation and white down-regulation. The analysis was performed using Genevestigator software (Zimmermann et al. 2014).

Figure S4.4: Alignment of all Remorin protein sequences. The alignment was presented by using Jalview software (Waterhouse et al. 2009), where the secondary structure was predicted.

Figure S5.1: Syntenic relationships between *Theobroma cacao* CAP160 (Tc) gene and many other orthologous genes in the matching micro-chromosomal segments (100 Kb) from different plant species as analysed by Plant Genome Duplication Database (PGDD), according to Lee et al. (2013).

Figure S5.2: Alignment of all retrieved CAP160 protein sequences. The alignment was presented by using Jalview software (Waterhouse et al. 2009) where the secondary structure and intrinsically disordered regions were predicted.

Figure S5.3: Analysis and graphing of cis-acting regulatory DNA elements in promoters of different plant CAP160 homologous genes according to Higo et al. (1999) and Austin et al. (2016), where Z-score threshold 5 was selected and calculated as the number of standard deviations by which the number of promoter cis-elements binding sites in specific group deviates from the mean of background distributions. Significance is considered with Z-scores threshold of 5.

Figure S5.4: Microarray based differential gene expression screening meta-analysis of some plant CAP160 homologous genes in Arabidopsis, rice, barley, maize and wheat. The goal of this screening is to track treatment conditions where the selected genes are differentially expressed below or above a cut-off fold-change value of 3 and with a p-value equals or less than 0.05. The analysis was performed using Genevestigator software (Zimmermann et al. 2014).

Figure S5.5: Bayesian phylogenetic analysis of clade I where the phylogenetic tree is rooted by using Amborella trichopoda (Atr) sequence. Predicted MEME-Multiple EM for Motif Elicitation motifs (Bailey et al. 2009) were graphed in order with respect to each sequence by using the online tool iTOL (Letunic and Bork 2016).

Figure S5.6: Bayesian phylogenetic analysis of clade II where the phylogenetic tree is rooted by using Phoenix dactylifera (Pd) sequence. Predicted MEME-Multiple EM for Motif Elicitation motifs (Bailey et al. 2009) were graphed in order with respect to each sequence by using the online tool iTOL (Letunic and Bork 2016).

Figure S5.7: Bayesian phylogenetic analysis of clade III where the phylogenetic tree is rooted by using Eucalyptus grandis (Eg) sequence. Predicted MEME-Multiple EM for Motif Elicitation motifs (Bailey et al. 2009) were graphed in order with respect to each sequence by using the online tool iTOL (Letunic and Bork 2016).

3. List of Appendix Tables

Table S3.1: The summary of the selected candidate genes with annotation of their predicted functions based on blastx results (NCBI Resource Coordinators 2016). Previously uncharacterized genes that were reported in literature as upregulated in response to cold were selected for this study.

Table S4.1: Identification of consensus sequence of TaREM using MEME and their function by prosite and Eukaryotic Linear Motif resource programs. The motif numbers are the same to those described in Figure 4.4.

Table S4.2: The cis-acting regulatory DNA elements of 20 TaREM promoters.

Table S4.3: REM Genevestigator identifiers that were used to generate the heatmaps in Figures S4.2 and S4.3.

Table S4.4: The qRT-PCR primers sequences that were used in the present study.

Table S5.1: Identifiers of Plant RD29/CAP160/ CDeT11-24 genes and promoters from different genome databases.

Table S5.2: Assessment of multiple sequence alignment quality using VerAlign.

Table S5.3: Cacao gene annotations of micro-syntenic analysis as deduced from NCBI BLASTp search and their asynonymous (Ka) and synonymous (Ks) values of each matching gene pair.

Table S5.4: Codons of CAP160 gene homologs under pervasive positive/diversifying selection and their site-specific parameter values as estimated by fixed effects likelihood approaches (FEL;

Kosakovsky Pond & Frost, 2005b). Thirteen sites were found to be under pervasive positive selection with a p-value threshold of 0.1. Underlined codons are five sites of the thirteen which were found to be significant with a p-value threshold of 0.05. FEL results display parameters for each site where α represents synonymous rate at the site, β constitutes nonsynonymous rate and the rate estimate under neutral model (α = β). FEL uses likelihood ratio test (LRT) to infer the significance of (β > α) for a specific site.

Table S5.5: Codons of CAP160 gene homologs under pervasive negative/purifying selection and their site-specific parameter values as estimated by fixed effects likelihood approaches (FEL; Kosakovsky Pond & Frost, 2005b). Four hundred and eighty sites were found to be under pervasive negative selection with a p-value threshold of 0.1, three hundred and seventy-three sites out of them were found to be significant with a p-value threshold of 0.05. FEL results display parameters for each site where α represents synonymous rate at the site, β constitutes nonsynonymous rate and the rate estimate under neutral model (α = β). FEL uses likelihood ratio test (LRT) to infer the significance of (α > β) for a specific site.

Table S5.6: Molecular characteristics of CAP160 protein homologs from different plant species.

Table S5.7: Subcellular localization of different plant CAP160 proteins as predicted by different tools.

Table S5.8: Predicted *MEME*-Multiple EM for Motif Elicitation motifs (Bailey et al. 2009) and the motif logo alignment with their potential functional sites as retrieved from ELM-Eukaryotic Linear Motif (Dinkel et al. 2016).

Chapter One: General Introduction

The low temperature (0-15 °C) and freezing conditions (< 0 °C) affect plant growth and development and limits the geographical distribution of plants through their damaging effects on the development and productivity of sensitive plant species. However cold and freezing-tolerant plant species can tolerate these conditions to various degrees (Theocharis et al. 2012). The most of the global land area has an average minimum temperature of below 0 °C, which remains as a major barrier for expansion of the agriculture (Rihan et al. 2017). Many temperate plant species have developed different degrees of tolerance to frost conditions. The low, non-freezing temperature during the pre-frost period plays an important role in cold acclimation leading to the development of molecular and biochemical responses for cold tolerance in plants (Janská et al. 2010; Rihan et al. 2017).

In contrast, varieties of the same plant species that inhabit geographic regions with subtropical climatic conditions over long periods of time are not tolerant to frost conditions and do not show cold acclimation. Plants that respond to cold acclimation or develop frost tolerance are generally known as winter varieties whereas plants that cannot positively respond to cold acclimation or develop frost tolerance are classified as spring varieties (Preston and Sandve 2013). Responding positively to cold acclimation involves many physiological, biochemical and molecular changes that enable plants to adjust their metabolism, growth and development under low temperature conditions to develop cold stress tolerance (Rihan et al. 2017). Although most plants develop cold acclimation through similar genetic networks, some plants possess unique systems for developing cold tolerance (Sandve et al. 2011; Preston and Sandve 2013). Besides the inducible cold acclimation process, majority of cold-tolerant plant species have developed vernalization responsiveness to develop frost tolerance, protect reproductive structures and synchronize the flowering with favourable climatic conditions. However, the spring varieties of are unable to tolerate lower temperatures during vernalization period and show many cellular and physiological damages due to freezing (Preston and Sandve 2013).

Understanding the molecular mechanisms and evolutionary history through which cold tolerant species have developed tolerance to cold is essential for identifying new cryoprotective and antifreeze compounds, production of cold stress tolerant plant species, and overcoming the geographical limits for growing crop plants due to low-temperature conditions. During cold acclimation and vernalization periods, many protein-coding genes show significant differential

expression between winter and spring varieties of plants. Further investigations showed their functional importance of genes such as ICE (Inducer of CBF expression), CBF (C-repeat-binding factors) and COR (Cold- regulated) in developing cold tolerance in winter wheat varieties (Miura and Furumoto 2013; Wang et al. 2017).

Wheat is one of the globally important crops valued for its nutritional values with high demand for bread and starch production, and as a livestock feed. Wheat grains are a rich source of essential proteins, carbohydrates, vitamins and minerals, and bread alone constitutes the fifth of the average human daily consumption. Due to its high demand as a food source for humans, often inferior wheat cultivars with lower nutritional quality are used as a livestock feedstock. According to FAOStat, wheat cultivars dominate other crops in the area of its cultivation and has been increased from about 217 million ha in 2012 to 220 million ha in 2016 while its production continued a steady increase from around 672 million tonnes in 2012 up to 749 million tonnes in 2016 (FAOStat, http://www.fao.org/faostat/en/#home). According to FAOStat, the world top five exporter countries during the period from 2010 to 2013 are United States of America (USA), France, Australia, Canada and Russia while the top five importers countries are Egypt, Italy, Brazil, Algeria and Japan which may indicate that wheat production plays a significant role in the economy of developed countries.

In contrast to other important crops such as maize and rice, which are chilling-sensitive, wheat is cultivated in a wide range of geographical area due to its diverse genotypes that can grow in contrasting climatic condition ranging from tropical to temperate regions. Spring wheat cultivars are usually cultivated in subtropical and tropical climatic conditions due to its chilling-sensitivity while winter wheat cultivars grow within temperate regions due to its tolerance and requirement of lower temperatures. Besides their different physiological responses to different climatic conditions, winter and spring wheat cultivars also differ in the higher productive potential of winter wheat cultivars and the better baking quality of spring wheat cultivars (Koppel and Ingver 2008). Although winter wheat cultivars grown in the temperate climates, their production and geographical distribution in the northern hemisphere constitutes most of the global land area and is restricted due to severe cold conditions (Andrews et al. 1997).

The overall goal of this thesis is focused on the identification of cold tolerance associated genes in wheat and the characterization of the selected cold tolerance associated genes through *in silico* and expression analyses. My thesis will include a General introduction (Chapter 1), a Literature review on wheat and mechanisms of cold stress tolerance (Chapter 2), Identification of

cold tolerance associated genes in wheat (Chapter 3), Genome-wide identification and characterization of the wheat remorin (TaREM) gene family and its association with cold tolerance (Chapter 4), Evolution and function predictions of plant CAP160 genes (Chapter 5) and a General conclusion (Chapter 6).

Chapter Two: Literature Review
The Mechanisms of Cold Stress Tolerance in Wheat

Abstract

Understanding the mechanisms of abiotic stress tolerance in plants is essential for developing stress tolerant crop plants to achieve global food security and to mitigate the damaging effects of the changes in climate. The fluctuations above or below the optimum temperature and moisture regime remain as major abiotic stresses that cause losses in crop yield. Thus, identifying the physiological and molecular mechanisms related to heat, cold and drought tolerance in plants is crucial for development of appropriate management strategies to maximize crop yield. This review presents a broad overview of the underlying mechanisms of cold stress tolerance in plants using examples from either wheat or Arabidopsis. The choice of wheat is due to its economic importance and Arabidopsis as a model plant with substantial experimental advances. Cold and drought stresses are related to the creation of similar downstream signalling effects on plants, therefore investigating cold tolerance is important as it is the major limitation for agriculture expansion. Many plant varieties of the same species have developed different degrees of tolerance to cold conditions and serves as genetic material for improving crops for adapting to changes in the climate. This review elucidates the mechanisms of cold signal perception, transduction, and roles of abscisic acid (ABA) and jasmonic acid (JA) in cold acclimation and vernalization.

2.1 Wheat and Cold Stress Tolerance

Wheat is one of the most important crops, and its scale of production is approximately equivalent to maize and rice (Shewry and Hey 2015). It belongs to the family Poacea. In general, wheat refers to either the bread wheat *Triticum aestivum,* about 95% of wheat cultivated worldwide, or pasta wheat, *T. durum* which covers about 5% of cultivated wheat (Arzani and Ashraf 2017). Both are polyploids where durum wheat is a tetraploid with AABB genome (2n=4x=28), and bread wheat is hexaploid with AABBDD genome (2n = 6x = 42). Peng et al. (2011) reviewed evolutionary studies and showed that the D genome in bread wheat originated from *Aegilops tauschii,* while the A and B genomes originated from the domesticated *Triticum dicoccum*. The complexity and large size of the hexaploid bread wheat genome hindered the progress towards determining the complete genome sequence for a long time. However, using 454-pyrosequencing technology, Brenchley et al. (2012) sequenced 17-gigabase-pairs of the bread

wheat genome, and showed that the long process of wheat domestication along with polyploidization affected many gene family members. Recently, the International Wheat Genome Sequencing Consortium (IWGSC) announced the first version of the reference genome sequence of the bread wheat variety, Chinese Spring (IWGSC RefSeq v1.0), with annotation of genes, non-coding RNAs, and transposable elements (https://wheat-urgi.versailles.inra.fr/Seq-Repository/Annotations).

The domestication of wheat led to the broad diversification with spring, winter, and facultative ecotypes. The spring and winter wheat varieties differ in their growth habits, vernalization requirement, and their response to various stresses. Studying genetic differences among wheat varieties distributed in different geographic regions will provide means for developing new wheat varieties with more resistant to diseases, abiotic stresses or high yield potential.

Winter wheat is cultivated in the autumn, as the low temperatures during the winter season stimulate the recessive *Vrn1* gene, returning healthy growth and head development under higher temperatures. Thus, plants become ready to be harvested in July. On the other extreme, spring wheat has the dominant *Vrn1* gene, characterized by constitutive expression without the need of low temperature or photoperiod stimuli. These plants grow faster and require approximately three months before harvesting in the summer season when planted during the spring season. Any fluctuation in climate may have detrimental effects on wheat yield and remains as one of the challenges for cultivating wheat in harsh environments with either cold or hot climatic conditions. Furthermore, understanding the differences in molecular mechanisms between spring and winter wheat varieties is useful for developing plants resistant to abiotic conditions.

Cold stress is one of the critical environmental factors that limit plant distribution in many regions of the world and sudden drops in temperature leads to productivity losses of many economically important crops. Plants are sessile organisms that cannot escape from changing habitats, so they must develop mechanisms to sustain cellular homeostasis in situ to protect themselves from the surrounding harsh environmental conditions. Species that are unable to adapt to environmental stochasticity may go extinct. Individuals that can survive under severe stress conditions may develop different mechanisms for maintaining stress tolerance. Severe cold stress or frost stress induces crystallization in two steps: first by enhancing the formation of ice particle clusters at a nanometer scale (Nucleation), then by promoting ice crystal growth under extended periods of low temperature (Crystal growth) (Rihan et al. 2017). This process damages plant cells,

while frost-tolerant individuals can slow down this process through various mechanisms, including the production of unique cryoprotective and antifreeze proteins. One example of a frost tolerant species is winter-varieties of wheat, which develop tolerance based on their geographic location.

Most cold-tolerant plants acquire resistance to cold by prior exposure to an initial low temperature where ice cannot be formed (Supercooling temperature) during their vegetative phase (Rihan et al. 2017). Similarly, plants can be acclimated to survive high-temperature conditions with short-term exposure to an initial high temperature, a process known as acquired thermotolerance. Winter wheats should be cold-acclimated for at least a period of one to two weeks, so they can survive under freezing conditions. In nature, plants have an acclimatization period during the fall season, before winter, or in the spring, before summer. Although cold acclimation improves ability of winter wheat varieties to tolerate freezing stress, sub-zero temperatures always cause injury even for most winter cultivars. This injury is more pronounced in older leaves than younger leaves, where the former die at – 4 °C, the latter can survive up to – 20 °C. The difference in temperature at injury may be due to younger leaves' higher extracellular ice nucleation activity and better ability to lower relative water content allowing cells to drop their equilibrium freezing points (Burke et al. 1976; Griffith 2005). Extracellular ice nucleation activity drives water movement from the cytoplasm to apoplast thus lowering the freezing point (enhancing supercooling ability) of these tissues. Livingston et al., (2018) used high-definition infrared thermography technology to trace the freezing events in winter wheat (CV Shirley) at – 4.6 °C. They found that the first stage of freezing occurs rapidly for six seconds where the freezing occurs in xylem vessels of the vascular bundles and ends by reaching the tip of the plant leaves. After 14 seconds, the second stage starts when the cells come to equilibrium freezing, where the freezing next includes mesophyll tissues and ends by reaching the tip of the plant leaf for the second time in a slower but a more uniform manner. It takes around 10 minutes for wheat leaf cells to reach the equilibrium after this stage. When thawed at higher temperature, wheats can recover after the second stage of freezing, but more subsequent freezing will be lethal. Understanding these mechanisms is necessary for improving cold tolerance traits of winter grasses.

2.2 Cold Signal Perception

2.2.1 Accumulation of Various Osmolytes

Cold-tolerant plants perceive low temperature by producing many different classes of osmolytes that act as osmoprotectants, which moderate the severe impact of dehydration. The

gradual accumulation of soluble sugars is reported in many trees, either during autumn or winter seasons (Oleksyn et al. 2000; Wong et al. 2003; Eris et al. 2007), or during periods of cold-acclimation or cold stress (Sasaki et al. 1996; Wanner and Junttila 1999; Saghfi and Eivazi 2014). The accumulation of soluble sugars in plants as an aspect of physiological protection is not only correlated with cold stress, but also with heat stress, drought, and salinity (Rosa et al. 2009). At all events, these stresses decrease water activity in the cytosol. Therefore, soluble sugar accumulation protects the cells from severe dehydration, in addition to acting as nutrient reserves and protectants to the cellular membranes (Yuanyuan et al. 2010).

Furthermore, soluble sugars tend to lower the freezing point of the cytoplasm and accordingly increase frost resistance (Sauter et al. 1996; Ouellet 2007). The accumulation of soluble sugars is associated with starch hydrolysis in sugar maple (Wong et al. 2003), reducing photosynthetic activity and stimulating senescence (Wong et al. 2003; Rosa et al. 2009; Yuanyuan et al. 2010). However, the reduction of photosynthetic activity may lead to soluble sugar accumulation and not be directly correlated with it (Nebauer et al. 2011). Others suggest that sugars may play a role as a signalling molecule that cross-communicates with phytohormones, other nutrients, and regulates the expression of sugar-regulated genes, enabling them to tailor photosynthetic efficiency under stress conditions (Biswal et al. 2011). Perception of cold does not only support soluble sugar accumulation, but also reallocates solutes, such as sucrose and fructose from the symplast to the apoplast, forming a barrier between the plasma membrane and ice crystals, thus hindering the growth rate of ice formation (Gusta et al. 2005). In addition to the accumulation of soluble sugars, other chemical compounds like organic acids, amino acids, polyamines, and lipids have been noticed to accumulate due to cold stress and during cold acclimation periods, as reviewed by Ouellet (2007), Yadav (2010), and Thakur and Nayyar (2013). These low-temperature stress-responsive metabolites act as osmolytes to protect the cell and reduce damage.

2.2.2 Encoding stress signal perception by calcium

Variability of the accumulated osmolytes depends mainly on the nature of stress conditions while this accumulation happens in a slow, gradual, and constant manner, to maintain protection and proper metabolism. However, as a fast ephemeral response to cold signals, living cells uptake more Ca^{2+} ions in a phenomenon known as stress-specific "calcium signature." The signature varies from one stress to another but cytosolic $[Ca^{2+}]_{cyt}$ may increase by 10 to 20 times in a moment

during each spike (Bose et al. 2011). In the case of ABA treatment, the signature has many spikes of Ca^{2+}, while there is only one spike signature for anoxia.

The intensity of the spike differs under the same treatment by different manners, as in the unique biphasic spike signature of cold treatment. The first spike represents the uptake of calcium ions from the external medium while the second represents their release from the vacuole, this second spike shows an enhanced peak in cold-acclimated Arabidopsis relative to non-acclimated plants (Knight and Knight 2000). Subsequently, after each spike, living cells use their cytosolic buffering system to restore the basal level of $[Ca^{2+}]_{cyt}$ rapidly after each spike (Plieth et al. 1999; Schwaller 2009). Once $[Ca^{2+}]_{cyt}$ is in its peak concentration inside the cell, K^+ channels will open to drive potassium ions outside the cell until its equilibrium potential (E_K) in the repolarization phase (Hermann et al. 2012). Signal stress triggers the plant cells action potential above its threshold guided depolarization, enabling many calcium-binding proteins to catch the high calcium ions, as most of these proteins have 'EF' hand motif(s). 'EF' hand motif is a conserved helix-loop-helix (HLH) structure that mainly consists of two alpha helices connected by a short loop region, where the Ca^{2+} ion can bind (Day et al. 2002). Most known examples of 'EF' hand motif-containing proteins are calcium-dependent protein kinases (CPK), calmodulin-dependent protein kinases (CaM), calmodulin-like proteins (CML), calcineurin B-like proteins (CBL), and calreticulin (CRT) (Ranty et al. 2006; Xiang et al. 2015; Mohanta et al. 2017). A cytosolic buffering system constitutes plenty of calcium-binding proteins, where many of them act as signal transducers to transfer the stress signal in a specific downstream response cascade. Using chemical inhibitors of calcium channels not only lowers $[Ca^{2+}]_{cyt}$ concentration, but also negatively affects the expression of *KIN1* (a cold-responsive gene marker and one of the CBF gene family members) which points out that calcium signalling is upstream of the CBF-gene regulon, and an essential signal for a proper perception of stress (Knight et al. 1996). However, there is still the question of whether the calcium channels themselves are the primary receptors for the stress signal or if signalling occurs upstream.

2.2.2.1 Calcium influx systems

Ca^{2+}-permeable channels manage the temporarily elevated increase of cytosolic calcium from extracellular surroundings and intracellular compartments. These channels encompass a voltage potential-based manner into three main categories: depolarization-activated calcium channels (DACCs), hyperpolarization-activated calcium channels (HACCs), and voltage-independent calcium channels (VICCs). The diversity of Ca^{2+}-permeable channels in plants is less

than that of animals and include only five protein families. These families are cyclic nucleotide-gated channels (CNGCs), glutamate-receptors like channels (GLRs), two-pore channels (TPCs), mechanosensitive channels (MCAs), and hyperosmolality-gated calcium-permeable channels (OSCAs) (Edel et al. 2017). The activation of Ca^{2+}-influx channels drive calcium into plant cell cytosol (Bose et al. 2011). Some of these channels have been detected to be localized only in the plasma membrane, such as MCAs, CNGCs, and GLRs. Therefore, the function of these channels is mainly to drive Ca^{2+} from extracellular space into the cell. CNGCs and GLRs channels are permeable to either monovalent and divalent ions while MCAs and TPCs channels have an EF-hand domain that is highly specific to Ca^{2+} ions (Chen et al. 2015; Guo et al. 2015). The interactions with other molecules direct the activity of Ca^{2+}-permeable channels. For example, CNGCs and GLRs have a defined negative feedback regulation mechanism when bound to CaM binding domain that overlaps with either cAMP or cGMP, while GLRs are positively regulated through binding with glutamate, glycine, alanine, serine, aspartic acid, cysteine or glutathione (Chen et al. 2015). DeFalco et al. (2016) introduced a distinct mechanism of the interaction between CNGC12 and CaM where apoCaM constitutively associates with C-terminal isoleucine-glutamine (IQ) motif of AtCNGC12 and AtCNGC12 inhibition by the interaction of their N-terminal (NT) motifs with CaM-binding domain (CaMBD) to form a bridge that physically impedes $[Ca^{2+}]_{ext.}$ influx. Releasing calcium from vacuole to cytosol is controlled by TPC channels which have an exclusive two-pore domain. TPCs are only localized and expressed in the vacuole membrane (Guo et al. 2015), where their embedment in the membrane is through numerous transmembrane domains. Their intervening cytosolic EF-hand domain adopts their ability to recognize calcium ions.

Furthermore, they have a non-selective nature relative to other monovalent ions. OSCA channels act mainly as osmosensors, and loss-of-function mutants have a calcium spike of reduced intensity under osmotic stress when compared with wild-type plants (Yuan et al. 2014). The relative low diversity of Ca^{2+}-influx systems in plants, compared to counterparts in animals and algae, may be because many of the components in plants are not discovered yet (Edel et al. 2017).

2.2.2.2 Calcium efflux systems

The primary purpose of the calcium efflux system is to alleviate the amplitude of cellular Ca^{2+} concentrations that have arisen during stress signal perception. Although calcium is a beneficial element that is essential for maintaining plasma membrane integrity, cell wall structure,

and many other metabolic processes in the plant cell, usually its extracellular concentration is below its cellular concentration, under untreated conditions. If $[Ca^{2+}]_{cyt}$ concentration increased suddenly as in the case of the depolarization phase, but without recovery to its optimal concertation, this ultimately leads to cytotoxic effects as calcium may cause precipitation of proteins and nucleic acids. Numerous metabolic disorders and other adverse effects will also occur if the cellular Ca^{2+} concentration is being held below its optimal concentration, as is seen at the end of the repolarization phase. That is why hyperpolarization is an essential physiological response that maintains the appropriate integrity of the living cells. Bose et al. (2011) reviewed the optimal concentration of Ca^{2+} cations in plant cell to be 1-10 mM in the apoplast, 0.2-10 mM in the vacuole, 0.002-0.006 mM in the chloroplast stroma, and ~1mM in the endoplasmic reticulum, while its lowest concentration has been reported in the cytosol as only 0.0001-0.0002 mM, indicating that all cell compartments have higher Ca^{2+} than the cytosol by at least 20 times. Stress signals bring Ca^{2+} into the cytosol either from extracellular surroundings or intracellular compartments during depolarization. Consequently, cytosolic calcium increases in a concentration higher than 0.001 mM to initiate the first cytosolic Ca^{2+} transient or oscillation. Afterwards, the role of the calcium efflux system is essential to alleviate its concentration elevation. Calcium efflux system components constitute several classes (Tuteja and Mahajan 2007; Bose et al. 2011; Edel et al. 2017) including P-type ATPases, mitochondria calcium uniporter complexes, cation/Ca2+ exchangers.

These are ion channels that are mostly universal in all living organisms. According to Palmgren and Nissen (2011), their structure consists of five domains, three of which are cytoplasmic, and two are membranous. Cytoplasmic domains consist mainly of an actuator domain, nucleotide binding domain, and phosphorylation domain. The two membranous domains are a transport domain and a class-specific support domain.

P-type ATPases can be divided into five classes, from PI to PV, according to the transported substance. PIA and PIB are responsible for pumping potassium and heavy metals, while PIIC is either Na^+/K^+ or H^+/K^+, P2D is a Na^+ pump, PIIIA is an H^+ pump, and PIV is a putative lipid flippase that mainly transports phospholipids. PV has no assigned specificity. HMA1 channels, classified under PIB group, have been reported as a uniporter channel that localizes in the inner membrane of the chloroplast of many plants, including barley, and shows sensitivity to many heavy elements, including calcium (Mikkelsen et al. 2012; Hanikenne and Baurain 2014). On the other hand, PII (type A and B) are fundamentally responsible for calcium transport.

P-type ATPase II:

A- **PIIA-ATPases** (known as Ca^{2+}/H^{+}-ATPase or ER-Type Ca^{2+}-ATPases "ECAs")

B- **PIIB-ATPases** (known as Ca^{2+}-ATPase or Autoinhibited Ca^{2+}-ATPases "ACAs")

Although both of PIIA and PIIB promote ATP hydrolysis after binding with Ca^{2+} ions, type IIA needs two Ca^{2+} ions to start ATP hydrolysis, while only one Ca^{2+} ion is needed for type IIB to initiate ATP hydrolysis. This makes type IIB more putative with response to Ca^{2+} ion concentration. Another advantage of type IIB channels is their N-terminal autoregulation ability, being positively regulated by binding with CaM protein and negatively regulated by Ca^{2+}-dependent protein kinase (CDPK). A phosphorylation reaction of its serine-residue phosphorylation site initiates the binding activity. On the other hand, PIIA type has a broad nucleotide specificity (Tuteja and Mahajan 2007; Palmgren and Nissen 2011).

2.2.2.2.1 Mitochondria Calcium Uniporter Complex (MCUC)

MCUC channels are Ca^{2+} uniporter channels that localize in the inner mitochondrial membrane to drive calcium ions inside the mitochondrial matrix via its EF-hand binding domain (Teardo et al. 2016; Edel et al. 2017).

2.2.2.2.2 Cation/Ca2+ Exchangers (CCX)

The Cation/Ca^{2+} exchangers can transport cytosolic Ca^{2+} against its downhill concentration by using the downhill gradient of other cation species such as Na^{+1}, K^{+1}, and H^{+1}. Consequently, according to the type of the cation species, they can be named H^{+1}/Ca^{+2} exchangers or Na^{+1}/Ca^{+2} exchangers (Cai and Lytton 2004). H^{+1}/Ca^{+2} exchangers (CAX) were first discovered in plant systems, localized in the plasma membrane and tonoplast. Wang et al. (2012) has reported the localization of Na^{+1}/Ca^{+2} exchangers (NAX) in the plasma membrane of Arabidopsis. Post-translational events control CCX channel activity by interacting with small molecules, other proteins, phosphorylation, or pH homeostasis (Bose et al. 2011). In brief, CCX channels are essential to modulate cytosolic Ca^{2+} elevation in response to abiotic stress like CAX channels that bring calcium into the vacuole against its gradient and restore protons inside the cytosol.

It has been reported that the calcium influx is coupled with the early phase of membrane depolarization that occurs in response to cold signals (Penfield 2008; Teardo et al. 2016), although it is still unknown which is upstream of which. As depolarization occurs with the increase of $[Ca^{2+}]_{cyt}$, Plieth et al. (1998) used manganese quench techniques to show that cytosolic Ca^{2+} increase is from the cell compartments, not from outside. In such a case, pushing calcium ions from cell compartments can be triggered by a variety of secondary messenger molecules, where

the elevated level of inositol triphosphate guide the efflux of Ca^{2+} from endoplasmic reticulum (Wacke et al. 2003), which is, in turn, a hydrolytic product of the cell membrane phosphatidylinositol 4,5-biphosphate (Plieth 2005; Berridge 2016). Knight and Knight (2012) have described membranes as cellular thermometers during cold signal perception. In their review, they highlighted many types of research that have used chemical agents which either increase or decrease membrane fluidity, finding that they have a direct effect on cold sensing. They also acknowledge many mutant studies that affect membrane fatty acids, directly reducing cold sensing.

2.2.2.3 Membranes as temperature sensors

Membranes respond to stress by modifying their chemistry, but this modification depends mainly on the nature of the stress. For example, in contrast to increasing the content of saturated and monounsaturated fatty acids as a response towards high temperature, plants react to cold by having membranes with a higher amount of polyunsaturated fatty acids and lower amount of saturated fatty acids. Therefore, the freezing points of the membranes of cold-tolerant plants may reach below – 20 °C when compared to membranes of cold-sensitive plants that may solidify at only 10°C (Yadav 2010). The presence of a high amount of unsaturated fatty acids in cold-resistant plants is correlated with a cold acclimation phase, during which the expression of glycerol-3-phosphate acyltransferase is induced (S. Sanghera et al. 2011). That is why genetically engineered *Saccharomyces cerevisiae* with desaturase genes from sunflower have an enhanced tolerance towards cold and salinity conditions, due to the increase in unsaturated lipids of cell membranes (Rodríguez-Vargas et al. 2007). Additionally, transgenic tobacco seedlings expressing a plastid-specific omega-3-fatty acid desaturase gene (FAD7), exhibit greater tolerance under low-temperature conditions due to an increase in the amount of trienoic fatty acids (Kodama et al. 1995; Khodakovskaya et al. 2006). Thus, some members of desaturase genes have roles in conferring cold tolerance traits to plants. Instead of increasing the amount of fatty acid desaturase gene transcripts, cold tolerant plants use low temperature to increase the stability of their gene-of-interest transcripts, and thus can use protein turnover mechanisms to increase the amount of fatty acid desaturase proteins, as is seen in the endoplasmic reticulum targeting protein (FAD3) in the root tips of wheats (Horiguchi et al. 2000). Accumulation of polyunsaturated fatty acids increases cell membrane rigidification which may negatively affect the proper function of many integral proteins (Upchurch 2008). Cold acclimated plants show more active plasma membrane H^+-ATPase to avoid the decrease of ion exchange and water availability, imminent from membrane solidification. This mechanism facilitates the movement of ions either across cell membranes or

through active transport processes, triggering cytoplasmic alkalinization by transporting protons out of the cytoplasm (Kasamo 2003; Martz et al. 2006). A significant observation from the activation of H^+-ATPases is that they rely directly on the unsaturation degree of biological membranes, and H^+-ATPase activation is crucial for many physiological events during stress conditions, such as plasma membrane hyperpolarization, proton efflux from the cytoplasm, apoplast acidification, ions and water uptake, stomatal opening, solute transport, and cell growth (Kasamo 2003; Martz et al. 2006). Accordingly, membrane fluidity is upstream of proton-ATPase pumps during the signalling mechanism (Martz et al. 2006). As a result, plants that can perceive the cold acclimation signal properly are those that can accumulate and redistribute polyunsaturated fatty acids in a mode that orchestrates the activity of ionic-pumping channels in the plasma membrane. During cold signal perception, plants do not add or remove any novel molecules to their biological membranes. Instead, they change the relative proportions of the present molecules with their ability to increase the unsaturated phosphatidylcholine and phosphatidylethanolamine. This leads to a total increase in phospholipids, in line with the obvious decrease in cerebrosides (Uemura et al. 2006). In addition to the change in the membrane lipid composition, membrane protein profiles change to adapt plants during cold acclimation. Likewise, cold signals trigger the enhancement of phosphatidic acid (PA) biosynthesis (Yadav 2010) from either acylation of lysophosphatidic acid by lysophosphatidic acid-acyltransferase, hydrolysis of structural phospholipids by phospholipase D, or phosphorylation of diacylglycerol (DAG) by diacylglycerol kinase (DGK) (Yadav 2010; Arisz et al. 2013). Phosphatidic acid is thought to be involved in recruiting enzymes and dehydrins to their respective functional sites (Yadav 2010; Testerink and Munnik 2011). Zhang et al. (2004) showed that PA binds to ABSCISIC ACID-INSENSITIVE 1 (ABI1), a protein phosphatase with a calcium-binding EF-hand motif, thus preventing its negative effect on ABA production (Figure 2.1). Accumulated membrane proteins work principally in a cryoprotective manner to protect membranes from dehydration and to enhance their freezing tolerance. Examples of these proteins are membrane-anchored lipocalins (Frenette Charron et al. 2002; Charron et al. 2005), early responsive dehydration protein 14 (ERD14) (Uemura et al. 2006), annexins such as Ca^{2+}-regulated membrane-binding proteins and COR410 – a peripheral membrane protein that accumulates near the membrane during cold acclimation in wheat (Danyluk et al. 1998). Annexin accumulation may act to protect membranes during cold acclimation conditions (Breton et al. 2000; Rescher and Gerke 2004). Membranes respond to various abiotic stress signals by changing three main things: first, by altering membrane electrical potential

through either activation or deactivation of specific ionic pumps that are distributed through the membrane. Second, by shifting their membrane fluidity in response to the nature of stress, and third by de-accumulating and accumulating various types of membrane proteins. Regardless of which event happens first, these modifications enable the biological membranes to tune up electrochemical gradients between intracellular and extracellular spaces. Consequently, this suggests that living cells perceiving abiotic signals have other upstream temperature sensors that may able to send proper signals to start cell acclimatization/modification of their membranes.

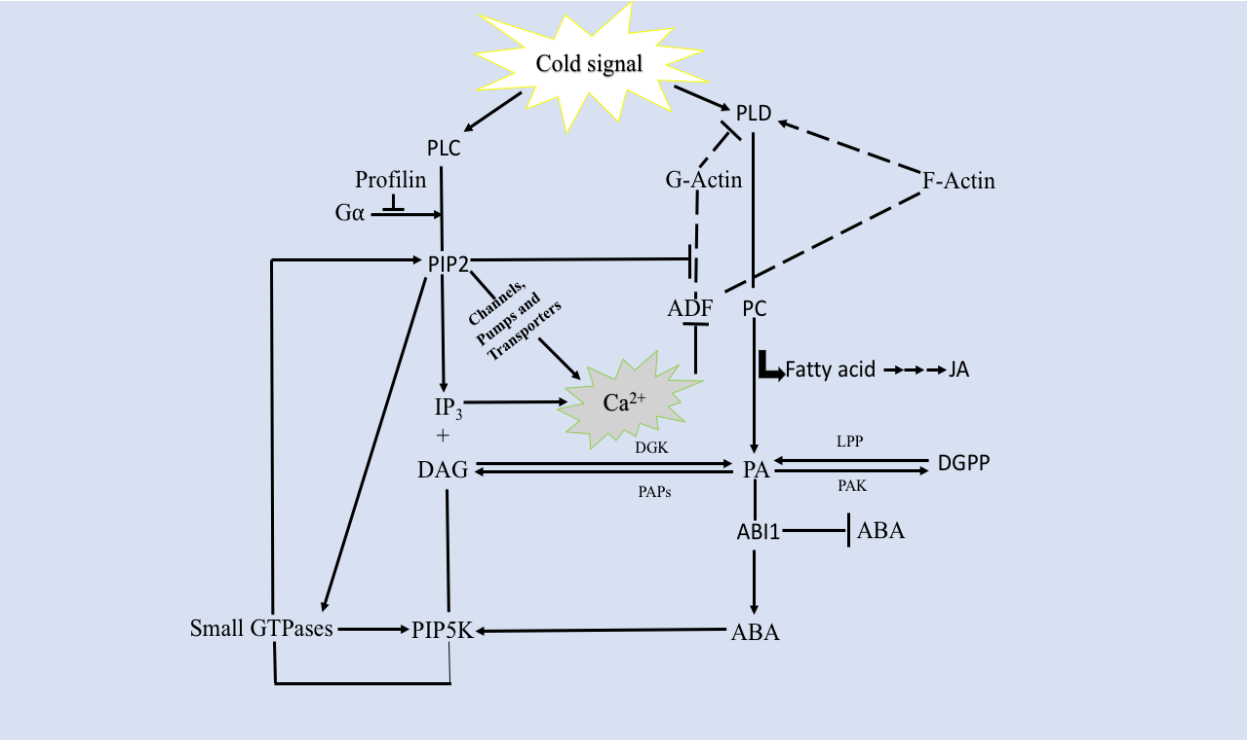

Figure 2.1: Scheme to illustrate the most common early events of cold signal perception in plants. Cold signal perception leads to increasing the calcium ions uptake and some plant hormones such as ABA and JA.

2.2.2.4 Cytoskeleton as a functional stress signal receptor

The cytoskeleton responds to cold signals by depolymerizing its microfilaments and microtubules. It is unlikely that this depolymerization event is responsible for the fast increase in $[Ca^{2+}]_{cyt}$ as cytoskeleton rearrangements require more extended periods of time (Knight and Knight 2012). However, Thion et al. (1996) proposes that cytoskeleton disruption somehow positively regulates the activity of voltage-dependent calcium channels. Many other researchers support this claim, (Örvar et al. 2000; Sangwan et al. 2001) where they suggest that cytoskeleton rearrangement

may be directed by cold-stimulated membrane rigidification. Cytoskeleton structure is mainly from microtubules (MT) and actin filaments (AF), through which the cytoskeleton can interact with many diverse cellular elements. Both cytoskeleton cortical actin and microtubules are linked to the plasma membrane and cell wall (Akashi et al. 1998; Collings et al. 1998). Cytoskeleton tubulin dimers have interaction sites for calcium and magnesium ions (Solomon 1977). Besides this, actin-binding proteins (ABPs) and microtubule-associated proteins (MAPs) regulate cytoskeleton rearrangements through their interaction with many diverse interacting-molecules like kinases and phosphatases (Wasteneys and Yang 2004). For example, phospholipase D (PLD) acts as a signalling molecule and as a structural protein that binds to actin, microtubules, and the plasma membrane (Gardiner et al. 2003; Drøbak et al. 2004) where cytoskeleton components regulate PLD activity as monomeric actin inhibits its activity and F-actin enhances it (Figure 2.1). Abiotic stress induces heterotrimeric G-proteins which regulates cytoskeleton organization, ion channels and phospholipases activity (Millner 2001; Dave et al. 2009). Plant G-proteins and phospholipases constitute large proteins families with diverse functions. Figure 2.1 shows Phosphatidylinositol 4,5-bisphosphate (PIP_2) as an important signalling molecule that activates actin regulatory proteins, ion channels and phospholipases C and D and its synthesis is regulated by Small GTPases and Phosphatidic acid (PA) through phosphoinositide 5-kinase (PIP5K) isoforms (Oude Weernink et al. 2007). Profilin competes with PLC for its interaction with PIP2, thus hindering PIP2 hydrolysis by phospholipases C as specified in Figure 2.1 (Goldschmidt-Clermont et al. 1990). Previous work indicated that G-protein activates Phospholipase C (PLC) to hydrolyze PIP2 which produces essential signalling proteins like inositol 1,4,5-triphosphate (IP_3) and Diacylglycerol (DAG) where the former stimulates the efflux of Ca^{2+} ions from cellular compartments, and the latter is phosphorylated by DAG kinase (DGK) to Phosphatidic acid (PA) (Khatri et al. 2012; Li et al. 2012).

Additionally, PA correlates positively with increasing F-actin density and polymerization (Figure 2.1). Therefore, cytoskeleton binding proteins are valuable in regulating essential signalling pathways in plants and organizing the cytoskeleton itself. F-actin enhances the activity of phospholipase D β (PLDβ), but G-actin inhibits it (Wasteneys and Yang 2004; Li et al. 2012).Actin-depolymerizing factors (ADF), also known as cofilins, are essential actin remodelling proteins, whose activity that is controlled by Ca^{2+}-gradients and pH, but can be hindered by phosphorylation done through a Ca^{2+}-dependent protein kinase on their conserved serine residue, Ser6 in a temperature-dependent manner (Viswanathan and Zhu 2002; Drøbak et al. 2004). PIP2

molecules tend to bind cofilins and thus stop their interaction with G-actin (Yonezawa et al. 1990). It has been stated that wheat *TaADF* gene is highly induced after two days of cold acclimation and has a higher induction in winter cultivars rather than spring (Ouellet et al. 2001; Viswanathan and Zhu 2002). Its expression does not reach this level of induction in response to ABA, drought, heat, or salinity treatments which indicates that a specific cytoskeleton reorganization is necessary for cold acclimation in wheat. These results are consistent with Abdrakhamanova et al. (2003) who showed that freezing-tolerant wheat cultivars develop transient and partial disassembly of microtubules during the early stage of cold acclimation. This contrasts with sensitive cultivars where applying an artificially-enhanced microtubule disassembly chemical named pronamide leads to enhanced freezing tolerance in sensitive cultivars. Moreover, (Örvar et al. 2000) found that jasplakinolide, an actin microfilament stabilizer, inhibits calcium influx and a cold acclimation-specific gene's (cas30) activity at 4°C, while cytochalasin, an actin microfilament destabilizer, induces calcium influx and cas30 gene activity at 25°C. These findings indicate that cytoskeleton dynamics have a significant role in configuring plants to cold stress conditions.

2.3 Cold Signal Transduction in Plants

Since plant cells perceive cold signals or any other abiotic signal, they must transduce this signal via messengers to administrate stress gene expression regulation. Plant susceptibility to cold stress may be attributed to the incompetence of the plant receptors to perceive the cold signal adequately or due to an error in the signal transduction cascades of some essential cold-regulated genes. As signal transduction is the bridge between plant-sensors and gene expression, other stresses may induce the same regulon if perceived by the same or related sensors as cold, drought, and ABA sensors.

One of the most critical cold regulatory pathways is the C-repeat binding factor /dehydration responsive element binding protein, abbreviated to CBF/DREB pathway (Chinnusamy et al. 2003; Chinnusamy et al. 2007). Yamaguchi-Shinozaki and Shinozaki (2005) found that the expression of CBF/DREB genes in Arabidopsis is ABA-independent, as the expression of genes is triggered by cold stress in *abi* and *aba* mutants. The CBF or DREB proteins are members of the AP2 family of transcription factors that bind to DRE/CRT or LTRE cis-elements' promoters of stress-regulated genes since they identify the motives of COR genes' promoters that have the sequence (A/GCCGAC). Once they bind to the promoter, they activate COR gene expression (Gilmour et al. 2000; Akhtar et al. 2012). It has been demonstrated that

abiotic stress factors such as low temperature regulate CBF/DREB expression via a nuclear constitutive protein ICE1 (Chinnusamy et al. 2003). Polyubiquitination of ICE1 is induced in normal conditions by the HOS1, a (Really Interesting New Gene) RING -type ubiquitin E3 ligase that is found upstream of CBF. As the temperature goes down, a SUMO E3 ligase SIZ1-mediated sumoylation prevents the polyubiquitination action enhanced by HOS1 and thus increases the ICE1 stability (Ishitani et al. 1998; Dong et al. 2006). Miura et al. (2009) showed that SIZ1 inactivates ABI5 by sumoylation where phosphorylation by SnRKs activates desumoylated ABI5 (Figure 2.2). The phosphorylated ABI5 can induce the transcription of ABA-responsive genes. Thus SIZ1 is not only a positive regulator in CBF-dependent pathway but also a negative regulator in ABA signalling pathway. Chinnusamy et al. (2003) used *ice1* mutants in Arabidopsis and showed that ICE1, an upstream transcription factor of CBF genes, enhances CBF3 expression by binding with its promoter as it recognizes its motif that has an MYC-recognition sequence (CANNTG). Many overlapped posttranslational events control ICE1; its phosphorylation by one of the protein kinases named Open Stomata 1 (OST1) enhances its activity to induce CBF regulon, however, other MPK-mediated ICE1 phosphorylation has been reported to lead to its degradation by E3 ligase (Li, Ding, et al. 2017). Consequently, the occurrence of these phosphorylation events on different sites of ICE1 protein is essential for determining its cellular role.

Additionally, Ding et al. (2018) demonstrated that cold inducing OST1 phosphorylation drives the phosphorylation of basic transcription factor 3 (BTF3) and BTF3-like proteins which in turn enhance CBF protein stability through protein-protein interaction besides acting as transcription factors to upregulate CBF gene expression (Figure 2.2). Under normal conditions, MYB15 represses CBF transcription by binding to its promoter MYB-elements whereas during cold acclimation ICE1 may lead to decreasing MYB15 repression upon CBF regulon either by physical interaction with it (Agarwal et al. 2006).

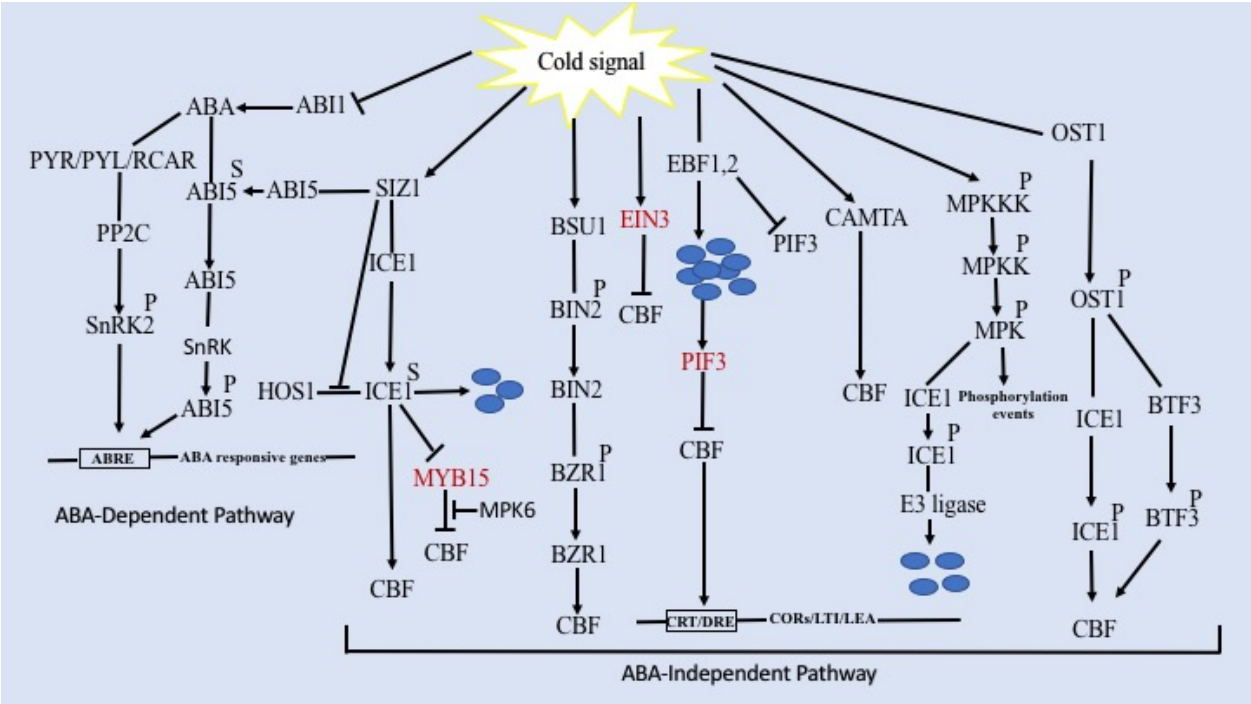

Figure 2.2: Examples of significant signalling transduction pathways related to inducing the transcriptional regulatory network of ABA-independent and ABA-dependent pathways as triggered by cold signal perception. These examples show how either ABA-dependent, ABA-independent and MPK cascade can be interconnected together to orchestrate different signalling defence mechanisms in plants. Superscripted letters on symbols are used to highlight the post-translational events where "P" refers to phosphorylation and "S" refers to sumoylation.

Further studies show that repressing MYB gene transcription may occur either by sumoylated form of ICE1 (Miura et al. 2007) or by its phosphorylation by cold-induced MPK6. The MYB phosphorylated form has less binding affinity with DNA and a mutation of its phosphorylation site on Ser168 enhances its repression effect on CBF (Kim et al. 2017; Li, Ding, et al. 2017). Doherty et al. (2009) reported calmodulin-binding transcription factor (CAMTA) as a positive CBF regulator that binds to CBF promoter to induce CBF gene transcription. CAMATA proteins have a definite affinity to a calcium-binding protein calmodulin through their IQ C-terminal domains thus they may transduce calcium signals into regulation of gene expression (Leng et al. 2015). H. Li, Ye, et al. (2017) identify the dephosphorylated form of Brassinazole-

Resistant 1 (BZR1) as a positive regulator of many stress-responsive genes like CBF, WKRY6, PYL6, SOC1, JMT, SAG21 and ESM1 (Figure 2.2). Cold or Brassinosteroid treatment induces BSU1 to dephosphorylate BIN2 and thus enhancing BIN2 degradation by 26 proteasomes. Since BIN2 is the protein that phosphorylates BZR1, its degradation will enhance the accumulation of BZR1 dephosphorylated form. Therefore, BSU1 is a CBF positive regulator upstream of BZR1 and BIN2 is a CBF negative regulator downstream of BSU1.

A different mechanism for CBF gene transcription regulation has been introduced by Shi et al. (2012), where cold induces the protein accumulation of Ethylene-Insensitive 3 (EIN3), a CBF negative regulator transcription factor (Figure 2.2). Moreover, cold treatment was found to indirectly induce the stability of Phytochrome-Interacting Factor 3 (PIF3), a CBF transcriptional repressor, by enhancing the degradation of EIN3-Binding F-Box 1(EBF1) and EBF2 which target PIF3 for 26S proteasome-mediated degradation (Jiang et al. 2017). Other CBF repressor proteins work only under certain circumstances like PHYB, PIF4, and PIF7 that repress CBF only under extended day conditions (Lee and Thomashow 2012).

Further studies using transgenic plants found that the expression of CBF1/DREB1b and CBF3/DREB1a enhanced freezing, drought, and salt tolerance (Chinnusamy et al. 2006). Predominantly CBF2/DREB1c negatively controls CBF2 expression as revealed by a *cbf2* null mutant (Novillo et al. 2004). Fursova et al. (2009) identified another transcription factor ICE2, a structural relation to the ICE1, that is involved in freezing tolerance up to – 20°C by endorsing CBF1 gene expression. The performance of other transcription factors such as HOS9, a putative homeodomain protein, and HOS10, an R2R3-type MYB transcription factor, were identified in Arabidopsis to positively regulate frost-tolerance independently from the CBF pathway (Zhu et al. 2004; Zhu et al. 2005). Moreover, the same authors found that mutant plants of hos9 and hos10 showed less freezing tolerance but with the routine induction of CBFs and regular expression of COR genes. Thus, many cold-regulated genes are separate from the CBF pathway.

Cold stress-regulated genes that require the ABA-dependent pathway have been previously reviewed (Gusta et al. 2005) and found that they contain either DRE/CRT or ABRE cis-acting elements in their promoter. Therefore, most of the cold-regulated genes are related to other abiotic stresses like drought and salinity. Yadav, (2010) found that the ABA-responsive element (PyACGTGGC) differs from the CBF/DREB responsive element, which is (A/GCCGAC). However, exogenous application of ABA during the period of cold acclimation enhanced the freezing tolerance of many different plants (Robertson et al. 1994; Bravo et al. 1998). Spraying

ABA on cold-sensitive rice seedling improved freezing and heat tolerance without prior exposure to cold (Shinkawa et al. 2013). Within reason, ABA can increase the induction of DRE/CRT-containing genes as has been reviewed by Yamaguchi-Shinozaki and Shinozaki, (2005). Since DRE/CRT promoter elements may act as coupling elements for the functional activation of genes-containing ABRE elements, this confirms the communication between ABA-dependent and ABA-independent pathways. Additionally, ABA, drought, and salinity induce the transcription factors bZIP and ABA-responsive element binding protein (AREBs) which binds with ACGT-containing ABA response elements (ABRE) to induce the expression of ABRE-containing genes like RD29A, RD29B, and RD22 (Uno et al. 2000). Mutants hos9-1 show upregulation of RD29A gene expression and HOS10 positively regulates 9-CIS-EPOXYCAROTENOID DIOXYGENASE3 (NCED3), a gene encodes a key enzyme in abscisic acid biosynthesis, where MeJA induces its expression (Hossain et al. 2011). Therefore, HOS9 and HOS10 transcription factors are thought to regulate cold tolerance in Arabidopsis through the ABA-mediated pathway (Zhu et al. 2004; Zhu et al. 2005).

Another significant signalling pathway is the MAPK signal transduction pathway that is not only associated with cold stress, but also to other biotic and abiotic stresses. This signal cascade transfers the signal from the cell surface to many cytosolic proteins and to the nucleus where it can initiate the transcription of many transcription factors. In Alfalfa plants, a MAPK signal was induced in response to cold, drought, and mechanical stress but not by ABA, heat, or salt treatments (Jonak et al. 1996). Other Arabidopsis MAPK genes like MAPK3 shows more accumulation of its transcript by drought, cold, salinity, and H_2O_2 , while Arabidopsis MPK7 activation is regulated through the ABA-dependent pathway (Mizoguchi et al. 1996; Danquah et al. 2015). Sinha et al. (2011) found that the MAPK pathway comprises three core components which are MAP kinase (MAPK), MAPK kinase (MAPKK, MAP2K or MEK) and MAPK kinase kinase (MAPKKK, MAP3K or MEKK). These form the cascade which is stimulated and related to each other by phosphorylation events where MAPKKK is upstream and phosphorylates MAPKK upon its activation. Teige et al. (2004) showed that MKK2 is upstream of and targets MPK4 and MPK6 enhanced cold and salt tolerance in Arabidopsis, as revealed by mkk2 null mutant plants that were sensitive to cold and salt stresses. Furthermore, MKK2 overexpression increases MPK4 and MPK6 transcripts which can also be activated by downstream MEKK1-mediated phosphorylation that controls the activation of MKK1, MKK2 and MPK4 which can result in the cold- and salt-tolerant plants. Cold stress tolerance in plants was also shown to be controlled by MPK4 and MPK6, as

they are substrates for MKK2 in Arabidopsis (Sinha et al. 2011). Cold stress has been found to upregulate many kinases in a variety of plants, inducing cold-regulated genes such as SAMK, cbMAKP3, GhMAPK, ZmMPK3, ZmMAPK5, ZmMPK5, OsMAPK5, SbMAPKK, NtNPK1, OsMEK1, MsSAMK, and OsWJUMK1 (Sinha et al. 2011; Šamajová et al. 2013). Danquah et al. (2014) reviewed the link between the ABA signalling pathway and different kinases, where ABA drives the activation of SnRKs and many members of MAPK family. Thus, ABA-dependent or independent mechanisms can initiate MAPK cascade activation.

2.4 Roles of plant hormones

Plant hormones or plant growth regulators are chemical compounds that can act locally or can move inside the plant body and cause a cellular response through specific signal transduction pathways, depending on the kind of plant hormone and its concentration. Through their diverse structure and classes, they not only orchestrate the development of all plant growth phases but also play important roles when exposing the plant to either biotic or abiotic stress. Once the plant perceives the cold signal, either through its plasma membrane or an unknown receptor, the transduction of the signal changes the expression of many genes. These changes affect plant hormones to standardize different biological processes like growth and development through playing diverse and complicated roles in coordinating different signal transduction pathways and gene expression during stress conditions. Phytohormones constitute many classes, the most famous of which are auxins, gibberellins (GA), abscisic acid (ABA), ethylene, jasmonic acid (JA), salicylic acid (SA), cytokinins (CKs), and brassinosteroids (BRs). Other studies consider polyamines as a class of phytohormones (Upreti and Sharma 2016). These hormones have different receptors and potentiate different entangled metabolic pathways during biotic and abiotic stress conditions. The two most intriguing questions in the aim to understand their mode of action during stress conditions are how stress signal perception drives plants to change their hormonal profiles, and which proteins recognize these growth regulators to generate the corresponding downstream signalling events. This review will shed light on the roles of ABA and JA during abiotic stress tolerance as examples.

2.4.1 Abscisic acid (ABA)

Abscisic acid is known for its role in protecting plants during abiotic and biotic stress conditions, as its increase during stress-induced stomatal closure induces stress-responsive gene expression, like many late embryogenesis abundant proteins (LEA), and accumulation of many compatible solutes. Stress-responsiveness in plants includes ABA-dependent and ABA-independent pathways (Rihan et al. 2017). In the ABA-dependent pathway, many protecting genes that have ABA-responsive cis-acting elements (ABRE) in their promoters are provoked to upregulate their transcripts. Eyidogan et al. (2012) indicated that ABA ability to disable the role of 2C protein phosphatases (PP2C) on sucrose nonfermenting 1-related protein kinase 2 (SnRK2) dephosphorylation initiates this event. Thus, ABA indirectly enhances SnRK2 phosphorylation. The phosphorylated form of SnRK2 subsequently phosphorylates ABA-responsive element (ABRE)-binding factors (AREBs/ABFs) to initiate ABA-regulated gene expression. In the absence of ABA, PP2C remains free and thus acts to dephosphorylate SnRK2 kinases, keeping SnRK2 kinases in their inactive forms. The authors confirmed its homology to other protein kinases, its accumulation in response to ABA, and identified many potential sites of phosphorylation in its sequence. Based on this scenario, ABA signalling cascades will be negatively regulated by the free forms of PP2C as it can form a phosphatase–kinase complex (PP2C–SnRK2) while positively regulated by phosphorylated forms of SnRK2.

Identification of which molecules bind to ABA remains controversial and the most well-known receptors are the soluble cytosolic pyrabactin resistance 1/pyrabactin resistance 1-like/regulatory component (PYR/PYL/RCAR) proteins. ABA acts as a facilitator molecule that develops the binding of PYR/PYL/RCAR proteins with PP2C, thus halting PP2C from dephosphorylating SnRK2, keeping SnRK2 in its active phosphorylated form (Pokotylo et al. 2017).

ABA treatment causes an alteration in the expression of many enzyme-coding genes in the lipid-signalling pathways. Besides altering membrane fluidity, ABA increases the activity of phospholipase D (PLD) and other enzymes like phosphatidic acid kinase and N-ethylmaleimide-sensitive PA phosphatase thus Diacylglycerol pyrophosphate (DGPP) and Diacylglycerol (DAG) accumulate respectively from these enzymatic activities on phosphatidic acid (PA) (Zhang et al. 2009; Pokotylo et al. 2017). ABA treatment causes transient accumulation of PA as shown in barley aleurone (Villasuso et al. 2013). This scenario supports the mutant study on Arabidopsis thaliana that illustrates ABA's effect on downregulating LPP2 activity and the dependence of ABA-induced PAK activity on LPP2 disruption (Paradis et al. 2011). This effect of ABA on lipid-signalling enzymes supports the hypothesis that there may be another unknown receptor of ABA

in the membrane rather than the cytosolic (PYR/PYL/RCAR) proteins. Pokotylo et al. (2017) found that some lipids perform similar physiological responses as ABA does. For example, PA is able to induce stomatal closure even in the absence of ABA and ABA is unable to induce stomatal closure during the inhibition of PLD-mediated PA production through its activity on phosphatidylcholine (PC). Accordingly, PLD activity is necessary for ABA signal cascade since PA production relies on either PLD or phospholipase C/diacylglycerol kinase (PLC/DGK). Other than lipids, another organic molecule (IP_3) produced with DAG by the hydrolysis of phosphatidylinositol 4,5-bisphosphate (PIP2) has also been shown to induce stomatal closure. Thus, ABA treatment increases IP_3 accumulation level in stomata. It is worth mentioning that both IP_3 and DAG are involved in releasing Ca^{+2} from cellular organelles (Dong et al. 2012). Hence, ABA induces many physiological responses through its effects on phospholipid activity, many other organic molecules, and through controlling cellular Ca^{+2} distribution. Hallouin et al. (2002) showed that ABA-activation of PLD acts upstream of plasma anion channels, taking *RAB18* as a gene marker for detecting ABA stimulation effects. Guo and Wang (2012) state that this signal perception is done through membranes as calcium ions bind to the C-domain of PLDα1. This improves the binding of cytosolic PLDα1 with membrane lipids which, in turn, activates PA localized there to bind with sphingosine kinase (SPHK) forming PA-SPHK complex. This activated form of SPHK induces the generation of the phytosphingosine-1-phosphate (phyto-S1P) that activates PLDα1 in a positive feedback loop. This ABA-triggered PA activation is involved in SPHK activation which in turn activates PLDα1, as examined using *sphk1-1* and *sphk2-1* mutants of Arabidopsis (Liang Guo et al. 2012).

Most research was focused on PLD as ABA-mimic compounds until Zalejski et al. (2005) showed that PA triggers the activation of anion currents without affecting the accumulation of the *RAB18* transcript. In contrast, treating plants by diacylglycerol pyrophosphate (DGPP), a product from PA, imitates ABA on anion currents as well as *RAB18* transcript accumulation. PA enhances DGPP accumulation through its phosphorylation by phosphatidate kinase (PAK); thus, DGPP accumulation is detected only after PA accumulation. Affinity membrane studies showed that DGPP binds to glyceraldehyde-3-phosphate dehydrogenase (GAPDH), which is also increased in response to ABA treatment where this interaction may have a function in ABA signalling cascade (Astorquiza et al. 2016). GAPDH is one of the core enzymes in the glycolytic pathway where it provides energy in the form of NADH by oxidizing glyceraldehyde-3-phosphate to 1,3-

bisphosphoglycerate, where the former is the first precursor of ABA biosynthesis in plastids through the 2-C-methyl-D-erythritol-4-phosphate (MEP) pathway (L Guo et al. 2012).

2.4.2 Jasmonic acid (JA)

Free polyunsaturated fatty acids are essential for the biosynthesis of Jasmonates (Oxylipin compounds) and are synthesized from phosphoglycerolipids by lipases, such as the release of α-Linolenic acid from biological membranes by PLC enzymatic action. The released α-Linolenic acids will then be under a series of biochemical modifications beginning with the oxidation by lipoxygenases until the relief of JA. Zhao (2015) reviewed the occurrence of JA biosynthesis from the action of PLDs on PC and found PLD-produced PA positively regulates JA biosynthesis whereas PLDα1 and PLDβ1 mutation impairs it. The pathway of JA biosynthesis is known as the octadecanoid pathway (Turner et al. 2002; Pokotylo et al. 2017). One crucial JA precursor is 12-oxophytodienic acid (OPDA), which induces stomatal closure although MeJA does not trigger stomatal aperture (Montillet et al. 2013). The Ca^{2+} signalling pathway and MAPK cascade also control regulation of JA biosynthesis where calcium signalling regulates the expression of some lipoxygenase-encoding genes, and JA biosynthesis elevation occurs ultimately by Ca^{2+}-signalling activating lipoxygenases (Wasternack and Hause 2013). Jasmonic acids have been known for their prominent role during pathogenic infections and during grazing by wound-causing insects, acting as a promoter for synthesizing many defensive compounds. Many laboratory experiments have showed its crucial role in protecting plants during abiotic stress conditions such as drought, cold, salinity, and heat stress (Turner et al. 2002; Sharma and Laxmi 2016).

After its biosynthesis, JA is bound to isoleucine (Ile) forming a bioactive ligand, JA-Isoleucine (JA-Ile), which interacts with a receptor Coronatine Insensitive1 (COI1) to allow interaction with other transcription factors like MYC, MYB, and ICE or other signalling compounds like jasmonate ZIM-domain (JAZ) proteins (Thines et al. 2007; Sharma and Laxmi 2016). Sharma and Laxmi (2016) reviewed the importance of the discovery of JAZ proteins, which enhanced our understanding of the way by which JA launches a physiological response after its perception. Under normal growth conditions, JAZ proteins interact with various stress-controlled transcription factors (TFs) through its conserved C-terminal domain, where it halts TF from binding with cis-elements of stress-controlled gene promoters. Stress induces the biosynthesis of JA and its epimerization or isomerization into JA-Ile, which in turn is capable of binding with JAZ

proteins, causing the circulation of many TFs upon binding to stress-controlled gene promoters (Figure 2.3). Under normal growth conditions, JAZ proteins somehow halt many essential TFs that are involved in abiotic and biotic stress pathways such as MYC2, MYC3, MYC4, ICE1, and ICE2. Therefore, JA-Ile positively regulates ABA-independent pathway (CBF regulon) through releasing transcription factors like ICE1 and the ABA-dependent pathway via a bHLH transcription factor MYC2 (Figure 2.3).

ABA regulates the expression of MYC2, which upregulates the expression of many genes in ABA pathway by binding to G-box or Z-box elements in their promoters such as ABRE-element in PP2C gene promoter, G-box element is there to recruit MYC2 protein (Mine et al. 2017). Thus, some genes are regulated by both ABA and JA. Additionally, MYC2 upregulates the transcription of many genes involved in JA-biosynthesis like AOC1, DDE2 and LOX2. Aleman et al. (2016) showed that ABA facilitates the repression of JAZ6 that is positively regulated by MYC2 by enhancing the binding of MYC2 with ABA receptor PYL6, however, this ABA-mediated PYL6-MYC2 interaction induces JAZ8 transcription. Avramova (2017) found that high JA is noticed only in the early phase of stress like drought, but not in the second dehydration stress due to the induction of MYC2 in the first phase of stress only. However, the factor that suppresses MYC2 transcription in subsequent dehydration stress is still unknown.

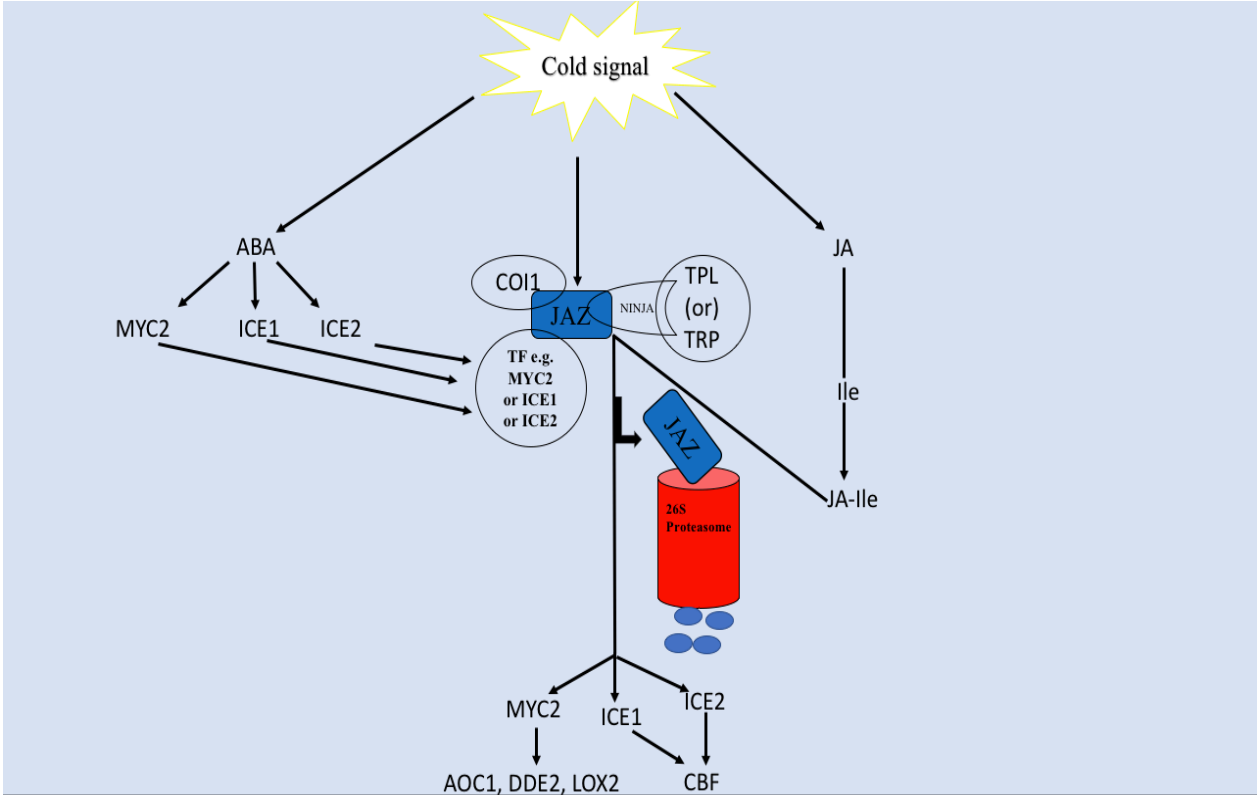

Figure 2.3: Proposed model for the crosstalk between ABA and JA during abiotic stress conditions such as cold stress.

Pauwels et al. (2010) show that JAZ proteins recruit Groucho/Tup1-type co-repressor TOPLESS (TPL) and TPL-related proteins (TPRs) through an adaptor protein INteractor of JAZ (NINJA) to induce epigenetic silencing of many critical hormone-synthesizing genes, including early JA-signalling genes. Therefore, JAZ proteins released by JA-Ile coordinate the cross-talk among different phytohormones. JA-Ile binds to JAZ repressor proteins through an F-box protein of the E3 ubiquitin ligase Skip-Cullin-F-box complex SCF^{COI1} which is encoded by COI1 locus. This SCF^{COI1} complex guides JAZ proteins aided by JA-Ile to be degraded through a ubiquitin-proteasome system (Wasternack and Hause 2013; Sharma and Laxmi 2016).

2.5 Cold acclimation: Cradle of Vernalization

The formation of ice causes the preliminary damage of cold stress in the apoplastic space due to its hypotonic nature. Water diffuses to the apoplastic space by the vapour pressure gradient, causing the formation of more ice crystals and the membrane to rupture in cold-sensitive plants (Yadav 2010). Because of this cold-induced dehydration, cold-sensitive plants and non-acclimated plants show signs of wilting, reduced development, and membrane damage. On the other hand, cold-tolerant plants can produce antifreeze proteins (AFP) that accumulate mostly in the apoplast to surround the ice crystals to prevent recrystallization (Bravo and Griffith 2005) or in the cytosol, chloroplast, and mitochondria. Plants are capable of developing cold-tolerance ability either inherently or by cold-acclimation (Thakur and Nayyar 2013).

Plants, as sessile organisms distributed across various environments, have developed fundamental and unique mechanisms to help overcome harsh environmental conditions. One of these mechanisms is the ability of some plant species to be cold-acclimated. In the northern hemisphere, temperatures can reach around zero in the fall, and quite below zero in the winter, where ice crystals can quickly form in the living cells of plants. Cold acclimation is a period of partly low temperature during which plants are reprogrammed to enhance their chilling and freezing tolerance, and thus to be capable of vernalization. The ability of plants to be cold-acclimated relies mainly on their genetic architecture which can adequately respond to the cold acclimation period. The adaptation of plants in hot conditions over long periods of time causes them to tune their genetic makeup in a different way. One example can be seen in winter wheat

which can be cold acclimated, tolerate harsh winter conditions, and flower after an extended cold periods of acclimation (vernalization). This is in contrast with its spring variation. With their tremendous diversity, Kosová and Prásil (2012) stated that plants embody three main categories regarding their ability to tolerate cold conditions: (1) Chilling-sensitive plants, which can be partially cold-acclimated but with severe cellular damage that will affect plant performance and fitness. These are typically tropical plants like maize, rice, tomato, chickpea, and soybean. (2) Chilling-tolerant plants which tolerate the chilling period of cold acclimation but cannot tolerate frosts, like sub-tropical plants such as potato and sugar beet. (3) Frost (freezing)-tolerant plants that can be cold-acclimated well and tolerate frost conditions, like winter cereals from the tribe *Triticeae*.

Freezing tolerance as identified by Sãulescu and Braun (2001) is the plant's ability to survive ice formation without significant cellular damage. This ability differs within different plant tissues due to their diverse physio-types. Plant tissues do not exhibit the same resistance level towards freezing conditions where the root collar (crown tissue) is the most tolerant part (Chen et al. 1983). In this sense, collars should have a significant role in protecting the plant from freezing damage as recently infrared thermography showed that freezing starts from the base of the plant, root collar, and then go upwards where leaf collar hinders the progression of ice propagation to the leaves (Livingston et al. 2018). Sãulescu and Braun (2001) found that the freezing tolerance trait is associated with vernalization requirements, prostrate growth type, day-length response, accumulation of specific gliadin blocks, and phenotypic differences like tissue water content, accumulation of polysaccharides, free proline and cold-regulated proteins.

Studies that had focused on chilling-sensitive plants and compared them with cold-tolerant ones showed that sensitive plants could not modify their lipid and protein profiles during cold stress. Additionally, the biological membranes of the sensitive plants have a higher proportion of saturated fatty acids, rendering them to solidify faster from a semi-fluid state into a semi-crystalline state under low-temperature conditions. The transition temperature of the biological membranes of cold-sensitive plants was recorded to be around 10ºC (Yadav 2010). The solid state of water vapour pressure is shallow in comparison with its liquid state, thus, as ice is formed in the apoplastic space, a vapor pressure gradient will be created between the hypotonic apoplast and hypertonic cytosol. This forces water molecules to migrate to the apoplastic space which in turn increases the rate of ice crystal formation and drives cell rupturing in cold-sensitive plants (Yadav 2010). Through their capability to shape their lipid and protein profiles, frost-tolerant plants

develop mechanisms to overcome this physiological consequence by their ability to produce and accumulate unique apoplastic proteins with cryoprotective and antifreeze activities, enabling them to surround ice crystals and halt ice re-crystallization (Winfield et al. 2010). Cold acclimation includes many important events like cold-signal perception and transduction which are significantly different among the three classes that group plants by their responsiveness to cold.

In general, cold stress reduces most plant metabolic reactions as the stress negatively affects the rate of most enzymatic reactions including the activity of ribulose-1,5-biphosphate carboxylase/oxygenase (Rubisco) and phosphoenolpyruvate carboxylase (PEP). Photoinhibition exhibit the same physiological consequences and is associated with decreasing both ratios of chlorophylls *a* and *b* to carotenoids and the maximum quantum yield efficiency (Fv/Fm) with a stable rate of electron transport. These events surge the non-photochemical quenching (NPQ) to dissipate the excess energy as heat (photochemical dissipation), therefore maintaining photosystem II (PSII) integrity is important (Huner et al. 1998; Kosová and Prásil 2012). During cold acclimation periods, winter annual plants evolve distinctive mechanisms to dissipate excess energy and to maintain PSII integrity either by reducing energy transfer efficiency from PSII to PSI, surging NPQ rate, developing smaller size of PSII antenna, changing leaf angle, leaf optical properties, or by elevating the activity rates of Calvin cycle enzymes (Huner et al. 1998). In winter cereals, cold acclimation drives activity and accumulation of photosynthetic carbon metabolic-regulatory enzymes such as Rubisco, fructose biphosphate, and sucrose phosphate synthase. It also maintains the oxidation state of the first stable electron acceptor protein, named the primary quinone (Q_A) of PSII reaction centre. The plastoquinone (PQ) pool thus maintains its activity during cold acclimation periods to transmit the electron transport signals into the Calvin cycle in forms of NADPH and ATP (Huner et al. 1993; Huner et al. 1998; Ensminger et al. 2006). This ability to maintain oxidized Q_A is positively correlated with freezing tolerance and negatively affects photosynthesis (Ensminger et al. 2006; Janda et al. 2014). Accordingly, cold-acclimated plants develop mechanisms that balance consumed energy and light absorption, mimicking the process of photoacclimation to high light to avoid the photodamage of PSII (Ensminger et al. 2006). This kind of photoprotection mimicking cold acclimation protection contrasts the events which happen during cold stress where plants lose the ability to halt the photoinhibition of PSII. For example, the expressed levels of light harvesting complex proteins (LHC) and nuclear genes encoding PSII and PSI core proteins are induced during the day of the cold acclimation periods, while they are suppressed during cold stress, enhancing photosynthetic inhibition (Janda et al.

2014; Hüner et al. 2016). This balance between absorbed and consumed energy of photosynthesis, is known as "Photostasis" and it is only a feature of environmentally well-adapted plants that can keep the oxidized state PQ pool under a long period of environmental fluctuations (Ensminger et al. 2006). To keep the metabolic sink up to date with the photosynthetic activity and cold acclimation conditions, a cross-talk necessary. For example, the chilling-tolerant Arabidopsis species maintain the level of Calvin cycle gene expression during cold treatment and the accumulation of sugars with contrast to chilling-sensitive species. Other sugar-biosynthetic specific genes are light-dependent, and their transcripts accumulate under cold-hardening periods, like that of fructosyltransferase genes in wheat which has a role in increasing membrane stabilization and freezing tolerance (Sandve et al. 2011; Janda et al. 2014). These genes are up-regulated under water stress conditions, as seen in cell wall hydrolases that provide a source of energy to the plants under nutrient deficiency conditions. SnRK1 (a sucrose non-fermenting 1-related kinase 1 or SNF1-related protein kinase 1) is thought to be an upstream regulator of these genes as its activity is also upregulated under water stress conditions where it enhances catabolic pathways to provide another source of energy under low photosynthetic activity (Biswal et al. 2011). This accumulation of photoassimilates usually occurs in the early phase of cold acclimation periods, like in autumn or early winter, and acts as an energy source during long cold acclimation times. This photoacclimation strategy of plants increases carbon assimilation during the early phases of cold acclimation and carbon metabolism during late phases of cold acclimation periods (Sandve et al. 2011). With a focus on wheat cultivars, spring growth-habit plants show sensitivity towards cold due to photoinhibition of PSII, in line with their distinctive low expression of CBF regulon genes. However, winter growth-habit plants show more active photosynthetic performance, higher accumulation of photosynthetic gene transcripts, lower photorespiration, and higher expression of CBF regulon genes (Hüner et al. 2016). The unique signature of cold-acclimated plants is to maintain efficient photosynthesis together with the accumulation of soluble sugars which discriminate this event from that of the cold stress event, where sugar accumulation is negatively affecting the photosynthetic efficiency.

During the early phase of the cold acclimation period, plants begin to gradually accumulate unique proteins with cryoprotective and antifreeze activities in various cell compartments. This protects the cell from severe low-temperature conditions. Dehydrins are an essential set of Late Embryogenesis Abundant (LEA) proteins that accumulate during water-limiting conditions. LEA proteins are diverse and contain various groups, although in general they have been found in

maturing seeds, anhydrobiotic plants, animals, and microorganisms (Wise and Tunnacliffe 2004). Battaglia et al. (2008) have classified LEA proteins into seven main groups according to their structural and functional characteristics. Dehydrins are in group 2 of LEA proteins and recently in the group (D-11). Dehydrins include five distinct subgroups, recognized by their characteristic K-segment (EKKGIMDKIKEKLPG) that is predicted to form amphipathic α-helical structures that may protect membranes from dehydration and mediate specific protein-protein interactions and protect enzymes from inactivation. If the dehydrin protein has many K-segments, they may interact together forming a bundle with amphipathic alpha-helical conformations. In Arabidopsis, two dehydrins named early responsive dehydration proteins (ERD10 and ERD14) are found to protect many enzymes from dehydration (Kiyosue et al. 1994; Kovacs et al. 2008). Most LEA proteins and dehydrins pass the cryoprotective assay of freeze-liable enzymes (Lin and Thomashow 1992). In general, LEA proteins prevent protein inactivation through their "Molecular shield activity" which reduces protein aggregation, imminent from water stress, in addition to the solution effects of polysaccharides that minimize protein aggregation (Chakrabortee et al. 2012). Liu et al. (2016) identified a group three LEA protein in maize (ZmLEA3) which is upregulated in reduced water activity and ABA. While its over-expression enhances tolerance of tobacco towards low-temperature conditions, other proteins in LEA group three have been found in pea mitochondria (PsLEAm), which can interact with and protect liposomes from dehydration (Stupnikova et al. 2006). WCS19 has been characterized in wheat as an LEA which localizes in chloroplast stroma (NDong et al. 2002). The WAP27A and WAP27B are localized in the endoplasmic reticulum (Ukaji et al. 2001). A wheat protein (TaEm) which belongs to group one LEA showed an ability to protect citrate synthase and lactate dehydrogenase (LDH) from aggregation due to low water conditions (Battaglia et al. 2008). Other LEA proteins were still unique and not classified into any of the seven known groups. Sasaki et al. (2014) identified a novel LEA protein from wheat (WCI16) which showed a cryoprotective tendency to enzymes and DNA in vitro and was involved in conferring transgenic Arabidopsis plants with increased freezing tolerance.

In line with various LEA protein accumulation during cold acclimation, other unique groups called antifreeze proteins accumulate under low-temperature conditions in tolerant plant species, particularly in their apoplast. AFP are unique in their ability to either increase the difference between melting and hysteretic freezing points, known as Thermal Hysteresis (TH), or by their ability to inhibit ice recrystallization by surrounding ice crystals affecting its shape and preventing the growth of ice crystals. AFP surrounding ice crystals requires minor AFP activity in

comparison with TH (Preston and Sandve 2013; Duman and Wisniewski 2014). Antifreeze activity in plants is not only confined to proteins and glycoproteins, but also some non-proteinaceous molecules, such as antifreeze glycolipids. Sugar moieties in some antifreeze glycoproteins or glycolipids serve crucial roles due to their tendency to bind with ice (Gupta and Deswal 2014). While thermal hysteresis is most common in fish, insects, and plants, ice re-crystallization inhibition proteins (IRIP) are well-known in plants during cold acclimation (Urrutia et al. 1992; Preston and Sandve 2013). AFPs are highly upregulated in plants once they sense cold, such as that of LpIRI-a with which transcription is upregulated to 40-fold in *Lolium perenne* upon one hour of cold acclimation and can reach 8000-fold after seven days of acclimation.

Another example is TaIRI-1 from *Triticum aestivum,* where its transcript is upregulated in the first day of cold acclimation and keeps increasing between 6 days and 36 days of cold acclimation with increased accumulation in the winter wheat cultivar, Norstar as compared to the spring wheat cultivar Glenlea (Tremblay et al. 2005; Gupta and Deswal 2014). Plant AFPs show diverse physicochemical properties, some of which having pIs in the acidic range and others having basic pIs. Most of them are hydrophilic, but hydrophobic AFPs have been reported, with the majority of AFPs having a high aliphatic index (Gupta and Deswal 2014).

Metabolic modifications, photoacclimation, signal transduction, and accumulation of LEA and AFPs are some events that happen during cold acclimation periods. Cold acclimation is a multigenic, quantitative trait that implicates numerous physiological and biochemical events (Wisniewski and Gusta 2014). The cold acclimatization reprograms genetic and metabolic networks enabling the plant to withstand an extended period of low-temperature, thus it is an essential step for vernalization.

2.6 Vernalization: Qualification for Flowering

Vernalization is a prolonged period of cold acclimation which drives certain plant varieties towards competency to flower during normal conditions following vernalization, i.e. in spring season or during a deacclimation phase (Danyluk et al. 2003; Trevaskis 2010; Brian Fowler 2012). Not all plants need vernalization to flower, and this is usually only limited to winter varieties. Many efforts have been made to answer the question why spring wheat varieties can flower without any vernalization requirement while winter ones cannot. The discovery of the MADS-box transcription factor gene VRN1/VRT1 that is responsible for vernalization in cereals and which has high homology with *Arabidopsis thaliana* meristem identity gene *APETALA1* (*AP1*), opens

the door for understanding the mechanism of vernalization in cereals (Danyluk et al. 2003; Yan et al. 2003). These studies have shown that spring wheat cultivars have deletions in the VRN1/VRT1 gene promoter that impedes the VRN2 repressor in identifying its binding site, thus VRN1 keeps its constitutive expression without any need for vernalization in these spring cultivars. Whereas winter wheat varieties have VRN1 promoter sequence that can be recognized by VRN2 and only prolonged cold treatment liberates VRN2 from the VRN1 promoter to enhance the expression of the floral promoter gene (VRN1) (Danyluk et al. 2003; Yan et al. 2003; Yan et al. 2004). It has been found that VRN1 not only controls the transition from vegetative to reproductive phase in wheat where its radiation-induced deletion results in plants that never flower, but is also negatively correlated with the transcription of COR genes and degree of freezing tolerance (Danyluk et al. 2003; Shitsukawa et al. 2007).

Moreover, Distelfeld et al. (2009) found that vegetative-to-flowering transition is also associated with a VRN2 region deletion, resulting in wheats with spring growth habits. *ZCCT* gene-contained VRN2 regions that encode two similar functional putative proteins with Zinc-finger and CCT domains. The epistatic interaction between VRN1 and VRN2 is not accomplished by direct binding of VRN2 to the VRN1 promoter, though a repressor complex may be involved in this regulation. Kane et al. (2005) identified another gene in bread wheat named VRT2 that has been found to bind with the CArG motif (MADS-box-binding site) in the VRN1 promoter, and this binding may enhance VRN2 repressor complex formation which may regulate VRN1 activity. Other studies suggested that the binding of VRT2 to the VRN1-CArG motif promoter not interfere with VRN2-regulating VRN1 activity or vernalization requirement as many diploid *Triticum monococcum* accessions with VRN1-CArG-motif deletions still show winter-growth habit (Distelfeld et al. 2009; Pidal et al. 2009).

However, with looking into the effect of day length on VRN2 expression, Turner et al. (2013) showed that long days (LD) upregulate its expression rather than short days (SD). Dubcovsky et al. (2006) found that six weeks of SD treatment intervening LD treatment is enough to substitute the need for vernalization to suppress VRN2. However, this interruption of SD treatment never upregulates VRN1 until the plants are again at LD which may suggest the presence of another VRN1 repressor that is down-regulated during the LD retreatment. Kane et al. (2007) showed that SD treatment induces VRT2 expression in spring wheat (Figure 2.4). Thus, the VRN1 gene is repressed during the intervening SD treatment. However, Trevaskis et al. (2006) showed that day length in barley does not regulate VRT2 gene expression. Oliver et al. (2009) showed that

vernalization controls the epigenetic state of VRN1 in barley rather than VRN2 or VRN3. As vernalization stimulates VRN1 gene expression by increasing the level of histone 3 lysine 4 trimethylation (H3K4me3) and decrease the level of histone 3 lysine 27 trimethylation (H3K27me3), it thus activates chromatin at VRN1 locus. This epigenetic control of vernalization in Arabidopsis happens in a different way where vernalization provides FLC repression by inducing H3K27me3.

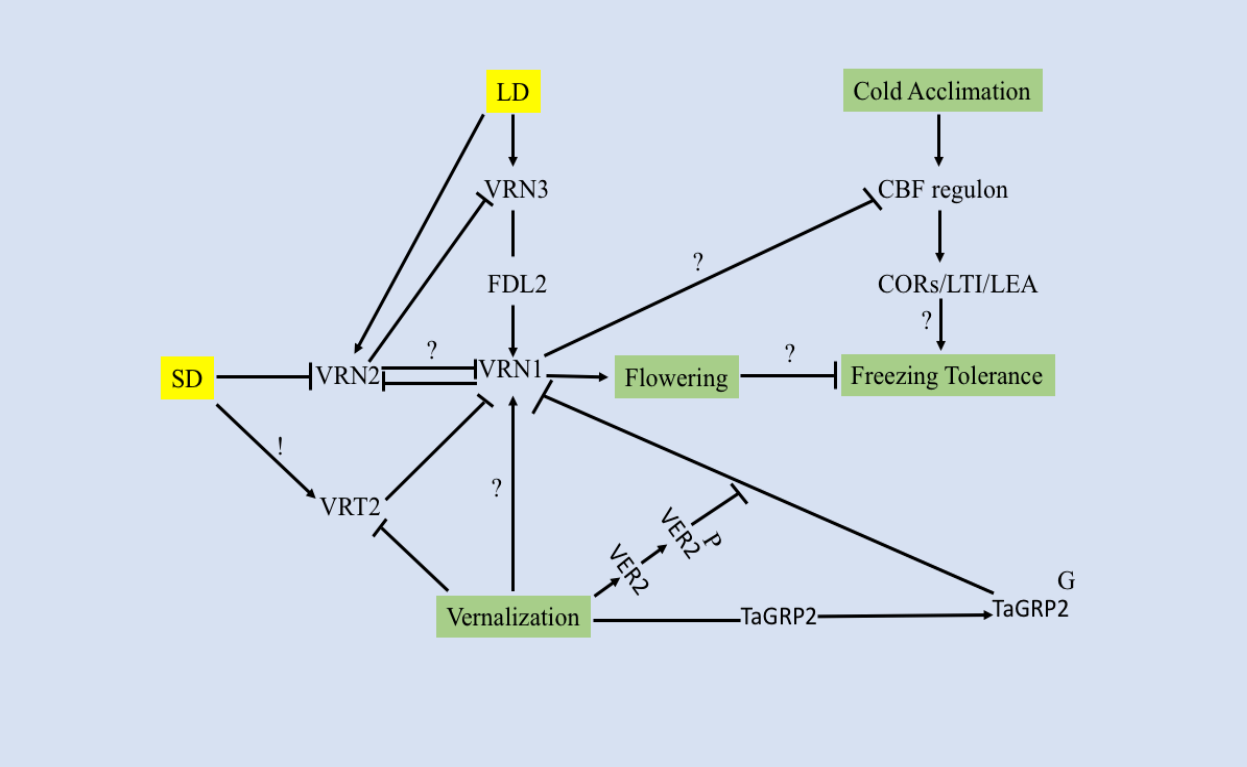

Figure 2.4: An overview of photoperiod, cold acclimation, vernalization and flowering crosstalk in wheat. Post-translational events are highlighted by superscripted letters on symbols where "P" refers to phosphorylation and "G" refers to *O*-glycosylation. Questions marks indicate that more elucidations are needed to indicate the exact molecular pathway while exclamation mark refers to a hypothetical model where SD effect or induce VRT2, but this effect is in need to be verified across different wheat varieties and under different treatments.

Continued analyses of wheat requirements for vernalization identified an essential gene named VRN3 whose expression upregulates VRN1 without vernalization, irrespective of day length (Yan et al. 2006). As shown in Figure 2.4, this occurs through the interaction of its protein with FD-LIKE2 (FDL2) and the VRN1 promoter (Li and Dubcovsky 2008). A transposable

element insertion associated with the dominant VRN3 allele promoter causes transgenic winter wheats with the spring wheat dominant VRN3 allele to upregulate the expression of VRN1 gene. Thus, these transgenic plants show rapid flowering without vernalization or short daylength requirements (Yan et al. 2006; Li and Dubcovsky 2008; Distelfeld et al. 2009). Moreover, transgenic wheats with reduced VRN2 transcript levels showed a significant increase in VRN3 transcript levels (Yan et al. 2004; Distelfeld et al. 2009). The loss of VRN2 results in rapid transition into the flowering stage only under long-day conditions (Karsai et al. 2005; Hemming et al. 2008; Trevaskis 2010).

As the VRN3 gene has been shown to be regulated by photoperiod with its induction during the long day conditions, it has been suggested that VRN2 represses VRN3 under extended day conditions (Distelfeld et al. 2009; Trevaskis 2010). Transgenic polyploid wheat studies showed that the abundance of VRN1 transcripts downregulates VRN2 genes in isogenic lines carrying different combinations of dominant and recessive VRN1 alleles, rather than isogenic lines carrying only recessive vrn1 alleles (Loukoianov 2005; Distelfeld et al. 2009). Another mechanism has been introduced by Xiao et al. (2014) to interpret the regulation mode of VRN1 gene activation during vernalization of wheat plants. They found that vernalization induces VER2 expression in the shoot apex nuclei and stimulates O-GlcNAcylation of TaVRN1 pre-mRNA repressor protein (TaGRP2) at Thr17. Phosphorylated VER2 proteins bind only to O-GlcNAc-TaGRP2 during vernalization to release its repression effect on TaVRN1 pre-mRNA, thus promoting flowering (Figure 2.4).

Vernalization is a complicated process that is controlled by many genetic elements, where all components collaborate efficiently with genetic-network controlling photoperiodism and flowering. Cold acclimation and vernalization are highly coordinated, as vernalization is a long-term cold acclimation that allows winter varieties to flower only under suitable conditions. During cold acclimation, winter varieties show biomass accumulation in line with increased photosynthetic capacity, building up the energy needed for rapid flowering and seed formation after vernalization (Hüner et al. 2016). Moreover, freezing tolerance is to be built up during cold acclimation and if plants grow at low-temperature conditions until they reach the vernalization saturation point where they are ready to flower. Subsequently, plants begin to lose their frost tolerance by down-regulating many frost tolerance controlling genes like CBF and COR genes (Trevaskis 2010).

2.7 Evolutionary Aspects

Domestication of crop plants drives many permanent modifications in phenotypes through loss-of-function mutations and cis-regulatory changes, or in their metabolic pathways via selection on structural and regulatory genes (Olsen and Wendel 2013). These phenotypic and metabolic changes are a product of genotype-by-environment interactions (Hansen et al. 2012). However, local populations of wheat differentiate immensely due to limited gene flow among these populations. Regardless of its life cycle and the complexity of its genome, wheat is one of the ideal organisms for genotype-by-environment interaction studies. Cereals originate from the artificial selection of wild grasses, by which they got their current diverse phenotypic, physiological, and genetic changes as domestication changes ancestral genetic loci (Pozzi et al. 2005). Over past centuries, artificial selection in wheat plants selected for agronomic traits such as free-threshing and yield components as well as plant performance to fill the needs blooming human populations. This process of artificial selection along with geographic isolation decreased the genetic diversity of modern wheat landraces compared to wild wheat species (Nevo et al. 2012). Domestication of the crop plant in different climatic conditions results in opposing adaptive machinery. For example, wheat domestication has resulted in the evolution of winter, spring, and facultative wheats regarding cold tolerance. Another example is the response of wheat genotypes to different levels of heat stress during their filling period since the selection of the resistant genotypes is significant for wheat breeding (Castro et al. 2007).

During cold acclimation and vernalization periods, spring and winter plant varieties show opposing phenotypic plasticity which is due to long-term natural selection (adaptive evolution) in the tropics and temperate climate conditions. Körner (2016) has reviewed three evolutionary adaptation characters that plants have developed during the cold-adaptation of their genome: 1) their ability to maintain the movement of water molecules from the cytosol to the apoplast, 2) fine-tuning their phenology during different seasons, and 3) keeping small stature in response to cold. Spring varieties of plants respond to cold acclimation periods by showing more resistance to damage, while winter varieties show higher responsiveness to decrease the negative impacts of damage. Both tolerance and resistance traits have opposing trends in these varieties (Agrawal et al. 2004).

With a focus on the subfamily Pooideae, winter varieties accumulate multifarious compounds like IRI-like proteins and dehydrins during cold acclimation periods. These compounds protect them from injury due to freezing, and the evolution of their functionality may

have evolved independently or from a common ancestor. Sandve et al. (2008) assumed that IRI-like proteins evolved their ice-recrystallization inhibitory activities through gene duplication events after rice-Pooideae divergence, which has been detected by an ice-binding domain. Moreover, no orthologous genes have so far been identified for the cold acclimation wheat WCS120 gene outside the tribe Triticeae, indicating the independent evolution of cold acclimation traits (Schubert et al. 2017). However, the similarity of the flanking regions of the IRI-domain in the subfamily Pooideae within the rice leucine-rich repeat domain in phytosulfokine receptor kinase (OsLRR-PSR), raises the hypothesis that the IRI-domain may have evolved from the OsLRR-PSR domain by a series of genetic modifications. Likewise, the evolutionary study of 47 different AFPs using the unweighted pair group method with arithmetic mean (UPGMA) grouped the 12 IRI-containing AFPs from Pooideae into a subsister clade, indicating the presence of a common ancestor (Gupta and Deswal 2014). A different example is the neofunctionalisation of core Pooideae cold acclimation genes, CBFIII and CBFIV, as they did not show the same expression patterns, which may indicate their role in cold acclimation outside the core Pooideae (Schubert et al. 2017). These authors showed that cold stress marker genes like HvDHN8 and HvDHN13 have the same expression patterns with a more conserved protein structure and absence of duplication events, as these show a sign of sharing general responsiveness to cold with their most recent common ancestor.

In wheat, VRN genes play an adaptive role that is linked to freezing tolerance and heading time. It has been found that winter wheat varieties with FROST TOLERANCE 2 allele T (FR-A2-T) and three VRN-A1 copies tolerate frost conditions more than varieties with less VRN-A1 copies (Zhu et al. 2014). Kippes et al. (2018) reported 3 SNPs in the first intron of the VRN-A1 gene, the binding site of the GRP2 protein, that are associated with a significant earlier heading time of the winter wheat haplotype. Although, winter wheat varieties with various VRN-A1 copies did not show this significant difference in the heading time.

The vernalization-regulatory genetic network has evolved independently across dicots, whereas in monocots it has evolved through neo-functionalization where orthologous genes possess different functions – sometimes even amongst different dicot plants (Kim and Sung 2014). The Flowering Locus C (FLC), a MADS-box floral repressor gene, is the principal regulator for vernalization in Arabidopsis since a variation in its promoter, first exon, and first intron drives different responses to vernalization. FLC down-regulation by cold releases the repression of the Flowering Locus T (FT), FLOWERING LOCUS D (FD), and the suppressor of overexpression of

CO1 (SOC1). In turn, this release upregulates many other genes that develop the transition from vegetative to the flowering stage after vernalization like the floral homeotic gene APETALA1 (AP1) (Trevaskis et al. 2007; Trevaskis 2010; Preston and Sandve 2013). The positive regulator FRIGIDA (FRI) is an upstream regulator gene which also accounts for the natural variation in vernalization requirements and the autonomous pathway genes as negative regulators (Trevaskis et al. 2007; Kim and Sung 2014). Vernalization in Arabidopsis acts by downregulating the FLC gene. The transcription of FT and AP1 genes is induced, while in wheat it acts mainly by upregulating the VRN1 gene, which in turn downregulates the VRN2 gene (a repressor of VRN3/FT). Thus, VRN3 transcription is induced (Trevaskis et al. 2007). Although VRN3 in wheat is the orthologous gene of the FT gene in Arabidopsis, evolutionary studies did not show any orthologs of VRN2 outside temperate cereals or any FLC-like genes in monocots, regarding the function only, both VRN2 and FLC in temperate cereals and many dicots respectively act to repress the FT gene.

Furthermore, vernalization downregulates both VRN2 and FLC to release the repression of the VRN3/FT gene (Yan et al. 2006; Trevaskis et al. 2007; Trevaskis 2010). Vernalization may have evolved independently, but the intercommunication between vernalization and freezing tolerance seems to be tightly regulated, as vernalization ensures the onset of flowering which in turn reduces freezing tolerance. It has been found that temperate cereals with active VRN1 alleles show reduced expression of CBF genes (Stockinger et al. 2007; Dhillon et al. 2010; Deng et al. 2015).

Chapter Three: Identification of Cold-Tolerance Associated Genes in Wheat

Abstract

The low temperature and freezing conditions affect growth and development of plants reducing the productivity of crops. Identification of cold tolerance related genes is crucial for developing cold tolerant crop plants to increase agricultural productivity. Although many molecular mechanisms, metabolic pathways and genes involved in cold acclimation in plants are known, recent microarray-based gene expression data revealed many genes in plants that are differentially expressed in response to exposure to cold. The function of many of these genes are unknown and serves as an invaluable resource for identification and characterization of cold tolerance genes in plants. The present study is focused on i) selecting genes in wheat (*Triticum aestivum*) that show microarray based evidence for differential expression in response to exposure to cold, ii) verifying their expression in wheat plants treated with cold for short and long durations and iii) predicting their function through bioinformatics approaches, and iv) analysing the expression of the selected genes in response to Abscisic acid (ABA) and Methyl Jasmonate (MetJ), two of the signalling molecules involved in stress response, including cold response in plants.

The 40 selected genes with uncharacterized functions that showed increased expression in response to cold treatments were clustered into four groups namely i) Defense related regulators, ii) Transcriptional and epigenetic regulators, iii) Post-transcriptional and post-translational regulators, and iv) Genes of unknown function. The Real Time Quantitative PCR (RT-qPCR) analyses of cold exposed wheat plants revealed differential regulation of many genes in response to cold treatment, including i) Remorin - upregulated in response to cold, ii) a novel gene with remote homology to RD29B of Arabidopsis – upregulated in response to cold and ABA and iii) an unknown gene upregulated by both ABA and MetJA.

Introduction

A great deal of research focuses on understanding the mechanisms by which winter cultivars of the grass family, Poaceae, can tolerate low-temperature conditions more than spring cultivars of the same species. Species with spring-cultivating backgrounds are not competent enough to develop frost tolerance traits during the cold-acclimation period (Preston and Sandve 2013). The ability of temperate grasses to acquire a diverse transcriptomic network under low-

temperature environments has gained much interest in the scientific community, and many global gene expression studies have tried to designate the reshaping of their transcriptomes.

Global gene differential expression has often been investigated using DNA Microarray technology, although newer, more precise and advanced technology has now become available, such as RNA-Seq. Before using gene expression tools to thoroughly study the function of specific genes related to cold acclimation, it is crucial to validate the results of the global gene expression tool used. Exploring microarray data from previously published works (Skinner 2009; Laudencia-Chingcuanco et al. 2011; Kane et al. 2013; Li et al. 2018) and highlighting candidate genes that have a role in cold acclimation of wheat plants is the first step for investigating gene expression in temperate grasses. Selection of genes from previously published microarray data results in forty genes of interest that can be re-evaluated by qPCR under specifically designed cold conditions. The selected genes have been annotated from NCBI and are found to have various functions ranging from defence regulation, transcriptional, epigenetic, post-transcriptional and post-translational functions, while genes with unknown functions are kept together in one separate group.

When plants are exposed to low temperatures, some genes are differentially expressed during the short-phase of low-temperature exposure (i.e. cold acclimation), while others are induced only during the long-phase of low-temperature exposure (i.e. vernalization). However, early-induced genes are essential for the induction of genes during vernalization. One example of this is the induction of the CBF regulon that is essential for the activation of the VRN1 gene through an unknown mechanism. Cold acclimated plants gain their cold tolerance traits during the first phase of low-temperature exposure by the induction of ICE, a transcription factor which in turn induces the CBF regulon that turns on the transcription of LEA and COR genes. The developing of plant's cold tolerance traits lead to the induction of vernalization genes and the down-regulation of CBF regulon (Trevaskis 2010). The cross-talk mechanism between vernalization genes and the CBF regulon are not yet fully understood. To better understand the function of these identified genes, it is important to know whether it is induced only during the short phase or the long-phase of low-temperature exposure. For this purpose, we designed two experiments where we analyzed the expressions of the selected genes under the cold acclimation period (short-growth kinetics) and the long-phase of low-temperature exposure (long-growth kinetics).

Tissue specificity in gene expression is another significant factor to consider as genes orchestrate the physiology and development of plants by different levels of expression throughout the day (circadian genes) and in different tissues (tissue-specific genes). Many genes have been previously observed to accumulate in specific tissues under low-temperature conditions. Chauvin et al. (1993) identified a leaf specific light-stimulated WcS3.19 gene that is induced during cold acclimation periods, while NDong et al. (1997) showed that the Fcor3 gene is specific to leaves and its expression profoundly declined in strawberry leaves during cold acclimation. On the other extreme, some genes do not show tissue specificity, such as Wcor410 that accumulates in the plasma membrane of either leaves, roots, or crowns under low-temperature conditions (Danyluk et al. 1998). We investigated the expression of the selected genes in different plant tissues, namely roots, crowns, stems, and leaves. Due to the variation in physiological states of cells in the same tissue, leaves are partitioned into three parts; tip of the leaf, the middle parts of the leaves, and leaf base. We separated the stem into two different segments: the lower part of the stem and upper part. Our study on gene expression regulation in different plant tissues will improve the understanding of where the transcription of the candidate gene is mainly needed. In this study, we flagged forty genes, determined their expression profiles, and evaluated their necessity across different wheat tissues under short- and long-cold conditions.

Materials and Methods

Exploratory data mining and selection of candidate genes

Many candidate genes with increased expression under cold exposure but no identified roles in cold acclimation in wheat *Triticum aestivum* (cv. Norstar) were manually selected from microarray data of published articles (Skinner 2009; Laudencia-Chingcuanco et al. 2011; Kane et al. 2013; Li et al. 2018). Some of the genes were selected based upon the functions related to homologous with genes in Arabidopsis (Duque 2011). The selection process was made based on two main criteria (1) differential gene expression observed in microarray data where upregulated genes in response to cold treatment were selected (at least ≤ 3 fold change) and (2) the predicted functions of the candidate genes where most of the selected genes have unknown/speculative functions in winter wheats that survive under cold acclimation or freeze tolerance conditions. Forty genes were selected and were anticipated to be promising for further studies. Probe sets IDs were used to retrieve the identifiers from Netafex (Liu et al. 2003). These identifiers were used as queries

in the nucleotide BLAST program (NCBI Resource Coordinators 2016) to retrieve gene accession numbers in the genus (*Triticum*), then the translated nucleotides were used as queries in blastx to identify the closest annotated homologous proteins, and whenever possible, start and stop codons of the chosen candidate were predicted from the blastx results. Table S3.1 summarizes these data, and for convenience, the selected candidates were given numbers from 1 to 40 and then grouped according to their predicted functions into four main groups (I) Defence-related regulators (II) Transcriptional and epigenetic regulators (III) Post-transcriptional and post-translational regulators (IV) genes of unknown function.

Plant material and growth conditions

Two kinds of growth experiments were set up to validate the expression of the selected candidate genes under short and long cold treatments.

Short kinetics growth condition:

Wheat, *Triticum aestivum* L. cv. Norstar (Grant 1980) plants were grown in a growth chamber under controlled conditions of 20°C, long days (LD) (16 h at 320 μmol m^{2} s^{-1}). For cold treatment, seven-day old plants were grown under 4°C and sampled after one more day (CA-I) and eight more days (CA-II). Untreated seven-day old wheat seedlings were grown and sampled after one more day (NC-I) and three days (NC-II). Sampling was always started at 12:00 PM. Different plant tissues were sampled from each plant, including the roots (R), crowns (Cr), lower part of the stem (S1), upper part of the stem (S2), leaf base (L1), middle part of the leaf (L2) and upper part of the leaf (L3). The partitioning of stems was done into two halves while leaves into three thirds, equally divided based on their lengths. Samples were kept in dry ice for less than a half-hour until all the samples were collected, then stored at -80°C for further analysis.

Long kinetics growth condition:

Wheat crowns of Norstar (Grant 1980) and Manitou (Campbell 1967) grown under field conditions were collected at five time points in 2010 as described by Q. Li et al. (2017), where T1, T2, T3, T4 and T5 refer to sampling on 22 September, 4 October, 18 October, 25 October and 5 November, respectively. Biological samples were collected for each sampling date and immediately frozen in liquid nitrogen and stored at −80°C for analysis.

Hormone Treatment:

ABA and MetJ treatments were performed as described previously (Danyluk et al. 1998; Diallo et al. 2014). Briefly, two groups of seedlings were sprayed and watered with 150 μM MetJ

or 100 µM ABA dissolved in 0.1% tween 20 solutions respectively. Each group of treated plants was watered with the same treatment solution. The untreated plants received a mock treatment of 0.1% Tween 20 solution and used as a control. The samples were collected after four hours of the treatments.

Gene expression analysis

RNA Extraction:

Total RNA was extracted from different sample tissues using Qiagen kit as follows: one sample was ground in a pre-chilled mortar, and 0.1 mg was taken as a representative sample and extracted with 100 µl plant aid and 1000 µl lysis buffer. For crowns, approximately ten crowns were weighed and ground in a pre-chilled mortar in plant aid (w:v ratio was 1:1) and lysis buffer (w:v ratio was 1:10). The mixture was left for 5 minutes at room temperature after homogenization and then centrifuged at 15000 rpm for 5 minutes. A volume for 500 µL supernatant was taken, and 50 µl miRNA homogenate was added to it; the tubes were then vortexed three times and kept in ice for 10 minutes. Acid-phenol chloroform (500 µL) was added, followed by vortexing of the tube several times. Samples were then centrifuged for 7 minutes, and the upper phase was carefully removed and mixed with 1.25 volume of pure 100% ethanol by pipetting. The mixture was filtered through the Qiagen Yo filter in two successive runs and centrifugation (10,000 rpm/ 15 sec) was applied in each one, followed by discarding the flow-through. Each filter membrane was then washed one time with Solution1 700µl and two times with Solution2/3 500µl, centrifugation (10,000 rpm/ 15 sec) with discarding the flow-through at each washing step. The filter was then centrifuged for 1 minute at 10,000 rpm and then 5 minutes to make sure that no more washing solutions are remaining. The membrane was then eluted by a preheated (95°C) elution buffer (80 µL) in two successive steps by applying 40 µL to the center of the filter followed by centrifugation 60 sec./10,000 rpm in each step. Extracted RNA was then stored at -20°C. A Nanodrop spectrophotometer was used then measured RNA concentration.

Formaldehyde RNA gel:

Agarose (1.5 gm) was dissolved in pure distilled water (100 ml) by heating in a microwave for two minutes. Once it was at a safe temperature (~ 40°C), a mixture of MOPS 10x (10 ml) pH 7 and formaldehyde (16.2 ml) was added to the agarose solutions, and the flask was swirled to mix the gel buffer with the agarose solution. The gel was poured into the gel casting and given time to solidify. Gel hydration solution [MOPS 10x (20 ml), distilled water (144.2 ml), and Formaldehyde

(38.8 ml)] were then added to cover the gel, and a glass plate was applied on the gel to minimize formaldehyde evaporation. The gel was left like this under the fume hood for at least 40 minutes. An RNA sample loading buffer was prepared as follows [Formamide (10 µL), Formaldehyde (4 µL) MOPS 10x (2.5 µL), Ethidium Bromide (10 mg ml^{-1}) (0.1 µL)], all of which was added to 6 µL of RNA. Samples were heated to 70°C for 10 minutes, then kept in ice for 5 minutes and loaded into wells. The running gel buffer that was used consisted of MOPS (1x), with a run time of 60 to 90 minutes at 90V.

Genomic DNA elimination reaction:

RNA samples were diluted by RNase free water to make a final concentration of (900ng), and 2µl of gDNA wipeout buffer was added to make a final volume of 14 µL. RNA Samples were then incubated at 42°C for 10 minutes and then stored in ice.

cDNA preparation:

Reverse transcription master mix (RT) and None-reverse transcriptase (NRT) reactions were prepared on ice as follows:

Component	Volume/ RT reaction	Volume/NRT reaction
Quantiscript reverse transcriptase	1 µL	-
Quantiscript RT buffer	4 µL	4 µL
RT primer mix	1 µL	1 µL
RNase free water	-	1 µL

A total of 6 µL from either RT master mix or NRT master mix was added to each template RNA (14 µL). The tubes were incubated at 42°C for 30 minutes, and the reaction was terminated at 95°C for 3 minutes and chilled on ice.

Quantitative real-time PCR:

cDNA (RT and NRT) was diluted 10-fold with RNase free water. Quantiscript SYBR Green PCR (2x) Master Mix was prepared as follow:

Component	Volume (µL)/reaction
SYBR Green (2x)	12.5
Primer (A+B)	0.75
RNase free water	9.75

A volume of 2 µL of the diluted cDNA was added in each 96 PCR plate according to the plate design. The master mix was then distributed to 23 µL for a total reaction of 25 µL in each well. The18S rRNA was used as an internal standard for normalization of expression levels with the delta-delta-Cq method for the calculation of relative expression. The plate was then centrifuged (2500 rpm/4°C/5 minutes). Real-time PCR analysis was performed in a Roche Light Cycler 480 according to the manufacturer's instructions. The program used contains four steps: the first step is the initial activation at 95°C for 15 min, the next step is the PCR amplification, performed up to 40 cycles with 94°C for 15 s, 57 °C for 30 s and 70 °C for 30 s. The third step is the melting curve for one cycle (95 °C for 5 s, 65 °C for 30 s and 95 °C continuous), and the last step of the program is cooling for one cycle at 37°C for 5 minutes. Melting curve analysis was used to assess the specificity of the qRT-PCR products. Primers for the forty selected candidate genes were designed by primer3 and are listed in Supplementary File S3.2.

Data Curation

Raw Cq data values were normalized to 18S Cq values and one day cold acclimated crown sample was used in all plates as an inter-plate calibrator to balance any variations among different PCR runs, and $\log_2$ relative expressions were calculated (Schmittgen and Livak 2008). All graphics and statistical analysis were done using R programming (R Development Core Team 2013) and R package ggplot2 (Wickham 2009). Linear regression model was used to assess the relationship of $\log_2$ relative gene expressions and different sampling times in the long-kinetics experiment. Moreover, the adjusted R-squared (R2) and p-values (p) were estimated to the assess the significance of the linear model. Estimated p-values from a t-test were used to evaluate the significance between one day non-acclimation of one-week old wheat seedlings (NC-I) versus one-day cold-acclimation of one-week old wheat seedlings (CA-I), and three-days cold-acclimation of one-week old wheat seedlings (CA-I) versus one-week cold-acclimation of one-week old wheat seedlings (CA-II). Both p-values and 95% confidence intervals were used in the experiments with two biological replicates.

Results

Bioinformatics-assisted gene annotation and functional domain prediction

The previously selected genes (Skinner 2009; Laudencia-Chingcuanco et al. 2011; Kane et al. 2013; Li et al. 2018) were categorized into four main groups based on their functions as

predicted through their protein domains (Table S3.1) (NCBI Resource Coordinators 2016). For the matter of convenience, all candidates were given different numerical identifiers.

Group I contained all proteins that play a role in increasing plant defence against pathogens. Predicting protein domains revealed that more than 50% coverage of candidate number 1 protein had a conserved domain that belonged to Alpha-amylase inhibitors, lipid transfer and seed storage protein (AAI-LTSS) superfamily. Candidate number 2 protein had many kelch repeats and homology with nitrile-specifier protein that had a role in changing myrosinase-catalyzed hydrolysis of glucosinolates to form nitrile in place of isothiocyanate in the glucosinolate degradation system (Kong et al. 2012). Candidate gene number 3 encoded a dirigent-like protein that had been given a role in lignan production and was usually induced in response to diseases (Behr et al. 2015). Although candidate number 4 protein had homology with RNA-binding protein Fus, its protein had a ricin B lectin domain that was able to bind to simple sugars like galactose and lactose. Lectins with the ricin-B domain were classified as R- type lectins (Cummings and Etzler 2009). Candidate gene number 5 encoded a mannose/glucose-specific lectin and had two domains, a dirigent domain and Jacalin-like domain (NCBI Resource Coordinators 2016). The last candidate in this group was annotated to be a remorin gene. Most remorins were thought to be induced either under abiotic stress or pathogen infection (Raffaele et al. 2007).

Group II contained all candidates with a significant function of DNA-binding activity. Candidate gene number 7 was annotated as a member that encoded whirly (WHY) transcription factors that had multifarious functions, such as maintaining nuclear and plastid genome stability, RNA splicing, transcription activator for the PR1 gene in potato, and as a transcription repressor for the KP1 gene in Arabidopsis (Desveaux et al. 2000; Grabowski et al. 2008; Majeran et al. 2012; Zhang et al. 2013). Candidate gene number 8 encoded a CAAT-binding transcription factor, Qu et al. (2015) showed that overexpression of wheat CAAT-binding transcription factor enhanced wheat plant growth and grain yield under different nitrogen and phosphorus supply levels. Candidate gene number 9 encoded basic helix-loop-helix 19 (bHLH19) transcription factor, bHLH genes were differentially expressed under cold conditions in rice (Chawade et al. 2013), also bHLH19-like in *Tripogon loliiformis* was down-regulated by MiR5059 (Njaci 2016). A putative nuclease HERBI1 was encoded by gene candidate number 10, the encoded protein has two domains, one domain belonging to the DDE superfamily endonucleases, and the other was a transcriptional regulator ICP4. Candidate gene number 11 encoded a protein with a SANT domain that had a DNA-binding activity (Zhang et al. 2016). MYB transcription factors had this domain

localized in their N-terminal (Bi et al. 2016), though the domain had a principal role in allowing its protein to interact with histones for chromatin remodelling (Boyer et al. 2004). Domains of the translated protein of candidate gene number 12 revealed that it might be a cytosine-S DNA methyltransferase that was responsible for silencing genes by an epigenetic mechanism, through adding a methyl group to the carbon number 5 of the targeted cytosine residues (Zhang and Jacobsen 2006; Pavlopoulou and Kossida 2007). Another DNA-binding protein was gene candidate number 13 that encoded a high mobility group domain (HMG-box) that was found to be conservative in all eukaryotic organisms. Proteins with this domain showed diverse nuclear functions, some functioned as transcription factors or subunits of chromatin remodelling or modulating DNA recombination and repair, while others were recognized to unwind and bend the DNA helix through binding with its minor groove as a manner to induce the assembly of nucleoprotein complexes (Antosch et al. 2012).

Group III candidates included genes that had a post-transcriptional or post-translational activity. Candidate gene number 14 encoded one of a group of pseudo-response regulators (PRRs) which are known to have a function in regulating plant circadian clocks (Kim et al. 2010). This annotation is based on this protein which has an N-terminal signal receiver domain (REC) and C-terminal CCT domain (Farré and Liu 2013). Gene candidate number 15 had a DEAD-box helicase domain which is required for many RNA processing mechanisms, such as splicing, ribosome biogenesis, and RNA degradation (Macovei et al. 2012). Protein candidate number 15 had a methyltransferase domain, with NCBI blastp results (NCBI Resource Coordinators 2016) showing a high homology with the protein arginine N-methyltransferase (PRMT) that catalyses the transfer of a methyl group from S-adenosyl-L-methionine (SAM) to arginines in proteins that may be either RNA-binding proteins or proteins that were involved in transcription (Ahmad et al. 2011). Candidate gene number 17, 18, 19, 20, and 21 encoded mainly as alternative splicing regulators, as all of them had RNA recognition motif domains (RRM domain) for RNA recognition. They were, however, diverse proteins since in addition to their RRM domain they had other distinctive domains. For example, candidate gene number 17 encoded a pre-mRNA processing factor (RSZ22) which was known as serine-arginine rich 22 which had an N-terminal RRM domain and C-terminal arginine-serine rich domain (RS-rich domain) that are mainly involved in controlling alternative splicing mechanisms (Duque 2011). Candidate number 18 had two more zinc-finger domains which were zf-CCHC and ZnF_C2HC next to its RRM domain, while candidate number 20, which annotated as U2 small nuclear ribonucleoprotein auxiliary factor (U2AF), could

recognize 3‘-splice sites, and only had a zf-CCCH domain next to its RRM domain. Candidate 19 had two RRM domains, and candidate 21 had only one RRM domain. Candidate numbers 22 and 23 mainly acted as post-translational regulators with two diverse functions. Because of its UBC domain, regulator number 22 is annotated as ubiquitin-conjugating enzyme E2, and proteins with this domain could covalently attach ubiquitin to target proteins in guiding them to be degraded through proteasome (Xu et al. 2009; Wang et al. 2016). Candidate number 23 may perform a different post-translational function because it is annotated as pyrrolidone-carboxylase peptidase (Pcp). This enzyme was recognized to cleave pyroglutamate (pGlu) from the N-terminal of target proteins to facilitate their degradation by other proteases (Awadé et al. 1994).

Group IV had fifteen genes where some of them were found to have proteins with unknown domain function. For example, gene candidate numbers 39 and 40 are annotated, but they had anonymous function and are not characterized yet. Candidates 37 and 38 were found to not code for any proteins, and so they may be non-coding RNA species. These candidates were grouped in group number IV.

Validation of gene expression under cold treatment conditions by quantitative RT-PCR

In the Group I, target number 1 showed a significant induction under short-kinetics cold conditions in the roots (R), lower part of stems (S2) and leaves (L) after 8 days of cold acclimation in comparison with three days non-acclimated plants (Figure 3.1). While, candidate gene number 2 showed significant upregulation only in roots of 8 days of cold-acclimated plants (Figure 3.1). Target number 3 did not seem to have a clear pattern of induction due to short-kinetics cold treatment, but it was only induced in the lower part of the stems (S) after one day of cold acclimation in comparison with one day non-acclimated plants (Figure 3.1) and showed a significant induction in crown tissues under long-kinetics filed experiment (Figure 3.2). Additionally, Target numbers 4, 5 and 6 showed a significant induction in crown tissues under long-kinetics filed experiment (Figure 3.2). Although, gene number 5 was induced in a consistent pattern in crowns during the field experiment, its expression in the growth chamber experiment showed significant repression due to cold treatment in different tissues (Figure 3.1 and Figure 3.2). Gene number 6 showed a significant induction in both experiments, with more induction in leaf tissues in short-kinetics cold treatments (Figure 3.1 and Figure 3.2).

Regarding the DNA-binding regulators, candidate gene number 7 showed a significant induction in stems and over time during the field cold conditions (Figure 3.3 and Figure 3.4). Gene

numbers 8, 9, 11, 12 and 13 were not significantly regulated by cold treatment in the field (Figure 3.3 and Figure 3.4). On the other extreme, target number 10 was significantly repressed by cold over time in the field (Figure 3.4). Targets 11, 12, and 13 tended to be repressed by cold treatments at 63 days in the long-kinetics experiment (Figure 3.4). All the targets in this group showed a significant regulation by cold during short-kinetics experiment during at least one of the tested points (Figure 3.3).

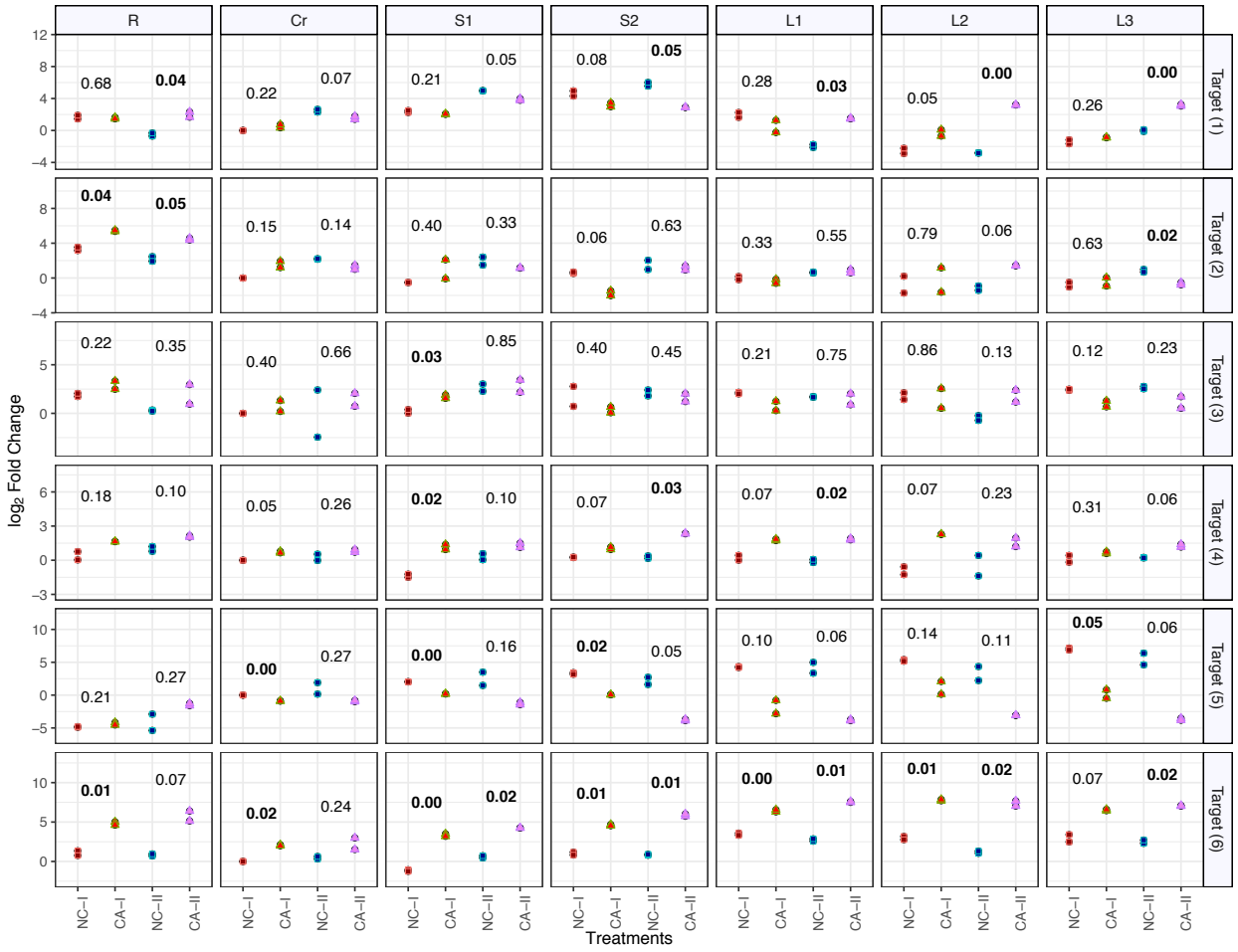

Figure 3.1: Quantitative RT-PCR analysis of targeted candidate genes 1 to 6 (Table S3.1) in different tissues of wheat plants under various cold treatments. Different tissues were coded as R for roots, Cr for crowns, S1 for the lower parts of the stems, S2 for the upper parts of the stems, L1 for the lower part of the leaves, L2 for the middle part of the leaves, and L3 upper parts of the leaves. The log_2 transformed relative expression values of candidate genes in one-week old seedlings subjected to 1 day and 8 days cold (4^0C) exposure treatment were plotted. The t-tests were performed by comparing Log_2 transformed candidate gene expression levels between one-week old seedlings exposed to one day of cold (CA-I) with 8 days old non-treated seedlings (NC-

I), and one-week old seedlings exposed to eight days of cold (CA-II) with 10 days old non-treated seedlings (NC-II). The p-values ≤ 0.05 were considered as statistically significant and indicated in boldface.

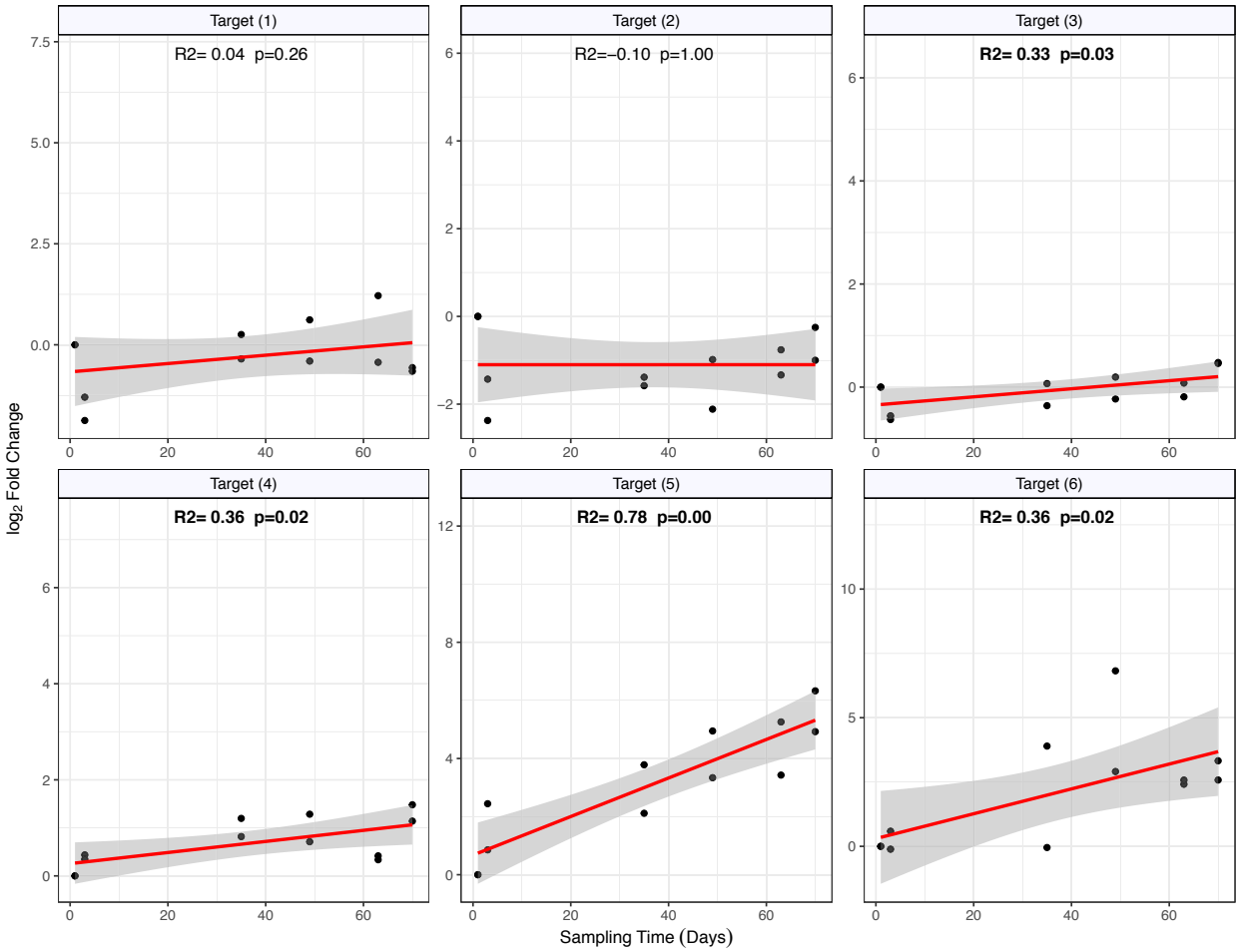

Figure 3.2: Quantitative RT-PCR analysis of targets 1 to 6 (Table S3.1) of wheat crowns sampled at different times from the field experiment according to Q. Li et al. (2017). The sampling times were at days 1, 3, 35, 49, 63 and 70 days. The values are plotted on the graph represent log_2 transformed relative gene expressions levels at different sampling times. The gene expression over time is given as linear regression with adjusted R-square (R2) and p-values (p) were estimated. The p-values ≤ 0.05 were considered as statistically significant and indicated in boldface.

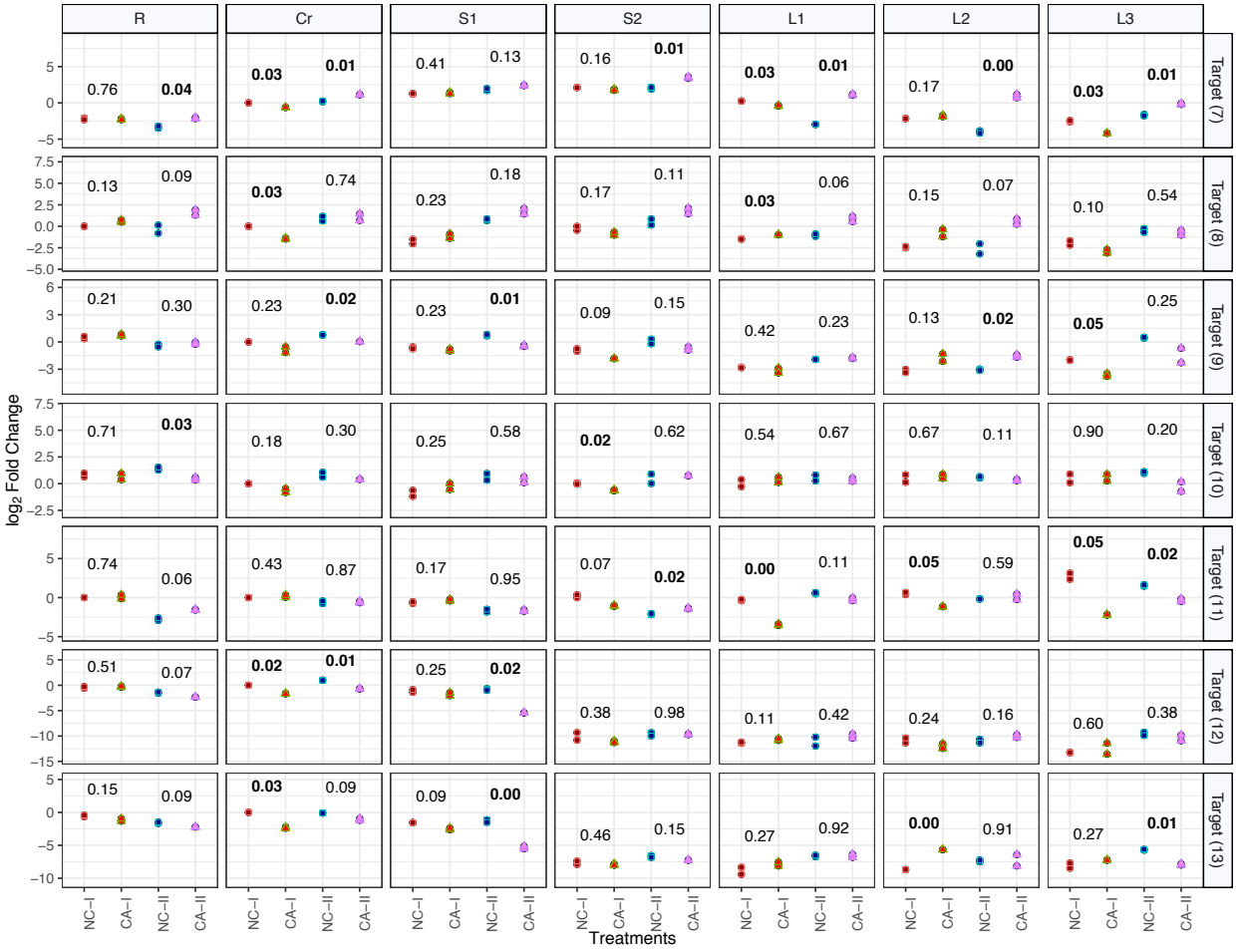

Figure 3.3: Quantitative RT-PCR analysis of targeted candidate genes 7 to 13 (Table S3.1) in different tissues of wheat plants under various cold treatments. Different tissues were coded as R for roots, Cr for crowns, S1 for the lower parts of the stems, S2 for the upper parts of the stems, L1 for the lower part of the leaves, L2 for the middle part of the leaves, and L3 upper parts of the leaves. The log_2 transformed relative expression values of candidate genes in one-week old seedlings subjected to 1 day and 8 days cold (4^0C) exposure treatment were plotted. The t-tests were performed by comparing Log_2 transformed candidate gene expression levels between one-week old seedlings exposed to one day of cold (CA-I) with 8 days old non-treated seedlings (NC-I), and one-week old seedlings exposed to eight days of cold (CA-II) with 10 days old non-treated seedlings (NC-II). The p-values ≤ 0.05 were considered as statistically significant and indicated in boldface.

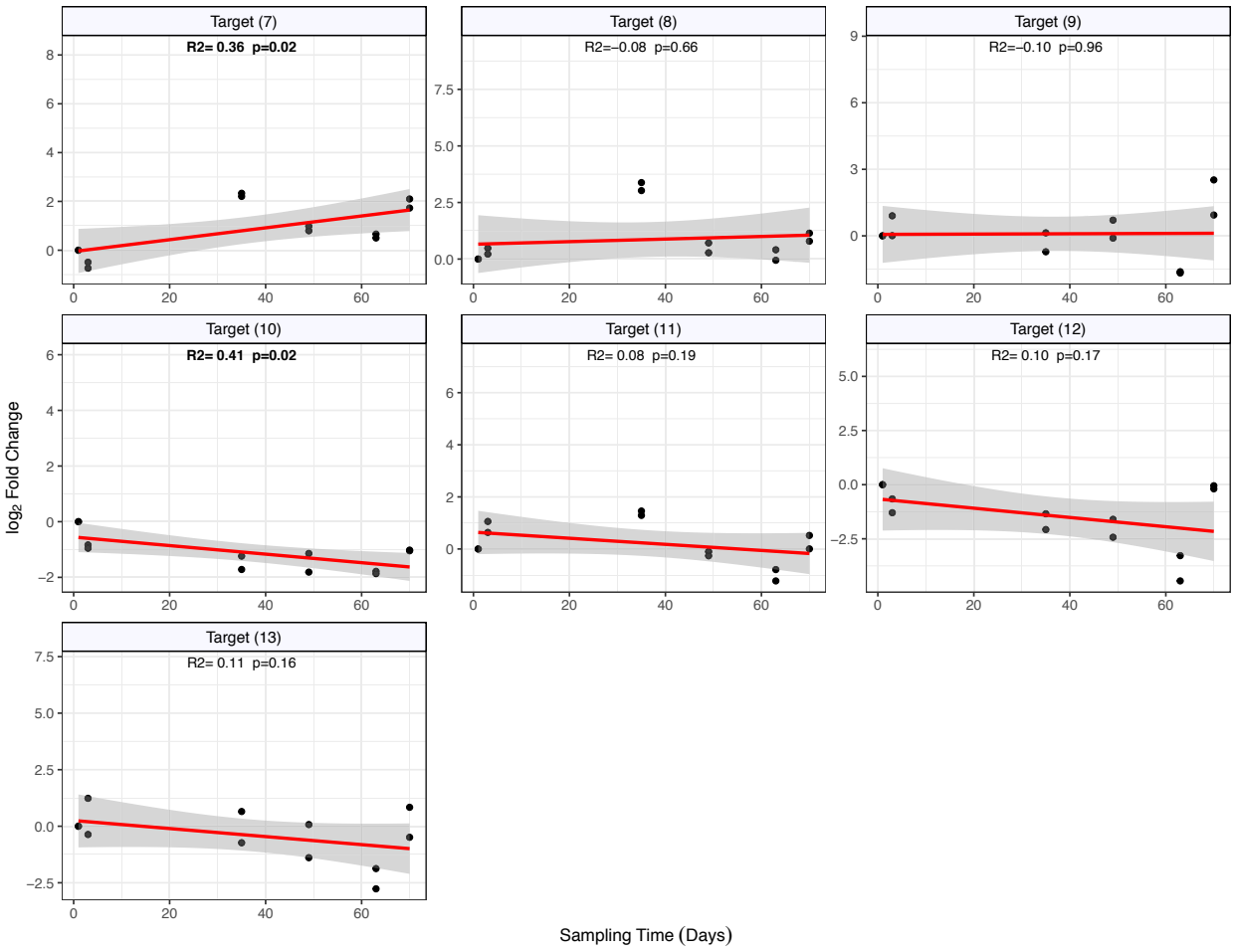

Figure 3.4: Quantitative RT-PCR analysis of targets 7 to 13 (Table S3.1) of wheat crowns sampled at different times from the field experiment according to Q. Li et al. (2017). The sampling times were at days 1, 3, 35, 49, 63 and 70 days. The values are plotted on the graph represent log_2 transformed relative gene expressions levels at different sampling times. The gene expression over time is given as linear regression with adjusted R-square (R2) and p-values (p) were estimated. The p-values ≤ 0.05 were considered as statistically significant and indicated in boldface.

The third group consisting of posttranscriptional and post translational showed slight repression under cold, short kinetics conditions for numbers 14, 17, 18, 19, 20, 21, and 23 in most tissues (Figure 3.5). Moreover, their expression mostly showed a repression pattern in the field

experiment, with regulator number 19 and 23 showed a significant repression as affected by cold in the field with R2=0.47 and p=0.01 (Figure 3.6). On the other hand, target numbers 14 and 15 were significantly upregulated by cold in the field over time (Figure 3.6). Cold treatments in both experiments very slightly induce regulators numbers 15 and 16, however regulator number 15 was repressed only at points 3 and 35 days in the long kinetics experiment (Figure 3.5 and Figure 3.6). Regulator number 22 was slightly induced in almost all tissues with a significant induction in the upper part of the stem (S1) and the middle part of the leaf (L2) (Figure 3.5).

In the last group of genes with unknown functions, numbered 24, 26, 36, and 39 were significantly induced by cold treatments in both experiments (Figure 3.7, Figure 3.8 and Figure 3.9), while genes 27, 28, 38 and 40 showed a significant induction in some tissues, and in the long kinetics experiment, especially in the late points of cold acclimation (Figure 3.7, Figure 3.8 and Figure 3.9). In this group, only candidate number 29 showed a significant repression due to cold treatment in the field (Figure 3.9). Although gene numbers 25, 30, 31, 32, 33, 34, 35 and 37 showed no significant indication of being regulated by cold in the field, they tended to show a significant regulation by cold during at least one point of the short-kinetics experiment (Figure 3.7, Figure 3.8 and Figure 3.9).

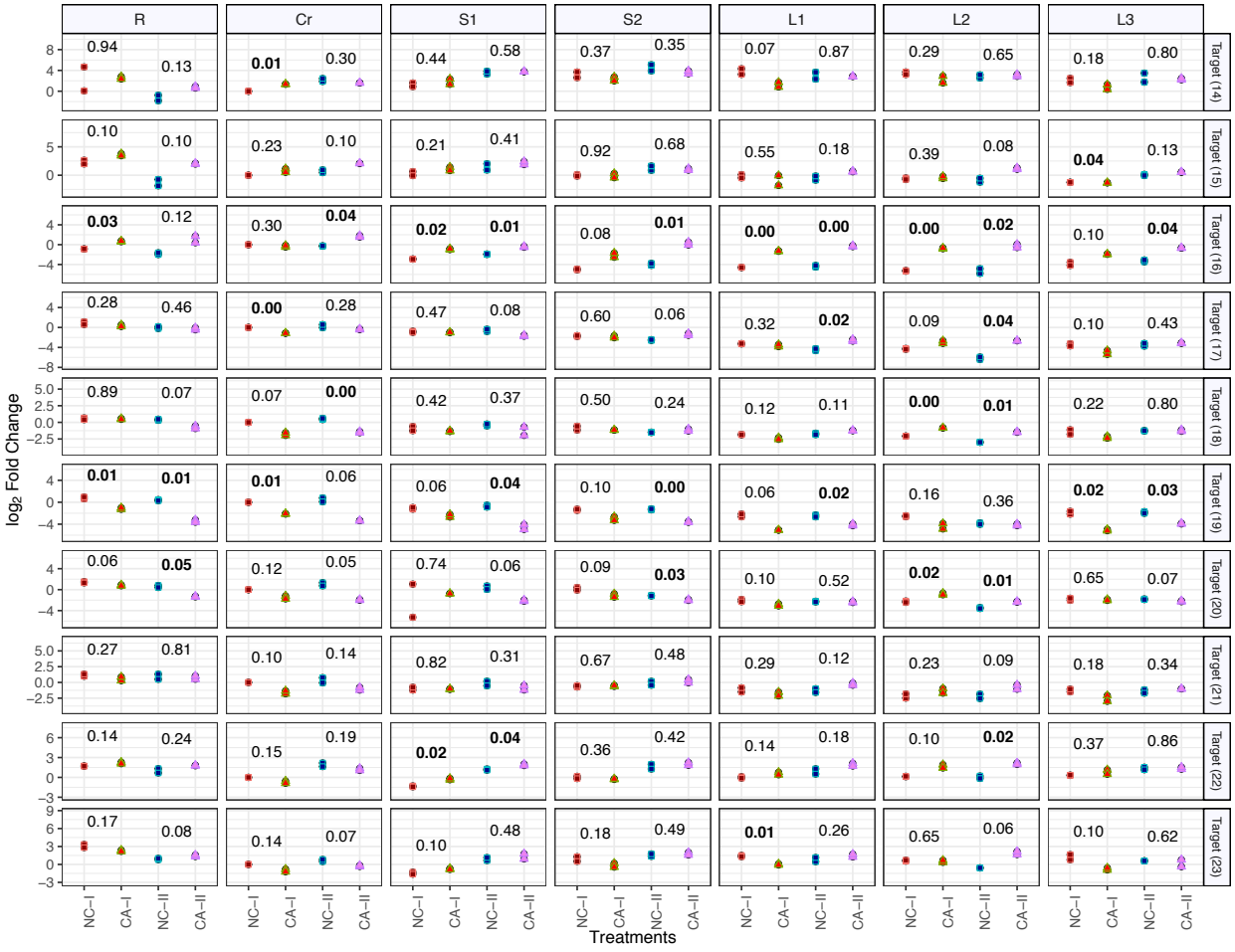

Figure 3.5: Quantitative RT-PCR analysis of targeted candidate genes 14 to 23 (Table S3.1) in different tissues of wheat plants under various cold treatments. Different tissues were coded as R for roots, Cr for crowns, S1 for the lower parts of the stems, S2 for the upper parts of the stems, L1 for the lower part of the leaves, L2 for the middle part of the leaves, and L3 upper parts of the leaves. The log_2 transformed relative expression values of candidate genes in one-week old seedlings subjected to 1 day and 8 days cold (4^0C) exposure treatment were plotted. The t-tests were performed by comparing Log_2 transformed candidate gene expression levels between one-week old seedlings exposed to one day of cold (CA-I) with 8 days old non-treated seedlings (NC-I), and one-week old seedlings exposed to eight days of cold (CA-II) with 10 days old non-treated seedlings (NC-II). The p-values ≤ 0.05 were considered as statistically significant and indicated in boldface.

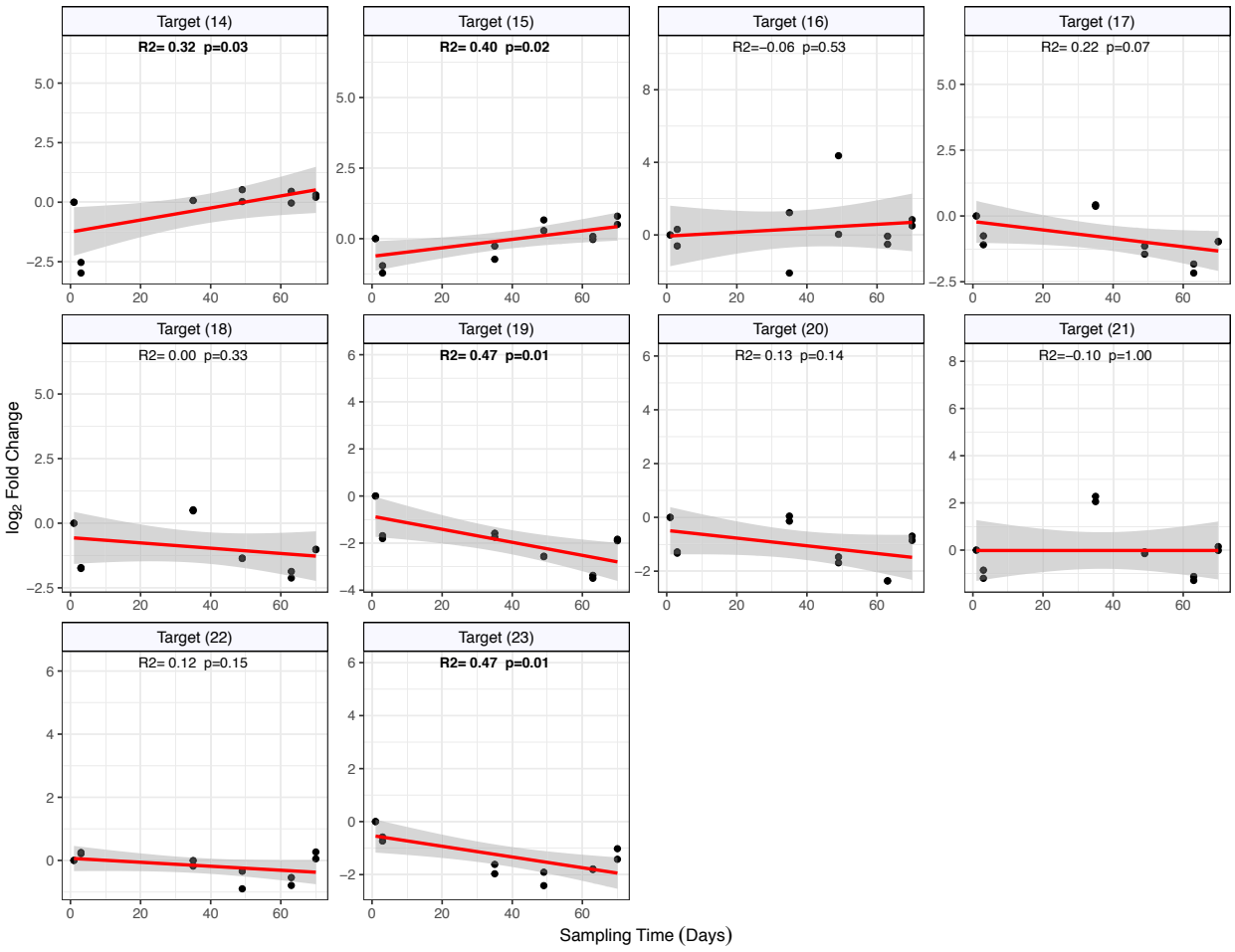

Figure 3.6: Quantitative RT-PCR analysis of targets 14 to 23 (Table S3.1) of wheat crowns sampled at different times from the field experiment according to Q. Li et al. (2017). The sampling times were at days 1, 3, 35, 49, 63 and 70 days. The values are plotted on the graph represent $\log_2$ transformed relative gene expressions levels at different sampling times. The gene expression over time is given as linear regression with adjusted R-square (R2) and p-values (p) were estimated. The p-values ≤ 0.05 were considered as statistically significant and indicated in boldface.

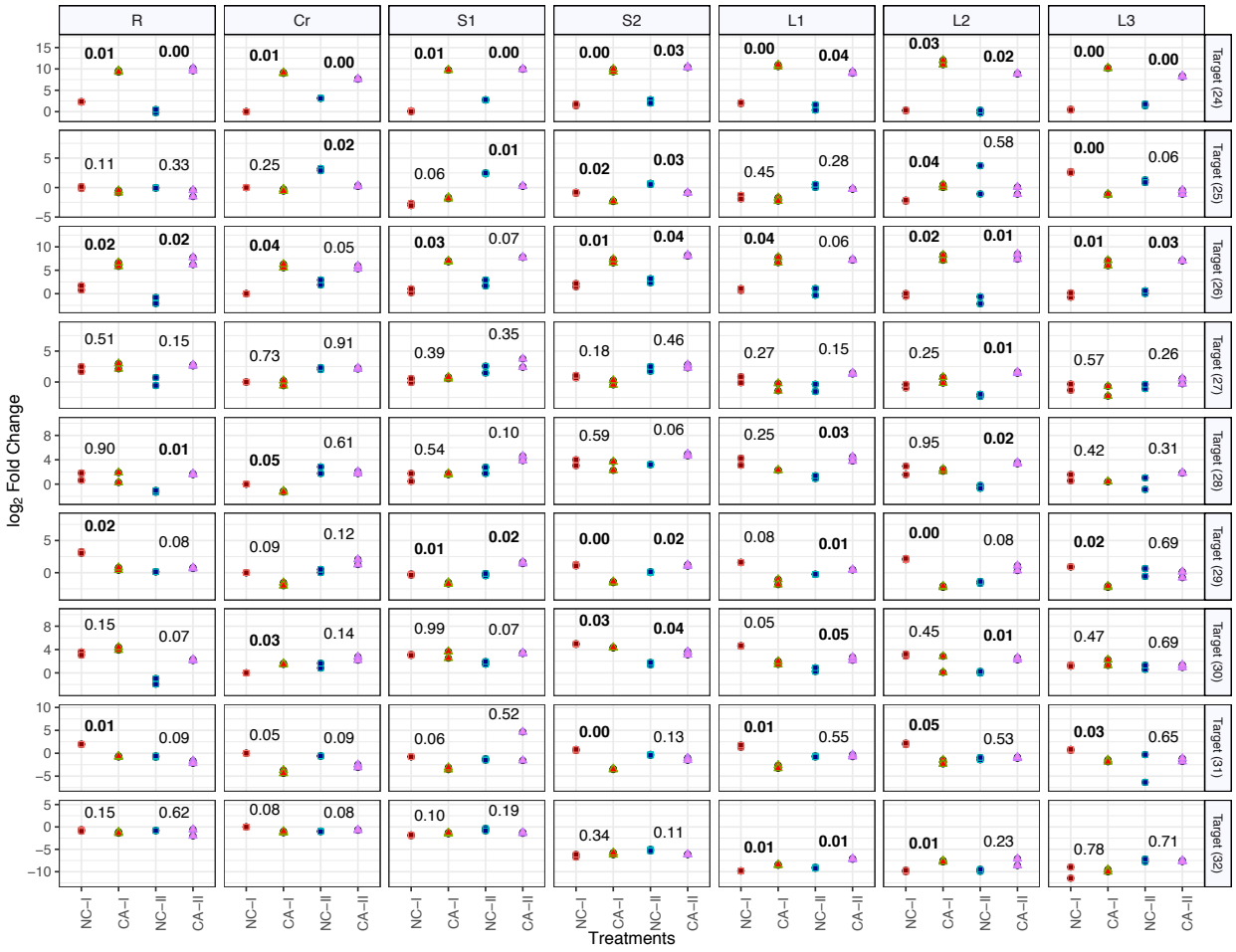

Figure 3.7: Quantitative RT-PCR analysis of targeted candidate genes 24 to 32 (Table S3.1) in different tissues of wheat plants under various cold treatments. Different tissues were coded as R for roots, Cr for crowns, S1 for the lower parts of the stems, S2 for the upper parts of the stems, L1 for the lower part of the leaves, L2 for the middle part of the leaves, and L3 upper parts of the leaves. The log_2 transformed relative expression values of candidate genes in one-week old seedlings subjected to 1 day and 8 days cold (4^0C) exposure treatment were plotted. The t-tests were performed by comparing Log_2 transformed candidate gene expression levels between one-week old seedlings exposed to one day of cold (CA-I) with 8 days old non-treated seedlings (NC-I), and one-week old seedlings exposed to eight days of cold (CA-II) with 10 days old non-treated seedlings (NC-II). The p-values ≤ 0.05 were considered as statistically significant and indicated in boldface.

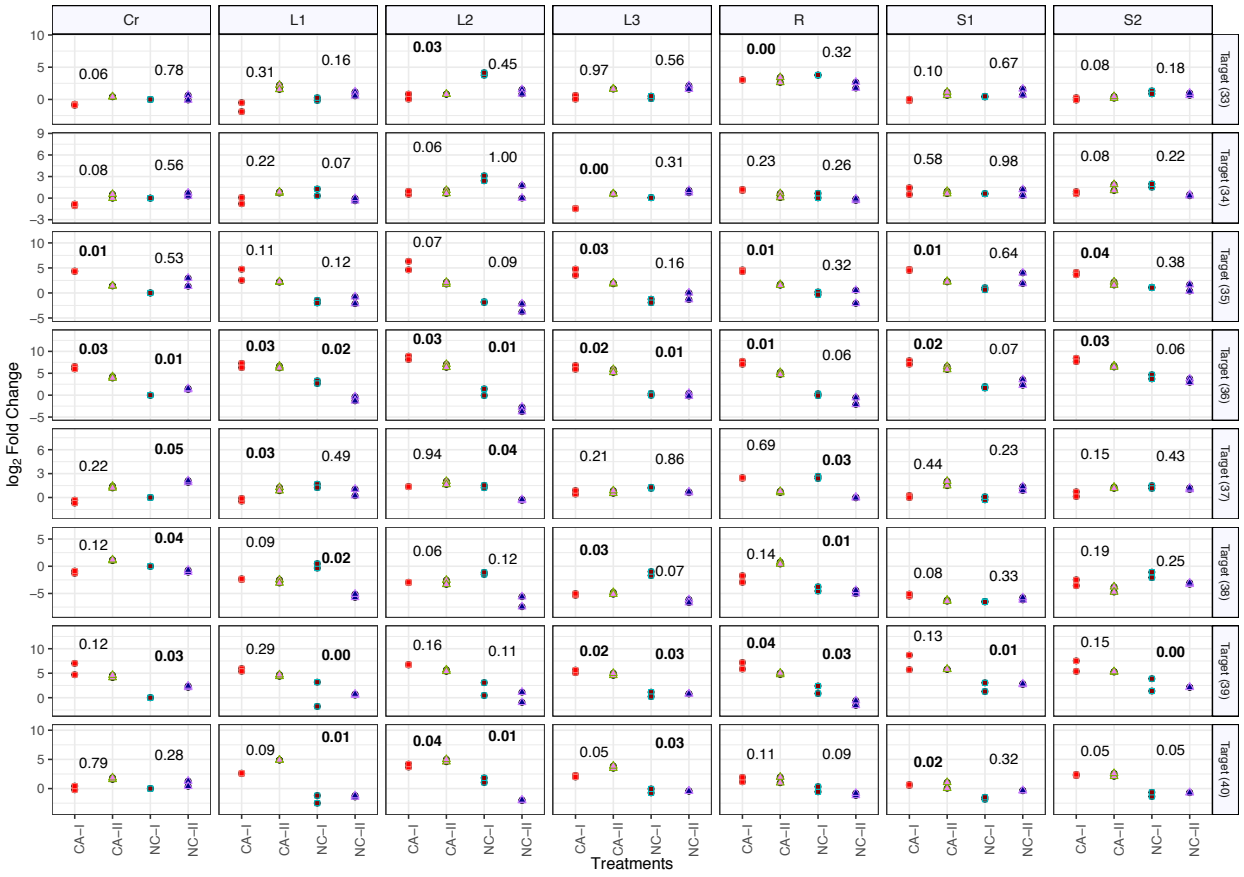

Figure 3.8: Quantitative RT-PCR analysis of targeted candidate genes 33 to 40 (Table S3.1) in different tissues of wheat plants under various cold treatments. Different tissues were coded as R for roots, Cr for crowns, S1 for the lower parts of the stems, S2 for the upper parts of the stems, L1 for the lower part of the leaves, L2 for the middle part of the leaves, and L3 upper parts of the leaves. The log_2 transformed relative expression values of candidate genes in one-week old seedlings subjected to 1 day and 8 days cold (4^0C) exposure treatment were plotted. The t-tests were performed by comparing Log_2 transformed candidate gene expression levels between one-week old seedlings exposed to one day of cold (CA-I) with 8 days old non-treated seedlings (NC-I), and one-week old seedlings exposed to eight days of cold (CA-II) with 10 days old non-treated seedlings (NC-II). The p-values ≤ 0.05 were considered as statistically significant and indicated in boldface.

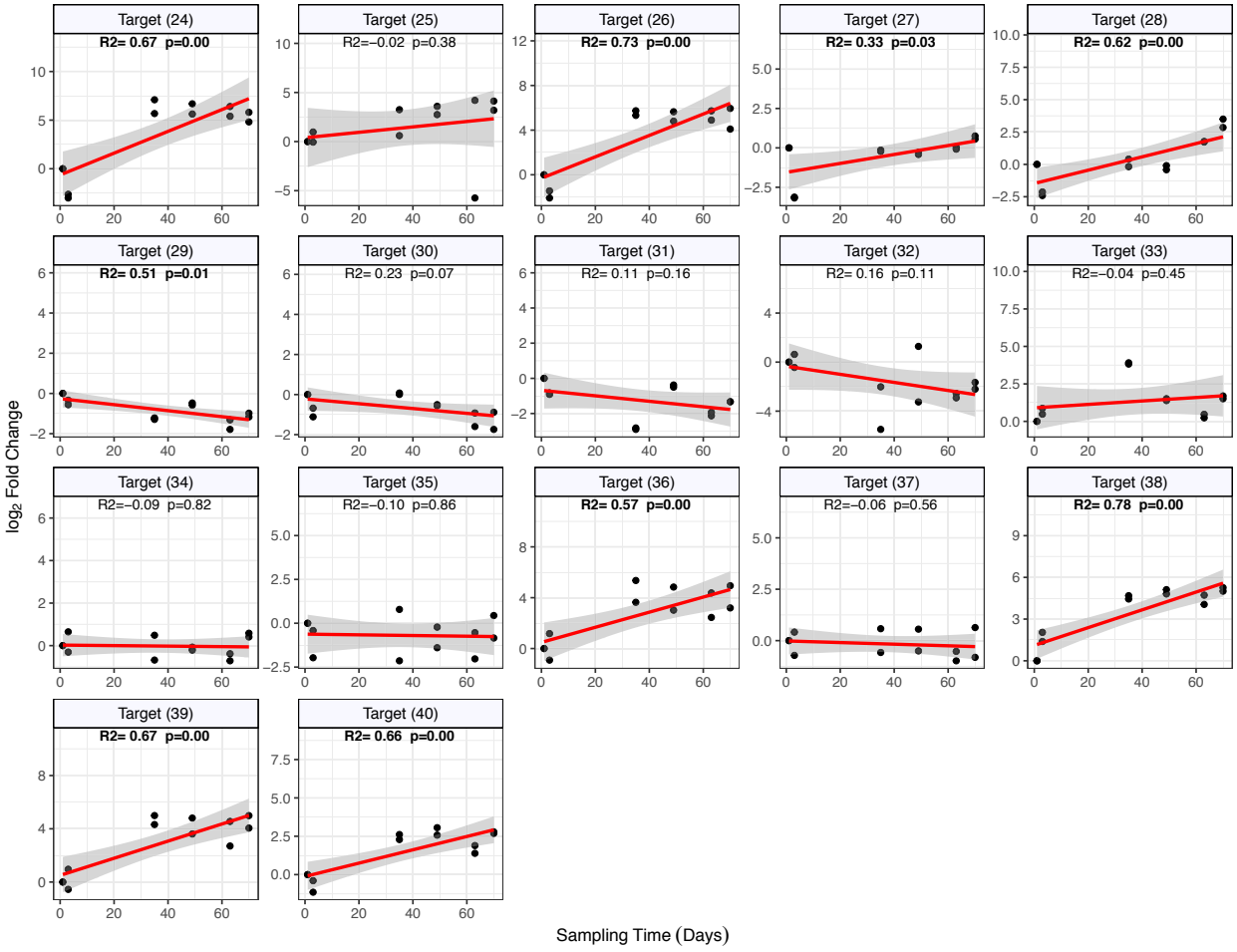

Figure 3.9: Quantitative RT-PCR analysis of targets 24 to 40 (Table S3.1) of wheat crowns sampled at different times from the field experiment according to Q. Li et al. (2017). The sampling times were at days 1, 3, 35, 49, 63 and 70 days. The values are plotted on the graph represent $\log_2$ transformed relative gene expressions levels at different sampling times. The gene expression over time is given as linear regression with adjusted R-square (R2) and p-values (p) were estimated. The p-values ≤ 0.05 were considered as statistically significant and indicated in boldface.

Detailed expression analyses of gene candidate gene numbers 24 and 39

The qPCR screening of the forty genes revealed many promising candidates whose functions are still unknown. From these candidates, we selected numbers 24 and 39 for more detailed analysis regarding their expression in winter versus spring wheat, across different tissues and as affected by ABA or JA treatments. The results showed that both genes are significantly

upregulated during the short and long phase of cold acclimation with a more significant increase during extended periods of cold acclimation in winter wheat Norstar versus spring wheat Manitou (Figures 3.10A and 3.11A). Additionally, both genes were expressed in all the selected tissues – leaves, stems, crowns and roots – with no significant differential expression among the tissues as indicated by ΔCq values (Figures 3.10B and 3.11B). Finally, both genes were significantly upregulated by ABA treatment while JA treatment significantly upregulates only gene number 24 and down-regulates number 39 (Figures 3.10C and 3.11C).

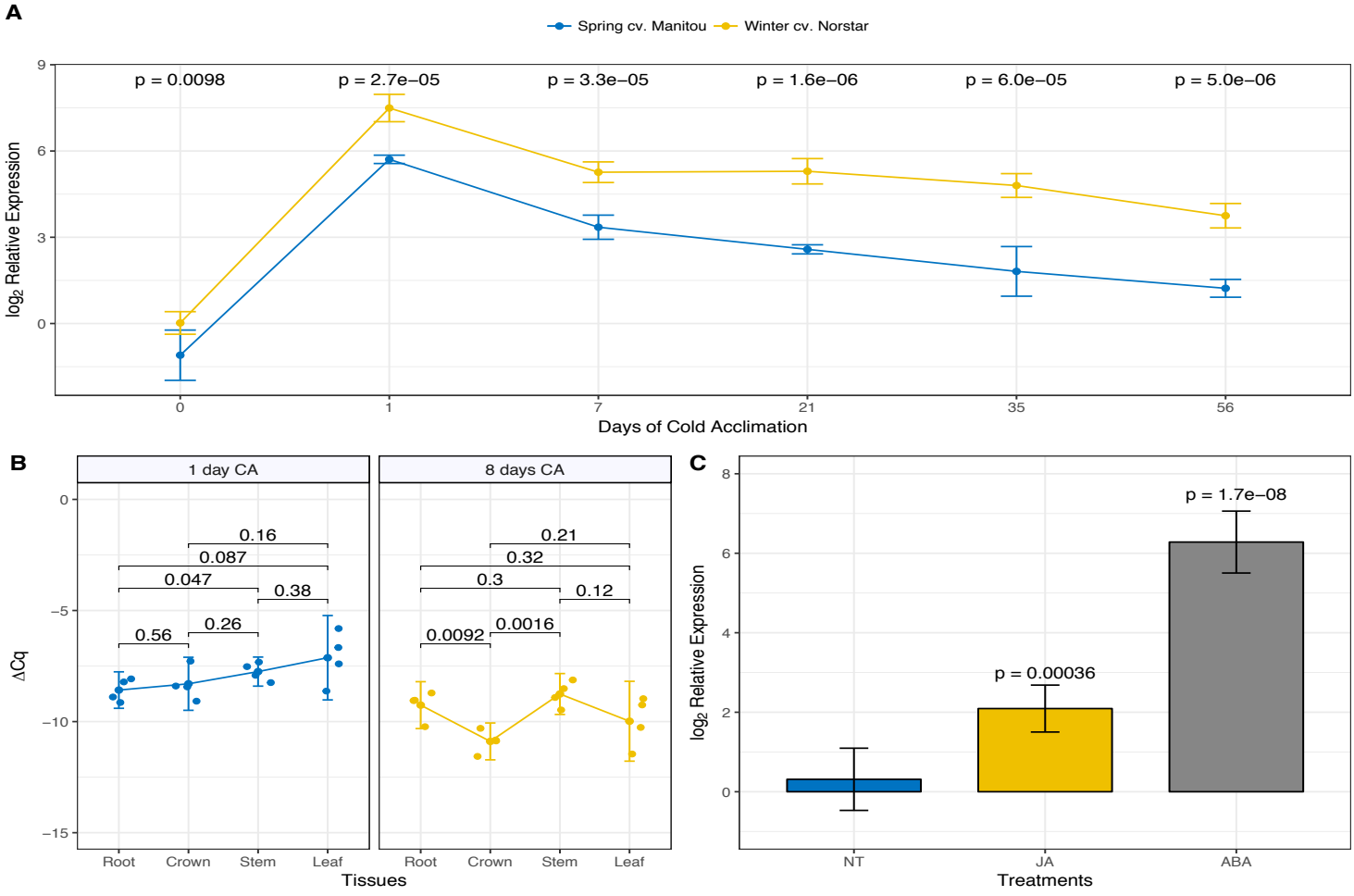

Figure 3.10: Relative expression analysis of the gene candidate number 24 (Table S3.1), including **(A)** relative expression analysis in the crowns of winter wheat norstar versus spring wheat manitou during different cold acclimation periods **(B)** relative expression analysis across different tissues and **(C)** relative expression analysis after four hours of hormone treatments versus NT (mock-treated plants). Statistical analysis was performed on two biological replicates for each point where

each biological replicate has two technical replicates. Error bars indicate the 95% confidence interval (CI) and the figure presents p-values between different points where as examples in (A) time point zero displays p-value significance of norstar versus manitou at this point and in (C) p-value displays significance regarding the treated versus mock-treated (NT).

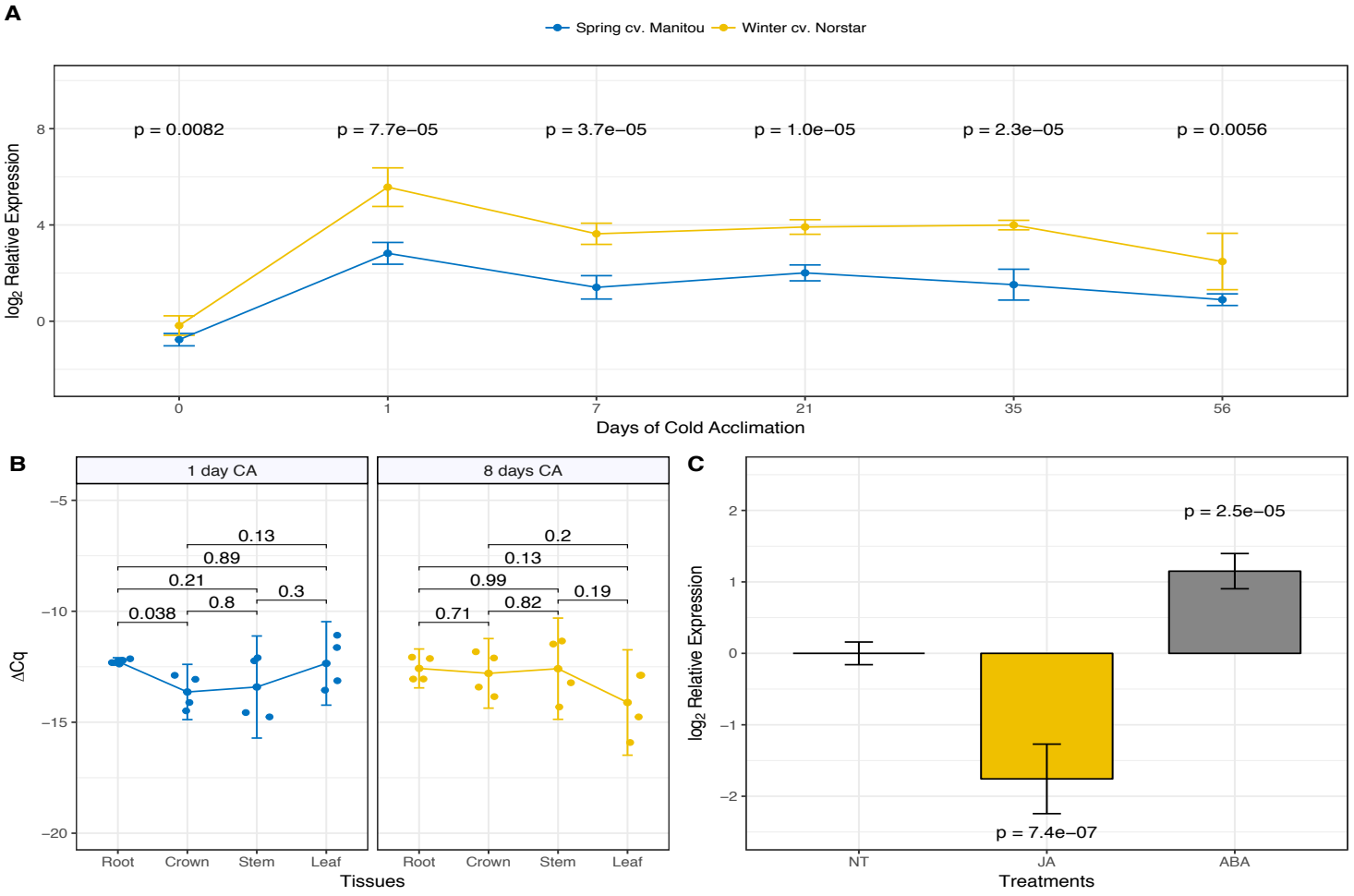

Figure 3.11: Relative expression analysis of the gene candidate number 39 (Table S3.1), including **(A)** relative expression analysis in the crowns of winter wheat norstar versis spring wheat manitou during different cold acclimation periods **(B)** relative expression analysis across different tissues and **(C)** relative expression analysis after four hours of hormone treatments versus NT (mock-treated plants). Statistical analysis was performed on two biological replicates for each point where each biological replicate has two technical replicates. Error bars indicate the 95% confidence interval (CI) and the figure presents p-values between different points where as examples in (A)

time point zero displays p-value significance of norstar versus manitou at this point and in (C) p-value displays significance regarding the treated versus mock-treated (NT).

Discussion

The ability of the cold-tolerant winter wheat plants to change their transcriptome in a manner to tolerate cold conditions is well studied by global gene expression technologies, such as microarrays and RNA-Seq (Skinner 2009; Laudencia-Chingcuanco et al. 2011; Kane et al. 2013; Li et al. 2018). We show the importance of exploring microarray data and validating them by qPCR to highlight the most significant genes that may play a crucial role in protecting wheat plants under icy conditions. We flagged forty candidate genes from their predicted protein domains and used qPCR to validate their expression in different tissues under short growth kinetics and in crowns under prolonged periods of cold treatments. Many of these candidates show a response either in one or both experiments, though further study is needed to investigate their function in the wheat plant under cold treatment.

Defence-related regulators

Studies have shown that some defence-related proteins accumulate during the periods of cold acclimation (Griffith and Yaish 2004; Dumont et al. 2011; Espevig et al. 2012). Regulator numbers 4 and 6 (R-type lectin and remorin, respectively), show a significant induction due to cold treatments in both experiments and across some different tissues (Figures 3.1 and 3.2). Lectins are a family of carbohydrate-binding proteins that play diverse roles in protecting plants against abiotic and biotic stresses (Jiang et al. 2010). Regulator number 4, with its ricin-B-lectin, is expected to play a role in defence mechanisms during cold acclimation conditions as most of the R-type lectins that accumulate either in the vacuole or the apoplast and can remove highly conserved adenine residues from the sarcin/ricin loop of 28S ribosomal RNA by their RNA N-glycosidase activity. Thus their proteins block other protein syntheses by inhibiting ribosomes from binding with elongation factor 2 (Lannoo and Van Damme 2014). Remorins are plant-specific proteins which are known to accumulate under abiotic and biotic stresses. Among large number of genes in the family, some are specific to pathogen attack, nodule formation, cold and drought conditions and they are also involved in coordinating hormone cross-talk (Raffaele et al. 2007; Gui et al. 2016). The molecular function of the wheat R-type lectins and remorins due to abiotic stress had not been studied before, while our results show that they may have functions in cold tolerance traits acquisition. Gene candidate number 5 shows a significant induction by cold over time in the field

(Figure 3.2), while it shows a significant repression during the first phase of cold-treatment in the short-kinetics experiment in crown, stems and upper part of the leaf tissues (Figure 3.1). This candidate is a member of mannose/glucose-specific lectins, with its dirigent and Jacalin-like domains, has a structural similarity with TaJA1 that is induced by jasmonic acid. Its overexpression in tobacco confers resistance against the pathogenic bacteria, *Pseudomonas syringe* (Ma et al. 2013). The unusual expression of this regulator may indicate a new functional mechanism in cold adaptation, as its transcript accumulates in crowns of wheat plants grown under field experiment (Figure 3.2). Yet its gene expression is repressed in all other tissues except the roots during the cold acclimation period of the short kinetics experiment (Figure 3.1). This gene expression behaviour demands further study to elucidate its function. Regulator number 1 shows a significant repression in the upper part of the stems. Though, it exhibits a significant induction during the second phase of the cold treatment in the short-kinetics experiment in crown, lower part of the stems and leaf tissues (Figure 3.1). Regulator number 4 is significantly induced in stems and lower part of the leaf during short cold acclimation conditions. While the function of regulator number 4 was not revealed, its klech repeat domains indicates homology with nitrile-specifier protein and raises the question as to whether some wheat tissues need to accumulate nitriles during short cold acclimation conditions rather than other tissues. Regulator number 1 is one member in the sizeable AAI-LTSS superfamily (Alpha-Amylase Inhibitors (AAI), Lipid Transfer (LT) and Seed Storage (SS) Protein family), and its function during cold acclimation is still speculative.

DNA-binding Proteins

Many of the screened genes that have been identified as DNA-binding proteins, did not show a high magnitude of regulation by cold treatment. However, the low magnitude of change may have a physiological role in abiotic stress tolerance. Targets number 10 and 12 seem to be down-regulated in crowns even with small decreases in the temperature of both experiments, and in the root tissues of the short-kinetics experiment (Figure 3.4). However, the significant repression was in the crowns and lower part of the stems for regulator number 12 and mostly in the leaf tissues for regulator number 11 (Figure 3.3). Regulator number 12 is annotated as a harbinger (HARBI1) protein which is not only known for its transposase activity but also its roles in controlling transcription of other genes and other epigenetic functions (Kapitonov and Jurka 2004). In addition to this, regulator number 12 is cytosine-5 DNA methyltransferase, which controls the transcription of other genes by an epigenetic silencing mechanism (Zhang and Jacobsen 2006).

Genes 7, 8, and 11 were highly induced in the wheat crown tissues under field conditions at 35 days, then the accumulation of their transcripts was down-regulated at 49 and 63 days, but slightly induced at 70 days (Figure 3.4). These three regulators have mostly the same expression patterns as affected by cold conditions in the field. The expressions of genes 7 and 8 were induced by low-temperature under short kinetics conditions in most tissues (Figure 3.3). As target number 7 is annotated as the WHY1 transcription factor, its function is likely to maintain plastid genome stability, regulating telomere length homeostasis, and controlling the transcriptional activity of other genes (UniProt Q9M9S3). Target number 8 which is annotated as CAAT-binding transcription factor B (Table S3.1) and a related protein in wheat is found to be necessary for root development, and its overexpression increases grain yield in wheat (Qu et al. 2015). Target number 11 is a DnaJ homolog subfamily C member 2; its exclusive SANT domain in the N-terminal suggests it is a nuclear protein (Zhang et al. 2016). This gene showed a significant down-regulation in wheat plant leaves of the short-kinetics experiment (Figure 3.3). The transcript of bHLH19 gene or candidate number 9 accumulates slightly in roots and significantly in the middle of the leaves, while it is repressed in crowns, stems, and the tip of the leaves. Moreover, the transcript of the HMG gene or regulator number 13 is repressed only in crowns, roots, and stems, though with their multiple functions it is hard to predict the role of their repression or accumulation in these distinct tissues.

Post-transcriptional and post-translational Genes

Candidate numbers 14, 15, 17, 18, 19, 20, 21, and 23 show a decline in their expressions once the temperature goes down as indicated in the field experiment (Figure 3.6), while their expressions varies across the tissue samples in the short kinetics experiment (Figure 3.5). These regulators control alternative splicing processes in the plant, except for regulator number 23 that is annotated as pyrrolidone carboxyl peptidase. Staiger and Brown (2013) showed the impact of alternative splicing in controlling most biological processes, such as the circadian clock, defence, development, and tolerance to biotic and abiotic stresses. Their work and this study support the notion that discovering the function of these genes and the timing of their expression is a crucial point to understand gene to gene regulation during stress conditions. Similarly, post-translational regulator elements that are vital in limiting the accumulation of other proteins, or in their production of mature functional proteins helps the cell to tolerate abiotic stresses.

Genes of unknown functions

Many genes with unknown function show either induction or repression under cold treatments (Figures 3.7, 3.8 and 3.9). Some encode proteins with unknown domain functions, and others are non-coding RNA species (genes number 37 and 38). Detailed expression analyses show that genes 24 and 39 are ABA-regulated genes while JA upregulates gene 24 and downregulates gene 39. Additionally, both genes show significant upregulation in the winter wheat versus the spring version especially during the extended period of cold acclimation (Figures 3.10 and 3.11). This indicates their significant prospective role in conferring cold-tolerance traits. Identifying the functions of these unknown genes are crucial in many biotechnological aspects.

Conclusion

In conclusion, this work sheds light on the value of data mining on gene function predictions and discovery. We have selected 40 genes with diverse functions from global gene expression studies of microarray or RNA-Seq technologies (Skinner 2009; Laudencia-Chingcuanco et al. 2011; Kane et al. 2013; Li et al. 2018), for investigating their transcripts' accumulations across different tissues in growth-champers (Short-growth kinetics) and crown tissues during different growth time points of cold acclimation in the field (long-growth kinetics). This gene expression study was performed using qPCR. According to their predicted functions, the selected genes were grouped into four main groups (Table 1). These groups are defence-related gene candidates, DNA-binding proteins, genes of unknown functions and post-transcriptional and post-translational genes.

The results showed that from the defence-related genes; regulators 4, 5 that are annotated as lectins, regulator 6 which is a remorin-encoding gene and regulator number 1 that belongs to AAI-LTSS superfamily are cold-regulated genes. Many speculative DNA-binding candidate proteins were found to be up-regulated during T3 time point (35 days) of cold-acclimation in the field, such as candidate numbers 7, 8 and 11 that are annotated as a WHY1 transcription factor, CAAT-binding transcription factor and DnaJ homolog superfamily C number 2, respectively.

On the other hand, candidate genes 15, 17, 18, 19, 20 and 21 that control alternative splicing events, were repressed in crown tissues as affected by low-temperature conditions in the field, with a significant pattern of repression over time for candidate numbers 15, 18 and 19 (Figure 3.6). Additionally, many genes with unknown functions were found to be cold-regulated genes, such as genes number 24 and 39 (Figures 3.7, 3.8 and 3.9). Furthermore, detailed expression of analyses

of candidate numbers 24 and 39, showed that the former is upregulated by ABA and JA while the latter by ABA only, and both are significantly upregulated in winter wheat more than spring wheat (Figures 3.10 and 3.11).

Finally, flagging candidate genes that are cold-regulated is the first step for more function studies that will enhance our understanding of the development of cold-tolerance associated traits in plants with a winter background.

Chapter Four: Genome-Wide Identification and Characterization of the Wheat Remorin (TaREM) Family and its Association with Cold Tolerance

Abstract

Remorins (REMs) are plant-specific proteins that play an essential role in plant-microbe interactions. However, their roles in vernalization and abiotic stress responses remain speculative. Most remorins have a variable proline-rich N-half and a more conserved C-half that is predicted to form coils. A search of the wheat database revealed the existence of twenty different remorin genes that we classified into six groups sharing a common phylogenetic and structure origin. Promoter analysis of TaREM genes revealed the presence of putative cis-elements related to diverse functions like development, hormonal regulation, biotic and abiotic stress responsiveness. Expression levels of TaREM genes were measured in plants grown under in field and laboratory conditions and in response to hormone treatment. Our analyses revealed twelve members of the remorin family that are regulated during cold acclimation of wheat in four different tissues (root, crown, stem and leaves), with the highest expression in roots. Differential gene expression was found between wheat cultivars with contrasting degree of cold tolerance suggesting the implication of TaREM genes in cold response and tolerance. Additionally, eight genes were induced in response to ABA and MetJA treatment. This genome-wide analysis of TaREM genes provides valuable resources for functional analysis aimed at understanding their role in stress adaptation.

Introduction

Remorins (REMs) are plasma membrane-associated proteins found explicitly in all embryophytes including angiosperms, gymnosperms, pteridophytes, and bryophytes (Checker and Khurana 2013). Although remorin proteins are specifically associated with the plasma membrane, they lack a transmembrane domain. They are characterized by a conserved C-terminal region with the signature coiled-coil structure (Marín et al. 2012), and a dynamic membrane-anchoring motif (Perraki et al. 2014). Experimental evidence showed that the C-terminal region plays a determinant role in the mechanism by which most REM proteins bind specifically to the inner leaflet of membrane domains. This binding is mediated by S-acylation of cysteine residues in a C-terminal hydrophobic core (Konrad et al. 2014). The N-terminal region is highly variable and harbours many residues that can be phosphorylated under a wide range of biological conditions (Marín et al. 2012; Marín and Ott 2012). Using yeast two-hybrid interaction assay in Arabidopsis, Marín et

al. (2012) demonstrated that the phosphorylation of Ser-residue (Ser-66) in the intrinsically disordered N-terminal region of AtREM1.3 mediates protein-protein interactions, and may constitute a regulatory domain stabilizing these interactions.

REMs have diverse functions in plant-microbe interactions (Campo et al. 2008; Jarsch and Ott 2011), and plant defence against some pathogens (Jacinto et al. 1993; Reymond et al. 1996; Raffaele et al. 2009), and have been found in membrane lipid rafts and plasmodesmata. It was been inferred that REMs impair cell-to-cell movement of the Potato Virus X by directly binding to the virus' movement protein TGBp1 (Raffaele et al. 2009). Other REMs, identified as membrane-raft-associated proteins, interact with signalling proteins such as receptor-like kinases (RLK) or act as scaffold proteins (Lefebvre et al. 2010).

Recent studies report that REMs are critical factors for plant signaling cascades, particularly during plant-microbe interactions (Raffaele et al. 2009; Lucau-Danila et al. 2010; Tóth et al. 2012; Demir et al. 2013), and play essential roles in signal transduction and plasma membrane trafficking (Reymond et al. 1996; Marín et al. 2012; Marín and Ott 2012; Tóth et al. 2012). REMs participate in plant hormone responses, as well as in the cross-talk in a variety of plant developmental processes (Bariola et al. 2004; Gui et al. 2016). They are also associated with apical, vascular and embryonic tissues (Bariola et al. 2004), involved in somatic embryogenesis as found in chicory (Lucau-Danila et al. 2010), and in regulating stem development and phloem formation in *Populus deltoides* (Li et al. 2013). OsREM4.1 protein coordinates the antagonistic interaction between abscisic acid (ABA) and brassinosteroid (BR) signalling pathways to regulate plant growth and development (Gui et al. 2016). In rice, the REM setting defect1 (GSD1) gene affects grain setting through regulating plasmodesmata conductance by interacting with actin. An over expression in GSD1 leads to a reduction in grain setting rate, carbohydrate accumulation in leaves, and soluble sugar content in the phloem exudates (Gui et al. 2014; Gui et al. 2015). Recently, Gui et al. (2016) found that the OsREM4.1 plays an essential function in equilibrating plant growth with the surrounding growth environments in rice.

In addition to their role in plant defence and development, there is evidence that REMs may play a role in plant adaptation to environmental conditions. The mulberry remorin (MiREM) transcript was induced during salt and water stress in mature leaves (Checker and Khurana 2013). In millet, the SiREM6 transcript was induced by high salt and cold treatment, but not by drought stress (Yue et al. 2014). The overexpression of these two remorin genes improved salt (Checker and Khurana 2013; Yue et al. 2014), and dehydration tolerance (Checker and Khurana 2013), in

transgenic Arabidopsis during seed germination and seedling developmental stages. Although, the remorin gene family has been investigated in potato (Jacinto et al. 1993), tobacco (Mongrand et al. 2004), tomato (Bariola et al. 2004), Arabidopsis (Bhat et al. 2005), rice (Raffaele et al. 2007), and Medicago (Lefebvre et al. 2007), the structural features, phylogenetics, and functional properties of the REMs gene family in common wheat (*T. aestivum*) have not been studied, especially in relation to cold tolerance and hormonal regulation.

In this study, 20 TaREM genes were identified from Ensembl wheat genome sequences and RNA-Seq data. Phylogenetic analysis, chromosomal localization, and expression profiling of these REMs were investigated during phenological development, cold acclimation, and in response to hormonal treatment. The analyses revealed that TaREMs are expressed in many different tissues. Several members of the wheat REM family were regulated during cold acclimation and associated with cold tolerance while others responded to ABA and Methyl jasmonate (MetJ) treatment. This genome-wide analysis of TaREM genes provides valuable resources for functional analysis to determine their role in stress adaptation.

Materials and Methods

Plant material and environmental conditions

Norstar (Grant 1980) winter, and Manitou (Campbell 1967) spring wheat (*T. aestivum* L.) cultivars were used for gene expression experiments where plants were grown in environmentally controlled growth chambers as previously described (Badawi et al. 2007). Cold treatment (4°C) and sampling dates are indicated in Figures 4.7 and 4.8. ABA and MetJ treatments were performed as described previously (Danyluk et al. 1998; Diallo et al. 2014). Briefly, two groups of seedlings were sprayed with 150 µM MeJA or 100 µM ABA dissolved in 0.1% tween 20 solutions respectively. Each group of treated plants was watered with the same treatment solution. The untreated plants received a mock treatment of 0.1% tween 20 solution and used as a control. The samples were collected at the indicated time points. For the tissue-specific experiment, different tissues representing the seedling, root, crown, stem and leaves were collected at each sampling date. For all experiments, two biological replicates were collected for each sample for expression analysis

For RNAseq analyses, developing crowns of Norstar and Manitou wheat grown under field conditions were collected at five-time points in 2010 as described by Q. Li et al. (2017). Two

biological replicates were collected for each sampling date and immediately frozen in liquid nitrogen and stored at −80°C for analysis.

Identification of the *REM* genes in *Triticum aestivum*

In order to investigate the REM gene family in wheat, all REM sequences of *O. Sativa* were used as queries for a blast search against the whole genome sequence of *T. aestivum* cv. Chinese Spring (release no. 31) from Ensembl Plants databases (http://plants.ensembl.org) (Kersey et al. 2014) with an expectation value of 0.01. All potential REM proteins were further screened to confirm the presence of the REM domain by NCBI. The REM sequences were confirmed based on the presence of a remorin domain, and the putative REM proteins were aligned to rice and Arabidopsis. Remorin proteins were classified into different groups, as described by Raffaele et al. (2007). All putative annotation of the REM genes was retrieved from the *T. aestivum* genome website (https://wheat-urgi.versailles.inra.fr/Seq-Repository/Annotations).

Phylogenetic and Mapping Analyses

Rice and wheat REM protein sequences were obtained from NCBI (http://www.ncbi.nlm.nih.gov/protein/) and Ensembl (http://plants.ensembl.org) (Kersey et al. 2014), databases. These sequences were analyzed and 20 TaREM and 20 OsREM genes were aligned using MUSCLE (http://www.ebi.ac.uk/Tools/msa/muscle/). A neighbor-joining (NJ) phylogenetic tree of remorin_C domain sequences was constructed with 500 bootstrap replicates implemented in the MEGA (Molecular Evolutionary Genetics Analysis) version 6 (Tamura et al. 2011). To confirm the phylogenetic analysis, Bayesian analysis was performed in a different way on the same set of the proteins. First, the proteins were aligned with default parameters using Probcons that is implemented Jalview (version 2.10.3b1) software (Waterhouse et al. 2009). The alignment with the predictions of preotein secondary strucutre is presented in the supplementary Figure S4.4. The best-fitted amino acid substitution model was selected with the lowest BIC score, using ProtTest v3.4.2 (Darriba et al. 2011) which was LG+G. Then, A Bayesian phylogenetic tree was constructed via MrBayes v3.2.6. (Ronquist et al. 2012) with the LG+G substitution model. The Markov Chain Monte Carlo parameters were: Ngen = 40×10^4, nchains = 8, burninfrac = 0.25. The constructed Bayesian phylogenetic tree is presented using the online tool iTOL (Letunic and Bork 2016) and it shows the posterior probabilities as percentages from 0 % to 100 % on the

branches. Graphical representation of TaREMs positions on chromosomes of *T. aestivum* was drawn using MapChart software (Voorrips 2002).

Conserved Motif Analyses

Genomic sequences and open reading frames (ORFs) of TaREMs were obtained from Ensembl (Kersey et al. 2014). Conserved motifs of the genes were analyzed using the Multiple Em for Motif Elucidation (MEME) program (http://meme.nbcr.net/meme/) (Bailey and Elkan 1994). The following parameters in MEME tool were used for the distribution of motif occurrences: any number of repetitions, the maximum number of motifs was set to 20 motifs; optimum motif width was set to 6–100 and minimum/maximum number of sites: 5/100. Identified MEME motifs other than C-remorin domain was achieved by PROSITE (Sigrist et al. 2013) and Eukaryotic Linear Motif resource (ELM, http://elm.eu.org/) (Gould et al. 2010), for functional sites in proteins.

Database searching and identification of cis-regulatory elements in the promoter regions

Putative cis-acting regulatory DNA elements in the promoter TaREM genes were identified from 1.5-kb upstream of the 5′-UTR as in previous studies (Badawi et al. 2008; Li et al. 2018), except for copies A of TaREM4.2, U (U represents unmapped genes in any wheat genome) of TaREM6.1 and B for TaREM6.6 whose promoter sequences are not complete. Promoter sequences were analyzed by the PlantCARE program (http://bioinformatics.psb.ugent.be/webtools/plantcare/html/) as previously described (Lescot et al. 2002). Protein subcellular localization was determined using CELLO (http://cello.life.nctu.edu.tw/).

Gene expression profile analysis

The RNA-Seq data corresponding to the TaREM genes was downloaded from the Norstar/Manitou wheat crown transcriptome database (Li et al. 2018). Illumina RNA-Seq data analyses were performed on crowns of plants grown under field conditions from early autumn to winter in 2010 (Li et al. 2018). The reads per million (RPM) were obtained from the field condition RNA-Seq database. The expression cluster for each TaREM gene for each cultivar/time point represents the total reads of the three copies (A, B and D) and the mean values of two replicates. A BLASTN search of the gene sequence obtained from the Ensembl wheat genome was performed

against TaREM genes identified in this study to find and confirm the corresponding Genevestigator REM identifiers (Table S4.3). One of the three homeologs was selected to represent the expression of the three homeologs, where the homeolog with the highest expression under different perturbations was selected (Table S4.3). The RNA-Seq databases of *T. aestivum* from different tissues and developmental stages were analyzed using Genevestigator tool (http://www.genevestigator.ethz.ch/) (Zimmermann et al. 2014). The expression patterns obtained are presented as heat maps in yellow/blue for different stresses and burgundy-white colour-coding for tissues and developmental stages.

RNA extraction and expression analyses by qRT-PCR of the *TaREM* genes

Total RNA was isolated from samples of all the experiments using the mirVana miRNA Isolation Kit (Ambion Inc. US). The purity and quality of RNA were analyzed by NanoDrop 2000c (Thermo-Scientific, USA). A 0.9 µg aliquot of total RNA was treated with gDNA wipeout buffer in QuantiTect Rev. Transcription Kit (QIAGEN, Carlsbad, CA, USA) and then reverse-transcribed using the QuantiTect Reverse Transcription Kit (QIAGEN, USA). Two Microliters of cDNA template (equivalent to 90 ng of total RNA) were used in qRT-PCR with LightCycler 480 SYBR Green I Master (Roche). The qRT–PCR was performed using FX96 Real-time Detection System (Bio-Rad, USA) according to the manufacturer's instructions. The PCR conditions were set as follows: 95°C for 15 minutes; 40 cycles of 95°C for 15 seconds and 55°C for 30 seconds; and 72°C for 30 seconds; the experiments were repeated for the two biological replicates. The ΔΔCT method was used to calculate relative expression levels of TaREM genes using 18S as the reference gene. The gene-specific primers were used to quantify the transcripts of TaREM. All the primers used for qRT-PCR were listed in Supplemental Table S4.4. Each reaction was conducted in duplicate to ensure reproducibility of results. Expression levels were calculated from the cycle threshold according to the delta-delta CT method (Livak and Schmittgen 2001). The statistical significance was assessed by InStat 3.0 using one-way ANOVA followed by Tukey's multiple range tests where the p-values < 0.05 were considered as significant. Then, the graphs were made using GraphPad Prism 6.0.

Results and Discussions

Analyses of gene families have become an essential step in the understanding of gene structure, protein function, and evolution. Here, we conducted a comprehensive analysis of the TaREM gene family to determine their potential functions in response to abiotic stresses (i.e. exceptionally cold temperatures), phenological development, and hormones such as MetJ and ABA.

Identification and phylogenetic analysis of the wheat remorin gene Family

Twenty rice REM genes were used to search the Ensembl database (release 31) and then used to identify genes encoding REMs in the wheat genome. Twenty TaREM coding sequences were identified. Based on their genomic location, these genes were present as two or three homeoallelic coding sequences on the three genomes of hexaploid wheat (A, B and D). To be consistent with the nomenclature established for the cereal species *O. sativa* (Raffaele et al. 2007); we assigned identical gene numbers to orthologs of hexaploid wheat (0.1–6). In total, 57 TaREMs copies were identified with their characteristic information such as the gene ID, position on the chromosomes, coding sequence (CDS) size and amino acids (Table 4.1). Most wheat REM gene loci have three copies distributed across the three wheat genomes except TaREM0.12, TaREM 1.3 and TaREM 6.6 that have only two copies (Table 4.1). Since all homeologs of TaREM6.4 were incomplete, we included the D genome progenitor, *Aegilops tauschii* (*A. tauschii*) ortholog (AtgREM6.4), as a substitute for sequence comparison. All identified TaREM proteins had a typical remorin motif at the C-terminus (Figures 4.1A and B). The TaREM-C motif contained a coiled-coil domain, a signature of the remorin family. The multiple sequence alignment of the C-terminal region of all identified wheat REM proteins revealed a highly conserved coiled-coil domain (Figure 4.1A). The number of identified REMs in rice, Arabidopsis and wheat are nineteen, sixteen and twenty, respectively, while there are only eight remorins in poplar (Raffaele et al. 2007), and eleven in millet (Yue et al. 2014), indicating that the REM family in the first three species has expanded over time. This expansion of TaREMs gene family is probably due to whole-genome duplication or segmental duplication. Gene duplication played a crucial role in the expansion of gene families creating the opportunity for changes in gene function, which in turn allowed for optimal adaptability to diverse environmental conditions (Xu et al. 2012).

Table 4.1: Characteristics of TaREM genes identified from the genome-wide search analysis, showing: putative REM gene names based on the phylogenetic analysis, Accession number (Gene

ID) and chromosome location from ensembl or NCBI, open reading frame in base pair (ORF bp) and the total numbers of deduced amino acids (aa) length. Since the gene TaREM6.4 was incomplete, the gene AtgREM6.4 from the D genome progenitor *Aegilops tauschii* was used. The star sign (*) indicates that this protein is complete in both *Triticum aestivum* and *Aegilops tauschii* genomes. U, unknown chromosome.

Gene name	GENE ID/Chromosome location	ORF (bp)	Total amino acid (aa)
TaREM1.1	TRIAE_CS42_6AL_TGACv1_474254_AA1534720.1	516	171*
	TRIAE_CS42_6BL_TGACv1_499375_AA1580240.1	522	173*
	TRIAE_CS42_6DL_TGACv1_527128_AA1698990.2	507	168*
TaREM1.2	TRIAE_CS42_1AL_TGACv1_000064_AA0001950.1	534	177*
	TRIAE_CS42_1BL_TGACv1_032062_AA0124920.1	534	177*
	TRIAE_CS42_1DL_TGACv1_061146_AA0186900.1	534	177*
TaREM1.3	TRIAE_CS42_5AL_TGACv1_375758_AA1226750.1	534	177*
	TRIAE_CS42_4DL_TGACv1_342748_AA1120910.1	528	175*
TaREM1.4	TRIAE_CS42_6AL_TGACv1_471085_AA1502500.1	582	193*
	TRIAE_CS42_6BL_TGACv1_500374_AA1603800.1	576	191*
	TRIAE_CS42_6DL_TGACv1_528469_AA1714380.1	576	191*
TaREM1.5	TRIAE_CS42_2AL_TGACv1_094593_AA0300040.1	632	210*
	TRIAE_CS42_2BL_TGACv1_129653_AA0391780.1	645	214*
	TRIAE_CS42_2DL_TGACv1_158509_AA0520480.3	645	214*
TaREM0.1	TRIAE_CS42_U_TGACv1_646021_AA2145870.1	1275	424*
	TRIAE_CS42_6BL_TGACv1_501473_AA1617960.1	1047	348
	TRIAE_CS42_6DL_TGACv1_528336_AA1713340.1	1275	424*
TaREM0.12	TRIAE_CS42_6BL_TGACv1_506147_AA1629390.1	1188	396
	TRIAE_CS42_6DL_TGACv1_530381_AA1719440.1	1284	427*
TaREM0.2	TRIAE_CS42_1AS_TGACv1_019235_AA0063720.1	1056	351*
	TRIAE_CS42_1BS_TGACv1_050175_AA0168550.1	1056	351*
	TRIAE_CS42_1DS_TGACv1_080889_AA0255170.1	1056	351*
TaREM0.23	TRIAE_CS42_4AS_TGACv1_307255_AA1018940.1	939	312*
	TRIAE_CS42_4BL_TGACv1_322745_AA1072920.2	942	313*
	TRIAE_CS42_4AS_TGACv1_307255_AA1018940.1	891	296
TaREM4.1	TRIAE_CS42_2AS_TGACv1_114832_AA0369660.1	936	311*
	TRIAE_CS42_2BS_TGACv1_147285_AA0481090.2	861	286
	TRIAE_CS42_2DS_TGACv1_178392_AA0594940.1	930	309*
TaREM4.2	TRIAE_CS42_5AL_TGACv1_374215_AA1194030.1	927	308*

	TRIAE_CS42_5BL_TGACv1_404576_AA1304770.1	921	306*
	TRIAE_CS42_5DL_TGACv1_433857_AA1423910.3	913	270
TaREM4.3	TRIAE_CS42_7AL_TGACv1_556525_AA1764760.1	855	284*
	TRIAE_CS42_7BL_TGACv1_576816_AA1855900.1	837	278*
	TRIAE_CS42_7DL_TGACv1_604984_AA2003590.1	834	277*
TaREM5.1	TRIAE_CS42_6AL_TGACv1_472197_AA1519020.2	1293	430 *
	TRIAE_CS42_6BL_TGACv1_502167_AA1623490.4	1293	430 *
	TRIAE_CS42_6DL_TGACv1_528653_AA1715370.5	1293	430 *
TaREM5.3	TRIAE_CS42_5AL_TGACv1_374503_AA1201850.3	1869	622 *
	TRIAE_CS42_U_TGACv1_640702_AA2069810.1	1806	601
	TRIAE_CS42_5DL_TGACv1_433202_AA1405370.1	1848	615 *
TaREM6.1	TRIAE_CS42_6AS_TGACv1_486089_AA1556650.1	1527	508 *
	TRIAE_CS42_6BS_TGACv1_514845_AA1665050.1	1527	508 *
	TRIAE_CS42_U_TGACv1_641607_AA2099410.1	1530	509*
TaREM6.2	TRIAE_CS42_5AL_TGACv1_374361_AA1197990.1	1269	422
	TRIAE_CS42_4BL_TGACv1_320542_AA1042610.1	1275	424
	TRIAE_CS42_4DL_TGACv1_343728_AA1138750.1	1410	469*
TaREM6.3	TRIAE_CS42_5AS_TGACv1_393298_AA1270840.1	1290	429
	TRIAE_CS42_5BSTGACv1_423765_AA1382870.1	1416	471*
	TRIAE_CS42_5DS_TGACv1_456797_AA1478190.1	1320	439
AtgREM6.4	ASM34733v1:Scaffold94581:24487:26802:1	1248	415*
TaREM6.5	TRIAE_CS42_4AL_TGACv1_289894_AA0978450.2	1050	349*
	TRIAE_CS42_4BS_TGACv1_329879_AA1104500.1	1065	354*
	TRIAE_CS42_4DS_TGACv1_361131_AA1161740.1	1062	353*
TaREM6.6	TRIAE_CS42_2BL_TGACv1_129903_AA0399020.1	1587	528*
	TRIAE_CS42_2DL_TGACv1_158356_AA0516500.1	1590	529*

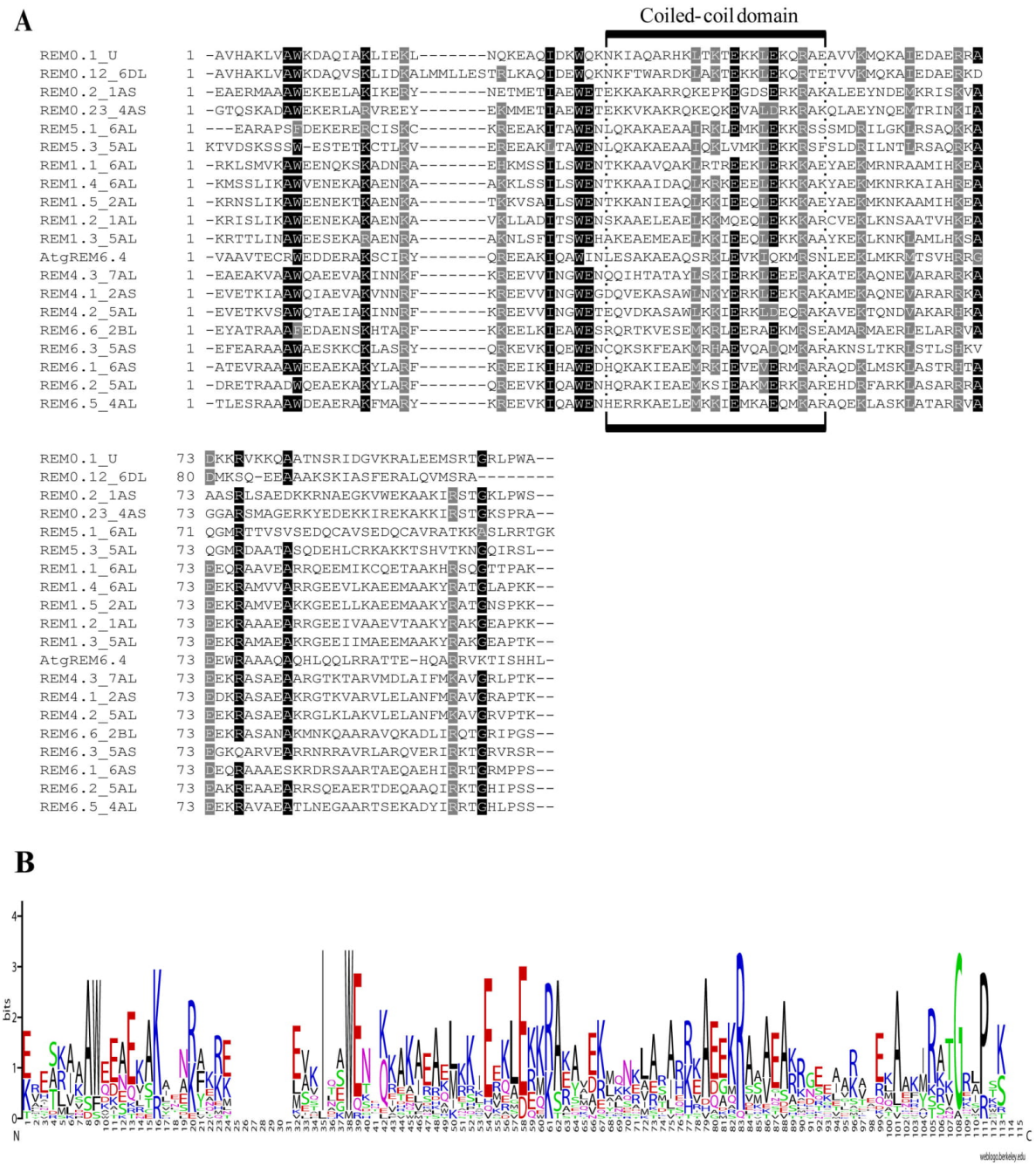

Figure 4.1: Conserved motif analysis of the REM C-terminal sequences in wheat. **(A)** Multiple sequence alignment of wheat REM motif is shown. The homeologous A copy from all REM genes were used in the analysis except for *TaREM0.12, TaREM6.6* and *TaREM0.1* genes where the B and U copies were used respectively. Since the gene *TaREM6.4* was incomplete, the gene AtgREM6.4 from D genome progenitor *Aegilops tauschii* was used. The coiled-coil domain in the REM motif is boxed. The conserved amino acid, and blocks of similar amino acid residues are shaded in black and gray, respectively. **(B)** Sequence representation LOGO derived from the

multiple sequence alignment of the Remorin-C motif. The x-axis represents the conserved sequence. The y-axis is a scale that reflects the conservation rate of each amino acid across all proteins.

Previously, Raffaele et al. (2007) had shown that some monocot and eudicot REM sequences are separated on a phylogenetic tree suggesting the existence of specific groups in monocots/eudicots. To study the phylogenetic relationships of the wheat REM family, we retrieved the REM proteins described by Raffaele et al. (2007), the 16 Arabidopsis REM members and the four Populus/Medicago group 2-specific members as representatives of eudicot REMs, and the twenty *O. sativa* REM members as additional monocot representatives. During our initial comparisons of REM proteins from different groups, it was difficult to align the entire protein of distant members with complete confidence. Therefore, we only aligned the amino acids encompassing the conserved C-motif from the 57 proteins. A Maximum Likelihood tree was derived from this alignment and is presented in Figure 4.2A. Additionally, Figure 4.2B shows a Bayesian phylogenetic tree that presented based on the alignment from Figure S4.4. Both analyses showed that REM proteins cluster into six monophyletic groups. Groups 0.2, 1 and 4 clearly show a separation of monocot and eudicot REM sequences suggesting that only one representative per group may have existed during eudicot/monocot divergence. These groups now account for ten REM proteins in each species.

(A)

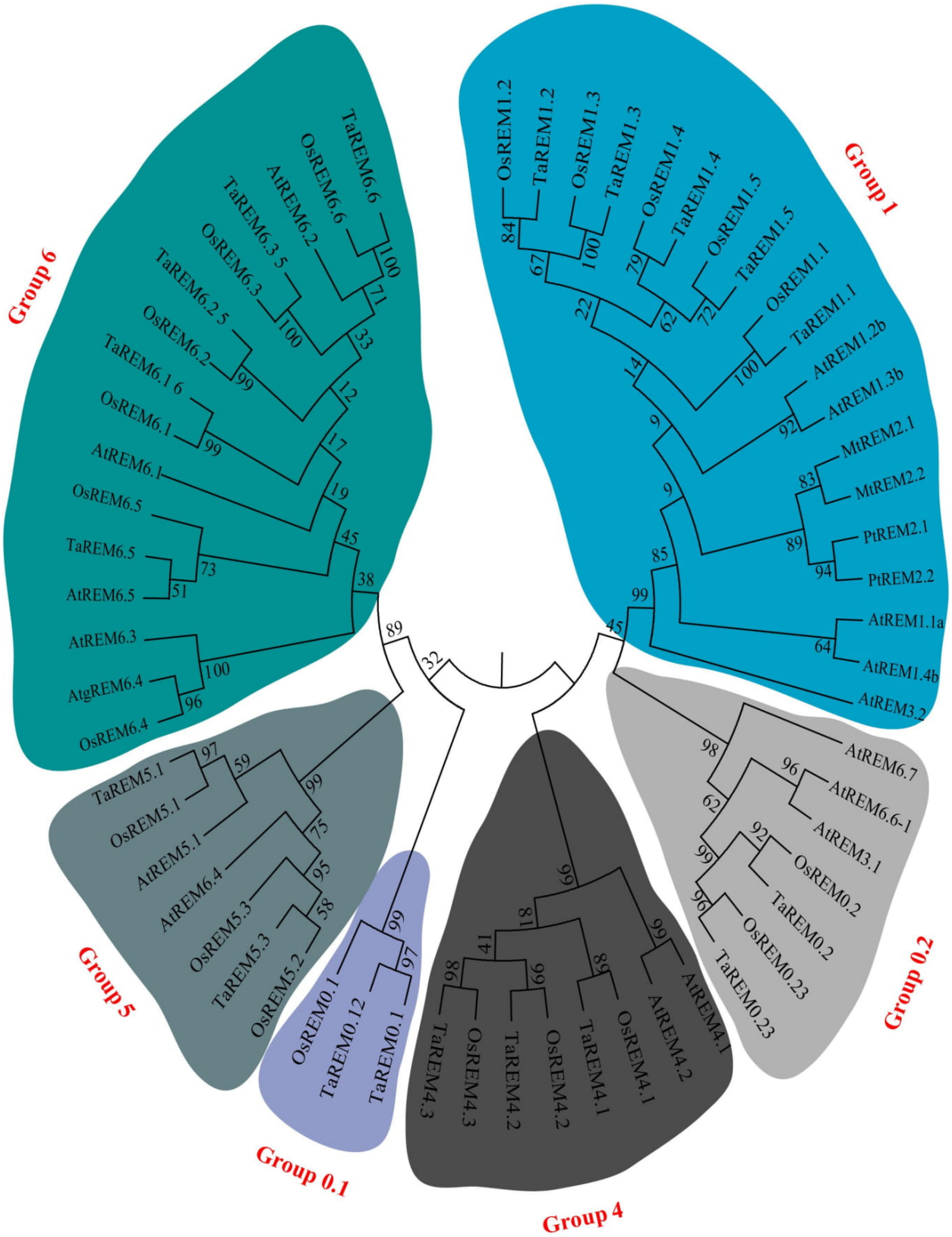
Group 6
TaREM6.6
OsREM6.6
AtREM6.2
TaREM6.3 5
OsREM6.3
TaREM6.2 5
OsREM6.2
TaREM6.1 6
OsREM6.1
AtREM6.1
OsREM6.5
TaREM6.5
AtREM6.5
AtREM6.3
AtgREM6.4
OsREM6.4
Group 1
OsREM1.2
TaREM1.2
OsREM1.3
TaREM1.3
OsREM1.4
TaREM1.4
OsREM1.5
TaREM1.5
OsREM1.1
TaREM1.1
AtREM1.2b
AtREM1.3b
MtREM2.1
MtREM2.2
PtREM2.1
PtREM2.2
AtREM1.1a
AtREM1.4b
AtREM3.2
Group 5
TaREM5.1
OsREM5.1
AtREM5.1
AtREM6.4
OsREM5.3
TaREM5.3
OsREM5.2
Group 0.1
OsREM0.1
TaREM0.12
TaREM0.1
Group 4
AtREM4.2
OsREM4.3
TaREM4.3
TaREM4.2
OsREM4.2
TaREM4.1
OsREM4.1
AtREM4.1
Group 0.2
AtREM6.7
AtREM6.6-1
AtREM3.1
OsREM0.2
TaREM0.2
OsREM0.23
TaREM0.23

(B)

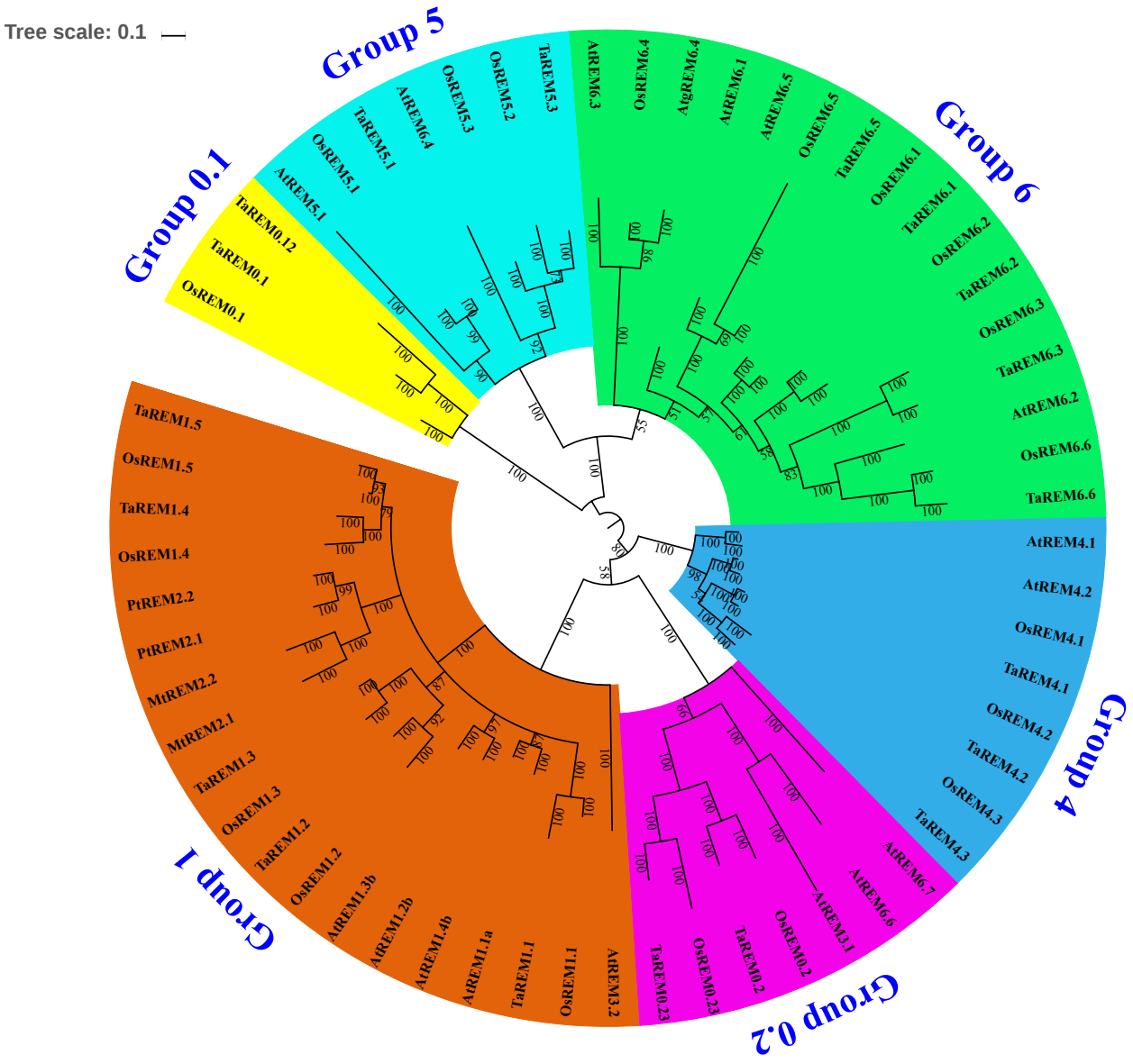

Figure 4.2: (A) Phylogenetic relationships between all remorin proteins from *T. aestivum*, *O. sativa* and Arabidopsis. The amino acids corresponding to the conserved C-motif from the three species were aligned by MUSCLE in MEGA6. A Maximum Likelihood tree (ML) was derived from this alignment using LG + Gamma model and bootstrap value with 500 replicates. In addition, four proteins from Populus/Medicago (group 2-specific remorins in Raffaele et al. (2007)) were included for comparison. The wheat remorins were grouped into six distinct groups and annotated with different colors. Genes belonging to the different groups are listed in Table 4.1. **(B)**

Phylogenetic Bayesian analysis of the same set of the proteins. The Markov Chain Monte Carlo parameters were: Ngen = 40×10^4, nchains = 8, burninfrac = 0.25. The constructed Bayesian phylogenetic tree is presented using the online tool iTOL (Letunic and Bork 2016) and it shows the posterior probabilities as percentages from 0 % to 100 % on the branches.

Groups 5 and 6 display two and four distinct branches that contain at least one REM member from each species suggesting that the amplification of genes within these groups preceded eudicot/monocot divergence. These groups now contain six, nine and eight REM proteins in Arabidopsis, rice and wheat, respectively. There were no Arabidopsis REM proteins clustered with members from group 0.1, suggesting its specificity to monocot group. The REM phylogenetic tree showed mostly the same clustering patterns in the two members of the grass family wheat and rice. The phylogenetic similarity between *T. aestivum* and *O. sativa* REM proteins suggests that they might have evolved conservatively. In total, 19 REM proteins out of 20 were clustered as pairs revealing their orthologous relationship.

Furthermore, TaREM0.12 and OsREM5.2 represent additional genes that may have explicitly duplicated in wheat and rice, respectively. Yue et al. (2014) showed that the eleven SiREMs (*Foxtail millet*) were classified into four phylogenetic groups. In Arabidopsis, all 16 AtREM genes were divided into five groups (1, 3, 4, 5 and 6). These results indicate that TaREM, OsREM, and AtREM genes may have undergone different duplication events. As shown in Figure S4.1, the orthologs from the A, B and D genomes tended to form an orthologous pair at the branch end indicating that the orthologs from A, B and D had a close relationship.

Chromosomal locations of wheat remorin members

TaREM genes were located on all the homoeologous groups of wheat chromosomes except group 3 (Figure 4.3), while no REM genes were found in rice chromosomes 1, 5, 6 and 7. As in wheat, REM genes in Arabidopsis were distributed among all five chromosomes (Raffaele et al. 2007). TaREM genes were overrepresented on group 6 and 4 chromosomes, which contain six and four genes respectively (Figure 4.3). Interestingly, the group 6 chromosomes have the most substantial number of COR genes (Li et al. 2018). TaREM4.2, TaREM5.3, and TaREM6.3 were located in group 5 chromosomes, which is known to harbour some regulatory genes that may regulate cold tolerance and development. Miller et al. (2006) stated that chromosome 5A has the freezing tolerance locus (FR2) and contains a cluster of CBF (C-repeat binding factor) genes.

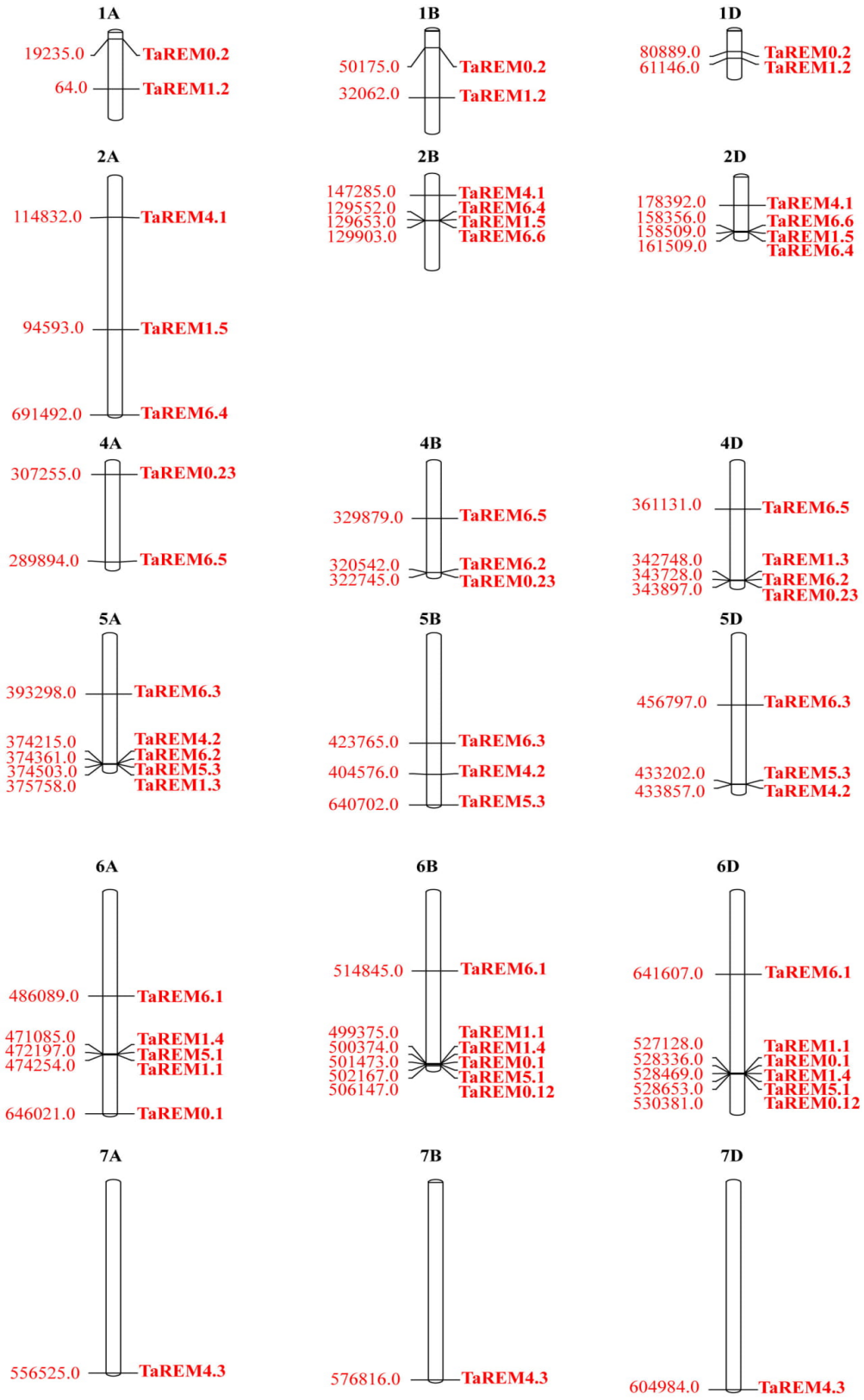

Figure 4.3: Chromosomal locations of *TaREM* genes in the wheat genome. The distributions of the 57 remorin genes was determined according to the scaffold number and are shown in red.

Chromosomes in the group number three do not have any remorins and was excluded in this figure. The numbers on the top indicate each chromosome number and the genome A, B or D. Positions are indicated in kilobases on chromosomes and bases on scaffolds.

Motifs and sub-cellular localization analysis

Putative motifs were identified using the MEME program (http://meme-suite.org/tools/meme) to study the diversity and conservation among the TaREMs. Twenty distinct motifs were identified among the 20 TaREMs proteins. The distribution of motifs in the different remorin groups, the protein motifs, and their consensus are shown in Figure 4.4, Table S4.1. The size of the identified motifs ranged from 10 to 107 amino acids (Table S4.1). The closely related genes within each group in the phylogenetic tree shared common motif sequences and positions (Figures 4.2 and 4.4). In general, remorins have a conserved C-terminal domain, considered to be a signature of the protein, a predicted coiled-coil and a variable N-terminal region. Motif analyses showed that the remorin-C domain (motif 1) is uniformly present in all wheat remorin proteins, suggesting that they have been evolutionarily conserved in plants.

The remorin-N domain is about 64 amino acids (motif 2) and was found only in group 1 remorins. This group has both Remorin-N and Remorin-C domains except for TaREM1.1, which is missing the Remorin-N domain but still contains high proline content as other members of group 1. Exclusively, group 4 members have similar numbers of proline in the N-terminal region. It was reported that group 1 remorins from dicots have a higher percentage of prolines in this region, but the biological significance remains unclear (Raffaele et al. 2007; Yue et al. 2014). We found that Group 1 Remorins have several motifs (3 to 10) in the N-terminal region. Group 4 was characterized by the presence of a serine-rich sequence in the N-terminal region that contains one specific motif (motif 11) corresponding to glycosylation site. Group 5 contains only one conserved motif in the N-terminal region and has a putative phosphorylation site (motif 14). Group 6 has four conserved motifs (motifs 15 to 18 corresponding to Collagen IV carboxyl-terminal, LDL-receptor class B, PKC_Protein kinase C and LIG_LIR_Gen_1) at the N-terminus except TaREM6.4 and TaREM6.5, which contained only two motifs (15 and 16).

Most of the closely related members in the phylogenetic tree had identical motif compositions, suggesting functional similarities among the REM proteins within the same group (Figures 4.2, 4.4 and Table S4.1). The motif distribution and organization showed that remorin proteins were conserved during evolution and the motif distribution in different groups of proteins

could be the source of the functional divergence in remorin genes over time. The presence of variable N-terminal regions in remorin genes suggests different structures and functions (Marín and Ott 2012).

Group	Gene Name	Motifs														
1	TaREM1.1	3			6											Remorin-C
	TaREM1.2	3	4	5	6		10		Remorin-N							Remorin-C
	TaREM1.3	3	4	5			10	9	Remorin-N							Remorin-C
	TaREM1.4	3	4	5			10		Remorin-N							Remorin-C
	TaREM1.5		4	5	6	7	8	9	Remorin-N							Remorin-C
4	TaREM4.1					11	12									Remorin-C
	TaREM4.2					11	12	13								Remorin-C
	TaREM4.3					11										Remorin-C
5	TaREM5.1									14						Remorin-C
	TaREM5.3									14						Remorin-C
6	TaREM6.1									15	16	17	18			Remorin-C
	TaREM6.2									15	16	17	18			Remorin-C
	TaREM6.3									15	16	17	18			Remorin-C
	TaREM6.4									15	16					Remorin-C
	TaREM6.5									15	16					Remorin-C
	TaREM6.6							9		15	16	17	18			Remorin-C
0.1	TaREM0.1													19		Remorin-C
	TaREM0.12													19		Remorin-C
0.2	TaREM0.2														20	Remorin-C
	TaREM0.23														20	Remorin-C

Figure 4.4: Schematic diagram of the conserved motifs in wheat 20 *REM* genes identified by MEME. Each colored number represents a motif. Yellow box Remorin-C domain represents motif number 1. Remorin-N domain represents motif 2. The other motifs are shown in different colours. The consensus sequences of these motifs identified by MEME and their function identified by prosite and Eukaryotic Linear Motif resource programs are presented in Table S4.1.

Subcellular localization of the TaREM proteins was predicted using the CELLO program. Putative TaREM protein subcellular localization showed that most TaREMs were concentrated in the nucleus. However, few REMs genes (TaREM1.2, TaREM1.3, TaREM1.5D and TaREM4.1B) were localized in the cytoplasm (Table 4.2). These differences may be related to the motif sequence and suggest that the subcellular localization of TaREMs is diverse and complex.

Table 4.2: Prediction of cell localization of wheat remorin proteins in comparison to rice and Arabidopsis prediction and to the experimental location in Arabidopsis. CELLO program was used for the localization prediction (http://cello.life.nctu.edu.tw/). U is a gene localized in unknown chromosomse. The asterisk (*) represents AtgREM6.4 from *Aegilops tauschii*. The minus sign (–) indicates that the gene is not existing in the species. Experimental localization of the Arabidopsis remorin C-terminal anchor was done by Konrad et al. (2014).

Gene name	**Prediction in wheat**	**Prediction In rice**	**Prediction in Arabidopsis**	**Experimental in Arabidopsis**
TaREM1.1 _6AL TaREM1.1 _6BL TaREM1.1 _6DL	Nuclear Nuclear Nuclear	OsREM1.1 Nuclear	AtREM1.1 Nuclear	Cytosol
TaREM1.2 _1AL TaREM1.2 _1BL TaREM1.2 _1DL	Cytoplasmic Cytoplasmic Cytoplasmic	OsREM1.2 Cytoplasmic	AtREM1.2 Nuclear	Cytosol
TaREM1.3_5AL TaREM1.3_4DL	Cytoplasmic Cytoplasmic	OsREM1.3 Nuclear	AtREM1.3 Cytoplasmic	Cytosol
TaREM1.4_6AL TaREM1.4_6BL TaREM1.4_6DL	Nuclear Nuclear Nuclear	OsREM1.4 Nuclear	AtREM1.4 Nuclear	Cytosol
TaREM1.5_2AL TaREM1.5-2BL TaREM1.5-2DL	Nuclear Nuclear Cytoplasmic	OsREM1.5 Nuclear	AtREM3.2 Nuclear	Cytosol
REM0.1_U REM0.1_6BL REM0.1_6DL	Nuclear Nuclear Nuclear	OsREM0.1 Nuclear	-	-
REM0.12_6BL REM0.12_6DL	Nuclear Nuclear	-	-	-
REM0.2_1AS REM0.2_1BS REM0.2_1DS	Nuclear Nuclear Nuclear	OsREM0.2 Nuclear	AtREM3.1 Nuclear AtREM6.6 Nuclear AtREM6.7 Nuclear	Cytosol Cytosol Plasma Membrane
REM0.23_4AS REM0.23_4BL REM0.23_4DS	Nuclear Nuclear Nuclear	-	-	-

TaREM4.1_2AS TaREM4.1_2BS TaREM4.1_2DS	Nuclear Cytoplasmic Nuclear	OsREM4.1 Nuclear	AtREM4.1 Nuclear	Cytosol
TaREM4.2_5AL TaREM4.2_5BL TaREM4.2_5DL	Nuclear Nuclear Nuclear	OsREM4.2 Nuclear	AtREM4.2 Nuclear	Cytosol
TaREM4.3_7AL TaREM4.3_7BL TaREM4.3_7DL	Nuclear Nuclear Nuclear	OsREM4.3 Nuclear	-	-
TaREM5.1_6AL TaREM5.1_6BL TaREM5.1_6DL	Nuclear Nuclear Nuclear	OsREM5.1 Nuclear OsREM5.2 Nuclear	AtREM5.1 Nuclear	Cytosol
TaREM5.3_5AL TaREM5.3_ U TaREM5.3_5DL	Nuclear Nuclear Nuclear	OsREM5.3 Nuclear	AtREM6.4 Nuclear	Plasma Membrane
TaREM6.1_6AS TaREM6.1_6BS TaREM6.1_U	Nuclear Nuclear Nuclear	OsREM6.1 Nuclear	AtREM6.1 Nuclear	Plasma Membrane
REM6.2_5AL REM6.2_4BL REM6.2_4DL	Nuclear Nuclear Nuclear	OsREM6.2 Nuclear	-	-
REM6.3_5AS REM6.3_5BS REM6.3_5DS	Nuclear Nuclear Nuclear	OsREM6.3 Nuclear	-	-
AtgREM6.4*	Nuclear	OsREM6.4 Nuclear	AtREM6.3 Nuclear	Cytosol
REM6.5_4AL REM6.5_4BS REM6.5_4DS	Nuclear Nuclear Nuclear	OsREM6.5 Nuclear	AtREM6.5 Nuclear	Cytosol
REM6.6_2BL REM6.6_2DL	Nuclear Nuclear	OsREM6.6 Nuclear	AtREM6.2 Nuclear	Plasma Membrane

Bioinformatics analysis of putative TaREM promoters

The transcriptional response elements of 19 TaREMs and REM6.4 from *A. tauschii* promoters were identified from the regions upstream to the start site in the *T. aestivum* genome using the PlantCARE promoter databases to elucidate the regulatory mechanisms of their genes.

All the putative TaREM promoters possessed typical TATA and CAAT boxes (Table 4.3, Table S4.2), which are the core elements in promoter and enhancer regions. The predicted regulatory cis-elements include transcription factor binding sites and numerous elements related to stress, phytohormone and light responses (Table 4.3). Light-responsive elements, which contain different core elements (Table S4.2), represent most predicted elements. Every promoter possessed 10 to 20 types of light core elements, indicating that light might differentially regulate TaREMs.

The presence of light-responsive element was reported in a soybean Remorin gene regulated under drought stress (Marcolino-Gomes et al. 2014). The thirteen predicted hormone-responsive regulatory elements are associated with ABA (ABRE, CE1, CE3 and motif IIb), ethylene (ERE), MeJA, (CGTCA and TGACG-motifs), GA (GARE-motif, TATC-box and P-box), auxin (AuxR-core, TGA-box and TGA element) and SA (TCA-element) responses. The ABA-responsive cis-elements in REM gene promoters were also found in *Foxtail millet* (Yue et al. 2014). Regulation of REM gene expression in response to hormone treatment including ABA, MetJ, IAA and/or salicylic acid has been reported in different species (Checker and Khurana 2013; Yue et al. 2014; Kong et al. 2016). The induction of MiREM and SiREM6 in response to exogenous ABA treatment in mulberry and millet suggest that these two genes could be involved in abiotic stress tolerance through the ABA-dependent signal pathway (Checker and Khurana 2013; Yue et al. 2014). The predicted TaREM promoters had many cis-elements related to endosperm expressions such as Skn-1 and GCN4, and the seed tissue-specific elements (RY and CCGTCC-box) as shown in Table S4.2.

The tissue specificity of REM genes has been reported in many tissue localization studies (Bariola et al. 2004; Li et al. 2013; Yue et al. 2014; Kong et al. 2016). Presence of the tissue-specific element in TaREM genes promoters reveals a vital role in plant development. Furthermore, putative TaREM promoters have different types of stress-responsive regulatory elements (abiotic and biotic) including LTRs and C-repeat/DRE, AREs, HSEs, MBSs, TC-rich repeats, and Box-W1s related to low-temperature, anaerobic induction, heat stress, drought stress, defence and fungal elicitors responses respectively (Table S4.2). Tissue-specific and stress-related cis-elements in the promoters may be responsible for many functions of TaREMs through complex regulatory mechanisms.

Table 4.3: In silico promoter analysis of *TaREM* genes using PlantCARE database program. Numbers of stress-related *cis*-elements, regulatory, development elements predicted in the upstream regions 1500 pb of *TaREM* genes. Sequences <1500bp were used for copies A of TaREM4.2, U of TaREM6.1 and B for TaREM6.6 promoter sequences because they are not complete. The cis motifs identified in TaREM candidate genes in relation to the transcription start site. DRE, dehydration-responsive element; ABRE, ABA-responsive element; MetJ, Methyl Jasmonate –responsive element; other hormone-responsive elements include (SA, Gibberellin, ethylene, Auxin); LRE, 45 different light-responsive elements (like G-box, ACE, GAG, Box 4, Sp1, BoxI, II, III, CAG motif ect.).; Regulatory, elements (AT-rich element, CAAT box, 3-AF3 binding site, 5UT Py-rich stretch, A-box and OBP-site); Development, elements (AC-I, AC-II and H-Box). For more information on LRE Regulatory and development elements see Table S3. Since the gene *TaREM6.4* was incomplete, the gene AtgREM6.4 from D genome progenitor *Aegilops* tauschii was used. The minus sign (–) indicates that the element does not exist in the promoter.

Gene name	DRE	ABRE	MetJ	Other hormones	LRE	Regulatory	Development	Promoter Size bp in different genomes
TaREM1.1	2	22	14	7	87	60	17	1500 (A, B, D)
TaREM1.2	9	17	11	6	73	39	20	1500 (A, B, D)
TaREM1.3	1	7	8	3	44	32	16	1500 (A, D)
TaREM1.4	4	4	20	6	57	45	18	1500 (A, B, D)
TaREM1.5	3	13	18	-	64	61	42	1500 (A, B, D)
TaREM0.1	-	1	10	12	36	72	14	1500 (U, B, D)
TaREM0.12	1	2	2	8	38	61	12	1500 (D)

TaREM0.2	2	3	12	9	36	54	30	1500 (A, B, D)
TaREM0.23	6	7	10	13	74	77	21	1500 (A, B, D)
TaREM4.1	6	4	12	12	49	46	15	1500 (A, B, D)
TaREM4.2	6	15	2	5	63	35	25	950 (A) 1500 (B) 1500 (D)
TaREM4.3	4	6	24	12	46	49	23	1500 (A, B, D)
TaREM5.1	16	13	8	2	75	33	14	1500 (A, B, D)
TaREM5.3	12	16	24	11	53	61	19	1500 (A, U, D)
TaREM6.1	8	1	18	7	43	67	17	1500 (A, B,) 750 (U)
TaREM6.2	1	6	4	5	45	48	9	1500 (A, B, D)
TaREM6.3	2	16	2	4	100	85	22	1500 (A, B, D)
Atg**REM6.4**	5	2	4	2	24	14	2	1500 (D)
TaREM6.5	1	1	14	4	48	55	15	1500 (A, B, D)
TaREM6.6	-	3	6	10	46	18	8	1100 (B) 1500 (D)

In silico expression profile of TaREM genes in crowns of two wheat genotypes grown under Autumn field condition

To understand the function of TaREM genes in response to cold acclimation and vernalization, we analyzed the transcriptome of developing crowns from five time points for two

genotypes grown under field conditions from early autumn to winter in 2010 at Saskatoon, Saskatchewan, Canada. The winter (Norstar) and spring (Manitou) wheat genotypes differ in vernalization requirement and freezing tolerance potential (Limin and Fowler 2002; Li et al. 2018). The transcript abundance of twenty TaREM genes was determined from the RNA-Seq data as reads per million (RPM) (Figure 4.5 A and B). Digital gene expression analysis revealed that wheat REM genes varied in their expression depending on the genotype and on the exposure time to cold.

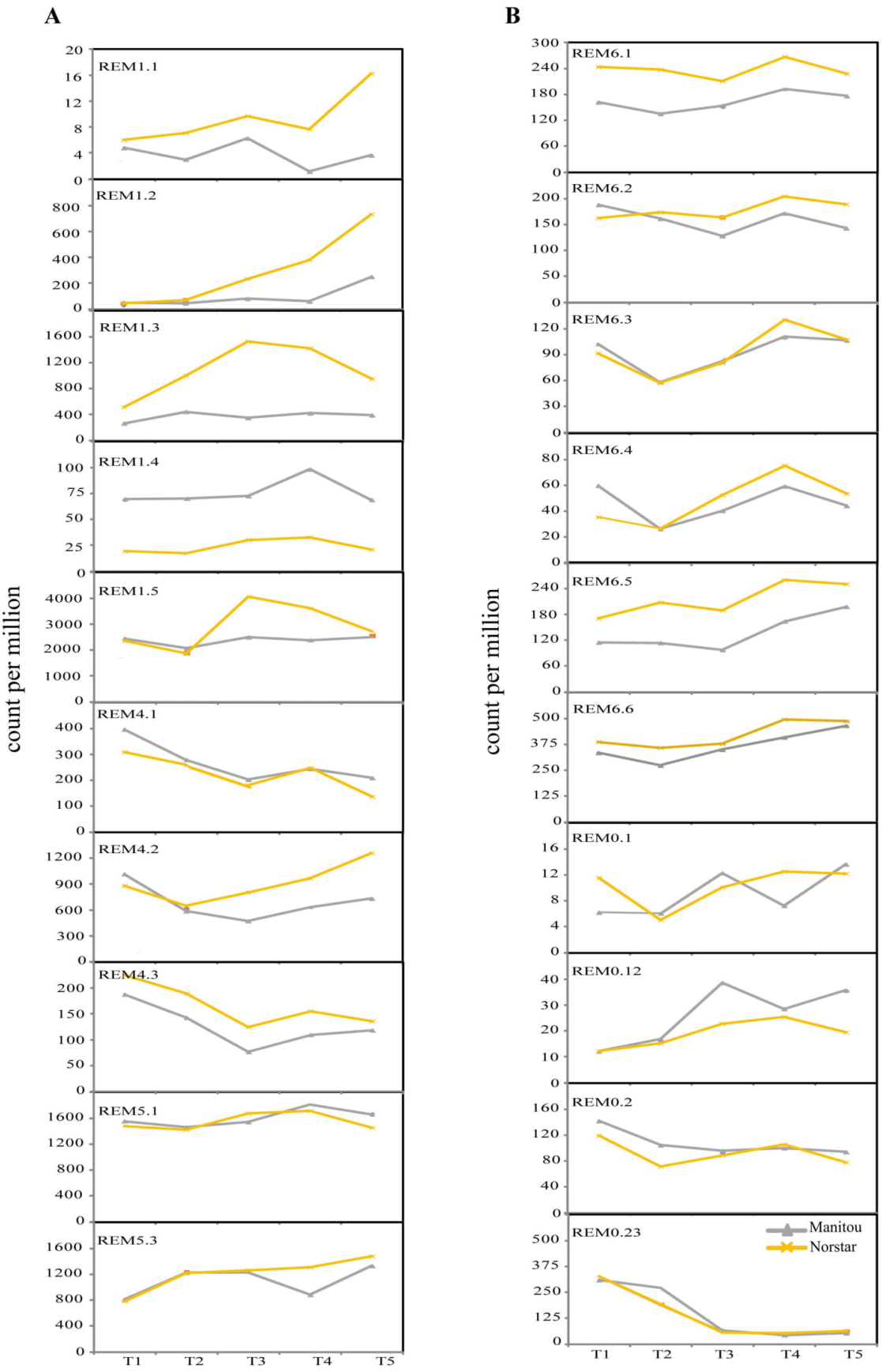
A
B
count per million
count per million
REM1.1
REM1.2
REM1.3
REM1.4
REM1.5
REM4.1
REM4.2
REM4.3
REM5.1
REM5.3
REM6.1
REM6.2
REM6.3
REM6.4
REM6.5
REM6.6
REM0.1
REM0.12
REM0.2
REM0.23
Manitou
Norstar
T1
T2
T3
T4
T5

Figure 4.5: Digital gene expression profiles of *TaREM* genes based on the transcriptome data from the field study of 2010. The expression profiles of 20 REMs representing each the combined counts of the three homeologous copies were deduced from the Illumina RNA-Seq data of winter genotype Norstar and spring genotype Manitou sampled from early autumn to winter. **(A)** Genes in phylogenetic group 1, 4 and 5; **(B)** Genes in phylogenetic group 6, 0.1 and 0.2. The y-axis represents count per million of remorin genes. The gene expression in this experiment represents the three copies added and then the mean between two the biological replicates are presented**.** T1, T2, T3, T4, and T5 represent the sampling five time points during autumn cold acclimation of crowns, where sampling were on 22 September, 4 October, 18 October, 25 October and 5 November, respectively, according to Q. Li et al. (2017).

TaREM genes were divided into three clusters based on their regulation in response to cold: up-regulated, down-regulated, or constitutively expressed. The up-regulated REM genes included the highly induced TaREM1.2 (30-fold) and the moderately induced TaREM1.3 (4-fold) and TaREM1.1 (2.5-fold). These genes have the putative CRT/DRE or low-temperature-responsive elements in their promoter regions (Table 4.3). Interestingly, their expression was higher in the cold tolerant Norstar than the less tolerant Manitou, indicating their possible association with freezing tolerance and vernalization in the crown tissue. TaREM0.12 showed an inverse association in the less tolerant Manitou. The down-regulated REM genes included 10-fold repression of TaREM0.23 and two-fold of TaREM4.1 and TaREM4.3. The other REM genes did not reveal any up- or down-regulation of more than two-fold and are considered here as constitutively expressed. Another interesting observation was that some genes were expressed in one genotype at a higher level across all-time points analyzed. The tolerant genotype shows higher expression of TaREM1.1, TaREM1.3, TaREM4.3, TaREM6.1, TaREM6.5 and TaREM6.6 whereas the less tolerant Manitou shows higher expression of TaREM1.4. The expression of these genes relies on the genetic background and could be considered positively or negatively associated with freezing tolerance and vernalization in the crown tissue.

Furthermore, the expressions of all the TaREM genes were examined in the publicly available data of spring wheat transcriptomics from multiple RNA-Seq experiments using different tissues and abiotic/biotic stress conditions (Zimmermann et al. 2014). Unfortunately, there is no public data available for winter wheat for comparison. The Genevestigator identifiers

corresponding to the TaREM genes are shown in Table S4.3. RNA-Seq data in Figure S4.2 showed that some TaREM genes (TaREM4.1, TaREM 4.2 and TaREM 4.3) are responsive to cold treatment (Zimmermann et al. 2014), while others were not. As reported in many species, REMs identified in this study are also responsive to drought and heat treatment (Figure S4.2). They were also expressed in different tissues and developmental stages (Figures S4.3 A and B). This suggests that REM genes have diverse functions during abiotic stresses.

Expression profiles of TaREM genes during cold acclimation under controlled environment

Real-Time quantitative PCR (qRT-PCR) was used to determine the expression levels of the 20 TaREM genes in aerial tissues of Norstar and Manitou to compare the RNA-Seq data from the field experiment with that of the controlled environment. The REM genes were classified into three groups according to their expression patterns: up-regulated, down-regulated, or constitutively expressed (Figure 4.6A and B). The first group represents those genes that were up-regulated in response to cold acclimation and correspond to TaREM1.1, TaREM1.2, TaREM4.1, TaREM4.2, TaREM4.3, TaREM6.3, TaREM6.4, TaREM0.1, TaREM0.12, and TaREM0.23. Interestingly, the entire group 4 remorins were strongly induced by cold. The highest increase in expression (7-fold) was found in TaREM4.3 followed by TaREM4.2 (4.5-fold) after 56 days of cold treatment suggesting an association with late cold response. In contrast, expression of the other 8 TaREMs peaked after seven days of cold treatment and then decreased towards the end of the treatment suggesting an association with early responses to cold. The second group represented the down-regulated genes and contained two genes from group 1 (TaREM1.3 and TaREM 1.4) that were also associated with the cold response. The third group contained eight constitutively expressed genes (TaREM0.2, TaREM1.5, TaREM5.1, TaREM5.3, TaREM6.1, TaREM6.2, TaREM6.5 and TaREM6.6) that were not significantly responsive to cold (Figure 4.6A and B).

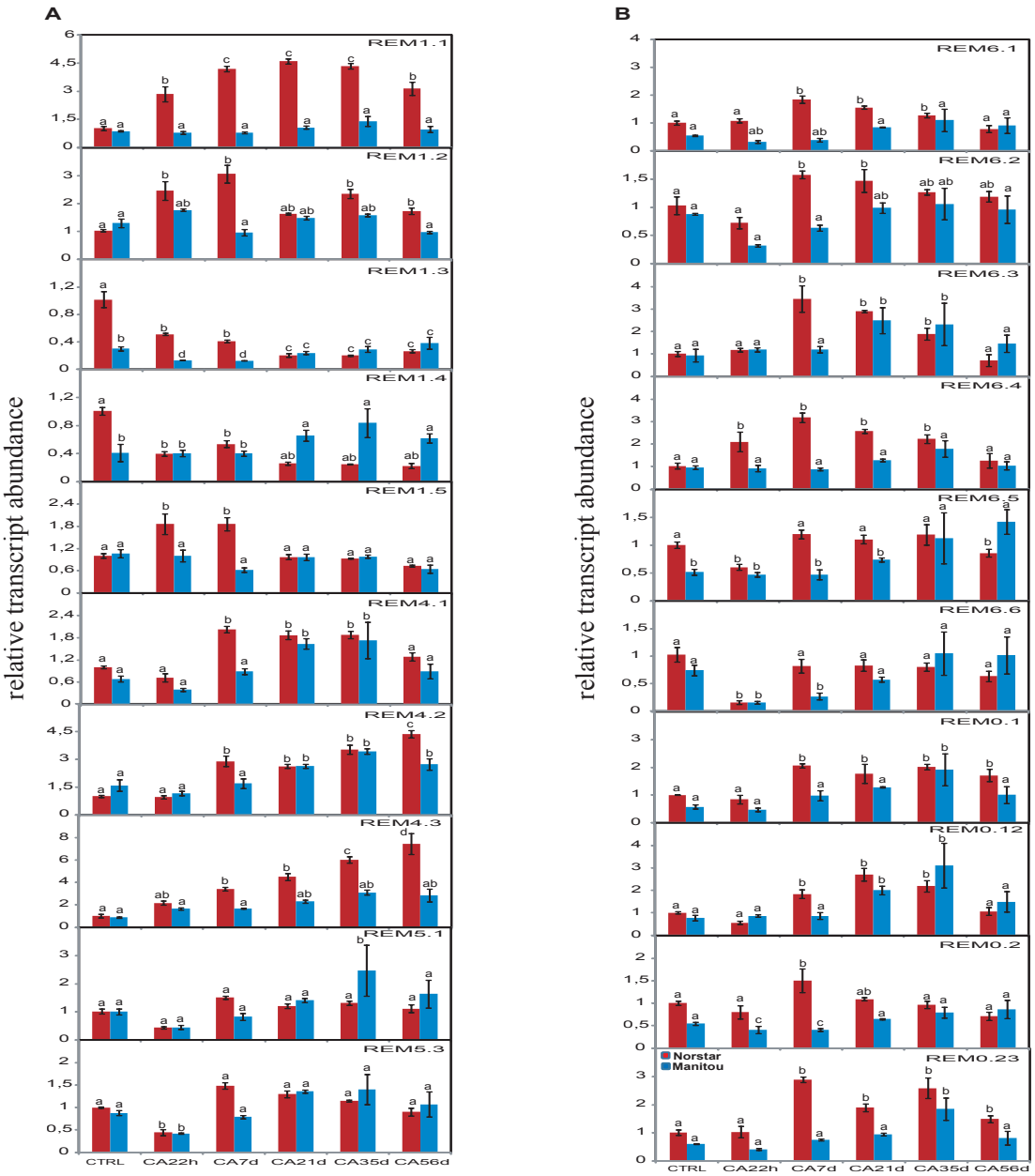

Figure 4.6: Expression profiles of *TaREM* genes in aerial tissues of winter (Norstar) and spring (Manitou) wheats during cold acclimation under experimental condition using qPCR. Expression of REMs genes was compared between control (CTR) and cold acclimated plants (CA) for 22 hours, 7, 21, 35 and 56 days, respectively using qPCR. (**A**), Genes in phylogenetic group 1, 4 and 5; (**B**), Genes in phylogenetic group 6, 0.1 and 0.2. The y-axis represents the relative expression levels of remorin genes compared to 18S. Bars represent the mean values of two biological and technical replicates ± standard deviation (SD). The small different letters present statistically significant differences between samples ($P < 0.05$ by Tukey's test).

Regulation of REM genes under abiotic stress has been reported in several species. In mulberry (*Morus indica*), MiREM was the first reported remorin gene involved in abiotic stress. The heterologous expression of MiREM in Arabidopsis improved drought and salinity tolerance during the germination and seedling stages (Checker and Khurana 2013). In another study, SiREM6 from *Foxtail millet* increased by 5.2-fold under high salinity, 4-fold in response to low temperature and 9.1-fold by ABA treatment. Overexpression of SiREM6 in Arabidopsis enhanced tolerance to high salt stress during seed germination and seedling development stages (Yue et al. 2014). This gene has a high sequence similarity with TaREM1.5, which increased in expression close to 2-fold after 7 days of cold treatment (Figure 4.6A). In a previous study, it was shown that several REMs in group 1 respond to abiotic stress and ABA treatment (Checker and Khurana 2013).

Interestingly, most of TaREMs contain the DRE/CRT element in their promoter (Table 4.2), suggesting that TaREMs can be regulated by DREB/CBF transcription factors in wheat. Byun et al. (2015) showed that DaCBF7 binds to the upstream region of an endogenous REM, which has a putative CRT/DRE. The overexpression of DaCBF7 in rice enhanced tolerance to cold stress through the up-regulation of dehydrin, remorin, and several unknown/hypothetical genes (Os03g63870, Os11g34790, and Os10g22630).

Moreover, all the induced TaREM genes were expressed to a significantly higher level in the winter cultivar in at least one-time point compared to the spring cultivar suggesting their potential implication in freezing tolerance and possible association with phenological development. Additional work is needed to confirm their role. The pattern of gene expression revealed by qPCR in aerial wheat tissues was similar to that which was detected in crowns using the RNA-Seq data for some REM genes such as (TaREM0.12, 1.1 and 1.2 (up-regulated) and TaREM1.5, 5.1, 5.3, 6.1, 6.2, 6.5 and 6.6 (constitutively expressed)).

Remarkably, TaREM0.12 and TaREM1.1 are located on chromosome 6, which is known to harbour the most considerable COR gene numbers (Li et al. 2018). These results support the possible role of TaREM0.12, TaREM1.1, and TaREM1.2 in a more generalized cold response. The differences observed in other REM expression profiles between both studies could be due to the type of tissues used (crowns vs. aerial tissues) and the different experimental conditions (field conditions vs. controlled conditions). Several transcriptional studies of cold acclimation in wheat have shown that changes observed under controlled environments can be different from those in

field studies (Campoli et al. 2009; Greenup et al. 2011; Laudencia-Chingcuanco et al. 2011; Wang et al. 2014), as plants grown under field conditions are exposed to more independent factors compared to controlled conditions.

Remorin regulation under hormone treatment

Plant hormones, such as ABA and MetJ, are involved in regulating several biotic and abiotic processes (Wasternack and Parthier 1997; Mittler and Blumwald 2015). Most TaREM genes considered in this study were down-regulated in response to ABA treatment (Figure 4.7A and B). Thirteen out of the twenty TaREM genes were repressed to different degrees, whereas the remaining genes showed no change (TaREM4.3, and 6.4), or were up-regulated (TaREM1.1, 1.2, 1.5, 4.2 and 0.23) under ABA treatment (Figure 4.7A and B). The up-regulated genes, TaREM1.2 and TaREM1.5, exhibited a high-level of transcript abundance with 15 and 3.5-fold increases, respectively. The REM genes from group 5 and 6 (TaREM5.1, 5.3, TaREM6.1, 6.5 and 6.6) were highly repressed by 50 to 400-fold changes. The other genes (TaREM0.1, 0.12. 0.2, 1.3, 1.4, 4.1, 6.2 and 6.3) were moderately repressed (2 to 21-fold changes) after ABA treatment (Figure 4.7A and B). These results indicate that 16 TaREM genes responded in an ABA-dependent manner and may play a role in ABA signalling. REM was also up-regulated in response to exogenous ABA in rice, suggesting that REM is involved in ABA signal transduction pathway (Lin et al. 2003). In Arabidopsis, REMs are induced through the binding of transcription factors to specific cis-elements in both ABA-dependent and ABA-independent pathways (Raffaele et al. 2007). These results demonstrate that TaREM1.1 and 1.2 are responsive to cold as well as to exogenous ABA treatment. In contrast, TaREM0.23 and TaREM4.3 are regulated in response to cold exposure, but not to ABA treatment; this suggests that ABA-dependent and independent pathways may regulate REM expression in response to cold acclimation.

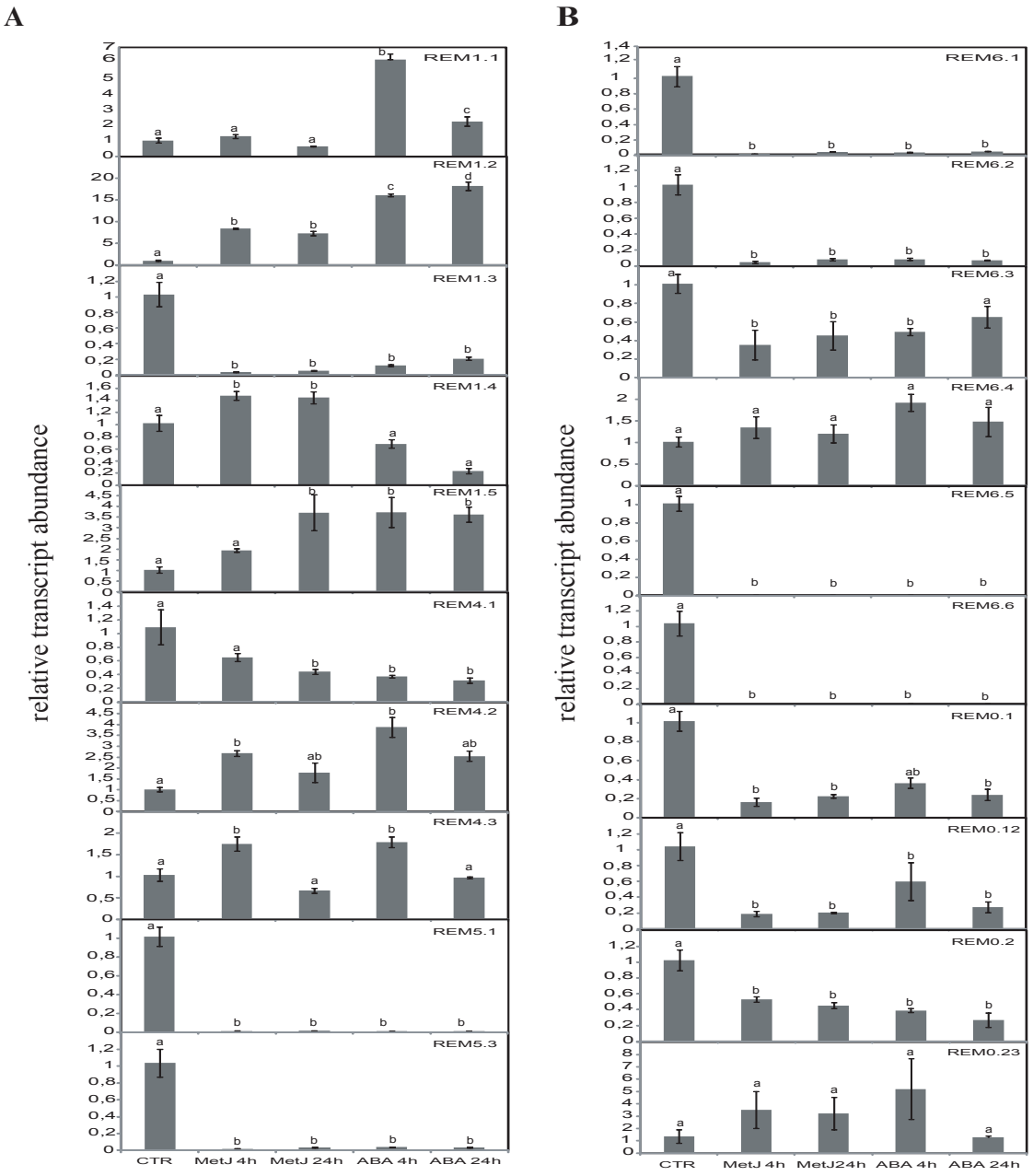

Figure 4.7: Expression profiles of *TaREM* genes in winter wheat (Norstar) in response to Methyl Jasmonate (MetJ) and ABA treatment using qPCR. Expression of REMs genes was compared between control (CTR) and plants treated by MetJ and ABA during 4 and 24 hours. **(A)**, Genes in phylogenetic group 1, 4 and 5; **(B)**, Genes in phylogenetic group 6, 0.1 and 0.2. The y-axis represents relative expression levels of remorin genes compared to 18S. Bars represent the mean values of two biological and technical replicates ± standard deviation (SD). The small different letters present statistically significant differences between samples ($P < 0.05$ by Tukey's test).

Recently, (Kong et al. 2016) showed that the StREMa4 expression level was regulated by SA, MeJA and ABA indicating that StREMa4, and perhaps other REMs, are part of a complex regulatory network affecting plant host interactions with pathogens (Kong et al. 2016). This gene has the strongest homology with wheat REM genes from group 1. The OsREM4.1 was induced by ABA signal through the transcriptional activator OsbZIP23 and plays a role in modulating BR signalling (Gui et al. 2016). Jasmonate positively regulates plant responses to freezing stress through a critical upstream signal of the ICE-CBF/DREB1 pathway to regulate Arabidopsis freezing tolerance (Zimmermann et al. 2014). In our study MetJ treatment induced the expression of TaREM1.2, 1.5, 4.2, and 0.23 genes (Figures 4.7A and B). The expression of TaREM1.1, 1.4, 4.3 and 6.4 showed no significant changes after the MetJ treatment (Figures 4.7A and B). As in the ABA treatment, the expression of TaREM5.1, 5.3, 6.1, 6.5 and 6.6 was severely repressed (55 to 111-fold changes). TaREM 0.1, 0.12, 0.2, 1.3, 4.1, 6.2, and 6.3 were moderately repressed in response to MetJ treatment (Figures 4.7A and B). These results suggest that the 16 differentially expressed genes may play a role in Jasmonic acid signalling. All REM genes identified in Arabidopsis were mostly involved in hormone and biotic/abiotic stress responses (Raffaele et al. 2007). REM accumulation in plants has often been associated with defence signalling molecules (Anderson et al. 2004; Chen and An 2006; Wu et al. 2006). Interestingly, in our study, the qPCR expression analyses revealed that the transcripts of TaREM1.2 and 4.2 accumulate upon exposure to low temperature (LT), ABA, and MetJ. This suggests that both ABA and MeJA may mediate their expression during cold acclimation.

TaREM gene expression in different tissues

REM gene expression is known to be tissue dependent (Raffaele et al. 2007), so to gain insight on tissue preference of TaREMs during cold acclimation of wheat, we examined the expression profiles of all REM genes in four organs (leaf, stem, crown and root) by qRT-PCR. All twenty TaREM genes were expressed in the tested tissues; the expression patterns reveal spatial variation in the expression of TaREM genes in different organs (Figure 4.8A and B). Some TaREMs are expressed preferentially in a specific tissue, and this includes TaREM1.2 in leaves, TaREM6.3 in stems, and TaREM1.1, TaREM1.3, TaREM1.4, TaREM4.2, TaREM4.3, TaREM0.23 in roots.

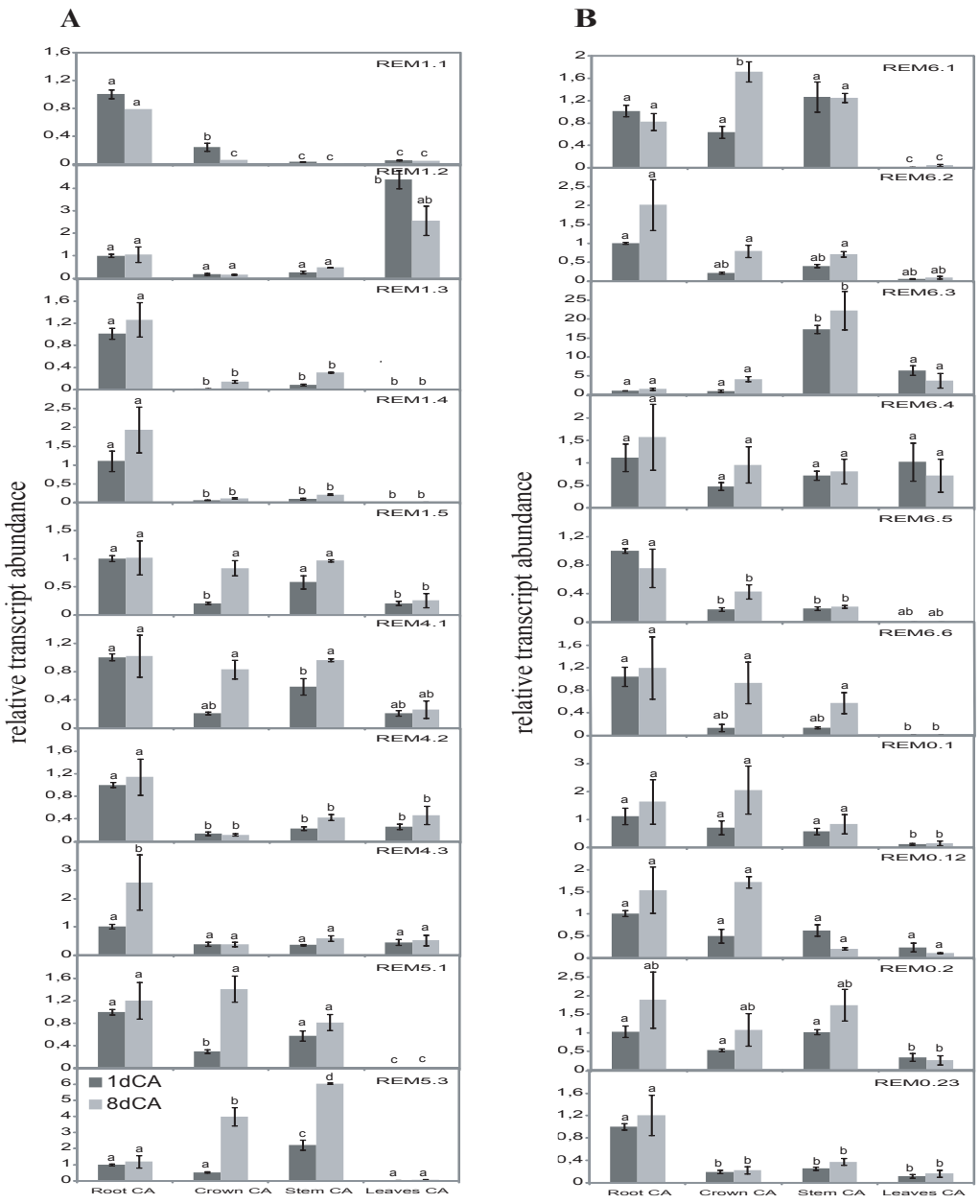

Figure 4.8: Expression profiles analysis of *TaREM* genes in different tissues of winter wheat Norstar during cold acclimation using qPCR**.**, Relative expression of REM genes was compared between roots, crown, stem and leaves from plants 1 and 8 days cold acclimated (1dCA, 8dCA). **(A)**, Genes in phylogenetic group 1, 4 and 5; **(B)**, Genes in phylogenetic group 6, 0.1 and 0.2. The y-axis represents relative expression levels of remorin genes compared to 18S. Bars represent the mean values of two biological and technical replicates ± standard deviation (SD). The small different letters present statistically significant differences between samples ($P < 0.05$ by Tukey's test).

TaREM gene expression was markedly less in leaves during cold acclimation. Seven TaREM genes (TaREM5.1, TaREM5.3, TaREM6.1, TaREM6.2, TaREM6.5, TaREM6.6, and TaREM0.1) displayed significantly less expression in leaves but otherwise did not display a pronounced preference for any other tissue. TaREM genes showed differential expression in various tissues as reported in other plants (Raffaele et al. 2007; Yue et al. 2014). The expression of 6 TaREMs was positively associated with preferential root expression while seven TaREMs showed a substantial loss of expression in leaves during cold acclimation. The higher expression level in roots indicates a possible role in root development during cold stress or may reflect the higher susceptibility of underground tissues to biotic stress under these conditions. The lower expression of TaREMs in leaves may stem from the reduced growth/developmental activity of the mature leaf tissue compared to stems or crowns in cereals. In tomato, millet, and Arabidopsis (group 1b genes), several members of the remorin family were expressed in the vascular system (Bariola et al. 2004; Yue et al. 2014). In millet seedlings, SiREM6 was expressed in different tissues (root, stem, leaf and inflorescences) in the early stage of vascular development (Yue et al. 2014). In *Populus deltoides*, PdREM was expressed in leaf buds, immature and mature phloem indicating the possible function of PdREM in stem development and phloem formation (Li et al. 2013). In rice, the REM gene GSD1 was localized at the plasma membrane and plasmodesmata of phloem companion cells and affected grain set by regulating the transport of photo-assimilates (Gui et al. 2015). According to the analysis of putative TaREM promoters, the TaREM gene family harbours different numbers and types of cis-elements involved in abiotic/biotic stresses, low-temperature, ABA, and MeJA responses. Additionally, TaREM genes showed tissue-specific responses during cold acclimation. Together these observations help to explain the complex response of TaREMs to abiotic stresses and hormonal treatments. These results indicate that TaREM genes have several functional roles in response to hormone and cold treatment.

Conclusions

In this study, we evaluated the functional importance of REM gene family members for the first time in wheat. Twenty non-redundant REM genes were identified and phylogenetically clustered into six distinct subfamilies. Phylogenetic analysis showed that TaREMs and other monocots REMs (rice) are homologous, suggesting a probable functional similarity among them. The responses of wheat REM genes to low temperature, ABA, and MeJA were determined where several genes were specific to low temperatures, while others responded to low temperature, ABA, and MeJA. This suggests that some REM genes may be regulated by cold through hormonal

signalling pathways. Cis-element analyses of putative REM promoters revealed the presence of cis-motifs specific to cold response, other abiotic stresses, hormone regulation, tissue specificity, and development which indicates that the expression of the REM genes is modulated in part by the regulatory elements in their promoters. Expression profiles of the twenty wheat REM genes in leaves, stems, crowns and roots showed that they were expressed in all tissues, with higher expression in roots. Comparisons between autumn field and controlled environments showed common expression for some TaREM genes, but not in others. The contradictions between the two experiments may be due to the type of tissues used and the different experimental conditions. The expression of REM genes at different wheat developmental stages and in different tissues and their association with cold acclimation and hormonal responses suggest a vital role during wheat development. Understanding the function of each gene during the wheat life cycle may help to select for varieties that tolerate higher biotic and abiotic stresses. One caveat of this study is that some the retrieved wheat remorin sequences were incomplete (Table 4.1).

Chapter Five: Evolutionary and In-Silico Functional Analysis of a Novel Cold Responsive Gene in Wheat

Abstract

Identification of cold responsive genes is essential for developing cold tolerant crop plants to increase agricultural productivity in the temperate regions. This study is focused on gaining insights into evolutionary history and in-silico functional characterization of a novel cold responsive gene in wheat. This gene in has a distant homology to known abiotic stress related genes in other plants including CAP160 in *Spinacia oleracea*, RD29B in *Arabidopsis thaliana* and CDeT11-24 in *Craterostigma plantagineum*. We investigated if these genes form a closely related gene family with close homologous relationship and shared ancestry or if they are a result of convergent evolution from unrelated proteins. Our results show that these genes are homologous and evolved from a common ancestor. The Bayesian phylogenetic analyses of the protein sequences of this gene from various plant species revealed three distinctive clades. Further analyses revealed that this gene has predominantly evolved neutral processes with some regions experiencing showing signatures of negative selections and some regions showing signatures of episodic positive selections. These genes contained common K-like segments and function predictions revealed that these protein-coding genes may share at least two functions related to abiotic stress conditions. One function is similar to the cryoprotective function of LEA protein, and the second function as a signalling molecule by binding specifically to phosphatidic acid.

Introduction

Abiotic stresses such as low temperatures (0-15 °C), freezing conditions (< 0 °C), heat (35-45 °C), and drought stresses have adverse effects on plant growth, development and productivity. These factors also determine the geographical distribution of many species. However, geographically wide-ranging plant varieties show great variation in their tolerance towards such stressful conditions: some varieties express tolerance whereas others, even within the same species, are sensitive. These contrasting physiological responses within the same species towards abiotic stresses are maintained by modifying the expression of various genes. Discriminative transcriptional networks were detected between sensitive and tolerant varieties, either at the level of intensity for some abiotic stress-regulated genes, or on the base of on-off gene regulation mechanism. The identification of abiotic stress-related genes – either through genome-wide studies

or by bioinformatic approaches – is essential for improving molecular studies and genetic improvements. The identification of plant CAP160 homologous genes revealed their regulation by abiotic stresses in both monocot and dicot plant species.

Identification of a new gene family or new genes within an existing gene family facilitates further study of the gene's pattern of evolution and its role during an organism's development. (Pearson 2013) states that identity, e-value, and bit-score are the common ways to infer homology as e-value and bit-score are useful in inferring homology. However, Pearson (2013) notes that a 30% identity cut-off may ignore many homologs that can be found with an e-value $<10^{-10}$ for nucleotide to nucleotide sequence comparison or e-value $<10^{-3}$, and bit-score > 50 for protein to protein sequence comparison. Presence of the same domain among proteins may infer function relatedness but not authentic homologous relationships. Thus the presence of a protein domain should be used to confirm homology, but not to validate it as many non-homologous proteins may share domains and be taken mistakenly as homologs (Joseph and Durand 2009). One limitation of using e-value, bit-score, and identity cut-offs is when retrieving homologs in protein super-families that include many analogous protein sub-families across different species where it is problematic for these measures only to infer authentic interspecies homology among related proteins as this may account for the availability of information in the query database during a blast search. A reciprocal blast should be used to verify the homologous relationship (Agostino 2013) and avoid a misleading result. Thus, the use of reciprocal blast along with using other measures like e-value cut-off is an essential step to infer authentic homology. Additionally, synteny can be used to verify the occurrence of homologous genes within the flanking regions surrounding the gene of interest across different species. This kind of comparative genomics provides insights not only into the homologous relationship but also into gene order, the pattern of gene evolution and duplication events, in addition to identifying these orthologous gene loci as possible linked evolutionary markers.

Our interest focuses on a new, cold-regulated gene from wheat that has an extremely distant homology with the CAP160 gene from spinach, the CDeT11-24 gene from *Craterostigma plantagineum,* and the RD29 gene from Arabidopsis. Although these genes are distantly related and have low identity values with the wheat gene, their expressions are similarly affected by abiotic stresses. Arabidopsis RD29 genes are abiotic stress marker genes that are regulated by ABA (Yamaguchi-shinozaki et al. 1992). These genes show discriminatory two-phase kinetics of expression: the first phase is induced through the ABA-independent pathway in less than 30

minutes from the onset of desiccation, whereas the second is provoked after three hours from the start of desiccation through the ABA-dependent pathway. Further analysis indicated that Arabidopsis has two RD29 genes located tandemly in an 8-kb region of its genome. One of them, RD29B, showed induction through an ABA-responsive manner only after three hours under either low-water activity or ABA conditions. The other, RD29A, accumulates its transcript after 3 hours of low-water activity or ABA conditions, and also within 20 minutes of low-water activity conditions in an ABA-independent manner (Yamaguchi-Shinozaki and Shinozaki 1993). It has been shown that the promoter motif analysis of RD29 genes revealed an AtRD29A promoter with DREs elements and one ABRE, while the RD29B promoter has three ABREs and one DRE elements (Msanne et al. 2011; Jia et al. 2012). ABA-treated Arabidopsis plants exhibited more induction of RD29A than RD29B, confirming their regulation through the ABA-signalling pathway, and inferring their prospective roles as either cellular protective proteins or regulatory proteins that may attenuate the negative effects of abiotic stresses, mainly water deficit conditions (Hoth et al. 2002). Additionally, the primary protein structure for the products of RD29 genes revealed high similarity regarding their hydrophilicity besides the presence of two acidic regions and one basic region and only one amino acid cysteine. The stress-responsive RD29A protein has two tandem repeats of 112 amino acids centrally located, and 21 amino acid tandem repeats near its C-terminal, which are absent in its paralogous protein, RD29B.

Arabidopsis RD29 genes have a remote homology with the cold acclimation protein CAP160 in spinach (Kaye et al. 1998). The protein profile of cold-acclimated spinach leaves versus non-acclimated plants showed the accumulation of many new polypeptides. Four of these proteins had been named CAP proteins and were denoted numbers for their molecular weights; for example CAP160 is a protein that has been identified as one of the four major accumulated proteins in the cold acclimated spinach leaves (Guy and Haskell 1987). Studies using ^{32}P-radiolabelling on cold-acclimated spinach seedlings indicates that CAP160 with its characteristic isoelectric point (pI) 4.5, is likely to be a phosphoprotein (Guy and Haskell 1989).

Velasco et al. (1998) identified a CDeT11-24 gene in *Craterostigma plantagineum* as a distant homologous gene of both spinach CAP160 and Arabidopsis RD29. The CDeT11-24 gene is upregulated in response to dehydration, salinity, and abscisic acid. This gene has a highly conserved lysine-rich domain, which resembles those in other LEA proteins. Liquid chromatography-tandem mass spectrometry techniques confirmed that its protein has many phosphorylation sites, which are subject to phosphorylation only in dehydrated tissues (Röhrig et

al. 2006). This is similar to what had been preliminarily demonstrated in its nearest homologous CAP160 gene, from spinach (Guy and Haskell 1989). It has been predicted that the dehydrin-like lysine-rich motif (K-like segment) near the CDeT11-24 N-terminal, may form a coiled-coil structure (Röhrig et al. 2006). This structure may be related to the function of this protein in providing cellular protection by its accumulation during abiotic stress conditions.

Plant cells gradually accumulate LEA proteins due to their cryoprotective and antifreeze activities in various cell compartments to protect the cell during severe low-temperature conditions or low water activity (Wise and Tunnacliffe 2004). Previous works have found that dehydrins are classified as a group II of LEA proteins which were previously identified as the group (D-11) (Wise and Tunnacliffe 2004; Battaglia et al. 2008). Although dehydrins are categorized into five distinct subgroups, all of these groups can only be structurally recognized by their characteristic K-segment (EKKGIMDKIKEKLPG) that is predicted to form the amphipathic α-helical structure, which acts to protect membranes from dehydration, mediate specific protein-protein interactions, and protect enzymes from inactivation (Kiyosue et al. 1994; Kovacs et al. 2008). The presence of many K-segments in the same dehydrin facilitate the formation of a bundle with amphipathic alpha-helical confirmation as a result of their interaction. In general, LEA proteins prevent protein inactivation through their "molecular shield activity", which reduces protein aggregation imminent from water stress, in addition to their solution effects that are similar to the impacts of polysaccharides in minimizing protein aggregation (Chakrabortee et al. 2012). Further studies on CDeT11-24 verified that its LEA group 2 (dehydrins) analogous characters are responsible for the protective role towards *in vitro* tested enzymes, and its ability to bind specifically to phosphatidic acid (PA) rather than other tested lipid molecules, where these behaviours are mainly due to its K-like dehydrin segment (Petersen et al. 2012).

Although diverse abiotic stresses regulate RD29, CAP160 and CDeT11-24 genes, the common characteristics of these genes have not yet been identified. A newly identified cold-regulated gene from wheat is distantly related to this group of genes which all have remote homology to one another. Due to this remote homology, only a limited number of genes have been identified to be distantly related to the SoCAP160 gene, and no genes have been discovered in the monocot clade. Thus, we aimed to test whether the cold-regulated gene from wheat is the authentic homologues gene of CAP160, CDeT11-24, and RD29 genes from spinach, *Craterostigma plantagineum,* and Arabidopsis, respectively. If these genes are homologs, we aim to identify other homologous genes that can potentially be found in monocots and dicots in order to study the

function, as well as the common and distinctive characteristics of this gene family. For the first time, we identified and verified many homologous proteins inside dicots and in monocots. We used structural alignment to accurately identify the most conserved structural and functional motifs in this unique family of LEA proteins. We also examined the evolution of CAP160 gene homologs. Our work found that CAP160 gene homologs constitute a family that is postulated to have evolved by vertical descent from a single common ancestor. Many intraspecies' "new" genes were found to arise from gene duplication events. The identification of this distinctive gene family supports future molecular and function characterization studies because we identified new dehydrin-like genes among different plant species. It was not our goal to provide an extensive study covering all plant CAP160 orthologous genes, nor to provide specific domains distinctive to this family, however, we answer the question of whether this gene family has been extended into monocot plants, and we attempt to predict its function during water deficit conditions.

Materials and Methods

Sequence retrieval

The sequence of a novel cold-regulated gene was retrieved from the RNA-Seq dataset of the cold experiment on wheat (Li et al. 2018). The gene was identified as XLOC_002283 and annotated by the authors through the International Wheat Genome Sequencing Consortium with IWGSC identifier as Traes_1AL_5184A1376. The gDNA, CDS, and protein sequence of this candidate are found in Dataset S5.1 with a symbol identifier Ta1.1. This wheat protein sequence was used as a query in a tblastn search with a cut-off e-value <1e-04 (Pearson 2013) to retrieve other homologous genes from wheat and other monocots, as well as against the *Theobroma cacao* genome database hosted by Ensembl Plants (http://plants.ensembl.org). The tblastn search against the *T. cacao* genome identified only one gene sequence that has been confirmed as an authentic homologous protein of the wheat and barley genes by the reciprocal blast. The retrieved protein sequence from *T. cacao* was used in a manual PSI-tBLASTn with the same cut-off e-value against many dicot plant genomes from different databases as indicated in Table S5.1, to retrieve all other dicot sequences. All the retrieved gDNA, CDS, and protein sequences used in this study are listed in Dataset S5.1.

Multiple sequence alignment and structure predictions

Retrieved protein sequences have been aligned by MAFFT version 7 (https://mafft.cbrc.jp/alignment/server/), T-COFFEE (Notredame et al. 2000; Di Tommaso et al. 2011), and Decipher, an R-based alignment software (Wright 2015). The quality of the alignments was assessed by sum-of-pairs (SP), column score (CS) and avg_SPdist score by comparing them with each other using the VerAlign online tool (Bawono et al. 2015). Protein secondary structure was predicted on the alignment using Jalview (version 2.10.3b1) software (Waterhouse et al. 2009). The PONDR program (http://www.pondr.com) was used to predict the folding states of some selected protein sequences. The amphipathic helices were selected and presented using the HELIQUEST tool (Gautier et al. 2008).

Phylogenetic analysis

The best-fitted amino acid substitution model was selected with the lowest BIC score, using ProtTest v3.4.2 (Darriba et al. 2011). A Bayesian phylogenetic tree was constructed via MrBayes v3.2.6. (Ronquist et al. 2012) with the Jones-Taylor-Thornton (JTT) amino acid substitution model, and (+I+G) for the rate of heterogeneity with (+F) for the empirical equilibrium of amino acid frequencies from the alignment. The Markov Chain Monte Carlo parameters were: Ngen = 10^6, nchains = 12, burninfrac = 0.25. The reconstructed phylogenetic tree of clade III was done using the same protein substitution model JTT+G+F+I for 6×10^5 generations while the model JTT+G+F suits clade I and clade II were done with 5×10^5 and 10^5 generations, subsequently.

Comparative genomics

Conserved gene order in micro-syntenic chromosomal regions (100-Kb) containing CAP160/RD29/CDeT11-24 gene homologs was compared in rice *Oryza sativa*, cotton *Gossypium raimondii*, tomato *Solanum tuberosum*, potato *Solanum lycopersicum*, sorghum *Sorghum bicolor*, pink shepherd's purse *Capsella rubella*, strawberry *Fragaria vesca*, rose gum *Eucalyptus grandis*, papaya *Carica papaya*, thale cress *Arabidopsis thaliana,* and amborella *Amborella trichopoda* against the matching genetic region in the cacao tree *Theobroma cacao* using the Plant Genome Duplication Database (PGDD) freely available at http://chibba.agtec.uga.edu/duplication/ (Lee et al. 2013).

Gene structure

The intron/exon structures of different genes were determined using the GSDS online tool (Hu et al. 2015) by comparing the full-length coding sequences with their counterparts genomic sequences (Dataset S5.1).

Analysis of enriched *cis*-regulatory elements in promoter regions

According to their availability, 2-Kb of upstream sequences relative to the translation start site were retrieved from the blast service hosted by the NCBI database (NCBI Resource Coordinators 2016), and all the retrieved promoter sequences were listed in Dataset S5.2. Distribution and occurrence of enriched PLACE *cis*-elements (Higo et al. 1999) were identified and graphed according to Austin et al. (2016). Only motifs with Z-scores more than 5 were presented, where the functional depth for position-specific scoring matrix (PSSM) was more than 0.35, and conditionally a minimum of 50% of the tested promoters in each group must have the selected motif.

Protein characters and subcellular localization

Protein molecular weights, and their isoelectric points were estimated according to Kozlowski (2017), and the grand average of hydropathy (GRAVY) was estimated according to Kyte and Doolittle (1982). Subcellular localization of each protein was predicted by five different tools which are LOCALIZER (Sperschneider et al. 2017), PredSL (Petsalaki et al. 2006), CELLO (Yu et al. 2006), Predotar (Small et al. 2004) and LocTree3 (Goldberg et al. 2014).

Protein conserved motif evaluation

Thirty protein conserved motifs were identified using Multiple EM for Motif Elicitation (*MEME*) at the website http://meme.sdsc.edu/meme/intro.html (Bailey et al. 2009), with default parameters. The predicted functional sites in these motifs were retrieved from the Eukaryotic Linear Motif (ELM) web-interface http://elm.eu.org/ (Dinkel et al. 2016). The retrieved *MEME* motif representations, locations and numbers were annotated on the Bayesian phylogenetic trees using the online tool iTOL (Letunic and Bork 2016).

Differential gene expression and Co-expression Analyses

Differential gene expression analysis of Arabidopsis, rice, barley, maize, and wheat CAP160 homologous genes within various microarray-based experiments and across different

treatments were retrieved from Genevestigator software (Zimmermann et al. 2014), using the appropriate gene identifiers. In Arabidopsis, AT5G52300.1 and AT4G25580.1 were used to represent the genes Ath1.1 and Ath1.2, respectively. In rice, Loc-Os10g36180.1 was used to represent the Os gene. In barley, Mloc_74793.3 was used to represent the Hv gene. In maize, GRMZM2G376743 was used to represent both Zm1.1 and Zm1.2 genes. For wheat, the Ta.8085.1.S1_at probe was used to represent Ta1.1, Ta1.2, and Ta1.3 genes, while the TaAffx.51089.1.S1_at probe was used to represent Ta1.3, Ta1.4 and Ta1.5 genes. Positively co-expressed genes of CAP160 homologs in Arabidopsis and rice were presented by using the same software, highlighting the annotations of the highly connected genes and their differential expression profiles.

Estimation of selection pressures

The alignment of protein-coding sequences from different species was used to evaluate the effect of natural selection on protein evolution across this gene family. Mixed-effects models of evolution (MEME) (Murrell et al. 2012) and the fixed effects likelihood approaches (FEL) (Kosakovsky Pond and Frost 2005a) were used to assess selection on individual sites that may be under episodic diversifying selection as determined by MEME, or pervasive selection, as measured by FEL. FEL measures ω (Ka/Ks) ratios across lineages at individual sites by inferring a maximum-likelihood tree, while MEME detects sites under positive selection where the rate of ω not only varies from site to site, but also from branch to branch. MEME is more sensitive in revealing sites under episodic positive selection through the same maximum-likelihood approach. One limitation of MEME is that it does not assign specific branches where individually selected sites that exhibit episodic positive selection. Therefore, to assess which branches and nodes demonstrated episodic positive selection during the evolution of this gene family, the adaptive branch site-random effects likelihood (aBSREL) method was used (Smith et al. 2015). The aBSREL test requires no prior knowledge about lineages-of-interest, and thus all the lineages across the entire phylogenetic tree were tested. These tools for estimating selection pressures are implemented in the Datamonkey web server (Kosakovsky Pond and Frost 2005b).

K-like segments Assessments

The amphipathic helical wheels from wheat was compared with its homologs in *Craterostigma plantagineum*, according to Gautier et al. (2008). Additionally, the tertiary

structures of these amphipathic wheels were predicted and presented, according to Reißer et al. (2014) and Schrödinger LLC (2016).

Results

Authentic homology assessment

A tBLASTn search with a cut-off e-value less than 1e-04 was used to test whether the retrieved proteins from the monocot clade, such as sequences from wheat and barley, contained any homologous genes in dicot plants. The proteins were used as queries against different dicot genome databases; this yielded no results in the tested dicot plants except against the *Theobroma cacao* genome database, where the tBLASTn algorithm identified only one gene sequence located on chromosome number 3 in cacao with identifiers TCM_015165 and EOY23189. A reciprocal blast search was performed against different monocot plant species, such as barley and wheat, to validate the homologous relationships. One advantage of this approach was that cacao, barley, and wheat, have their genome fully sequenced and publicly available, which diminishes the presence of any false results and accurately assesses the authentic homologous relationship. Using the cacao protein as a query in a tBLASTn search with an e-value parameter <1e-04 returns all known CAP160 proteins in various dicot species. These include CAP160, RD29, and CDeT11-24. The inability of wheat or barley proteins to retrieve these sequences by a simple tBLASTn algorithm may be due to the difficulty to establish a reliable alignment score among distantly related proteins. Hence, comparing cacao with barley proteins yields a low identity value (26%), the cacao protein query covers 83%, with a bit-score of 62.4; this indicates the limitation of using 30% identity cut-off in overlooking many homologs (Pearson 2013). Finally, using either cacao or barley protein as queries in a tblastn search with cut-off e-values <1e-04 against different dicot and monocot plant genome databases, respectively, we retrieved CAP160 homologous gene sequences from the different dicot or monocot species. To investigate plant CAP160 genes characteristics and evolution; many homologous gene sequences were retrieved this way from forty distinctive plant species that exemplify three different families from monocots, sixteen families from dicots, and Amborellaceae, a family that represents basal angiosperms (Table S5.1).

To further confirm the orthologous relationship between the retrieved cacao sequence gene and other genes from monocot or dicot clades, comparative genomics was used for the chromosomal segment-containing TCM_015165 from cacao with the corresponding chromosomal segments of eleven different plant species. Results showed that many syntenic anchors in cacao

match those in *Amborella*, rice, sorghum, and many other genes from dicot plants (Figure S5.1). Moreover, microsyntenic analysis confirms the duplication events in two genes from *Capsella* and for genes RD29B and CAP160 from Arabidopsis. Although two adjacent markers are enough to infer homologous synteny blocks, Figure S5.1 reveals at least the presence of four syntenic markers as in case of Cr1.2 and Ath1.2 genes. The presence of these syntenic anchors that match the gene from cacao, with their homologous genes within different monocot or dicot species, supports the orthologous relationship among these genes. With the conserved gene order among cacao and other species in the designated micro-syntenic chromosomal segment, the analysis confirmed the divergence of matching micro-syntenic anchors among distantly-related species, as indicated in Figure S5.1 and the annotations of the cacao matching genes from Table S5.3. Synonymous (Ks) and non-synonymous (Ka) substitution values presented an overall negative trend, where Ka-Ks < 0 among most diverse plant syntenic anchors when compared with the matching cacao genes except in the case of the two monocot plants rice and sorghum where Ka-Ks > 0 as seen in Table S5.3 (Xia and Kumar 2006). The Ka-Ks positive values in rice and sorghum indicates that their CAP160 gene pair and surrounding segments might be under positive selection where the fixation rate of useful sites spreads. This may imply opposing selection pressures in these micro-syntenic regions in monocots as represented only by rice and sorghum versus dicots.

Molecular phylogenetics

To estimate the evolutionary seeds of the newly identified ABA and cold-regulated gene in wheat, many homologous genes available in public databases were retrieved to investigate the origin and expansion of this gene family (Table S5.1 and Dataset S5.1). All the retrieved protein sequences were aligned by MAFFT version 7 (https://mafft.cbrc.jp/alignment/server/), T-COFFEE (Notredame et al. 2000; Di Tommaso et al. 2011), and Decipher, an R-based alignment software (Wright 2015). Testing the quality of different alignments by the VerAlign tool (Bawono et al. 2015) indicated that Decipher as a test alignment presents a higher sum of pairs (SP) score, column score (CS), and SPdist score (Table S5.2); this shows that Decipher outperforms the other two programs and has a higher quality of alignment. The Decipher outperformance may be due to the alignment of protein coding sequences based on the predictions of the secondary structures of their translated proteins by the GOR algorithm which is implemented in it (Wright 2015). Therefore, the output alignment from Decipher was used for further analyses. The secondary structure of the first protein in the alignment was predicted by Jpred4 (Drozdetskiy et al. 2015)

which is implemented in the Jalview software, to present the secondary structure prediction on the alignment.

Additionally, intrinsically disordered protein (IDP) regions were predicted by the IUPred method which is implemented in Jalview, and both secondary structure and IDP predictions were plotted on the alignment (Figure S5.2). The alignment showed the presence of a highly conserved region of amino acids near the N-terminal, which is highly predicted with an alpha helix motif structure and the existence of many IDP regions.

The Bayesian inference was performed using MrBayes v3.2.6. (Ronquist et al. 2012) to represent the evolutionary relationships among the retrieved proteins. By taking the protein from the basal angiosperm *Amborella trichopoda*, as an outgroup, the analysis showed that all the retrieved protein sequences could be clustered within three major clades (Figure 5.1). All monocot species except one duplicate protein from *Musa acuminate* (Ma1.2) are distinguished in clade II, with two common ancestors, which are *Phoenix dactylifera* (Pd) and *Musa acuminate* (Ma1.1), respectively. This result is in line with the phylogeny inference of Poales based on their plastid genome (Givnish et al. 2010) and phylogenetic analysis of angiosperms families based on fossil records (Magallón et al. 2015), where Arecales and Zingiberales are presented with older ages, respectively. Also, Figure 5.1 presents many monocot cold and drought-sensitive species in a separate clade originated from node 42 (N 42), which can be distinguished from cold and drought-tolerant monocot species which originate from node 21 (N 21). Clade III represents only species from dicots with *Eucalyptus grandis* (Eg) as a common ancestor, although fossil dating estimates an older age of Ranunculales than Myrtales (Magallón et al. 2015). Many duplicate genes from dicot species with one duplicate gene from monocot species represented by *Musa acuminate* (Ma1.1), were settled in a unique monophyletic group (Clade I) near the common outgroup (Figure 5.1) with a high posterior probability. This result supports the common origin of this unique gene family and signifies the value of gene duplication events in facilitating its expansion. The intron/exon organization showed pervasive symmetric exons, except for some genes from the genus Triticum and genes Eg, Bo1.1, Ah and Kf1.1 from Clade III (Figure 5.1). All symmetric exons are surrounded with phase 1 introns while asymmetric exons are bordered by phase 0 and phase 1. Numbers of introns ranged from 0 to 7, where cacao (Tc) is the only sequence in this dataset that shows the total absence of introns. Most sequences exhibit short lengths of introns in comparison with their surrounding exons.

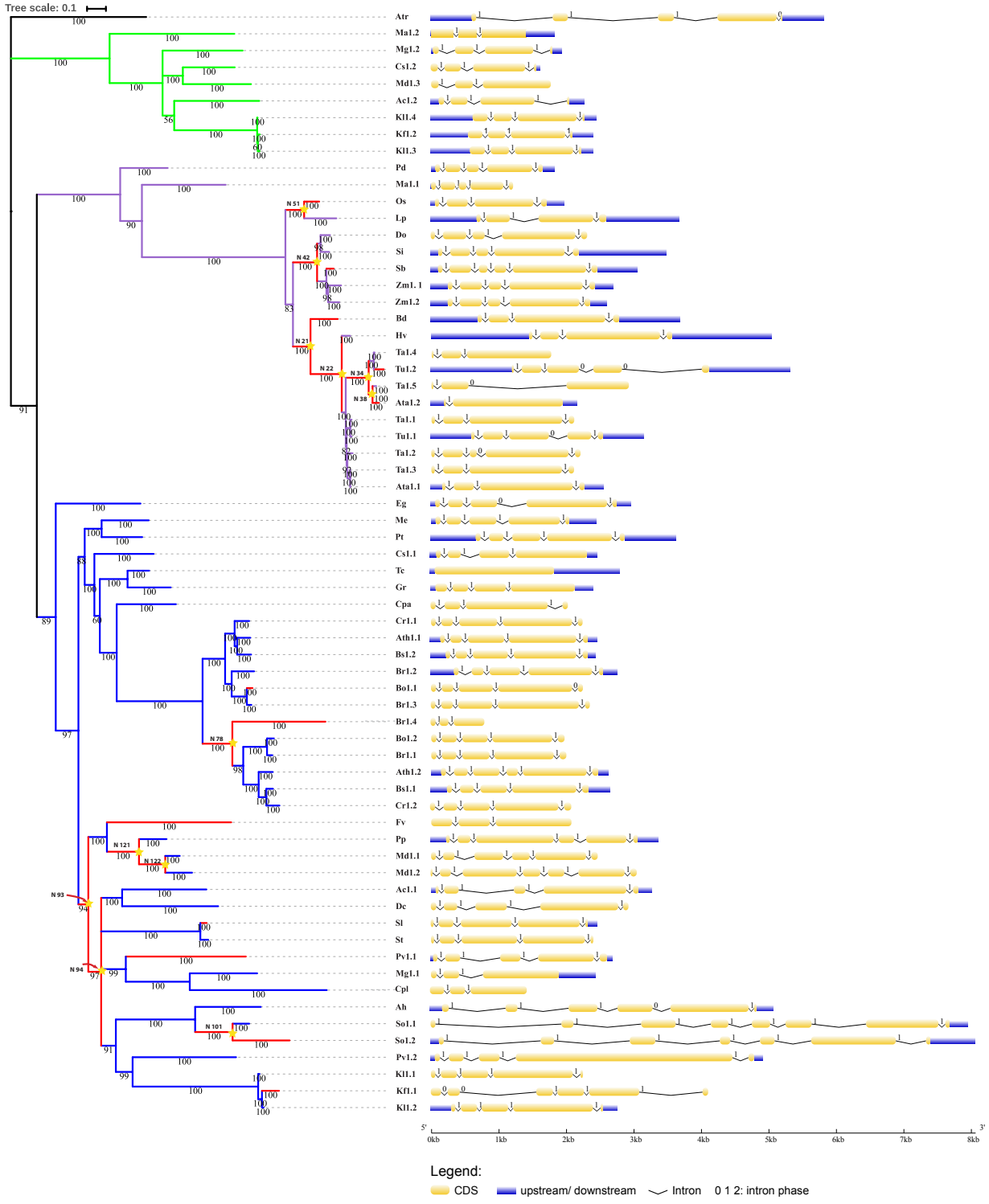

Figure 5.1: Bayesian phylogenetic analysis and gene structures with intron phase distributions of CAP160 homologous genes from different plant species. The phylogenetic tree is rooted by using the homologous sequence from *Amborella trichopoda* (Atr). The analysis reveals three distinctive

clades which are colored as green, violet, blue for clade I, clade II and clade III, respectively. Branches with red color and nodes with stars are verified with episodic diversifying selection according to aBS-REL method (Smith et al. 2015).

Signatures of natural selection

Protein coding sequence alignment of CAP160 gene homologs was used to evaluate the repercussions of natural selection on this gene family's evolution. The FEL analysis showed that 373 sites are significantly under pervasive negative selection (Table S5.5) while only five sites are positively selected with a p-value threshold of 0.05 (Table S5.4). These results indicated that the evolution of the plant CAP160 gene family could be best described by neutral theory where only 12.6% are under constrained selection, and a small portion around 0.17%, are positively selected. Mixed-effects model of evolution (MEME) was applied to test the presence of positively selected sites on specific lineages. MEME results detected twenty sites under episodic diversifying selection (Table 5.1); four of them were also significantly detected by FEL under pervasive positive selection (Table S5.4). These methods identify sites under positive selection, thus both methods agree on identifying these four codons under positive selection; since MEME is a more complex model that tests the evolution of sites under positive selection in any fraction of branches, it finds more sites under positive selection. Episodic selection model results indicated that sites 651, 682, 1110, 2237, and 2616 are positively selected in more fractions in the phylogenetic tree with only one site (682), that is selected within more than 50% of branches, where $\beta^+ > \alpha$ (Table 5.1).

Table 5.1: Codons of CAP160 gene homologs under episodic diversifying selection and their site-specific parameter values as estimated by mixed-effects models of evolution (MEME; Murrell et al., 2012). Twenty codons were detected under episodic diversifying selection with a p-value threshold of 0.05. MEME results display parameters for each site where α represents synonymous rate, β^- constitutes nonsynonymous rate at this site for lineages in the negative/neutral evolution component and β^+ is for the nonsynonymous rate at this specific site for positively-selected lineages. The probability of the tree evolving neutrally or under negative selection is represented by p^- while the probability of the tree evolving under positive selection is represented by p^+. MEME uses likelihood ratio test (LRT) to infer the significance of positive selection ($\beta^+ > \alpha$) for a specific site.

Codon	α	β^-	p^-	β^+	p^+	LRT	p-value
2	0.21	0.21	0.96	702.51	0.04	19.69	0
17	0.35	0.3	0.92	10.29	0.08	6.04	0.02
339	0.18	0.16	0.96	15.11	0.04	8.96	0
429	0.07	0.06	0.79	4.19	0.21	12.02	0
651	0.02	0	0.56	3.25	0.44	8.91	0.01
682	0	0	0.47	25.25	0.53	5.34	0.03
837	0	0	0.87	9.92	0.13	10.95	0
1110	0	0	0.52	1.63	0.48	7.61	0.01
1185	0.31	0.12	0.7	2.08	0.3	4.8	0.04
1966	0.26	0.16	0.87	7.65	0.13	7.52	0.01
1984	0.4	0.4	0.9	141.38	0.1	10.16	0
2040	0.59	0	0.77	5.73	0.23	6.04	0.02
2237	0.52	0.2	0.64	5.46	0.36	6.12	0.02
2332	0	0	0.77	10.31	0.23	10.97	0
2525	0.23	0	0.8	12.75	0.2	7.38	0.01
2616	0	0	0.67	5.32	0.33	6.16	0.02
2622	0	0	0	3.27	1	4.88	0.04
2631	0.44	0	0.84	33.82	0.16	9.83	0
2770	0.12	0.12	0.97	417.54	0.03	4.6	0.05
2917	0.15	0	0.53	2	0.47	4.62	0.05

To identify branches and nodes which have a fraction of sites under positive selection, aBSREL was applied and revealed that 34% of branches can be modelled with a single ω rate class, while 66% of branches can be only modelled with multiple ω rate classes and 24 branches have a proportion of sites under diversifying selection (Table 5.2). A total of twelve lineages and twelve nodes showed episodic positive selection (Figure 5.1 and Table 5.3). In most lineages, the portion of sites under positive selection was less than 30%, while the remaining sites exhibit neutral or negative selection where ω_1 ranges from 0.022 to 1 (Table 5.3). The episodic positive selection was detected only on some branches and nodes in Clade II and Clade III, whereas no signs of positive signatures were identified across Clade I sequences (Figure 5.1).

Table 5.2: Adaptive branch site-random effects likelihood (aBSREL) analysis results (Smith et al. 2015).

ω rate classes	# of branches	% of branches	% of tree length	# under selection
1	43	34%	0.069%	0
2	83	66%	100%	24

Table 5.3: Lineages and nodes with significant (p-value threshold of 0.05) signatures of positive selection as estimated by aBSREL (Smith et al. 2015).

Name	B	LRT	Test p-value	Uncorrected p-value	ω distribution over sites	
					ω_1 (Negative sites)	ω_2 (Positive sites)
Tu1.2	0.0000	139.3829	0.0000	0.0000	1.00 (94%)	10000 (5.5%)
Kf1.1	0.0000	180.6526	0.0000	0.0000	0.270 (90%)	7500 (10%)
Bo1.1	0.0000	28.0560	0.0000	0.0000	0.425 (99%)	10000 (1.1%)
Br1.4	0.0000	32.6475	0.0000	0.0000	0.0958 (70%)	10000 (30%)
Fv	0.0000	30.6036	0.0000	0.0000	0.225 (69%)	1470 (31%)
So1.2	0.0000	41.2442	0.0000	0.0000	0.747 (85%)	38.6 (15%)
N 22	0.0000	35.3608	0.0000	0.0000	0.0654 (84%)	11.1 (16%)

N 34	0.0000	44.5690	0.0000	0.0000	0.931 (93%)	127 (6.8%)
N 38	0.0000	63.4478	0.0000	0.0000	0.0220 (98%)	10000 (1.8%)
N 42	0.0000	48.5106	0.0000	0.0000	0.0634 (86%)	64.3 (14%)
N 122	0.0000	26.9252	0.0001	0.0000	0.116 (89%)	23.6 (11%)
N 21	0.0000	23.6973	0.0003	0.0000	1.00 (84%)	42.3 (16%)
Bd	0.0000	22.8978	0.0004	0.0000	0.109 (85%)	8.82 (15%)
Ata1.2	0.0000	20.2870	0.0015	0.0000	0.703 (99%)	10000 (0.95%)
N 121	0.0000	20.3229	0.0015	0.0000	0.601 (87%)	321 (13%)
N 51	0.0000	20.2926	0.0015	0.0000	0.152 (88%)	14.2 (12%)
N 78	0.0000	20.1171	0.0016	0.0000	0.161 (90%)	120 (9.6%)
N 93	0.0000	18.7646	0.0031	0.0000	0.230 (94%)	10000 (6.2%)

N 94	0.0000	17.3444	0.0062	0.0001	0.103 (92%)	150 (7.9%)
Sb	0.0000	16.7699	0.0082	0.0001	0.164 (98%)	95.6 (1.8%)
Os	0.0000	16.0266	0.0119	0.0001	0.255 (92%)	15.9 (7.6%)
Pv1.1	0.0000	15.7275	0.0136	0.0001	0.286 (70%)	13.6 (30%)
Sl	0.0000	15.2666	0.0170	0.0002	0.0593 (95%)	12.9 (5.1%)
N 101	0.0000	14.3266	0.0271	0.0003	0.149 (86%)	73.4 (14%)

Function predictions

Protein characters

The predicted isoelectric points of CAP160 homologous proteins reveal acidic tendency, where only Br1.4 has pI of 9.8 (Table S5.6), while other proteins have isoelectric points ranging from 4.4 to 6.7. Sizes of the proteins revealed that Br1.4 is the smallest predicted protein, with only 220 amino acids (24.12 kDa). This result may reveal the reason of its basic tendency, as this may be the effect of the conserved K-like segment which is rich with positively charged amino acids, mainly lysines. The biggest protein was Pv1.2 with 1299 amino acids (141.4 kDa), while other protein predicted sizes ranged from 34.1 to 100.7 kDa. GRAVY values showed that all proteins have negative scores which indicate their hydrophilic “water-loving” natures. The narrow range of sizes and isoelectric points of most surveyed proteins in this study confirms common biochemical characters among diverse CAP160 proteins.

Subcellular localization

Protein localization is essential for understanding cellular function and homologous proteins that share a common function mostly target the same cellular compartments. Different algorithms have been applied to predict the function of diverse CAP160 plant homologs. Both Loctree3 and CELLO use the hierarchical system of support vector machines (SVM), while the former has an advantage of employing a PSI-BLAST homology-based inference that is trained on SWISS-PROT database, and with a cut-off e-value $\leq 10^{-3}$ (Yu et al. 2006; Goldberg et al. 2014). Other tools that are based on machine learning were applied, such as Localizer, Predotar, and PredSL. The former is trained only on experimentally verified plant proteins, the second was trained on known proteins from the SWISS-PROT database, and the latter on proteins available in the UniProt database (Small et al. 2004; Petsalaki et al. 2006; Sperschneider et al. 2017). Using diverse approaches is necessary to confirm the prediction results where all the selected tools of prediction use either a different approach of prediction or were trained on a unique database. The results, as presented in Table S5.7 show that all Clade I proteins are nuclear proteins, however, PredSl predicts Kl1.4, Kf1.2 and Kl1.3 as mitochondrial proteins and Localizer predicts this set of proteins to be targeted to the nucleus or the chloroplast. Md1.3 is predicted by LocTree3 to localize in the plasma membrane based only on its homology to the signalling mucin HKR1 in yeast. The PSI-BLAST result indicates this homology-based annotation is established on the middle to the near end of the Md1.3 protein, not within its N- or C-terminal. Overall, Clade I proteins are frequently predicted as nuclear proteins. All tools predict Clade II proteins as either nuclear or cytoplasmic proteins. Most of the Clade III proteins are also predicted as either nuclear or cytoplasmic proteins. Although LocTree3 predicts Clade III proteins by machine-learning-based LocTree2, Pv1.2, and Ac1.1 were predicted by a PSI-BLAST homology-based inference as a nuclear protein and centriole-related protein, respectively. These proteins have distant homology with the mouse Npas4 (Neuronal PAS domain-containing protein 4) and *Caenorhabditis elegans* spd2 (Spindle-defective protein 2), respectively. Only Gr protein in Clade III was predicted with a signal peptide by PredSl and Predotar, while Fv was predicted as a secretory protein only by PredSl; this might be because both use a neural network-based approach that is trained only on known proteins. Like all other predictions, Atr that was used as an outgroup in the phylogenetic analysis, was predicted as either a cytoplasmic or nuclear protein.

Promoter *cis*-elements analysis

Promoter *cis*-elements are critical regulatory elements of gene expression. These are sequence motifs that are found in the core, proximal, or distal region from the transcription start site to direct the binding of particular transcription factors. The 2-kb promoter sequences upstream of the translational start sites were retrieved from many CAP160 homologous genes of different plant species to analyze the presence and distribution of different PLACE *cis*-elements motifs (Dataset S5.2 and Figure S5.3). Although this gene family is thought to be related to abiotic stress, the promoter analysis of species from clade I with the promoter of Atr did not show significant enrichment (Z-score > 5) of *cis*-elements that may regulate the expression of abiotic stress induced-genes. The promoters of genes Mg1.2, Cs1.2, Md1.3, and Ac1.2 from clade I were analyzed *in silico*. The results did not show the presence of motifs related to either the CBF-regulatory pathway or ABA-dependent pathway to be significantly detected under the cut-off values that were used in our analysis. However, the presence of motifs of low-temperature-responsive elements and ABA-related *cis*-elements were detected (Z-score < 5) in clade I (Data not shown). Phylogenetic analysis shows that gene duplicates Ma1.2 and Kf1.2 are ancestor alleles, and the enrichment of abiotic stress related cis-elements motifs in the promoters of their derived alleles may indicate adaptation to abiotic stress conditions. Promoter motifs related to development, light-dependent development or embryogenesis were significantly detected in promoters of clade I. CARGATCONSENSUS which is a *cis*-element motif that is responsible for recruiting FLC (Flowering repressor protein), was found in the promoter of Atr and Kf1.2 genes. This motif was also detected in the Mg1.1 promoter from Clade III. The gene promoters of clade II were analyzed in two separate groups, group IIA and IIB (Figure S5.3). The results confirmed the enrichment of ABA-responsive elements in both groups. The ABA-responsive core motif is (ACGT) which was represented in group IIB by the presence of ABREMOTIFIIIOSRAB16B, ACGTOSGLUB1, and DRE2COREZMRAB17, while it was only represented in group IIA by the presence of a related *cis*-acting element, IRO2OS. Group IIB was distinguished from group IIA by the significant enrichment of the CRT/DRE element (CCGAC) which was exemplified by the presence of CBFHV and LTRECOREATCOR15 *cis*-acting elements in their promoters. Groups from III to VII represent plant gene promoters of clade III, where their promoter analysis showed that the presence of ABA-responsive *cis*-acting elements is prevalent among all promoters. DRE/CRT elements were also detected in Pv1.2, So1.1 and So1.2 of group VII promoters. Most groups showed the enrichment of one or more elements related to light-dependent development. The

circadian regulation was enriched only in group IVA promoters where the CIACADIANLELHC motif was found in all of its members. To summarize, the results show that this gene family embraces many ABA-regulated genes although of the diminishment of ABA-responsive *cis*-elements in the analyzed clade I and Atr gene promoters. Additionally, the enrichment of DRE/CRT *cis*-elements in group IIB and VII confirms that many genes in this family are regulated through the CBF-dependent pathway.

Expression and co-expression analyses

Microarray-based differential expression analysis was explored across four different species; two genes from Arabidopsis that represent Clade III and four genes from barley, wheat, and rice that represent Clade II. The results revealed that almost all genes are upregulated by similar conditions such as ABA, cold, drought, and dehydration (Figure S5.4). Positive co-expression analysis was performed for two Arabidopsis genes and their homologous genes from rice (Dataset S5.3) to associate this gene family to distinct biological processes. The results indicated that many LEA genes are positively co-expressed with CAP160 homologous genes either from Arabidopsis or rice. In these LEA genes, many dehydrins (Group II LEA) were found to be positively co-expressed across different networks. This result signifies the functional similarity of the CAP160 homologous genes to dehydrins.

Three positively co-expressed genes in Arabidopsis were found to have an orthologous relationship with positively co-expressed genes in rice: AT3G22490 (RAB28), AT3G15670 (LEA76), AT5G66780 (LEA), and AT5G01300 (phosphatidylethanolamine-binding protein). The analysis of mutually correlated genes from our explored co-expression networks showed that hub genes from Arabidopsis and rice share significant and co-ordinated upregulation of their expression under ABA treatment or with conditions that instigate a decline in water activity. Moreover, the CAP160 homologous genes with these hub genes were downregulated during germination, hypoxia, and anoxia (Dataset S5.3C, F and I). The overall results of the expression and co-expression analyses link this gene family to the ABA-regulatory pathway and abiotic stress conditions. These results are consistent with the promoter analysis of the genes where it revealed the presence of many ABRE and CRT/DRE *cis*-regulatory elements.

Protein motifs and function predictions

In order to explore the role of these proteins as affected by ABA or during water deficit conditions, their protein sequence information was used by an online tool, *MEME* (Bailey et al. 2009), to identify functional motifs. The function of these motifs were predicted and explained through the ELM database (Dinkel et al. 2016). The raw data results of motif prediction by *MEME* were presented in Dataset S5.4. The analysis showed the presence of many conserved motifs across proteins from different species. Motif *MEME*-1 was found to present exclusively in all our tested sequences. This motif is found in the N-termini of all proteins (Figures S5.5, S5.6 and S5.7) where it localizes in or borders to the most conserved area under negative selection and contains the lysine-rich segment. The motif consensus sequence is SVLK (Figure S5.2) and has a corresponding homology with the [GS]IL[RK] sequence, known as the SILK motif (Table S5.8). The SILK motif is a feature in Protein Phosphatase 1-interacting proteins (PIPs), and is essential for inhibiting Protein Phosphatase 1 (PP1) activity, as the phosphorylated form of some PIPs act as pseudosubstrates to PP1 (Hendrickx et al. 2009; Dinkel et al. 2016).

Additionally, *MEME*-4 has a PPXY motif that interacts with a WW-domain when the S/T motif in the P(S/T)P sequence is phosphorylated. Another small motif (*MEME*-30) that is found only in some proteins of clade III and II recognizes the SH2 domain when the tyrosine of this motif is phosphorylated. Other motifs are related to the clathrin-mediated pathway where *MEME*-3 and *MEME*-13 recruit adaptor proteins for clathrin-coated vesicle formation and *MEME*-6 binds the VHS domain of clathrin-related adaptor proteins through its acidic dileucine motif. The phosphorylation of the first serine residue in the acidic dileucine motif enhances the interaction with the VHS domain. Almost all the screened proteins have one or more of these motifs. Many degron motifs where found across all the tested proteins, guiding them for degradation. These degron motifs are represented by *MEME*-5, *MEME*-9, *MEME*-18, *MEME*-24, *MEME*-10, *MEME*-26 and *MEME*-28. It has been reported that phosphorylation controls some of these protein interaction-guided degradations. For example, under normal condition KEAP1 inhibitor protein binds to the degron motif, marking the target protein for degradation, while under stress condition the phosphorylated form of this motif inhibits KEAP1 binding, and thus prevents the degradation of the target protein (Atia and Abdullah 2014). Two motifs were found as a recognition site for the Inhibitor of Apoptosis Proteins (IAPs): *MEME*-12 and *MEME*-27. Four short linear motifs were identified by their predicted ability to recognize protease enzymes such as separase: *MEME*-14, *MEME*-16, *MEME*-21, and *MEME*-22, which may guide the cleavage of the target protein. More motifs were found to mediate protein-protein interaction where *MEME*-8, *MEME*-15, and *MEME*-

17 were predicted with motifs that may recognize the UEV domain and *MEME*-23 was predicted to have a motif that may recognize the WD40 repeat domain. Only two motifs were detected as DNA binding motifs: *MEME*-7 and *MEME*-20. One motif (*MEME*-29) was predicted to bind with DEAD-box helicase to mediate the degradation of aberrant RNAs, . Motifs *MEME*-11 and *MEME*-25 were predicted as possible sites for post-translationally modification by C-terminal amidation. One motif (*MEME*-19) had homology with the MM[NDE][EDNAG]F[LMA] motif that is found in the N-terminal half of the cytosolic soluble Pex5 protein to mediate protein import into peroxisomes. Finally, *MEME*-2, which was found in all clades and near the C-terminal of the screened proteins, was predicted as a binding site for TRAF2, a cytosolic protein tumour necrosis factor receptor (TNFR). Many plant TRAF proteins were identified with roles in either plant development or during abiotic stress such as SEVEN IN ABSENTIA 2 (SINA2), a TRAF-like family protein that is involved in ABA-mediated drought stress signalling in Arabidopsis (Bao et al. 2014). The functions of most predicted *MEMEs* were found to mediate and regulate miscellaneous classes of protein-protein interactions where phosphorylation regulates many of them.

Intrinsically disorder analysis

To test the folding state of wheat protein (Ta1.1) and other proteins from different clades, the PONDR VL-XT algorithm integrated three different neural networks to identify unstructured regions in the tested proteins. Overall results showed the presence of many large unstructured regions in all the tested proteins and showed that this protein family are IDPs, where many large regions (> 30 amino acids) are natively unfolded (Figure 5.2). Similar results were predicted by the IUPred method (Figure S5.2). The thick, black lines in Figure 5.2 indicate predicted disordered regions that may change their conformations upon interaction with other molecules or under different physiological conditions. Petersen et al. (2012) showed that CDeT11-24 protein maintains its solubility with heat treatment and adopts many α-helical contents upon dehydration, as experimented by trifluoroethanol (TFE). Thus, these predicted natively disordered regions might hold α-helical structures upon dehydration, a feature of dehydrins. PONDR VL-XT predicts the K-like segments within these random coil regions where they can form α-helical structures upon dehydration or biochemical interactions.

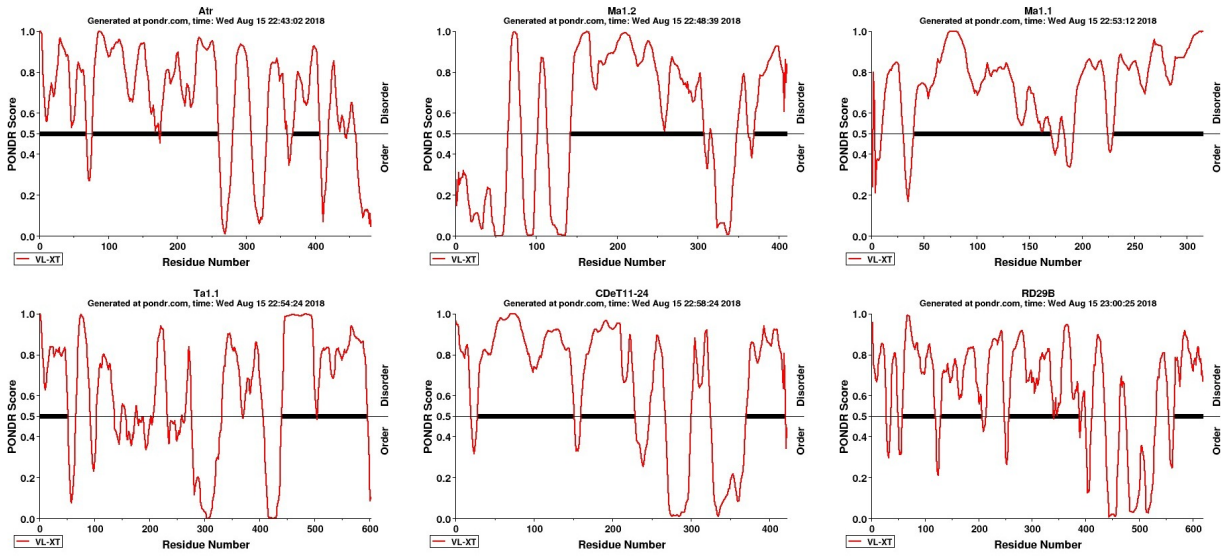

Figure 5.2: Predictions of intrinsically disordered regions in some CAP160 homologous proteins from different clades by PONDR program hosted at http://www.pondr.com.

Amphipathic helices assessment

The K-like segment identified by Petersen et al. (2012) in CDeT11-24 (Cpl) protein from *Craterostigma plantagineum* was suggested to harbour the amphipathic helix (AH). Our phylogenetic analysis showed that this lysine-rich sequence element maintains its conservation through purifying selection, and a similar AH can be proposed through other homologous proteins. Thus, to test this hypothesis, HELIQUEST (Gautier et al. 2008) was used to test AH formation across the N-termini from Atr, Pd, Eg, Ath1.1, Ta1.1 and Cpl proteins, where the helices in the K-like segments and with the higher Hydrophobic moments (μH) were selected for comparison. The results confirmed the conservation of the N-terminal of the lipid binding amphipathic helix among species of different clades, where six hydrophobic amino acids constitute the hydrophobic surface, and the hydrophilic surface establishes approximately 60% of the wheel (Figure 5.3).

Triticum aestivum

(Ta1.1)

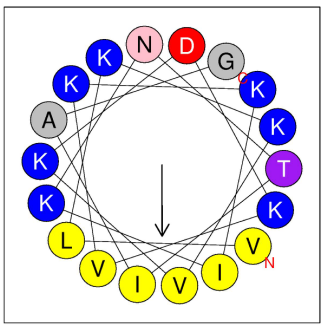

H = 0.068

μH = 0.584

Z = 6

Polar Surface

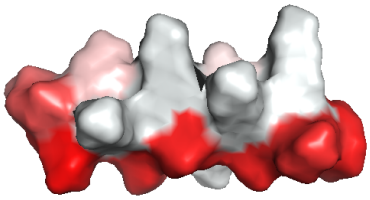

Hydrophobic Surface

Craterostigma plantagineum

(CDeT11-24, Cpl)

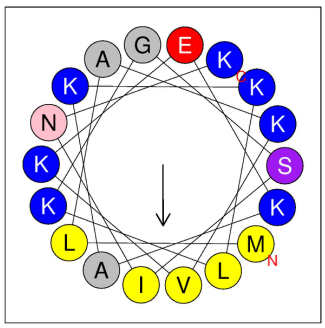

H = 0.003

μH = 0.498

Z = 6

Polar Surface

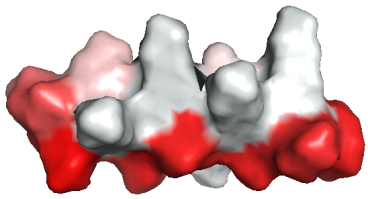

Hydrophobic Surface

Figure 5.3: Helical wheel representations according to (Gautier et al. 2008), and their tertiary strutute predictions according to (Reißer et al. 2014) and 3D model graphing (Schrödinger LLC 2016) of these wheels from the K-like segments in wheat and *Craterostigma plantagineum* proteins.

Discussion

Results of this study revealed that CAP160 from *Spinacia oleracea*, CDeT11-24 from *Craterostigma plantagineum*, and RD29B from *Arabidopsis thaliana* are homologous genes which belong to one gene family that has been descended vertically from a common ancestor and have orthologous genes in dicot and monocot species. Furthermore, this gene family was expanded by gene duplication in several species. The overall analysis showed that these genes are upregulated

synchronously with many other LEA and dehydrins in response to water deficit conditions and may have functions similar to dehydrins in providing cellular protection during abiotic stress conditions.

In plants, only two CAP160 distantly-related genes were characterized. These were CDeT11-24 gene from *Craterostigma plantagineum* and RD29 genes from *Arabidopsis thaliana* (Yamaguchi-shinozaki et al. 1992; Velasco et al. 1998). Due to their remote homology, their orthologous relationship was not assigned. At this moment, we have identified a new cold-regulated gene from wheat that has a remote homology with the genes above. Our protocol was to use a manual PSI-BLAST of the orthologous protein from cacao to identify other orthologous genes from monocot and dicot clades, with e-value cut-off <1e-04 as recommended by Pearson (2013), and with confirming the authentic homologous relationship by reciprocal BLAST. This protocol revealed that CAP160 gene from spinach has many orthologous genes across various plant species. Due to a lack of domain information, we have used the full protein sequences to construct our phylogenetic analysis, and as of their rapid evolutionary rate, we have aligned the retrieved proteins based on their predicted secondary structure, which revealed common conserved K-like segments near the N-termini among all tested proteins (Figure S5.2). To elucidate the evolutionary patterns inside this gene family, we used the orthologous gene from *Amborella trichopoda* (Atr) as the root of our phylogenetic analysis. The Bayesian phylogenetic inference grouped all the tested proteins in three different clades with proteins from monocot origin in one separate clade (clade II), and one clade representing both monocot and dicot species (clade I); clade III represents only dicot species (Figure 5.1). All genes from clade I have intraspecies duplicates that have diverged in either clade II or III. Bayesian inference indicated the early origin of clade I, and that clade II and III alleles may have arisen by divergent evolution from clade I. Thus, clade I represents ancestral CAP160 alleles. Sharing the K-like segment does not only support the hypothesis of divergent evolution, but authentic homology assessment and synteny analysis reject the hypotheses that this gene family may arise from convergent or parallel evolution. Since comparative genomics confirmed the inheritance of syntenic blocks surrounding CAP160 genes across different species (Figure S5.1), this supports the notion that these CAP160 genes have evolved from a common ancestor.

Given the long divergence time between clades II and III, a posterior probability value of 91% should be sufficient to support the hypothesis of divergent evolution (Figure 5.1). Gene structure revealed that most introns are symmetric, which may facilitate alternative splicing

besides the absence of phase 2 during intron evolution across the tested proteins. Figure 5.1 shows some degree of similarity of gene structures among different genes from different species and the prevalence of phase 1 introns which may further support the evolutionary descent of these genes from a common ancestor.

Based on the Bayesian phylogenetic analysis, fixed effects likelihood approaches indicated the dearth of both background and differentiating selections supported by the similarity of non-synonymous (β) and synonymous (α) substitution rates per site-basis (Table S5.5). Presence of only 12.6% sites under pervasive negative selection indicates the presence of selective pressures that change the features of the encoded proteins and reveals the higher evolutionary rate inside this gene family. Table S5.5 shows that the codons which encode the K-like segments are under negative selection, signifying the existence of selective constraints that preserve the features of this alpha-helix fragment. Although the typical appearance of neutral evolution with some signatures of pervasive negative selection was apparent, only five sites showed positive selection as detected by FEL, and 20 sites by MEME. Thus, these sites could be essential for protein function as their evolutionary changes can be explained by natural selection (Kimura 1991). Table 5.2 indicates that 24 branches have significantly experienced episodic diversifying selection and Table 5.3 and Figure 5.1 display these hypothetical taxonomic units (HTUs), operational taxonomic units (OTUs), and branches under episodic diversifying selection as detected by the branch model (aBSREL). These results denote the presence of adaptive protein evolution on specific sites in some plant species which may be related to a specific function as this was absent over the ancestor alleles from clade I, suggesting the recency of these adaptive evolution signatures.

The high numbers of mutant substitutions did not affect the semblances of most protein characters such as solubility and acidic nature among proteins from different clades. Additionally, all subcellular predictions were pointed to predict this protein family as either nuclear or cytoplasmic proteins; the nuclear-targeting predictions were based only on the most conserved alpha-helical region (K-like segment), as seen by Localizer (Table S5.7). Although predictions of nuclear localizations are based on the conserved K-like segment, the cytoplasmic localizations are predicted based on the lack of target peptides. If the K-like segment function is not to target these proteins to the nucleus, these proteins can be favourably predicted as cytoplasmic proteins. Based on LocTree3 predictions of gene ontologies, most proteins were either with GO:000564 based on their nuclear localization predictions or GO:0005737 as of their cytoplasmic localization predictions. To compare these results with the experimentally verified proteins, Kaye et al. (1998)

showed that spinach CAP160 protein (So1.2) can be detected in the soluble fraction and mitochondria, rather than other subcellular fractions of spinach leaf and hypocotyl tissue. Msanne et al. (2011) found that GFP-tagged AtRD29A or AtRD29B (Ath1.1) cDNA trace these proteins in the cytoplasm only, with the comparison to GFP expression in the nucleus and cytoplasm as a positive control. Immunolocalization is a different approach that was used to localize CAP160 protein of *Craterostigma plantagineum* (Cpl) CDeT11-24 gene product (dsp11-24), where distinct physiologically treated plant tissues were incubated with dsp11-24 antiserum (Velasco et al. 1998), and the results showed that dsp11-24 protein localizes in the cytoplasm. Accordingly, the experimental validations and *in silico* predictions agree on the cytoplasmic subcellular localization of CAP160 proteins.

Figure S5.3, shows the promoter cis-elements analysis that the CAP160 gene family encompasses mainly ABA-regulated genes, with a prominent enrichment of ABRE elements in the derived alleles (Uno et al. 2000). These results are in line with the expression meta-analysis of CAP160 genes from Arabidopsis, rice, barley, and wheat where all were upregulated by ABA as confirmed by numerous microarray experiments (Figure S5.4). Furthermore, results in Figure S5.3 shows that the co-expression analysis of CAP160 genes from Arabidopsis and rice with many LEA proteins, mostly under the ABA-dependent pathway (van Dam et al. 2017). The enrichment of CRT/DRE elements is established in Group IIB that represents CAP160 gene promoters from monocot crops with a winter background, rather than Group IIA that represents monocot summer crops. This may highlight the value of the CAP160 gene for increasing tolerance towards cold conditions in plant species with a winter genetic background (Gusta et al. 2005). This result agrees with the marked $\log_2$ expression values of CAP160 genes from barley and wheat, in comparison with rice (Figure S5.4). Many other motifs related to development, embryogenesis and light regulation are enriched along promoters from different clades, which indicates that the expression of CAP160 genes can be controlled by the developmental stage and other surrounding factors, which is in accordance with the CAP160 gene expressions when found to be regulated by light treatments and circadian rhythms (Figure S5.4). Moreover, the enrichment of CArG cis-elements in the promoters of ancestral alleles rather than derived alleles supports the upstream regulation of the plant MADS-box transcription factors in the ancestor alleles (de Folter et al. 2005).

Given the fact that CDeT11-24 is an intrinsically disordered protein (Petersen et al. 2012), and CAP160 is a similar and homologous protein (Figure 5.2) supports the role of the plant CAP160 proteins as molecular shields but also enhances their flexibility to engage in different

biological interactions (Petersen et al. 2012; Wright and Dyson 2015). Remarkably, divergent sequences of IDPs can tolerate mutations and maintain similar functions (Zarin et al. 2017); this feature was noticed from our analysis of protein motifs where many motifs with similar functions were well-conserved among separated clades. Our protein motif predictions confirm the fact that this family encompasses a class of phosphoproteins, where many motifs are subject to phosphorylation which in turn control subsequent interactions. These results are supported by the mass spectrometric analysis results of CDeT11-24 (Röhrig et al. 2006). Moreover, three verified phosphorylated sites correspond with three different *MEME*s of our predictions. Phosphorylation site 473A in Figure S5.3 is predicted within an alpha helix and is harboured by *MEME*-2 which binds to TRAF proteins; this site corresponds to site 1969 in the protein alignment (Dataset S5.5A) and is detected significantly by FEL under negative selection (Table S5.5). Phosphorylation site 318P within *MEME*-18, a degron motif that has redundant functions with other *MEME*s (*MEME*-5, *MEME*-9, *MEME*-24, *MEME*-10, *MEME*-26, and *MEME*-28), leads to the same functional outputs among diverged proteins. Finally, *MEME*-6 that supports the phosphorylation site 552S, is located within a predicted and well-conserved alpha-helix that binds with the VHS domain when the serine residue is phosphorylated. This serine site is maintained by negative selection, as detected by FEL under codon number 2807 (Table S5.5). This result indicates that although CAP160 has divergent sequences, the proteins could maintain similar functions where most *MEME*s are either conserved by negative selection or have redundant functions. The primary signature of this family which is the K-like segment, adopts an amphipathic helical structure where the hydrophilic face can be clearly distinguished from the hydrophobic one, and the segment is verified to bind specifically with phosphatidic acid rather than other lipids (Petersen et al. 2012). This result indicates a conserved signalling function in the ABA-dependent pathway.

Chapter Six: General Conclusion

Identification and characterization of genes associated with abiotic stress tolerance in wheat are crucial for developing tolerant varieties and understanding the molecular mechanisms underlying abiotic stress tolerance. Wheat is an economically important plant and was used here as a model organism, where we showed that the spring variety was sensitive to cold treatment while the winter variety was cold-tolerant. Cold tolerance traits in winter plant varieties have developed within temperate plants as an adaptation for the low-temperature conditions dominating these geographic locations. These adaptive mechanisms result in physiological variations between spring and winter plant varieties, where varieties of the same species respond differently at the molecular level to cold treatment. For example, during cold acclimation, winter varieties accumulate more sugars and dehydrins in comparison with spring varieties (Sandve et al. 2008; Sandve et al. 2011; Janda et al. 2014). Furthermore, on the molecular level winter varieties progressively accumulate VRN1 gene transcript during cold treatment significantly more than spring varieties (Danyluk et al. 2003; Yan et al. 2003; Yan et al. 2004). The identification of cold-responsive genes in winter wheat variety is crucial for understanding molecular mechanisms of adaptation during cold acclimation or vernalization.

In this thesis, I identified genes associated with the cold-tolerance trait in winter wheat cv. Norstar. Forty genes were selected from different microarray databases, and their expressions were validated by qPCR across experiments conducted in the field or in growth chambers. Several genes were found to be promising for further studies, such as candidate number 6 which was annotated as a remorin gene and is significantly upregulated by cold treatment (Figure 3.1). Candidate number 24 has had an unknown function until now, as preliminary screening showed that it is an orphan gene found only in the grass family (Data not shown). Candidate number 24's transcript was accumulated in response to cold treatment and in response to ABA and JA, where there was a significant upregulation in the winter wheat variety rather than the spring variety (Figure 3.10). Finally, we found that candidate number 39 has a remote homology with LTI65 gene in Arabidopsis and also shows a significant upregulation in winter wheat variety (Figure 3.11) in response to cold treatment, while it was significantly upregulated and downregulated by ABA and JA treatment, respectively. We then focused on identifying and characterizing candidate numbers 6 and 39.

The characterization of candidate number 6 showed that a large family of wheat genes were remorins. In both varieties of wheat, we retrieved, identified, and determined the expression of all remorin genes among different tissues and under ABA or JA treatments. Our results found twenty remorin genes in wheat where twelve of them were regulated during cold acclimation across different tissues, and eight genes were induced in response to either ABA or JA treatments. These results of TaREM genes facilitate the understanding of the different functions of remorin genes during stress adaptation.

Finally, the evolution and functional predictions of candidate number 39 showed that CAP160 homologous genes are not only found in plant dicot species but also in plant monocot species. This discovery assists future work by providing new abiotic stress marker genes in the monocot clade. Additionally, it improves the understanding of the evolution of remotely distant homologous genes. This study shows that plant CAP160 homologous genes have evolved by vertical descent from a single common ancestor and have maintained their function despite their remote, distant homology.

References

Abdrakhamanova A, Wang QY, Khokhlova L, Nick P. **2003**. Is microtubule disassembly a trigger for cold acclimation? Plant Cell Physiol. 44(7):676–686. doi:10.1093/pcp/pcg097.

Agarwal PK, Agarwal P, Reddy MK, Sopory SK. **2006**. Role of DREB transcription factors in abiotic and biotic stress tolerance in plants. Plant Cell Rep. 25(12):1263–1274. doi:10.1007/s00299-006-0204-8.

Agostino M. **2013**. Reciprocal BLAST: Confirming Identities. In: Practical Bioinformatics. Garland Science, Taylor & Francis Group, LLC. p. Chapter 6, pp.127–130.

Agrawal AA, Conner JK, Stinchcombe JR. **2004**. Evolution of plant resistance and tolerance to frost damage. Ecol Lett. 7(12):1199–1208. doi:10.1111/j.1461-0248.2004.00680.x.

Ahmad A, Dong Y, Cao X. **2011**. Characterization of the PRMT gene family in rice reveals conservation of arginine methylation. PLoS One. 6(8). doi:10.1371/journal.pone.0022664.

Akashi T, Makishima H, Tanaka K. **1998**. Involvement of the cytoskeleton in the intracellular distribution of mannoproteins in hyphal cells of Candida albicans. J Plant Res. 111(4):531–540. doi:10.1007/BF02507788.

Akhtar M, Jaiswal A, Taj G, Jaiswal JP, Qureshi MI, Singh NK. **2012**. DREB1/CBF transcription factors: their structure, function and role in abiotic stress tolerance in plants. J Genet. 91(3):385–95. [accessed 2017 Nov 16]. http://www.ncbi.nlm.nih.gov/pubmed/23271026.

Aleman F, Yazaki J, Lee M, Takahashi Y, Kim AY, Li Z, Kinoshita T, Ecker JR, Schroeder JI. **2016**. An ABA-increased interaction of the PYL6 ABA receptor with MYC2 Transcription Factor: A putative link of ABA and JA signaling. Sci Rep. 6. doi:10.1038/srep28941.

Anderson JP, Badruzsaufari E, Schenk PM, Manners JM, Desmond OJ, Ehlert C, Maclean DJ, Ebert PR, Kazan K. **2004**. Antagonistic Interaction between Abscisic Acid and Jasmonate-Ethylene Signaling Pathways Modulates Defense Gene Expression and Disease Resistance in Arabidopsis. Plant Cell. 16(12):3460–3479. doi:10.1105/tpc.104.025833.

Andrews CJ, Pomeroy MK, Seaman WL, Butler G, Bonn PC, Hoekstra G. **1997**. Relationships between planting date, winter survival and stress tolerances of soft white winter wheat in eastern Ontario. Can J Plant Sci. 77:507–513. doi:10.4141/P96-124.

Antosch M, Mortensen SA, Grasser KD. **2012**. Plant Proteins Containing High Mobility Group Box DNA-Binding Domains Modulate Different Nuclear Processes. Plant Physiol. 159(3):875–883. doi:https://doi.org/10.1104/pp.112.198283.

Arisz SA, van Wijk R, Roels W, Zhu JK, Haring MA, Munnik T. **2013**. Rapid phosphatidic acid accumulation in response to low temperature stress in Arabidopsis is generated through diacylglycerol kinase. Front Plant Sci. 4:1–15. doi:10.3389/fpls.2013.00001.

Arzani A, Ashraf M. **2017**. Cultivated Ancient Wheats (Triticum spp.): A Potential Source of Health-Beneficial Food Products. Compr Rev Food Sci Food Saf. 16(3):477–488. doi:10.1111/1541-4337.12262.

Astorquiza PL, Usorach J, Racagni G, Villasuso AL. **2016**. Diacylglycerol pyrophosphate binds and inhibits the glyceraldehyde-3-phosphate dehydrogenase in barley aleurone. Plant Physiol Biochem. 101:88–95. doi:10.1016/j.plaphy.2016.01.012.

Atia A, Abdullah A. **2014**. The Nrf2-Keap1 signalling pathway: Mechanisms of ARE transcription regulation in antioxidant cellular defence. Int J PharmTech Res. 6(1):154–167.

Austin RS, Hiu S, Waese J, Ierullo M, Pasha A, Wang TT, Fan J, Foong C, Breit R, Desveaux D, et al. 2016. New BAR tools for mining expression data and exploring Cis-elements in Arabidopsis thaliana. Plant J. 88(3):490–504. doi:10.1111/tpj.13261.

Avramova Z. **2017**. The jasmonic acid-signalling and abscisic acid-signalling pathways cross talk during one, but not repeated, dehydration stress: a non-specific 'panicky' or a meaningful response? Plant Cell Environ. 40(9):1704–1710. doi:10.1111/pce.12967.

Awadé AC, Cleuziat P, GonzalèS T, Robert-Baudouy J. **1994**. Pyrrolidone carboxyl peptidase (Pcp): An enzyme that removes pyroglutamic acid (pGlu) from pGlu-peptides and pGlu-proteins. Proteins Struct Funct Bioinforma. 20(1):34–51. doi:10.1002/prot.340200106.

Badawi M, Danyluk J, Boucho B, Houde M, Sarhan F. **2007**. The CBF gene family in hexaploid wheat and its relationship to the phylogenetic complexity of cereal CBFs. Mol Genet Genomics. 277(5):533–554. doi:10.1007/s00438-006-0206-9.

Badawi M, Reddy YV, Agharbaoui Z, Tominaga Y, Danyluk J, Sarhan F, Houde M. **2008**. Structure and functional analysis of wheat ICE (inducer of CBF expression) genes. Plant Cell Physiol. 49(8):1237–1249. doi:10.1093/pcp/pcn100.

Bailey TL, Boden M, Buske FA, Frith M, Grant CE, Clementi L, Ren J, Li WW, Noble WS. **2009**. MEME Suite: Tools for motif discovery and searching. Nucleic Acids Res. 37(SUPPL. 2). doi:10.1093/nar/gkp335.

Bailey TL, Elkan C. **1994**. Fitting a Mixture Model by Expectation Maximization to Discover Motifs in Bipolymers. Proc Second Int Conf Intell Syst Mol Biol.:28–36. doi:citeulike-article-id:878292.

Bao Y, Wang C, Jiang C, Pan J, Zhang G, Liu H, Zhang H. **2014**. The tumor necrosis factor receptor-associated factor (TRAF)-like family protein SEVEN IN ABSENTIA 2 (SINA2) promotes drought tolerance in an ABA-dependent manner in Arabidopsis. New Phytol. 202(1):174–187. doi:10.1111/nph.12644.

Bariola PA, Retelska D, Stasiak A, Kammerer RA, Fleming A, Hijri M, Frank S, Farmer EE. **2004**. Remorins form a novel family of coiled coil-forming oligomeric and filamentous proteins associated with apical, vascular and embryonic tissues in plants. Plant Mol Biol. 55(4):579–594. doi:10.1007/s11103-004-1520-4.

Battaglia M, Olvera-Carrillo Y, Garciarrubio A, Campos F, Covarrubias AA. **2008**. The Enigmatic LEA Proteins and Other Hydrophilins. PLANT Physiol. 148(1):6–24. doi:10.1104/pp.108.120725.

Bawono P, Van Der Velde A, Abeln S, Heringa J. **2015**. Quantifying the displacement of mismatches in multiple sequence alignment benchmarks. PLoS One. 10(5). doi:10.1371/journal.pone.0127431.

Behr M, Legay S, Hausman JF, Guerriero G. **2015**. Analysis of cell wall-related genes in organs of Medicago sativa L. Under different abiotic stresses. Int J Mol Sci. 16(7):16104–16124. doi:10.3390/ijms160716104.

Berridge MJ. **2016**. The Inositol Trisphosphate/Calcium Signaling Pathway in Health and Disease. Physiol Rev. 96(4):1261–1296. doi:10.1152/physrev.00006.2016. [accessed 2017 Nov 15]. http://www.ncbi.nlm.nih.gov/pubmed/27512009.

Bhat RA, Miklis M, Schmelzer E, Schulze-Lefert P, Panstruga R. **2005**. Recruitment and interaction dynamics of plant penetration resistance components in a plasma membrane microdomain. Proc Natl Acad Sci U S A. 102(8):3135–3140. doi:https://doi.org/10.1073/pnas.0500012102.

Bi H, Luang S, Li Y, Bazanova N, Morran S, Song Z, Perera MA, Hrmova M, Borisjuk N, Lopato S. **2016**. Identification and characterization of wheat drought-responsive MYB transcription factors involved in the regulation of cuticle biosynthesis. J Exp Bot. 67(18):5363–5380. doi:10.1093/jxb/erw298.

Biswal B, Joshi PN, Raval MK, Biswal UC. **2011**. Photosynthesis, a global sensor of environmental stress in green plants: Stress signalling and adaptation. Curr Sci. 101(1):47–56. doi:10.2307/24077862.

Bose J, Pottosin II, Shabala SS, Palmgren MG, Shabala S. **2011**. Calcium efflux systems in stress signaling and adaptation in plants. Front Plant Sci. 2:85. doi:10.3389/fpls.2011.00085. [accessed 2017 Nov 15]. http://www.ncbi.nlm.nih.gov/pubmed/22639615.

Boyer LA, Latek RR, Peterson CL. **2004**. The SANT domain: A unique histone-tail-binding module? Nat Rev Mol Cell Biol. 5(2):158–163. doi:10.1038/nrm1314.

Bravo LA, Griffith M. **2005**. Characterization of antifreeze activity in Antarctic plants. J Exp Bot. 56(414):1189–1196. doi:10.1093/jxb/eri112.

Bravo LA, Zuniga GE, Alberdi M, Corcuera LJ. **1998**. The role of ABA in freezing tolerance and cold acclimation in barley. Physiol Plant. 103(1):17–23. doi:10.1034/j.1399-3054.1998.1030103.x.

Brenchley R, Spannagl M, Pfeifer M, Barker GLA, D'Amore R, Allen AM, McKenzie N, Kramer M, Kerhornou A, Bolser D, et al. 2012. Analysis of the bread wheat genome using whole-genome shotgun sequencing. Nature. 491(7426):705–710. doi:10.1038/nature11650.

Breton G, Vazquez-Tello A, Danyluk J, Sarhan F. **2000**. Two Novel Intrinsic Annexins Accumulate in Wheat Membranes in Response to Low Temperature. Plant Cell Physiol. 41(2):177–184. doi:10.1093/pcp/41.2.177.

Brian Fowler D. **2012**. Wheat production in the high winter stress climate of the great plains of north America-An experiment in Crop Adaptation. Crop Sci. 52(1):11–20. doi:10.2135/cropsci2011.05.0279.

Burke MJ, Gusta L V, Quamme H a, Weiser CJ, Li PH. **1976**. Freezing and Injury in Plants. Annu Rev Plant Physiol. 27(1):507–528. doi:10.1146/annurev.pp.27.060176.002451.

Byun MY, Lee J, Cui LH, Kang Y, Oh TK, Park H, Lee H, Kim WT. **2015**. Constitutive expression of DaCBF7, an Antarctic vascular plant Deschampsia antarctica CBF homolog, resulted in improved cold tolerance in transgenic rice plants. Plant Sci. 236:61–74. doi:10.1016/j.plantsci.2015.03.020.

Cai X, Lytton J. **2004**. The cation/Ca2+ exchanger superfamily: Phylogenetic analysis and structural implications. Mol Biol Evol. doi:10.1093/molbev/msh177.

Campbell AB. **1967**. Registration of Manitou Wheat (Reg. No. 468). Crop Sci. 7:406.

Campo S, Manrique S, García-Martínez J, San Segundo B. **2008**. Production of cecropin A in transgenic rice plants has an impact on host gene expression. Plant Biotechnol J. 6(6):585–608. doi:10.1111/j.1467-7652.2008.00339.x.

Campoli C, Matus-Cádiz MA, Pozniak CJ, Cattivelli L, Fowler DB. **2009**. Comparative expression of Cbf genes in the Triticeae under different acclimation induction temperatures. Mol Genet Genomics. 282(2):141–152. doi:10.1007/s00438-009-0451-9.

Castro M, Peterson CJ, Rizza MD, Dellavalle PD, Vazquez D, Ibanez V, Ross A. **2007**. Influence of heat stress on wheat grain characteristics and protein molecular weight distribution.

Chakrabortee S, Tripathi R, Watson M, Kaminski Schierle GS, Kurniawan DP, Kaminski CF, Wise MJ, Tunnacliffe A. **2012**. Intrinsically disordered proteins as molecular shields. Mol Biosyst. 8(1):210. doi:10.1039/c1mb05263b.

Charron J-BF, Ouellet F, Pelletier M, Danyluk J, Chauve C, Sarhan F. **2005**. Identification, expression, and evolutionary analyses of plant lipocalins. Plant Physiol. 139(4):2017–28. doi:10.1104/pp.105.070466.

Chauvin LP, Houde M, Sarhan F. **1993**. A leaf-specific gene stimulated by light during wheat acclimation to low temperature. Plant Mol Biol. 23(2):255–265. doi:10.1007/BF00029002.

Chawade A, Lindlöf A, Olsson B, Olsson O. **2013**. Global expression profiling of low temperature induced genes in the chilling tolerant japonica rice Jumli Marshi. PLoS One. 8(12). doi:10.1371/journal.pone.0081729.

Checker VG, Khurana P. **2013**. Molecular and functional characterization of mulberry EST encoding remorin (MiREM) involved in abiotic stress. Plant Cell Rep. 32(11):1729–1741. doi:10.1007/s00299-013-1483-5.

Chen J, Gutjahr C, Bleckmann A, Dresselhaus T. **2015**. Calcium signaling during reproduction and biotrophic fungal interactions in plants. Mol Plant. 8(4):595–611. doi:10.1016/j.molp.2015.01.023.

Chen K, An YQC. **2006**. Transcriptional responses to gibberellin and abscisic acid in Barley aleurone. J Integr Plant Biol. 48(5):591–612. doi:10.1111/j.1744-7909.2006.00270.x.

Chen TH, Gusta L V, Fowler DB. **1983**. Freezing injury and root development in winter cereals. Plant Physiol. 73(3):773–777. doi:10.1104/pp.73.3.773.

Chinnusamy V, Ohta M, Kanrar S, Lee B ha, Hong X, Agarwal M, Zhu JK. **2003**. ICE1: A regulator of cold-induced transcriptome and freezing tolerance in arabidopsis. Genes Dev. 17(8):1043–1054. doi:10.1101/gad.1077503.

Chinnusamy V, Zhu J, Zhu JK. **2006**. Gene regulation during cold acclimation in plants. Physiol Plant. 126(1):52–61. doi:10.1111/j.1399-3054.2006.00596.x.

Chinnusamy V, Zhu J, Zhu JK. **2007**. Cold stress regulation of gene expression in plants. Trends Plant Sci. 12(10):444–451. doi:10.1016/j.tplants.2007.07.002.

Collings D a., Asada T, Allen NS, Shibaoka H. **1998**. Plasma Membrane-Associated Actin in Bright Yellow 2 Tobacco Cells1. Plant Physiol. 118:917–928. doi:10.1104/pp.118.3.917.

Cummings RD, Etzler ME. **2009**. Antibodies and Lectins in Glycan Analysis. In: Varki A, Cummings R, Esko JD, et al., editors. Essentials of Glycobiology 2nd Edition. 2nd editio. New York: Cold Spring Harbor (NY): Cold Spring Harbor Laboratory Press. p. 633–648.

van Dam S, Võsa U, van der Graaf A, Franke L, de Magalhães JP. **2017**. Gene co-expression analysis for functional classification and gene–disease predictions. Brief Bioinform.:bbw139. doi:10.1093/bib/bbw139.

Danquah A, de Zélicourt A, Boudsocq M, Neubauer J, Frei dit Frey N, Leonhardt N, Pateyron S, Gwinner F, Tamby J-P, Ortiz-Masia D, et al. 2015. Identification and characterization of an ABA-activated MAP kinase cascade in Arabidopsis thaliana. Plant J. 82(2):232–244. doi:10.1111/tpj.12808.

Danquah A, de Zelicourt A, Colcombet J, Hirt H. **2014**. The role of ABA and MAPK signaling pathways in plant abiotic stress responses. Biotechnol Adv. 32(1):40–52. doi:10.1016/j.biotechadv.2013.09.006.

Danyluk J, Kane NA, Breton G, Limin AE, Fowler DB, Sarhan F. **2003**. TaVRT-1, a putative transcription factor associated with vegetative to reproductive transition in cereals. Plant Physiol. 132(4):1849–1860. doi:10.1104/pp.103.023523.

Danyluk J, Perron A, Houde M, Limin A, Fowler B, Benhamou N, Sarhan F. **1998**. Accumulation of an acidic dehydrin in the vicinity of the plasma membrane during cold acclimation of wheat. Plant Cell. 10(4):623–638. doi:10.1105/tpc.10.4.623.

Darriba D, Taboada G, Doallo R, Posada D. **2011**. ProtTest 3: fast selection of best-fit models of protein evolution. Bioinformatics. 27(8):1164–5. doi:10.1093/bioinformatics/btr088. Epub 2011.

Dave RH, Saengsawang W, Yu JZ, Donati R, Rasenick MM. **2009**. Heterotrimeric G-proteins interact directly with cytoskeletal components to modify microtubule-dependent cellular processes. NeuroSignals. 17(1):100–108. doi:10.1159/000186693.

Day IS, Reddy VS, Shad Ali G, Reddy ASN. **2002**. Analysis of EF-hand-containing proteins in Arabidopsis. Genome Biol. 3(10):RESEARCH0056. doi:10.1186/gb-2002-3-10-research0056.

DeFalco TA, Marshall CB, Munro K, Kang H-G, Moeder W, Ikura M, Snedden WA, Yoshioka K. **2016**. Multiple Calmodulin-binding Sites Positively and Negatively Regulate Arabidopsis CYCLIC NUCLEOTIDE-GATED CHANNEL12. Plant Cell.:tpc.00870.2015. doi:10.1105/tpc.15.00870.

Demir F, Horntrich C, Blachutzik JO, Scherzer S, Reinders Y, Kierszniowska S, Schulze WX, Harms GS, Hedrich R, Geiger D, et al. 2013. Arabidopsis nanodomain-delimited ABA signaling pathway regulates the anion channel SLAH3. Proc Natl Acad Sci. 110(20):8296–8301. doi:10.1073/pnas.1211667110.

Deng W, Casao MC, Wang P, Sato K, Hayes PM, Finnegan EJ, Trevaskis B. **2015**. Direct links between the vernalization response and other key traits of cereal crops. Nat Commun. 6:5882. doi:10.1038/ncomms6882.

Desveaux D, Despres C, Joyeux A, Subramaniam R, Brisson N. **2000**. PBF-2 is a novel single-stranded DNA binding factor implicated in PR-10a gene activation in potato. Plant Cell. 12(8):1477–1489. doi:Doi 10.2307/3871144.

Dhillon T, Pearce SP, Stockinger EJ, Distelfeld A, Li C, Knox AK, Vashegyi I, Vagujfalvi A, Galiba G, Dubcovsky J. **2010**. Regulation of Freezing Tolerance and Flowering in Temperate Cereals: The VRN-1 Connection. PLANT Physiol. 153(4):1846–1858. doi:10.1104/pp.110.159079.

Diallo AO, Agharbaoui Z, Badawi MA, Ali-Benali MA, Moheb A, Houde M, Sarhan F. **2014**. Transcriptome analysis of an mvp mutant reveals important changes in global gene expression and a role for methyl jasmonate in vernalization and flowering in wheat. J Exp Bot. 65(9):2271–2286. doi:10.1093/jxb/eru102.

Ding Y, Jia Y, Shi Y, Zhang X, Song C, Gong Z, Yang S. **2018**. OST1-mediated BTF3L phosphorylation positively regulates CBFs during plant cold responses. EMBO J.:e98228. doi:10.15252/embj.201798228.

Dinkel H, Roey K, Michael S, Kumar M, Uyar B, Altenberg B, Milchevskaya V, Schneider M, Kühn H, Behrendt A, et al. 2016. ELM 2016 - Data update and new functionality of the eukaryotic linear motif resource. Nucleic Acids Res. 44(D1):D294–D300. doi:10.1093/nar/gkv1291.

Distelfeld A, Li C, Dubcovsky J. **2009**. Regulation of flowering in temperate cereals. Curr Opin Plant Biol. 12(2):178–184. doi:10.1016/j.pbi.2008.12.010.

Doherty CJ, Van Buskirk HA, Myers SJ, Thomashow MF. **2009**. Roles for Arabidopsis CAMTA Transcription Factors in Cold-Regulated Gene Expression and Freezing Tolerance. PLANT CELL ONLINE. 21(3):972–984. doi:10.1105/tpc.108.063958.

Dong C-H, Agarwal M, Zhang Y, Xie Q, Zhu J-K. **2006**. The negative regulator of plant cold responses, HOS1, is a RING E3 ligase that mediates the ubiquitination and degradation of ICE1. Proc Natl Acad Sci. 103(21):8281–8286. doi:10.1073/pnas.0602874103.

Dong W, Lv H, Xia G, Wang M. **2012**. Does diacylglycerol serve as a signaling molecule in plants? Plant Signal Behav. 7(4):472–475. doi:10.4161/psb.19644.

Drøbak BK, Franklin-Tong VE, Staiger CJ. **2004**. The role of the actin cytoskeleton in plant cell signaling. New Phytol. 163(1):13–30. doi:10.1111/j.1469-8137.2004.01076.x.

Drozdetskiy A, Cole C, Procter J, Barton GJ. **2015**. JPred4: A protein secondary structure prediction server. Nucleic Acids Res. 43(W1):W389–W394. doi:10.1093/nar/gkv332.

Dubcovsky J, Loukoianov A, Fu D, Valarik M, Sanchez A, Yan L. **2006**. Effect of photoperiod on the regulation of wheat vernalization genes VRN1 and VRN2. Plant Mol Biol. 60(4):469–480. doi:10.1007/s11103-005-4814-2.

Duman JG, Wisniewski MJ. **2014**. The use of antifreeze proteins for frost protection in sensitive crop plants. Environ Exp Bot. 106:60–69. doi:10.1016/j.envexpbot.2014.01.001.

Dumont E, Bahrman N, Goulas E, Valot B, Sellier H, Hilbert JL, Vuylsteker C, Lejeune-Hénaut I, Delbreil B. **2011**. A proteomic approach to decipher chilling response from cold acclimation in pea (Pisum sativum L.). Plant Sci. 180(1):86–98. doi:10.1016/j.plantsci.2010.09.006.

Duque P. **2011**. A role for SR proteins in plant stress responses. Plant Signal Behav. 6(1):49–54. doi:10.4161/psb.6.1.14063.

Edel KH, Marchadier E, Brownlee C, Kudla J, Hetherington AM. **2017**. The Evolution of Calcium-Based Signalling in Plants. Curr Biol. 27(13):R667–R679. doi:10.1016/j.cub.2017.05.020.

Ensminger I, Busch F, Huner NPA. **2006**. Photostasis and cold acclimation: Sensing low temperature through photosynthesis. Physiol Plant. 126(1):28–44. doi:10.1111/j.1399-3054.2006.00627.x.

Eris A, Gulen H, Barut E, Cansev A. **2007**. Annual patterns of total soluble sugars and proteins related to coldhardiness in olive (*Olea europaea L.'Gemlik'*). J Hortic Sci Biotechnol. 82(4):597–604. doi:10.1080/14620316.2007.11512279. [accessed 2017 Nov 14]. http://www.tandfonline.com/doi/full/10.1080/14620316.2007.11512279.

Espevig T, Xu CP, Aamlid TS, DaCosta M, Huang BR. **2012**. Proteomic Responses during Cold Acclimation in Association with Freezing Tolerance of Velvet Bentgrass. J Am Soc Hortic Sci. 137(6):391–399.

Eyidogan F, Oz MT, Yucel M, Oktem H a. 2012. Phytohormones and Abiotic Stress Tolerance in Plants. Phytohormones Abiotic Stress Toler Plants.:1–49. doi:10.1007/978-3-642-25829-9.

Farré EM, Liu T. **2013**. The PRR family of transcriptional regulators reflects the complexity and evolution of plant circadian clocks. Curr Opin Plant Biol. 16(5):621–629. doi:10.1016/j.pbi.2013.06.015.

de Folter S, Immink RGH, Kieffer M, Pařenicová L, Henz SR, Weigel D, Busscher M, Kooiker M, Colombo L, Kater MM, et al. 2005. Comprehensive Interaction Map of the Arabidopsis MADS Box Transcription Factors. Plant Cell. 17(5):1424–1433. doi:10.1105/tpc.105.031831.

Frenette Charron JB, Breton G, Badawi M, Sarhan F. **2002**. Molecular and structural analyses of a novel temperature stress-induced lipocalin from wheat and Arabidopsis. FEBS Lett. 517(1–3):129–132. doi:10.1016/S0014-5793(02)02606-6.

Fursova O V., Pogorelko G V., Tarasov VA. **2009**. Identification of ICE2, a gene involved in cold acclimation which determines freezing tolerance in Arabidopsis thaliana. Gene. 429(1–2):98–103. doi:10.1016/j.gene.2008.10.016.

Gardiner J, Collings DA, Harper JDI, Marc J. **2003**. The effects of the phospholipase D-antagonist 1-butanol on seedling development and microtubule organisation in Arabidopsis. Plant Cell Physiol. 44(7):687–696. doi:10.1093/pcp/pcg095.

Gautier R, Douguet D, Antonny B, Drin G. **2008**. HELIQUEST: A web server to screen sequences with specific α-helical properties. Bioinformatics. 24(18):2101–2102. doi:10.1093/bioinformatics/btn392.

Gilmour SJ, Sebolt AM, Salazar MP, Everard JD, Thomashow MF. **2000**. Overexpression of the Arabidopsis CBF3 transcriptional activator mimics multiple biochemical changes associated with cold acclimation. Plant Physiol. 124(December):1854–1865. doi:10.1104/pp.124.4.1854.

Givnish TJ, Ames M, McNeal JR, McKain MR, Steele PR, dePamphilis CW, Graham SW, Pires JC, Stevenson DW, Zomlefer WB, et al. 2010. Assembling the Tree of the Monocotyledons: Plastome Sequence Phylogeny and Evolution of Poales [1]. Ann Missouri Bot Gard. 97(4):584–616. doi:10.3417/2010023.

Goldberg T, Hecht M, Hamp T, Karl T, Yachdav G, Ahmed N, Altermann U, Angerer P, Ansorge S, Balasz K, et al. 2014. LocTree3 prediction of localization. Nucleic Acids Res. 42(W1). doi:10.1093/nar/gku396.

Goldschmidt-Clermont PJ, Machesky LM, Baldassare JJ, Pollard TD. **1990**. The actin-binding protein profilin binds to PIP2 and inhibits its hydrolysis by phospholipase C. Science. 247(4950):1575–1578. doi:10.1126/science.2157283.

Gould CM, Diella F, Via A, Puntervoll P, Gemünd C, Chabanis-Davidson S, Michael S, Sayadi A, Bryne JC, Chica C, et al. 2010. ELM: The status of the 2010 eukaryotic linear motif resource. Nucleic Acids Res. 38(SUPPL.1). doi:10.1093/nar/gkp1016.

Grabowski E, Miao Y, Mulisch M, Krupinska K. **2008**. Single-stranded DNA-binding protein Whirly1 in barley leaves is located in plastids and the nucleus of the same cell. Plant Physiol. 147(4):1800–1804. doi:10.1104/pp.108.122796.

Grant MN. **1980**. Registration of Norstar wheat. Crop Sci. 20:552.

Greenup AG, Sasani S, Oliver SN, Walford SA, Millar AA, Trevaskis B. **2011**. Transcriptome analysis of the vernalization response in barley (Hordeum vulgare) seedlings. PLoS One. 6(3). doi:10.1371/journal.pone.0017900.

Griffith M. **2005**. Antifreeze Proteins Modify the Freezing Process In Planta. PLANT Physiol. 138(1):330–340. doi:10.1104/pp.104.058628.

Griffith M, Yaish MWF. **2004**. Antifreeze proteins in overwintering plants: A tale of two activities. Trends Plant Sci. 9(8):399–405. doi:10.1016/j.tplants.2004.06.007.

Gui J, Liu C, Shen J, Li L. **2014**. Grain setting defect1, Encoding a Remorin Protein, Affects the Grain Setting in Rice through Regulating Plasmodesmatal Conductance. PLANT Physiol. 166(3):1463–1478. doi:10.1104/pp.114.246769.

Gui J, Zheng S, Liu C, Shen J, Li J, Li L. **2016**. OsREM4.1 Interacts with OsSERK1 to Coordinate the Interlinking between Abscisic Acid and Brassinosteroid Signaling in Rice. Dev Cell. 38(2):201–213. doi:10.1016/j.devcel.2016.06.011.

Gui J, Zheng S, Shen J, Li L. **2015**. Grain setting defect1 (GSD1) function in rice depends on S-acylation and interacts with actin 1 (OsACT1) at its C-terminal. Front Plant Sci. 6(804).

Guo J, Zeng W, Chen Q, Lee C, Chen L, Yang Y, Cang C, Ren D, Jiang Y. **2015**. Structure of the voltage-gated two-pore channel TPC1 from Arabidopsis thaliana. Nature. 531(7593):196–201. doi:10.1038/nature16446. [accessed 2017 Nov 15]. http://www.ncbi.nlm.nih.gov/pubmed/26689363.

Guo L, Devaiah S, Narasimhan R, Pan X, Zhang Y, Zhang W, Wang X. **2012**. Cytosolic Glyceraldehyde-3-Phosphate Dehydrogenases Interact with Phospholipase D to Transduce Hydrogen Peroxide Signals in the Arabidopsis Response to Stress. Plant Cell. 24(5):2200–2212. doi:10.1105/tpc.111.094946.

Guo L, Mishra G, Markham JE, Li M, Tawfall A, Welti R, Wang X. **2012**. Connections between sphingosine kinase and phospholipase D in the abscisic acid signaling pathway in Arabidopsis. J Biol Chem. 287(11):8286–8296. doi:10.1074/jbc.M111.274274.

Guo L, Wang X. **2012**. Crosstalk between Phospholipase D and Sphingosine Kinase in Plant Stress Signaling. Front Plant Sci. 3. doi:10.3389/fpls.2012.00051.

Gupta R, Deswal R. **2014**. Antifreeze proteins enable plants to survive in freezing conditions. J Biosci. 39(5):931–944. doi:10.1007/s12038-014-9468-2.

Gusta L V., Trischuk R, Weiser CJ. **2005**. Plant cold acclimation: The role of abscisic acid. J Plant Growth Regul. 24(4):308–318. doi:10.1007/s00344-005-0079-x.

Guy CL, Haskell D. **1987**. Induction of Freezing Tolerance in Spinach Is Associated with the Synthesis of Cold Acclimation Induced Proteins'. Plant Physiol. 84:872–878. doi:10.1104/pp.84.3.872.

Guy CL, Haskell D. **1989**. Preliminary characterization of high molecular mass proteins associated with cold acclimation in spinach. Plant Physiol Biochem. 27(5):777–784.

Hallouin M, Ghelis T, Brault M, Bardat F, Cornel D, Miginiac E, Rona JP, Sotta B, Jeannette E. **2002**. Plasmalemma abscisic acid perception leads to RAB18 expression via phospholipase D activation in Arabidopsis suspension cells. Plant Physiol. 130(1):265–272. doi:10.1104/pp.004168.

Hanikenne M, Baurain D. **2014**. Origin and evolution of metal P-type ATPases in Plantae (Archaeplastida). Front Plant Sci. 4. doi:10.3389/fpls.2013.00544.

Hansen MM, Olivieri I, Waller DM, Nielsen EE. **2012**. Monitoring adaptive genetic responses to environmental change. Mol Ecol. 21(6):1311–1329. doi:10.1111/j.1365-294X.2011.05463.x.

Hemming MN, Peacock WJ, Dennis ES, Trevaskis B. **2008**. Low-Temperature and Daylength Cues Are Integrated to Regulate FLOWERING LOCUS T in Barley. PLANT Physiol. 147(1):355–366. doi:10.1104/pp.108.116418.

Hendrickx A, Beullens M, Ceulemans H, Den Abt T, Van Eynde A, Nicolaescu E, Lesage B, Bollen M. **2009**. Docking Motif-Guided Mapping of the Interactome of Protein Phosphatase-1. Chem Biol. 16(4):365–371. doi:10.1016/j.chembiol.2009.02.012.

Hermann A, Donato R, Weiger TM, Chazin WJ. **2012**. S100 calcium binding proteins and ion channels. Front Pharmacol. 3 APR. doi:10.3389/fphar.2012.00067.

Higo K, Ugawa Y, Iwamoto M, Korenaga T. **1999**. Plant cis-acting regulatory DNA elements (PLACE) database: 1999. Nucleic Acids Res. 27(1):297–300. doi:10.1093/nar/27.1.297.

Horiguchi G, Fuse T, Kawakami N, Kodama H, Iba K. **2000**. Temperature-dependent translational regulation of the ER omega-3 fatty acid desaturase gene in wheat root tips. Plant J. 24(6):805–13. doi:10.1111/j.1365-313X.2000.00925.x.

Hossain MA, Munemasa S, Uraji M, Nakamura Y, Mori IC, Murata Y. **2011**. Involvement of Endogenous Abscisic Acid in Methyl Jasmonate-Induced Stomatal Closure in Arabidopsis. PLANT Physiol. 156(1):430–438. doi:10.1104/pp.111.172254.

Hoth S, Morgante M, Sanchez J-P, Hanafey MK, Tingey S V, Chua N-H. **2002**. Genome-wide gene expression profiling in Arabidopsis thaliana reveals new targets of abscisic acid and largely impaired gene regulation in the abi1-1 mutant\r10.1242/jcs.00175. J Cell Sci.

Hu B, Jin J, Guo AY, Zhang H, Luo J, Gao G. **2015**. GSDS 2.0: An upgraded gene feature visualization server. Bioinformatics. 31(8):1296–1297. doi:10.1093/bioinformatics/btu817.

Hüner NPA, Dahal K, Bode R, Kurepin L V., Ivanov AG. **2016**. Photosynthetic acclimation, vernalization, crop productivity and 'the grand design of photosynthesis.' J Plant Physiol. 203:29–43. doi:10.1016/j.jplph.2016.04.006.

Huner NPA, Öquist G, Hurry VM, Krol M, Falk S, Griffith M. **1993**. Photosynthesis, photoinhibition and low temperature acclimation in cold tolerant plants. Photosynth Res. 37(1):19–39. doi:10.1007/BF02185436.

Huner NPA, Öquist G, Sarhan F. **1998**. Energy balance and acclimation to light and cold. Trends Plant Sci. 3(6):224–230. doi:10.1016/S1360-1385(98)01248-5.

Ishitani M, Xiong L, Lee H, Stevenson B, Zhu JK. **1998**. HOS1, a genetic locus involved in cold-responsive gene expression in arabidopsis. Plant Cell. 10(7):1151–61. doi:10.1105/tpc.10.7.1151.

Jacinto T, Farmer EE, Ryan CA. **1993**. Purification of Potato Leaf Plasma Membrane Protein pp34, a Protein Phosphorylated in Response to Oligogalacturonide Signals for Defense and Development. Plant Physiol. 103(4):1393–1397. doi:10.1104/pp.103.4.1393.

Janda T, Gondor OK, Yordanova R, Szalai G, Pál M. **2014**. Salicylic acid and photosynthesis: signalling and effects. Acta Physiol Plant. 36(10):2537–2546. doi:10.1007/s11738-014-1620-y.

Janská A, Maršík P, Zelenková S, Ovesná J. **2010**. Cold stress and acclimation - what is important for metabolic adjustment? Plant Biol. 12(3):395–405. doi:10.1111/j.1438-8677.2009.00299.x.

Jarsch IK, Ott T. **2011**. Perspectives on Remorin Proteins, Membrane Rafts, and Their Role During Plant–Microbe Interactions. Mol Plant-Microbe Interact. 24(1):7–12. doi:10.1094/MPMI-07-10-0166.

Jia H, Zhang S, Ruan M, Wang Y, Wang C. **2012**. Analysis and application of RD29 genes in abiotic stress response. Acta Physiol Plant. 34(4):1239–1250. doi:10.1007/s11738-012-0969-z.

Jiang B, Shi Y, Zhang X, Xin X, Qi L, Guo H, Li J, Yang S. **2017**. PIF3 is a negative regulator of the CBF pathway and freezing tolerance in Arabidopsis. Proc Natl Acad Sci U S A. 114(32):E6695–E6702. doi:10.1073/pnas.1706226114.

Jiang SY, Ma Z, Ramachandran S. **2010**. Evolutionary history and stress regulation of the lectin superfamily in higher plants. BMC Evol Biol. 10(1). doi:10.1186/1471-2148-10-79.

Jonak C, Kiegerl S, Ligterink Wilc, BARKERt PJ, HUSKISSONt NS, by Winslow Briggs CR. **1996**. Stress signaling in plants: A mitogen-activated protein kinase pathway is activated by cold and drought. Plant Biol. 93:11274–11279. doi:10.1073/pnas.93.20.11274.

Joseph JM, Durand D. **2009**. Family classification without domain chaining. In: Bioinformatics. Vol. 25.

Kane K, Dahal KP, Badawi MA, Houde M, Hüner NPA, Sarhan F. **2013**. Long-term growth under elevated CO2 suppresses biotic stress genes in non-acclimated, but not cold-acclimated winter wheat. Plant Cell Physiol. 54(11):1751–1768. doi:10.1093/pcp/pct116.

Kane N a, Danyluk J, Tardif G, Ouellet F, Laliberté J-F, Limin AE, Fowler DB, Sarhan F. **2005**. TaVRT-2, a member of the StMADS-11 clade of flowering repressors, is regulated by vernalization and photoperiod in wheat. Plant Physiol. 138(4):2354–2363. doi:10.1104/pp.105.061762.

Kane NA, Agharbaoui Z, Diallo AO, Adam H, Tominaga Y, Ouellet F, Sarhan F. **2007**. TaVRT2 represses transcription of the wheat vernalization gene TaVRN1. Plant J. 51(4):670–680. doi:10.1111/j.1365-313X.2007.03172.x.

Kapitonov V V, Jurka J. **2004**. Harbinger transposons and an ancient HARBI1 gene derived from a transposase. DNA Cell Biol. 23(5):311–324. doi:10.1089/104454904323090949.

Karsai I, Szucs P, Mészáros K, Filichkina T, Hayes PM, Skinner JS, Láng L, Bedo Z. **2005**. The Vrn-H2 locus is a major determinant of flowering time in a facultative x winter growth habit barley (Hordeum vulgare L.) mapping population. Theor Appl Genet. 110(8):1458–1466. doi:10.1007/s00122-005-1979-7.

Kasamo K. **2003**. Regulation of plasma membrane H + -ATPase activity by the membrane environment. J Plant Res. 116(6):517–523. doi:10.1007/s10265-003-0112-8. [accessed 2017 Nov 15]. http://www.ncbi.nlm.nih.gov/pubmed/12905076.

Kaye C, Neven L, Hofig a, Li QB, Haskell D, Guy C. **1998**. Characterization of a gene for spinach CAP160 and expression of two spinach cold-acclimation proteins in tobacco. Plant Physiol. 116(4):1367–1377. doi:10.1104/pp.116.4.1367.

Kersey PJ, Allen JE, Christensen M, Davis P, Falin LJ, Grabmueller C, Hughes DST, Humphrey J, Kerhornou A, Khobova J, et al. 2014. Ensembl Genomes 2013: Scaling up access to genome-wide data. Nucleic Acids Res. 42(D1). doi:10.1093/nar/gkt979.

Khatri N, Katiyar A, Mudgil Y. **2012**. Role of G Protein Signaling Components in Plant Stress Management. In: Pandey GK, editor. Stress-Mediated Signaling in Plants I . Plant Stress 6 (Special Issue 1). Global Science Books. p. 1–9.

Khodakovskaya M, McAvoy R, Peters J, Wu H, Li Y. **2006**. Enhanced cold tolerance in transgenic tobacco expressing a chloroplast omega-3 fatty acid desaturase gene under the control of a cold-inducible promoter. Planta. 223(5):1090–1100. doi:10.1007/s00425-005-0161-4.

Kim D-H, Sung S. **2014**. Genetic and Epigenetic Mechanisms Underlying Vernalization. Arabidopsis Book. 12:e0171. doi:10.1199/tab.0171.

Kim SH, Kim HS, Bahk S, An J, Yoo Y, Kim JY, Chung WS. **2017**. Phosphorylation of the transcriptional repressor MYB15 by mitogen-activated protein kinase 6 is required for freezing tolerance in Arabidopsis. Nucleic Acids Res. 45(11):6613–6627. doi:10.1093/nar/gkx417.

Kim W, Salomé P, Fujiwara S, Somers D, McClung C. **2010**. Characterization of pseudo-response regulators in plants. Simon MI, Crane BR, Crane A, editors.

Kimura M. **1991**. The neutral theory of molecular evolution: a review of recent evidence. Japanese J Genet. 66(4):367–386. doi:10.1266/jjg.66.367.

Kippes N, Guedira M, Lin L, Alvarez M, Brown-Guedira G, Dubcovsky J. **2018**. Single nucleotide polymorphisms in a regulatory site of VRN-A1 first intron are associated with differences in vernalization requirement in winter wheat. Mol Genet Genomics.:1–13. doi:10.1007/s00438-018-1455-0.

Kiyosue T, Yamaguchi-Shinozaki K, Shinozaki K. **1994**. Cloning of cDNAs for genes that are early-responsive to dehydration stress (ERDs) in Arabidopsis thaliana L.: identification of three ERDs as HSP cognate genes. Plant Mol Biol. 25(5):791–798. doi:10.1007/BF00028874.

Knight H, Knight MR. **2000**. Imaging spatial and cellular characteristics of low temperature calcium signature after cold acclimation in Arabidopsis. J Exp Bot. 51(351):1679–86. doi:10.1093/jexbot/51.351.1679.

Knight H, Trewavas AJ, Knight MR. **1996**. Cold Calcium Signaling in Arabidopsis Involves Two Cellular Pools and a Change in Calcium Signature after Acclimation. PLANT CELL ONLINE. 8(3):489–503. doi:10.1105/tpc.8.3.489. [accessed 2017 Nov 15]. http://www.ncbi.nlm.nih.gov/pubmed/8721751.

Knight MR, Knight H. **2012**. Low-temperature perception leading to gene expression and cold tolerance in higher plants. New Phytol. 195:737–751. doi:10.1111/j.1469-8137.2012.04239.x. [accessed 2017 Nov 15]. http://onlinelibrary.wiley.com/store/10.1111/j.1469-8137.2012.04239.x/asset/j.1469-8137.2012.04239.x.pdf?v=1&t=ja1upafs&s=50c1917557cbefcd098bfde01d67601a96f64544.

Kodama H, Horiguchi G, Nishiuchi T, Nishimura M, Iba K. **1995**. Fatty Acid Desaturation during Chilling Acclimation Is One of the Factors Involved in Conferring Low-Temperature Tolerance to Young Tobacco Leaves. Plant Physiol. 107(4):1177–1185. doi:10.1104/pp.107.4.1177.

Kong CY, Luo Y ping, Duan TT, Xue Z, Gao XD, Zhao X, Gao G. **2016**. Potato remorin gene StREMa4 cloning and its spatiotemporal expression pattern under Ralstonia solanacearum and plant hormones treatment. Phytoparasitica. 44(4):575–584. doi:10.1007/s12600-016-0536-z.

Kong XY, Kissen R, Bones AM. **2012**. Characterization of recombinant nitrile-specifier proteins (NSPs) of Arabidopsis thaliana: Dependency on Fe(II) ions and the effect of glucosinolate substrate and reaction conditions. Phytochemistry. 84:7–17. doi:10.1016/j.phytochem.2012.08.004.

Konrad SSA, Popp C, Stratil TF, Jarsch IK, Thallmair V, Folgmann J, Marín M, Ott T. **2014**. S-acylation anchors remorin proteins to the plasma membrane but does not primarily determine their localization in membrane microdomains. New Phytol. 203(3):758–769. doi:10.1111/nph.12867.

Koppel R, Ingver A. **2008**. A COMPARISION OF THE YIELD AND QUALITY TRAITS OF WINTER AND SPRING WHEAT. Agron VĒSTIS (Latvian J Agron. LLU(11):83–88.

Körner C. **2016**. Plant adaptation to cold climates. F1000Research. 5:2769. doi:10.12688/f1000research.9107.1.

Kosakovsky Pond SL, Frost SDW. **2005a**. Not so different after all: A comparison of methods for detecting amino acid sites under selection. Mol Biol Evol. 22(5):1208–1222. doi:10.1093/molbev/msi105.

Kosakovsky Pond SL, Frost SDW. **2005b**. Datamonkey: Rapid detection of selective pressure on individual sites of codon alignments. Bioinformatics. 21(10):2531–2533. doi:10.1093/bioinformatics/bti320.

Kosová K, Prásil IT. **2012**. Annual field crops. In: Storey, K. B., Tanino KK, editor. Temperature adaptation in a changing climate: nature at risk. Wallingford: CABI. p. 186–207. [accessed 2017 Nov 17]. http://www.cabi.org/cabebooks/ebook/20113380766.

Kovacs D, Kalmar E, Torok Z, Tompa P. **2008**. Chaperone Activity of ERD10 and ERD14, Two Disordered Stress-Related Plant Proteins. PLANT Physiol. 147(1):381–390. doi:10.1104/pp.108.118208.

Kozlowski LP. **2017**. Proteome-pI: Proteome isoelectric point database. Nucleic Acids Res. 45(D1):D1112–D1116. doi:10.1093/nar/gkw978.

Kyte J, Doolittle RF. **1982**. A simple method for displaying the hydropathic character of a protein. J Mol Biol. 157(1):105–132. doi:10.1016/0022-2836(82)90515-0.

Lannoo N, Van Damme EJM. **2014**. Lectin domains at the frontiers of plant defense. Front Plant Sci. 5. doi:10.3389/fpls.2014.00397.

Laudencia-Chingcuanco D, Ganeshan S, You F, Fowler B, Chibbar R, Anderson O. **2011**. Genome-wide gene expression analysis supports a developmental model of low temperature tolerance gene regulation in wheat (Triticum aestivum L.). BMC Genomics. 12:299. doi:1471-2164-12-299 [pii]\r10.1186/1471-2164-12-299.

Lee C-M, Thomashow MF. **2012**. Photoperiodic regulation of the C-repeat binding factor (CBF) cold acclimation pathway and freezing tolerance in Arabidopsis thaliana. Proc Natl Acad Sci. 109(37):15054–15059. doi:10.1073/pnas.1211295109.

Lee TH, Tang H, Wang X, Paterson AH. **2013**. PGDD: A database of gene and genome duplication in plants. Nucleic Acids Res. 41(D1). doi:10.1093/nar/gks1104.

Lefebvre B, Furt F, Hartmann M-A, Michaelson L V., Carde J-P, Sargueil-Boiron F, Rossignol M, Napier JA, Cullimore J, Bessoule J-J, et al. 2007. Characterization of Lipid Rafts from Medicago truncatula Root Plasma Membranes: A Proteomic Study Reveals the Presence of a Raft-Associated Redox System. PLANT Physiol. 144(1):402–418. doi:10.1104/pp.106.094102.

Lefebvre B, Timmers T, Mbengue M, Moreau S, Herve C, Toth K, Bittencourt-Silvestre J, Klaus D, Deslandes L, Godiard L, et al. 2010. A remorin protein interacts with symbiotic receptors and regulates bacterial infection. Proc Natl Acad Sci. 107(5):2343–2348. doi:10.1073/pnas.0913320107.

Leng X, Han J, Wang X, Zhao M, Sun X, Wang C, Fang J. **2015**. Characterization of a Calmodulin-binding Transcription Factor from Strawberry (Fragaria × ananassa). Plant Genome. 8(2):0. doi:10.3835/plantgenome2014.08.0039.

Lescot M, Déhais P, Thijs G, Marchal K, Moreau Y, Van de Peer Y, Rouzé P, Rombauts S. **2002**. PlantCARE, a database of plant *cis*-acting regulatory elements and a portal to tools for *in silico* analysis of promoter sequences. Nucleic Acids Res. 30(1):325–327. doi:10.1093/nar/30.1.325.

Letunic I, Bork P. **2016**. Interactive tree of life (iTOL) v3: an online tool for the display and annotation of phylogenetic and other trees. Nucleic Acids Res. 44(W1):W242–W245. doi:10.1093/nar/gkw290.

Li C, Dubcovsky J. **2008**. Wheat FT protein regulates VRN1 transcription through interactions with FDL2. Plant J. 55(4):543–554. doi:10.1111/j.1365-313X.2008.03526.x.

Li H, Ding Y, Shi Y, Zhang X, Zhang S, Gong Z, Yang S. **2017**. MPK3- and MPK6-Mediated ICE1 Phosphorylation Negatively Regulates ICE1 Stability and Freezing Tolerance in Arabidopsis. Dev Cell. 43(5):630–642.e4. doi:10.1016/j.devcel.2017.09.025.

Li H, Ye K, Shi Y, Cheng J, Zhang X, Yang S. **2017**. BZR1 Positively Regulates Freezing Tolerance via CBF-Dependent and CBF-Independent Pathways in Arabidopsis. Mol Plant. 10(4):545–559. doi:10.1016/j.molp.2017.01.004.

Li J, Pleskot R, Henty-Ridilla JL, Blanchoin L, Potocký M, Staiger CJ. **2012**. Arabidopsis capping protein senses cellular phosphatidic acid levels and transduces these into changes in actin cytoskeleton dynamics. Plant Signal Behav. 7(12):1727–1730. doi:10.4161/psb.22472.

Li Q, Byrns B, Badawi MY, Diallo AB, Danyluk J, Sarhan F, Laudencia-Chingcuanco D, Zou J, Fowler DB. **2018**. Transcriptomic insights into phenological development and cold tolerance of wheat grown in the field. Plant Physiol. 176:2376–2394. doi:10.1104/pp.17.01311.

Li S, Su X, Zhang B, Huang Q, Hu Z, Lu M. **2013**. Molecular cloning and functional analysis of the Populus deltoides remorin gene PdREM. Tree Physiol. 33(10):1111–1121. doi:10.1093/treephys/tpt072.

Limin AE, Fowler DB. **2002**. Developmental traits affecting low-temperature tolerance response in near-isogenic lines for the vernalization locus Vrn-A1 in wheat (Triticum aestivum L. em Thell). Ann Bot. 89(5):579–585. doi:10.1093/aob/mcf102.

Lin C, Thomashow MF. **1992**. A cold-regulated Arabidopsis gene encodes A polypeptide having potent cryoprotective activity. Biochem Biophys Res Commun. 183(3):1103–1108. doi:10.1016/S0006-291X(05)80304-3.

Lin F, Xu SL, Ni WM, Chu ZQ, Xu ZH, Xue HW. **2003**. Identification of ABA-responsive genes in rice shoots via cDNA macroarray. Cell Res. 13(1):59–68. doi:10.1038/sj.cr.7290151.

Liu G, Loraine AE, Shigeta R, Cline M, Cheng J, Valmeekam V, Sun S, Kulp D, Siani-Rose MA. **2003**. NetAffix: Affymetrix probesets and annotations. Nucleic Acids Res. 31(1):82–86. doi:10.1093/nar/gkg121.

Liu Y, Liang J, Sun L, Yang X, Li D. **2016**. Group 3 LEA Protein, ZmLEA3, Is Involved in Protection from Low Temperature Stress. Front Plant Sci. 07. doi:10.3389/fpls.2016.01011.

Livak KJ, Schmittgen TD. **2001**. Analysis of relative gene expression data using real-time quantitative PCR and the 2(-Delta Delta C(T)) Method. Methods. 25(4):402–408. doi:10.1006/meth.2001.1262.

Livingston DP, Tuong TD, Murphy JP, Gusta L V., Willick I, Wisniewski ME. **2018**. High-definition infrared thermography of ice nucleation and propagation in wheat under natural frost conditions and controlled freezing. Planta. 247(4):791–806. doi:10.1007/s00425-017-2823-4.

Loukoianov A. **2005**. Regulation of VRN-1 Vernalization Genes in Normal and Transgenic Polyploid Wheat. PLANT Physiol. 138(4):2364–2373. doi:10.1104/pp.105.064287.

Lucau-Danila A, Laborde L, Legrand S, Huot L, Hot D, Lemoine Y, Hilbert JL, Hawkins S, Quillet MC, Hendriks T, et al. 2010. Identification of novel genes potentially involved in somatic embryogenesis in chicory (Cichorium intybus L.). BMC Plant Biol. 10. doi:10.1186/1471-2229-10-122.

Ma QH, Zhen WB, Liu YC. **2013**. Jacalin domain in wheat jasmonate-regulated protein Ta-JA1 confers agglutinating activity and pathogen resistance. Biochimie. 95(2):359–365. doi:10.1016/j.biochi.2012.10.014.

Macovei A, Vaid N, Tula S, Tuteja N. **2012**. A new DEAD-box helicase ATP-binding protein (OsABP) from rice is responsive to abiotic stress. Plant Signal Behav. 7(9):1138–1143. doi:10.4161/psb.21343.

Magallón S, Gómez-Acevedo S, Sánchez-Reyes LL, Hernández-Hernández T. **2015**. A metacalibrated time-tree documents the early rise of flowering plant phylogenetic diversity. New Phytol. 207(2):437–453. doi:10.1111/nph.13264.

Majeran W, Friso G, Asakura Y, Qu X, Huang M, Ponnala L, Watkins KP, Barkan A, van Wijk KJ. **2012**. Nucleoid-Enriched Proteomes in Developing Plastids and Chloroplasts from Maize Leaves: A New Conceptual Framework for Nucleoid Functions. PLANT Physiol. 158(1):156–189. doi:10.1104/pp.111.188474.

Marcolino-Gomes J, Rodrigues FA, Fuganti-Pagliarini R, Bendix C, Nakayama TJ, Celaya B, Molinari HBC, De Oliveira MCN, Harmon FG, Nepomuceno A. **2014**. Diurnal oscillations of soybean circadian clock and drought responsive genes. PLoS One. 9(1). doi:10.1371/journal.pone.0086402.

Marín M, Ott T. **2012**. Phosphorylation of Intrinsically Disordered Regions in Remorin Proteins. Front Plant Sci. 3(86). doi:10.3389/fpls.2012.00086.

Marín M, Thallmair V, Ott T. **2012**. The intrinsically disordered N-terminal region of AtREM1.3 remorin protein mediates protein-protein interactions. J Biol Chem. 287(47):39982–39991. doi:10.1074/jbc.M112.414292.

Martz F, Sutinen M-L, Kiviniemi S, Palta JP. **2006**. Changes in freezing tolerance, plasma membrane H+-ATPase activity and fatty acid composition in Pinus resinosa needles during cold acclimation and de-acclimation. Tree Physiol. 26(6):783–90. [accessed 2017 Nov 15]. http://www.ncbi.nlm.nih.gov/pubmed/16510394.

Mikkelsen MD, Pedas P, Schiller M, Vincze E, Mills RF, Borg S, Møller A, Schjoerring JK, Williams LE, Baekgaard L, et al. 2012. Barley HvHMA1 Is a Heavy Metal Pump Involved in Mobilizing Organellar Zn and Cu and Plays a Role in Metal Loading into Grains. PLoS One. 7(11). doi:10.1371/journal.pone.0049027.

Miller AK, Galiba G, Dubcovsky J. **2006**. A cluster of 11 CBF transcription factors is located at the frost tolerance locus Fr-Am2 in Triticum monococcum. Mol Genet Genomics. 275(2):193–203. doi:10.1007/s00438-005-0076-6.

Millner PA. **2001**. Heterotrimeric G-proteins in plant cell signaling. In: New Phytologist. Vol. 151. p. 165–174.

Mine A, Berens ML, Nobori T, Anver S, Fukumoto K, Winkelmüller TM, Takeda A, Becker D, Tsuda K. **2017**. Pathogen exploitation of an abscisic acid- and jasmonate-inducible MAPK phosphatase and its interception by *Arabidopsis* immunity. Proc Natl Acad Sci. 114(28):7456–7461. doi:10.1073/pnas.1702613114.

Mittler R, Blumwald E. **2015**. The Roles of ROS and ABA in Systemic Acquired Acclimation. Plant Cell. 27(1):64–70. doi:10.1105/tpc.114.133090.

Miura K, Furumoto T. **2013**. Cold signaling and cold response in plants. Int J Mol Sci. 14(3):5312–5337. doi:10.3390/ijms14035312.

Miura K, Jin JB, Lee J, Yoo CY, Stirm V, Miura T, Ashworth EN, Bressan RA, Yun D-J, Hasegawa PM. **2007**. SIZ1-Mediated Sumoylation of ICE1 Controls CBF3/DREB1A Expression and Freezing Tolerance in Arabidopsis. PLANT CELL ONLINE. 19(4):1403–1414. doi:10.1105/tpc.106.048397.

Miura K, Lee J, Jin JB, Yoo CY, Miura T, Hasegawa PM. **2009**. Sumoylation of ABI5 by the Arabidopsis SUMO E3 ligase SIZ1 negatively regulates abscisic acid signaling. Proc Natl Acad Sci. 106(13):5418–5423. doi:10.1073/pnas.0811088106.

Mizoguchi T, Irie K, Hirayama T, Hayashida N, Yamaguchi-Shinozaki K, Matsumoto K, Shinozaki K. **1996**. A gene encoding a mitogen-activated protein kinase kinase kinase is induced simultaneously with genes for a mitogen-activated protein kinase and an S6 ribosomal protein kinase by touch, cold, and water stress in Arabidopsis thaliana. Proc Natl Acad Sci U S A. 93(2):765–769.

Mohanta TK, Kumar P, Bae H. **2017**. Genomics and evolutionary aspect of calcium signaling event in calmodulin and calmodulin-like proteins in plants. BMC Plant Biol. 17(1):38. doi:10.1186/s12870-017-0989-3. [accessed 2017 Nov 15]. http://www.ncbi.nlm.nih.gov/pubmed/28158973.

Mongrand S, Morel J, Laroche J, Claverol S, Carde JP, Hartmann MA, Bonneu M, Simon-Plas F, Lessire R, Bessoule JJ. **2004**. Lipid rafts in higher plant cells: Purification and characterization of triton X-100-insoluble microdomains from tobacco plasma membrane. J Biol Chem. 279(35):36277–36286. doi:10.1074/jbc.M403440200.

Montillet JL, Leonhardt N, Mondy S, Tranchimand S, Rumeau D, Boudsocq M, Garcia AV, Douki T, Bigeard J, Laurière C, et al. 2013. An Abscisic Acid-Independent Oxylipin Pathway Controls Stomatal Closure and Immune Defense in Arabidopsis. PLoS Biol. 11(3). doi:10.1371/journal.pbio.1001513.

Msanne J, Lin J, Stone JM, Awada T. **2011**. Characterization of abiotic stress-responsive Arabidopsis thaliana RD29A and RD29B genes and evaluation of transgenes. Planta. 234(1):97–107. doi:10.1007/s00425-011-1387-y.

Murrell B, Wertheim JO, Moola S, Weighill T, Scheffler K, Kosakovsky Pond SL. **2012**. Detecting individual sites subject to episodic diversifying selection. PLoS Genet. 8(7). doi:10.1371/journal.pgen.1002764.

NCBI Resource Coordinators. **2016**. Database resources of the National Center for Biotechnology Information. Nucleic Acids Res. 44(Database issue):D7–D19. doi:10.1093/nar/gks1189.

NDong C, Danyluk J, Wilson KE, Pocock T, Huner NPA, Sarhan F. **2002**. Cold-regulated cereal chloroplast late embryogenesis abundant-like proteins. Molecular characterization and functional analyses. Plant Physiol. 129(3):1368–81. doi:10.1104/pp.001925.

NDong C, Ouellet F, Houde M, Sarhan F. **1997**. Gene expression during cold acclimation in strawberry. Plant Cell Physiol. 38(7):863–870. doi:10.1093/oxfordjournals.pcp.a029245.

Nebauer SG, Renau-Morata B, Guardiola JL, Molina RV, Pereira J. **2011**. Photosynthesis down-regulation precedes carbohydrate accumulation under sink limitation in Citrus. Tree Physiol. doi:10.1093/treephys/tpq103.

Nevo E, Fu Y-B, Pavlicek T, Khalifa S, Tavasi M, Beiles A. **2012**. Evolution of wild cereals during 28 years of global warming in Israel. Proc Natl Acad Sci U S A. 109(9):3412–5. doi:10.1073/pnas.1121411109.

Njaci I. **2016**. THE ROLE OF MicroRNAs IN STRESS RESPONSE IN THE RESURRECTION By. Queensland University of Technology.

Notredame C, Higgins DG, Heringa J. **2000**. T-coffee: a novel method for fast and accurate multiple sequence alignment. J Mol Biol. 302(1):205–217. doi:10.1006/jmbi.2000.4042.

Novillo F, Alonso JM, Ecker JR, Salinas J. **2004**. CBF2/DREB1C is a negative regulator of CBF1/DREB1B and CBF3/DREB1A expression and plays a central role in stress tolerance in Arabidopsis. Proc Natl Acad Sci. 101(11):3985–3990. doi:10.1073/pnas.0303029101. [accessed 2017 Nov 16]. http://www.ncbi.nlm.nih.gov/pubmed/15004278.

Oleksyn J, Zytkowiak R, Karolewski P, Reich PBB, Tjoelker MG. **2000**. Genetic and environmental control of seasonal carbohydrate dynamics in trees of diverse Pinus sylvestris populations. Tree Physiol. 20:837–847. doi:10.1093/treephys/20.12.837.

Oliver SN, Finnegan EJ, Dennis ES, Peacock WJ, Trevaskis B. **2009**. Vernalization-induced flowering in cereals is associated with changes in histone methylation at the VERNALIZATION1 gene. Proc Natl Acad Sci. 106(20):8386–8391. doi:10.1073/pnas.0903566106.

Olsen KM, Wendel JF. **2013**. A Bountiful Harvest: Genomic Insights into Crop Domestication Phenotypes. Annu Rev Plant Biol. 64(1):47–70. doi:10.1146/annurev-arplant-050312-120048.

Örvar BL, Sangwan V, Omann F, Dhindsa RS. **2000**. Early steps in cold sensing by plant cells: the role of actin cytoskeleton and membrane fluidity. Plant J. 23(6):785–794.

Oude Weernink PA, López De Jesús M, Schmidt M. **2007**. Phospholipase D signaling: Orchestration by PIP2 and small GTPases. Naunyn Schmiedebergs Arch Pharmacol. 374(5–6):399–411. doi:10.1007/s00210-007-0131-4.

Ouellet F. **2007**. Cold Acclimation and Freezing Tolerance in Plants. Life Sci.(December). doi:10.1002/9780470015902.a0020093.

Ouellet F, Carpentier E, Cope MJ, Monroy a F, Sarhan F. **2001**. Regulation of a wheat actin-depolymerizing factor during cold acclimation. Plant Physiol . 125(1):360–8. doi:10.1104/pp.125.1.360.

Palmgren MG, Nissen P. **2011**. P-Type ATPases. Annu Rev Biophys. 40(1):243–266. doi:10.1146/annurev.biophys.093008.131331.

Paradis S, Villasuso AL, Aguayo SS, Maldiney R, Habricot Y, Zalejski C, Machado E, Sotta B, Miginiac E, Jeannette E. **2011**. Arabidopsis thaliana lipid phosphate phosphatase 2 is involved in abscisic acid signalling in leaves. Plant Physiol Biochem. 49(3):357–362. doi:10.1016/j.plaphy.2011.01.010.

Pauwels L, Barbero GF, Geerinck J, Tilleman S, Grunewald W, Pérez AC, Chico JM, Bossche R Vanden, Sewell J, Gil E, et al. 2010. NINJA connects the co-repressor TOPLESS to jasmonate signalling. Nature. 464(7289):788–791. doi:10.1038/nature08854.

Pavlopoulou A, Kossida S. **2007**. Plant cytosine-5 DNA methyltransferases: Structure, function, and molecular evolution. Genomics. 90(4):530–541. doi:10.1016/j.ygeno.2007.06.011.

Pearson WR. **2013**. An introduction to sequence similarity ("homology") searching. Curr Protoc Bioinforma.(SUPPL.42). doi:10.1002/0471250953.bi0301s42.

Penfield S. **2008**. Temperature perception and signal transduction in plants. New Phytol. 179(3):615–628. doi:10.1111/j.1469-8137.2008.02478.x.

Peng JH, Sun D, Nevo E. **2011**. Domestication evolution, genetics and genomics in wheat. Mol Breed. 28(3):281–301. doi:10.1007/s11032-011-9608-4.

Perraki A, Binaghi M, Mecchia MA, Gronnier J, German-Retana S, Mongrand S, Bayer E, Zelada AM, Germain V. **2014**. StRemorin1.3 hampers Potato virus X TGBp1 ability to increase plasmodesmata permeability, but does not interfere with its silencing suppressor activity. FEBS Lett. 588(9):1699–1705. doi:10.1016/j.febslet.2014.03.014.

Petersen J, Eriksson SK, Harryson P, Pierog S, Colby T, Bartels D, Röhrig H. **2012**. The lysine-rich motif of intrinsically disordered stress protein CDeT11-24 from Craterostigma plantagineum is responsible for phosphatidic acid binding and protection of enzymes from damaging effects caused by desiccation. J Exp Bot. 63(13):4919–4929. doi:10.1093/jxb/ers173.

Petsalaki EI, Bagos PG, Litou ZI, Hamodrakas SJ. **2006**. PredSL: A tool for the N-terminal sequence-based prediction of protein subcellular localization. Genomics, Proteomics Bioinforma. 4(1):48–55. doi:10.1016/S1672-0229(06)60016-8.

Pidal B, Yan L, Fu D, Zhang F, Tranquilli G, Dubcovsky J. **2009**. The CArG-box located upstream from the transcriptional start of wheat vernalization gene VRN1 is not necessary for the vernalization response. J Hered. 100(3):355–364. doi:10.1093/jhered/esp002.

Plieth C. **2005**. Calcium: Just another regulator in the machinery of life? Ann Bot. 96(1):1–8. doi:10.1093/aob/mci144.

Plieth C, Hansen UP, Knight H, Knight MR. **1999**. Temperature sensing by plants: The primary characteristics of signal perception and calcium response. Plant J. 18(5):491–497. doi:10.1046/j.1365-313X.1999.00471.x.

Plieth C, Sattelmacher B, Hansen U-P, Thiel G. **1998**. The action potential in Chara: Ca2+ release from internal stores visualized by Mn2+-induced quenching of fura-dextran. Plant J. 13(2):167–175. doi:10.1046/j.1365-313X.1998.00019.x. [accessed 2017 Nov 15]. http://doi.wiley.com/10.1046/j.1365-313X.1998.00019.x.

Pokotylo I, Janda M, Kalachova T, Zachowski A, Ruelland E. **2017**. Phosphoglycerolipid Signaling in Response to Hormones Under Stress. In: Mechanism of Plant Hormone Signaling under Stress. Hoboken, NJ, USA: John Wiley & Sons, Inc. p. 91–126. [accessed 2017 Nov 17]. http://doi.wiley.com/10.1002/9781118889022.ch22.

Pozzi C, Rossini L, Vecchietti A, Salamini F. **2005**. Gene and genome changes during domestication of cereals. In: Cereal Genomics. p. 165–198.

Preston JC, Sandve SR. **2013**. Adaptation to seasonality and the winter freeze. Front Plant Sci. 4. doi:10.3389/fpls.2013.00167.

Qu B, He X, Wang J, Zhao Y, Teng W, Shao A, Zhao X, Ma W, Wang J, Li B, et al. 2015. A Wheat CCAAT Box-Binding Transcription Factor Increases the Grain Yield of Wheat with Less Fertilizer Input. Plant Physiol. 167(2):411–423. doi:10.1104/pp.114.246959.

R Development Core Team. **2013**. R: A language and environment for statistical computing. R Foundation for Statistical Computing, Vienna, Austria. URL http://www.R-project.org/. R Found Stat Comput Vienna, Austria.

Raffaele S, Bayer E, Lafarge D, Cluzet S, German Retana S, Boubekeur T, Leborgne-Castel N, Carde J-P, Lherminier J, Noirot E, et al. 2009. Remorin, a Solanaceae Protein Resident in Membrane Rafts and Plasmodesmata, Impairs Potato virus X Movement. Plant Cell. 21(5):1541–1555. doi:10.1105/tpc.108.064279.

Raffaele S, Mongrand S, Gamas P, Niebel A, Ott T. **2007**. Genome-Wide Annotation of Remorins, a Plant-Specific Protein Family: Evolutionary and Functional Perspectives. Plant Physiol. 145(3):593–600. doi:10.1104/pp.107.108639.

Ranty B, Aldon D, Galaud J-P. **2006**. Plant calmodulins and calmodulin-related proteins: multifaceted relays to decode calcium signals. Plant Signal Behav. 1(3):96–104. [accessed 2017 Nov 15]. http://www.ncbi.nlm.nih.gov/pubmed/19521489.

Reißer S, Strandberg E, Steinbrecher T, Ulrich AS. **2014**. 3D hydrophobic moment vectors as a tool to characterize the surface polarity of amphiphilic peptides. Biophys J. 106(11):2385–2394. doi:10.1016/j.bpj.2014.04.020.

Rescher U, Gerke V. **2004**. Annexins--unique membrane binding proteins with diverse functions. J Cell Sci. 117(Pt 13):2631–2639. doi:10.1242/jcs.01245.

Reymond P, Kunz B, Paul-Pletzer K, Grimm R, Eckerskorn C, Farmer EE. **1996**. Cloning of a cDNA encoding a plasma membrane-associated, uronide binding phosphoprotein with physical properties similar to viral movement proteins. Plant Cell. 8(12):2265–2276. doi:10.1105/tpc.8.12.2265.

Rihan HZ, Al-Issawi M, Fuller MP. **2017**. Advances in physiological and molecular aspects of plant cold tolerance. J Plant Interact. 12(1):143–157. doi:10.1080/17429145.2017.1308568. [accessed 2017 Nov 16]. https://www.tandfonline.com/doi/full/10.1080/17429145.2017.1308568.

Robertson a. J, Weninger a., Wilen RW, Fu P, Gusta L V. 1994. Comparison of Dehydrin Gene Expression and Freezing Tolerance in Bromus inermis and Secale cereale Grown in Controlled Environments, Hydroponics, and the Field. Plant Physiol. 106(3):1213–1216.

Rodríguez-Vargas S, Sánchez-García A, Martínez-Rivas JM, Prieto JA, Randez-Gil F. **2007**. Fluidization of membrane lipids enhances the tolerance of Saccharomyces cerevisiae to freezing and salt stress. Appl Environ Microbiol. 73(1):110–116. doi:10.1128/AEM.01360-06.

Röhrig H, Schmidt J, Colby T, Bräutigam A, Hufnagel P, Bartels D. **2006**. Desiccation of the resurrection plant Craterostigma plantagineum induces dynamic changes in protein phosphorylation. Plant, Cell Environ. 29(8):1606–1617. doi:10.1111/j.1365-3040.2006.01537.x.

Ronquist F, Teslenko M, van der Mark P, Ayres DL, Darling A, Hohna S, Larget B, Liu L, Suchard MA, Huelsenbeck JP. **2012**. MrBayes 3.2: Efficient Bayesian phylogenetic inference and model choice across a large model space. Syst Biol. 61(3):539–542. doi:DOI 10.1093/sysbio/sys029.

Rosa M, Prado C, Podazza G, Interdonato R, González JA, Hilal M, Prado FE. **2009**. Soluble sugars--metabolism, sensing and abiotic stress: a complex network in the life of plants. Plant Signal Behav. 4(5):388–93. doi:10.4161/psb.4.5.8294.

S. Sanghera G, H. Wani S, Hussain W, B. Singh N. **2011**. Engineering Cold Stress Tolerance in Crop Plants. Curr Genomics. 12(1):30–43. doi:10.2174/138920211794520178.

Saghfi S, Eivazi AR. **2014**. Effects of cold stress on proline and soluble carbohydrates in two chickpea cultivars. IntJCurrMicrobiolAppSci. 3(2):591–595. [accessed 2017 Nov 14]. https://www.ijcmas.com/vol-3-2/Siamak Saghfi and Ali Reza Eivazi.pdf.

Šamajová O, Komis G, Šamaj J. **2013**. Emerging topics in the cell biology of mitogen-activated protein kinases. Trends Plant Sci. 18(3):140–148. doi:10.1016/j.tplants.2012.11.004.

Sandve SR, Kosmala A, Rudi H, Fjellheim S, Rapacz M, Yamada T, Rognli OA. **2011**. Molecular mechanisms underlying frost tolerance in perennial grasses adapted to cold climates. Plant Sci. 180(1):69–77. doi:10.1016/j.plantsci.2010.07.011.

Sandve SR, Rudi H, Asp T, Rognli O. **2008**. Tracking the evolution of a cold stress associated gene family in cold tolerant grasses. BMC Evol Biol. 8(1):245. doi:10.1186/1471-2148-8-245.

Sangwan V, Foulds I, Singh J, Dhindsa RS. **2001**. Cold-activation of Brassica napus BN115 promoter is mediated by structural changes in membranes and cytoskeleton, and requires Ca 2+ influx. Plant J. 27(1):1–12. doi:10.1046/j.1365-313X.2001.01052.x.

Sasaki H, Ichimura K, Oda M. **1996**. Changes in sugar content during cold acclimation and deacclimation of cabbage seedlings. Ann Bot. 78(3):365–369. doi:10.1006/anbo.1996.0131.

Sasaki K, Christov NK, Tsuda S, Imai R. **2014**. Identification of a novel LEA protein involved in freezing tolerance in wheat. Plant Cell Physiol. 55(1):136–147. doi:10.1093/pcp/pct164.

Sãulescu N, Braun H. **2001**. Breeding for adaptation to environmental factors. Cold tolerance. In: Reynolds MP, Ortiz-Monasterio JI, McNab A, editors. Application of physiology in wheat breeding. CIMMYT, Mexico DF. p. 111–123.

Sauter JJ, Wisniewski M, Witt W. **1996**. Interrelationships between ultrastructure, sugar levels, and frost hardiness of ray parenchyma cells during frost acclimation and deacclimation in poplar (Populus × canadensis Moench ‹robusta›) Wood. J Plant Physiol. 149(3–4):451–461. doi:10.1016/S0176-1617(96)80148-9.

Schmittgen TD, Livak KJ. **2008**. Analyzing real-time PCR data by the comparative CT method. Nat Protoc. 3(6):1101–1108. doi:10.1038/nprot.2008.73.

Schrödinger LLC. **2016**. The PyMOL Molecular Graphics System. Schrödinger LLC. Version 1.:http://www.pymol.org.

Schubert M, Grønvold L, Sandve SR, Hvidsten TR, Fjellheim S. **2017**. Evolution of cold acclimation in temperate grasses (Pooideae). bioRxiv. 661592(1):1–36. doi:10.1095/biolreprod.108.070177. [accessed 2017 Nov 17]. https://www.biorxiv.org/content/early/2017/10/27/210021.

Schwaller B. **2009**. The continuing disappearance of "pure" Ca2+ buffers. Cell Mol Life Sci. 66(2):275–300. doi:10.1007/s00018-008-8564-6.

Sharma M, Laxmi A. **2016**. Jasmonates: Emerging Players in Controlling Temperature Stress Tolerance. Front Plant Sci. 6:1129. doi:10.3389/fpls.2015.01129. [accessed 2017 Nov 17]. http://journal.frontiersin.org/Article/10.3389/fpls.2015.01129/abstract.

Shewry PR, Hey SJ. **2015**. The contribution of wheat to human diet and health. Food Energy Secur. 4(3):178–202. doi:10.1002/FES3.64.

Shi Y, Tian S, Hou L, Huang X, Zhang X, Guo H, Yang S. **2012**. Ethylene Signaling Negatively Regulates Freezing Tolerance by Repressing Expression of CBF and Type-A ARR Genes in Arabidopsis. Plant Cell. 24(6):2578–2595. doi:10.1105/tpc.112.098640.

Shinkawa R, Morishita A, Amikura K, Machida R, Murakawa H, Kuchitsu K, Ishikawa M. **2013**. Abscisic acid induced freezing tolerance in chilling-sensitive suspension cultures and seedlings of rice. BMC Res Notes. 6(1):351. doi:10.1186/1756-0500-6-351.

Shitsukawa N, Ikari C, Mitsuya T, Sakiyama T, Ishikawa A, Takumi S, Murai K. **2007**. Wheat SOC1 functions independently of WAP1/VRN1, an integrator of vernalization and photoperiod flowering promotion pathways. Physiol Plant. 130(4):627–636. doi:10.1111/j.1399-3054.2007.00927.x.

Sigrist CJA, De Castro E, Cerutti L, Cuche BA, Hulo N, Bridge A, Bougueleret L, Xenarios I. **2013**. New and continuing developments at PROSITE. Nucleic Acids Res. 41(D1). doi:10.1093/nar/gks1067.

Sinha AK, Jaggi M, Raghuram B, Tuteja N. **2011**. Mitogen-activated protein kinase signaling in plants under abiotic stress. Plant Signal Behav. 6(2):196–203. doi:10.4161/psb.6.2.14701.

Skinner DZ. **2009**. Post-acclimation transcriptome adjustment is a major factor in freezing tolerance of winter wheat. Funct Integr Genomics. 9(4):513–523. doi:10.1007/s10142-009-0126-y.

Small I, Peeters N, Legeai F, Lurin C. **2004**. Predotar: A tool for rapidly screening proteomes for N-terminal targeting sequences. Proteomics. 4(6):1581–1590. doi:10.1002/pmic.200300776.

Smith MD, Wertheim JO, Weaver S, Murrell B, Scheffler K, Kosakovsky Pond SL. **2015**. Less is more: An adaptive branch-site random effects model for efficient detection of episodic diversifying selection. Mol Biol Evol. 32(5):1342–1353. doi:10.1093/molbev/msv022.

Solomon F. **1977**. Binding Sites for Calcium on Tubulin. Biochemistry. 16(3):358–363. doi:10.1021/bi00622a003.

Sperschneider J, Catanzariti AM, Deboer K, Petre B, Gardiner DM, Singh KB, Dodds PN, Taylor JM. **2017**. LOCALIZER: Subcellular localization prediction of both plant and effector proteins in the plant cell. Sci Rep. 7. doi:10.1038/srep44598.

Staiger D, Brown JWS. **2013**. Alternative Splicing at the Intersection of Biological Timing, Development, and Stress Responses. Plant Cell. 25(10):3640–3656. doi:10.1105/tpc.113.113803.

Stockinger EJ, Skinner JS, Gardner KG, Francia E, Pecchioni N. **2007**. Expression levels of barley Cbf genes at the Frost resistance-H2 locus are dependent upon alleles at Fr-H1 and Fr-H2. Plant J. 51(2):308–321. doi:10.1111/j.1365-313X.2007.0141.x.

Stupnikova I, Benamar A, Tolleter D, Grelet J, Borovskii G, Dorne A-J, Macherel D. **2006**. Pea seed mitochondria are endowed with a remarkable tolerance to extreme physiological temperatures. Plant Physiol. 140(1):326–35. doi:10.1104/pp.105.073015.

Tamura K, Peterson D, Peterson N, Stecher G, Nei M, Kumar S. **2011**. MEGA5: Molecular evolutionary genetics analysis using maximum likelihood, evolutionary distance, and maximum parsimony methods. Mol Biol Evol. 28(10):2731–2739. doi:10.1093/molbev/msr121.

Teardo E, Carraretto L, Wagner S, Formentin E, Behera S, De Bortoli S, Larosa V, Fuchs P, Lo Schiavo F Lo, Raffaello A, et al. 2016. Physiological characterization of a plant mitochondrial calcium uniporter in vitro and in vivo. Plant Physiol.:pp.01359.2016. doi:10.1104/pp.16.01359.

Teige M, Scheikl E, Eulgem T, Doczi R, Ichimura K, Shinozaki K, Dangl JL, Hirt H. **2004**. The MKK2 pathway mediates cold and salt stress signaling in Arabidopsis. Mol Cell. 15(1):141–152. doi:10.1016/j.molcel.2004.06.023.

Testerink C, Munnik T. **2011**. Molecular, cellular, and physiological responses to phosphatidic acid formation in plants. J Exp Bot. 62(7):2349–2361. doi:10.1093/jxb/err079.

Thakur P, Nayyar H. **2013**. Facing the cold stress by plants in the changing environment: Sensing, signaling, and defending mechanisms. In: Plant Acclimation to Environmental Stress. p. 29–69.

Theocharis A, Clément C, Barka EA. **2012**. Physiological and molecular changes in plants grown at low temperatures. Planta. 235(6):1091–1105. doi:10.1007/s00425-012-1641-y.

Thines B, Katsir L, Melotto M, Niu Y, Mandaokar A, Liu G, Nomura K, He SY, Howe GA, Browse J. **2007**. JAZ repressor proteins are targets of the SCFCOI1 complex during jasmonate signalling. Nature. 448(7154):661–665. doi:10.1038/nature05960.

Thion L, Mazars C, Thuleau P, Graziana A, Rossignol M, Moreau M, Ranjeva R. **1996**. Activation of plasma membrane voltage-dependent calcium-permeable channels by disruption of microtubules in carrot cells. FEBS Lett. 393(1):13–18. doi:10.1016/0014-5793(96)00844-7.

Di Tommaso P, Moretti S, Xenarios I, Orobitg M, Montanyola a, Chang JM, Taly JF, Notredame C. **2011**. T-Coffee: a web server for the multiple sequence alignment of protein and RNA sequences using structural information and homology extension. Nucleic Acids Res. 39(Web Server issue):W13-7. doi:10.1093/nar/gkr245.

Tóth K, Stratil TF, Madsen EB, Ye J, Popp C, Antolín-Llovera M, Grossmann C, Jensen ON, Schüßler A, Parniske M, et al. 2012. Functional domain analysis of the remorin protein LjSYMREM1 in lotus japonicus. PLoS One. 7(1). doi:10.1371/journal.pone.0030817.

Tremblay K, Ouellet F, Fournier J, Danyluk J, Sarhan F. **2005**. Molecular characterization and origin of novel bipartite cold-regulated ice recrystallization inhibition proteins from cereals. Plant Cell Physiol. 46(6):884–891. doi:10.1093/pcp/pci093.

Trevaskis B. **2010**. Goldacre Paper: The central role of the VERNALIZATION1 gene in the vernalization response of cereals. Funct Plant Biol. 37(6):479–487. doi:10.1071/FP10056.

Trevaskis B, Hemming MN, Dennis ES, Peacock WJ. **2007**. The molecular basis of vernalization-induced flowering in cereals. Trends Plant Sci. 12(8):352–357. doi:10.1016/j.tplants.2007.06.010.

Trevaskis B, Tadege M, Hemming MN, Peacock WJ, Dennis ES, Sheldon C. **2006**. Short Vegetative Phase-Like MADS-Box Genes Inhibit Floral Meristem Identity in Barley. PLANT Physiol. 143(1):225–235. doi:10.1104/pp.106.090860.

Turner AS, Faure S, Zhang Y, Laurie DA. **2013**. The effect of day-neutral mutations in barley and wheat on the interaction between photoperiod and vernalization. Theor Appl Genet. 126(9):2267–2277. doi:10.1007/s00122-013-2133-6.

Turner JG, Ellis C, Devoto A. **2002**. The jasmonate signal pathway. Plant Cell. 14 Suppl:S153–S164. doi:10.1105/tpc.000679.

Tuteja N, Mahajan S. **2007**. Calcium signaling network in plants: an overview. Plant Signal Behav. 2(2):79–85. doi:10.4161/psb.2.2.4176.

Uemura M, Tominaga Y, Nakagawara C, Shigematsu S, Minami A, Kawamura Y. **2006**. Responses of the plasma membrane to low temperatures. Physiol Plant. 126(1):81–89. doi:10.1111/j.1399-3054.2005.00594.x.

Ukaji N, Kuwabara C, Takezawa D, Arakawa K, Fujikawa S. **2001**. Cold acclimation-induced WAP27 localized in endoplasmic reticulum in cortical parenchyma cells of mulberry tree was homologous to group 3 late-embryogenesis abundant proteins. Plant Physiol. 126(4):1588–97. doi:10.1104/pp.126.4.1588.

Uno Y, Furihata T, Abe H, Yoshida R, Shinozaki K, Yamaguchi-Shinozaki K. **2000**. Arabidopsis basic leucine zipper transcription factors involved in an abscisic acid-dependent signal transduction pathway under drought and high-salinity conditions. Proc Natl Acad Sci U S A. 97(21):11632–11637. doi:10.1073/pnas.190309197.

Upchurch RG. **2008**. Fatty acid unsaturation, mobilization, and regulation in the response of plants to stress. Biotechnol Lett. 30(6):967–977. doi:10.1007/s10529-008-9639-z.

Upreti KK, Sharma M. **2016**. Role of plant growth regulators in abiotic stress tolerance. In: Abiotic Stress Physiology of Horticultural Crops. p. 19–46.

Urrutia ME, Duman JG, Knight CA. **1992**. Plant thermal hysteresis proteins. Biochim Biophys Acta (BBA)/Protein Struct Mol. 1121(1–2):199–206. doi:10.1016/0167-4838(92)90355-H.

Velasco R, Salamini F, Bartels D. **1998**. Gene structure and expression analysis of the drought- and abscisic acid-responsive CDeT11-24 gene family from the resurrection plant Craterostigma plantagineum Hochst. Planta. 204(4):459–471. doi:10.1007/s004250050280.

Villasuso AL, Di Palma MA, Aveldaño M, Pasquaré SJ, Racagni G, Giusto NM, Machado EE. **2013**. Differences in phosphatidic acid signalling and metabolism between ABA and GA treatments of barley aleurone cells. Plant Physiol Biochem. 65:1–8. doi:10.1016/j.plaphy.2013.01.005.

Viswanathan C, Zhu J-K. **2002**. Molecular genetic analysis of cold-regulated gene transcription. Philos Trans R Soc Lond B Biol Sci. 357(1423):877–886. doi:10.1098/rstb.2002.1076.

Voorrips RE. **2002**. MapChart: Software for the Graphical Presentation of Linkage Maps and QTLs. J Hered. 93(1):77–78. doi:10.1093/jhered/93.1.77.

Wacke M, Thiel G, Hütt MT. **2003**. Ca2+ dynamics during membrane excitation of green alga Chara: Model simulations and experimental data. J Membr Biol. 191(3):179–192. doi:10.1007/s00232-002-1054-0.

Wang D-Z, Jin Y-N, Ding X-H, Wang W-J, Zhai S-S, Bai L-P, Guo Z-F. **2017**. Gene regulation and signal transduction in the ICE-CBF-COR signaling pathway during cold stress in plants. BIOCHEMISTRY-MOSCOW. 82(10):1103–1117. doi:10.1134/S0006297917100030.

Wang P, Li Z, Wei J, Zhao Z, Sun D, Cui S. **2012**. A Na+/Ca2+ exchanger-like protein (AtNCL) involved in salt stress in Arabidopsis. J Biol Chem. 287(53):44062–44070. doi:10.1074/jbc.M112.351643.

Wang S, Cao L, Wang H. **2016**. Arabidopsis ubiquitin-conjugating enzyme UBC22 is required for female gametophyte development and likely involved in Lys11-linked ubiquitination. J Exp Bot. 67(11):3277–3288. doi:10.1093/jxb/erw142.

Wang S, Wong D, Forrest K, Allen A, Chao S, Huang BE, Maccaferri M, Salvi S, Milner SG, Cattivelli L, et al. 2014. Characterization of polyploid wheat genomic diversity using a high-density 90 000 single nucleotide polymorphism array. Plant Biotechnol J. 12(6):787–796. doi:10.1111/pbi.12183.

Wanner LA, Junttila O. **1999**. Cold-induced freezing tolerance in Arabidopsis. Plant Physiol. 120(2):391–400. doi:10.1104/PP.120.2.391.

Wasteneys GO, Yang Z. **2004**. The cytoskeleton becomes multidisciplinary. Plant Physiol. 136(December):3853–3854. doi:10.1104/pp.104.900130.

Wasternack C, Hause B. **2013**. Jasmonates: Biosynthesis, perception, signal transduction and action in plant stress response, growth and development. An update to the 2007 review in Annals of Botany. Ann Bot. 111(6):1021–1058. doi:10.1093/aob/mct067.

Wasternack C, Parthier B. **1997**. Jasmonate-signalled plant gene expression. Trends Plant Sci. 2(8):302–307. doi:10.1016/S1360-1385(97)89953-0.

Waterhouse AM, Procter JB, Martin DMA, Clamp M, Barton GJ. **2009**. Jalview Version 2-A multiple sequence alignment editor and analysis workbench. Bioinformatics. 25(9):1189–1191. doi:10.1093/bioinformatics/btp033.

Wickham H. **2009**. ggplot2 Elegant Graphics for Data Analysis.

Winfield MO, Lu C, Wilson ID, Coghill JA, Edwards KJ. **2010**. Plant responses to cold: transcriptome analysis of wheat. Plant Biotechnol J. 8(7):749–771. doi:10.1111/j.1467-7652.2010.00536.x.

Wise MJ, Tunnacliffe A. **2004**. POPP the question: What do LEA proteins do? Trends Plant Sci. 9(1):13–17. doi:10.1016/j.tplants.2003.10.012.

Wisniewski M, Gusta L V. 2014. The biology of cold hardiness: Adaptive strategies. Environ Exp Bot. 106:1–3. doi:10.1016/j.envexpbot.2014.03.001.

Wong BL, Baggett KL, Rye AH. **2003**. Seasonal patterns of reserve and soluble carbohydrates in mature sugar maple (*Acer saccharum*). Can J Bot. 81(8):780–788. doi:10.1139/b03-079. [accessed 2017 Nov 14]. http://www.nrcresearchpress.com/doi/10.1139/b03-079.

Wright ES. **2015**. DECIPHER: Harnessing local sequence context to improve protein multiple sequence alignment. BMC Bioinformatics. 16(1). doi:10.1186/s12859-015-0749-z.

Wright PE, Dyson HJ. **2015**. Intrinsically Disordered Proteins in Cellular Signaling and Regulation. Nat Rev Mol Cell Biol. 16(1):18–29. doi:10.1038/nrm3920.

Wu C-Q, Hu H-H, Zeng Y, Liang D-C, Xie K-B, Zhang J-W, Chu Z-H, Xiong L-Z. **2006**. Identification of Novel Stress-responsive Transcription Factor Genes in Rice by cDNA Array Analysis. J Integr Plant Biol. 48(10):1216–1224. doi:10.1111/j.1672-9072.2006.00344.x.

Xia X, Kumar S. **2006**. Codon-based detection of positive selection can be biased by heterogeneous distribution of polar amino acids along protein sequences. Comput Syst Bioinforma Conf.:335–340. doi:9781860947575_0040 [pii].

Xiang Y, Hai Lu Y, Song M, Wang Y, Xu W, Wu L, Wang H, Ma Z. **2015**. Overexpression of a triticum aestivum calreticulin gene (TaCRT1) improves salinity tolerance in tobacco. PLoS One. 10(10). doi:10.1371/journal.pone.0140591.

Xiao J, Xu S, Li C, Xu Y, Xing L, Niu Y, Huan Q, Tang Y, Zhao C, Wagner D, et al. 2014. O-GlcNAc-mediated interaction between VER2 and TaGRP2 elicits TaVRN1 mRNA accumulation during vernalization in winter wheat. Nat Commun. 5. doi:10.1038/ncomms5572.

Xu G, Guo C, Shan H, Kong H. **2012**. Divergence of duplicate genes in exon-intron structure. Proc Natl Acad Sci. 109(4):1187–1192. doi:10.1073/pnas.1109047109.

Xu L, Ménard R, Berr A, Fuchs J, Cognat V, Meyer D, Shen WH. **2009**. The E2 ubiquitin-conjugating enzymes, AtUBC1 and AtUBC2, play redundant roles and are involved in activation of FLC expression and repression of flowering in Arabidopsis thaliana. Plant J. 57(2):279–288. doi:10.1111/j.1365-313X.2008.03684.x.

Yadav SK. **2010**. Cold stress tolerance mechanisms in plants. A review. Agron Sustain Dev. 30(3):515–527. doi:10.1051/agro/2009050.

Yamaguchi-shinozaki K, Koizumi M, Urao S, Shinozaki K. **1992**. Molecular cloning and characterization of 9 cDNAs for genes that are responsive to desiccation in arabidopsis thaliana: Sequence analysis of one cDNA clone that encodes a putative transmembrane channel protein. Plant Cell Physiol. 33(3):217–224. doi:10.1093/oxfordjournals.pcp.a078243.

Yamaguchi-Shinozaki K, Shinozaki K. **1993**. Characterization of the expression of a desiccation-responsive rd29 gene of Arabidopsis thaliana and analysis of its promoter in transgenic plants. Mol Gen Genet. 236(2–3):331–340. doi:10.1007/BF00277130.

Yamaguchi-Shinozaki K, Shinozaki K. **2005**. Organization of cis-acting regulatory elements in osmotic- and cold-stress-responsive promoters. Trends Plant Sci. 10(2):88–94. doi:10.1016/j.tplants.2004.12.012.

Yan L, Fu D, Li C, Blechl A, Tranquilli G, Bonafede M, Sanchez A, Valarik M, Yasuda S, Dubcovsky J. **2006**. The wheat and barley vernalization gene VRN3 is an orthologue of FT. Proc Natl Acad Sci. 103(51):19581–19586. doi:10.1073/pnas.0607142103.

Yan L, Loukoianov A, Blechl A, Tranquilli G, Ramakrishna W, SanMiguel P, Bennetzen JL, Echenique V, Dubcovsky J. **2004**. The Wheat VRN2 Gene Is a Flowering Repressor Down-Regulated by Vernalization. Science (80-). 303(5664):1640–1644. doi:10.1126/science.1094305. [accessed 2017 Nov 17]. http://www.ncbi.nlm.nih.gov/pubmed/15016992.

Yan L, Loukoianov A, Tranquilli G, Helguera M, Fahima T, Dubcovsky J. **2003**. Positional cloning of the wheat vernalization gene VRN1. Proc Natl Acad Sci. 100(10):6263–6268. doi:10.1073/pnas.0937399100.

Yonezawa N, Nishida E, Iida K, Yahara I, Sakai H. **1990**. Inhibition of the interactions of cofilin, destrin, and deoxyribonuclease I with actin by phosphoinositides. J Biol Chem. 265(15):8382–8386.

Yu C-S, Chen Y-C, Lu C-H, Hwang J-K. **2006**. Prediction of protein subcellular localization. Proteins. 64(3):643–51. doi:10.1002/prot.21018.

Yuan F, Yang H, Xue Y, Kong D, Ye R, Li C, Zhang J, Theprungsirikul L, Shrift T, Krichilsky B, et al. 2014. OSCA1 mediates osmotic-stress-evoked Ca2+ increases vital for osmosensing in Arabidopsis. Nature. 514(7522):367–371. doi:10.1038/nature13593. [accessed 2017 Nov 15]. http://www.ncbi.nlm.nih.gov/pubmed/25162526.

Yuanyuan M, Yali Z, Jiang L, Hongbo S. **2010**. Roles of plant soluble sugars and their responses to plant cold stress. J Biotechnol. 8(10):2004–2010.

Yue J, Li C, Liu Y, Yu J. **2014**. A remorin gene SiREM6, the target gene of SiARDP, from foxtail millet (Setaria italica) promotes high salt tolerance in transgenic Arabidopsis. PLoS One. 9(6). doi:10.1371/journal.pone.0100772.

Zalejski C, Zhang Z, Quettier A-L, Maldiney R, Bonnet M, Brault M, Demandre C, Miginiac E, Rona J-P, Sotta B, et al. 2005. Diacylglycerol pyrophosphate is a second messenger of abscisic acid signaling in Arabidopsis thaliana suspension cells. Plant J. 42(2):145–52. doi:10.1111/j.1365-313X.2005.02373.x.

Zarin T, Tsai CN, Nguyen Ba AN, Moses AM. **2017**. Selection maintains signaling function of a highly diverged intrinsically disordered region. Proc Natl Acad Sci. 114(8):E1450–E1459. doi:10.1073/pnas.1614787114.

Zhang F, Qi B, Wang L, Zhao B, Rode S, Riggan ND, Ecker JR, Qiao H. **2016**. EIN2-dependent regulation of acetylation of histone H3K14 and non-canonical histone H3K23 in ethylene signalling. Nat Commun. 7. doi:10.1038/ncomms13018.

Zhang W, Qin C, Zhao J, Wang X. **2004**. Phospholipase D 1-derived phosphatidic acid interacts with ABI1 phosphatase 2C and regulates abscisic acid signaling. Proc Natl Acad Sci. 101(25):9508–9513. doi:10.1073/pnas.0402112101.

Zhang X, Jacobsen SE. **2006**. Genetic analyses of DNA methyltransferases in Arabidopsis thaliana. Cold Spring Harb Symp Quant Biol. 71:439–447. doi:10.1101/sqb.2006.71.047.

Zhang Y, Zhu H, Zhang Q, Li M, Yan M, Wang R, Wang L, Welti R, Zhang W, Wang X. **2009**. Phospholipase dalpha1 and phosphatidic acid regulate NADPH oxidase activity and production of reactive oxygen species in ABA-mediated stomatal closure in Arabidopsis. Plant Cell. 21(8):2357–77. doi:10.1105/tpc.108.062992.

Zhang YF, Hou MM, Tan BC. **2013**. The Requirement of WHIRLY1 for Embryogenesis Is Dependent on Genetic Background in Maize. PLoS One. 8(6). doi:10.1371/journal.pone.0067369.

Zhao J. **2015**. Phospholipase D and phosphatidic acid in plant defence response: From protein-protein and lipid-protein interactions to hormone signalling. J Exp Bot. 66(7):1721–1736. doi:10.1093/jxb/eru540.

Zhu J, Pearce S, Burke A, See DR, Skinner DZ, Dubcovsky J, Garland-Campbell K. **2014**. Copy number and haplotype variation at the VRN-A1 and central FR-A2 loci are associated with frost tolerance in hexaploid wheat. Theor Appl Genet. 127(5):1183–1197. doi:10.1007/s00122-014-2290-2.

Zhu J, Shi H, Lee B -h., Damsz B, Cheng S, Stirm V, Zhu J-K, Hasegawa PM, Bressan RA. **2004**. An Arabidopsis homeodomain transcription factor gene, HOS9, mediates cold tolerance through a CBF-independent pathway. Proc Natl Acad Sci. 101(26):9873–9878. doi:10.1073/pnas.0403166101.

Zhu J, Verslues PE, Zheng X, Lee B, Zhan X, Manabe Y, Sokolchik I, Zhu Y, Dong C-H, Zhu J-K, et al. 2005. HOS10 encodes an R2R3-type MYB transcription factor essential for cold acclimation in plants. Proc Natl Acad Sci U S A. 102(28):9966–9971. doi:10.1073/pnas.0503960102.

Zimmermann P, Bleuler S, Laule O, Martin F, Ivanov N V., Campanoni P, Oishi K, Lugon-Moulin N, Wyss M, Hruz T, et al. 2014. ExpressionData - A public resource of high quality curated datasets representing gene expression across anatomy, development and experimental conditions. BioData Min. 7(1). doi:10.1186/1756-0381-7-18.